Global 3'-UTR Length Changes Form a Novel Layer of Regulation in the Macrophage Response to Interferon-Beta

Sarah Straub

ORCID ID: 0000-0002-6556-8110

from Bonn, Germany

Submitted in total fulfilment of the requirements of the joint degree of Doctor of Philosophy (PhD)

of

The Medical Faculty
The Rheinische Friedrich-Wilhelms-Universität Bonn

and

The Department of Microbiology and Immunology
The University of Melbourne

Bonn/Melbourne, 2022

Performed and approved by The Medical Faculty of The Rheinische Friedrich-Wilhelms-Universität Bonn and The University of Melbourne

1. Supervisor: Prof. Eicke Latz

2. Supervisor: Prof. Paul Hertzog

Original thesis submission: September 2nd 2021

Oral examination: April 14th 2022

Institute of Innate Immunity, Bonn

Director: Prof. Eicke Latz

Table of Contents

Abbreviations

ACC	Acetyl-CoA carboxylase
ACOD1	Cis-aconitate decarboxylase
ADAR1	Adenosine deaminase RNA specific
AGO2	Argonaute 2
AIP4	Itchy E3 ubiquitin protein ligase
AIM2	Absent in melanoma 2
ALPP	Alkaline phosphatase, placental
AMP	Adenosine monophosphate
ANOVA	Analysis of variance
AP1	Activator protein 1
APA	Alternative polyadenylation
APEX2	Apurinic/Apyrimidinic endodeoxyribonuclease 2
APOBEC3	Apolipoprotein B mRNA editing enzyme catalytic subunit 3
ARG1	Arginase 1
ARSA	Arylsulfatase A
ATF3	Activating transcription factor 3
ATG5	Autophagy protein 5
ATM	Serine/threonine protein kinase ATM
ATP	Adenosine triphosphate
AUF1	AU-rich element RNA-binding protein 1
BAD	BCL2-associated agonist of cell death
BAFFR	B-cell-activating factor-receptor
bp	Base pairs
BDNF	Brain-derived neurotrophic factor
BIRC3	Baculoviral inhibitors of apoptosis repeat-containing protein 3
BMDM	Mouse bone marrow-derived macrophage
CAMK2A	Calmodulin-dependent protein kinase 2 alpha

CARD	Caspase recruitment domain
CARKL	Carbohydrate kinase-like
CBX5	Chromobox 5
CCL	C-C chemokine ligand
CD	Cluster of differentiation
CDK	Cyclin-dependent kinase
CEBP1	Cytoplasmic polyadenylation element binding protein 1
CEBPB	CCAAT enhancer-binding protein beta
CF	Cleavage factor
cGAS	Cyclic GMP-AMP synthase
cGAMP	Cyclic GMP-AMP
CHX	Cycloheximide
CIC	Capicua transcriptional repressor
CLP1	Cleavage factor polyribonucleotide kinase subunit 1
CoA	Coenzyme A
COX5B	Cytochrome C oxidase subunit 5B
CPSF	Cleavage and polyadenylation specificity factor
CPT1A	Carnitine palmitoyltransferase 1A
CRISPR	Clustered regularly interspaced short palindromic repeats
CSTF	Cleavage stimulation factor
CXCR4	C-X-C motif chemokine receptor 4
DAMP	Damage-associated molecular pattern
DMSO	Dimethyl sulphoxide
DPBS	Dulbecco’s phosphate buffered saline
DC	Dendritic cell
DCTN1	Dynactin subunit 1
DNA	Deoxyribonucleic acid
DRP1	Dynamin-related protein 1
EDC3	Enhancer of mRNA decapping 3

EIF4E	Eukaryotic initiation factor 4 E
EIF4EBP/4EBP	EIF4E binding protein
EPRS	Glutamyl-prolyl-tRNA synthetase
ER	Endoplasmic reticulum
ERK	Extracellular signal-regulated kinase
ES cell	Embryonic stem cell
FAD	Flavin adenine dinucleotide
FAK	Focal adhesion kinase
FASN	Fatty acid synthase
FC	Fold change
FCS	Fetal calf serum
FDR	False discovery rate
FIP1	Factor interacting with poly-A polymerase
FISH	Fluorescence *in situ* hybridization
FOXP3	Forkhead box P3
fwd	Forward
G3BP1	Stress granule assembly factor 1
GAS	Gamma-activated sequence
GAS2	Growth arrest specific 2
GBP5	Guanylate binding protein 5
GFP	Green fluorescent protein
GMP	Guanosine monophosphate
H3K27	Histone 3 lysine 27
HAUS1	HAUS augmin-like complex subunit 1
HBA2	Hemoglobin subunit alpha 2
HBB	Hemoglobin subunit beta
HERC5	HECT and RLD domain-containing E3 ubiquitin protein ligase 5
HIF1α	Hypoxia-inducible factor 1 subunit alpha
HITS-CLIP	High-throughput sequencing of RNA isolated by crosslinking immunoprecipitation

HIV	Human immunodeficiency virus
HK2	Hexokinase 2
HMDM	Human blood monocyte-derived macrophage
HN1	Hematological and neurological expressed 1
HNRNP	Heterogeneous nuclear ribonucleoprotein
HSC	Hematopoietic stem cell
HSPA9	Heat shock protein family A
HO1	Heme oxygenase 1
HuR	Hu antigen R
IDH	Isocitrate dehydrogenase
IFIT	Interferon-induced protein with tetratricopeptide repeats
IFITM	Interferon-induced transmembrane
IFN	Interferon
IFNAR	IFN alpha receptor
IFNGR	IFN gamma receptor
IFNLR1	IFN lamba receptor 1
Ig	Immunoglobulin
IKK	Inhibitor of κB kinase
IL	Interleukin
IL10RB	IL10 receptor subunit beta
iNOS	Inducible nitric oxide synthase
IPEX	Immunodysregulation polyendocrinopathy enteropathy X-linked
iPSC	Induced pluripotent stem cells
IQGAP1	IQ motif-containing GTPase activating protein 1
IRAK	Interleukin 1 receptor-associated kinase 1
IRF	Interferon regulatory factor
IRG	Interferon-regulated gene
ISG15	Interferon-stimulated gene 15
ISRE	IFN-stimulated response element

ISGF3	IFN-stimulated gene factor 3
ITGA1	Integrin subunit alpha 1
JAK	Janus kinase
JNK	c-Jun N-terminal kinase
KARS1	Lysine-tRNA ligase
LGP2	Laboratory of genetics and physiology 2
LPS	Lipopolysaccharide
LTR	Long terminal repeat
LU	Long 3'-UTR
M2BP	Mac-2-binding protein
MAP kinase	Mitogen-activated protein kinase
MAM	Mitochondria-associated membranes
MAPKAP	MAP kinase-activated protein kinase
MARCH	Membrane-associated ring-CH-type finger
MAVS	Mitochondrial antiviral-signaling protein
MBD2	Methyl-CpG binding domain protein 2
MCL	Markov cluster
M-CSF	Macrophage colony-stimulating factor
MDA5	Melanoma differentiation-associated gene 5
MEF	Mouse embryonic fibroblast
MFI	Mean fluorescence intensity
MHC	Major histocompatibility complex
miRNA	microRNA
MKK	MAP kinase kinase
MNK	MAP kinase-interacting kinase
MPDZ	Multiple PDZ domain protein
MPG	DNA-3-methyladenine glycosylase
MRC1	Mannose receptor C-type 1
MSC	Multi-synthase-complex
MSI1	Musashi RNA-binding protein 1
MSK	Mitogen- and stress-activated protein kinase

MTFP1	Mitochondrial fission process 1
mTOR	Mechanistic target of rapamycin kinase
mTORC	mTOR complex
MX2	MX dynamin-like GTPase 2
MYD88	Myeloid differentiation factor 88
MYDGF	Myeloid-derived growth factor
NADH	Nicotinamide adenine dinucleotide
NADPH	Nicotinamide adenine dinucleotide phosphate
NDP	Nuclear dot protein
NEAT1	Nuclear paraspeckle assembly transcript 1
NEMO	NF-κB essential modulator
NFATC1	Nuclear factor of activated T cells 1
NFκB	Nuclear factor kappa B
NK cells	Natural killer cells
NLR	NOD-like receptor
NLRP3	NLR family pyrin domain-containing 3
NO	Nitric oxide
NOD	Nucleotide oligomerization domain
NRF2	Nuclear factor erythroid 2-related factor 2
NUDT21	Nudix hydrolase 21
NuRD	Nucleosome remodeling and deacetylase
ODC	Ornithine decarboxylase
OTUB	Ovarian tumor deubiquitinase
P2RY6	Pyrimidinergic receptor P2Y6
PABC	Poly-A binding protein C
PABPN1	Poly-A binding protein nuclear 1
PAMP	Pathogen-associated molecular pattern
PAP	Poly-A polymerase
PAS	Polyadenylation site
PAX3	Paired box 3
PCA	Principal component analysis

PCBP2	Poly rC-binding protein 2
PCF11	Pre-mRNA cleavage complex 2 protein Pcf11
PD1	Programmed cell death 1
pDC	Plasmacytoid dendritic cell
PDCD4	Programmed cell death 4
PFK2	Phosphofructokinase 2
PGC1β	Peroxisome proliferator-activated receptor gamma coactivator 1 beta
PGD	Phosphogluconate dehydrogenase
PHD	Prolyl hydroxylase domain
PI3K	Phosphoinositide 3-kinase
PKC	Protein kinase C
PKR	Protein kinase R
PKM2	Pyruvate kinase M2
POLR2	RNA polymerase 2
Poly I:C	Polyinosinic-polycytidylic acid
PP2A	Protein phosphatase 2
rev	Reverse
PRPP	Phosphoribosyl pyrophosphate
PRR	Pattern recognition receptor
PTEN	Phosphatase and tensin homolog
RAC1	Rac family small GTPase 1
RAD23	UV excision repair protein RAD23
RALA	RAS like proto-oncogene A
RBBP6	RB-binding protein 6
RBP	RNA-binding protein
RIG-I	Retinoic acid-inducible gene I
RLR	RIG-I-like receptor
RNA	Ribonucleic acid
RNF	Ring finger protein
ROS	Reactive oxygen species

RPS28B	Ribosomal protein S28B
RRS	Arginyl-tRNA synthetase
RSK	p90 ribosomal S6 kinase
S6K1	Ribosomal protein S6 kinase 1
SAMD4A	Sterile alpha motif domain-containing 4A
SAMHD1	SAM and HD domain-containing deoxynucleoside triphosphate triphosphohydrolase 1
SDH	Succinate dehydrogenase
SGK1	Serum- and glucocorticoid-regulated kinase 1
sgRNA	Single guide RNA
SIRPα	Signal-regulatory protein alpha
SLC15A3	Solute carrier family 15 member 3
SLN11	Schlafen 11
SMARCA4	SWI/SNF-related matrix-associated actin-dependent regulator of chromatin subfamily A member 4
SNP	Single nucleotide polymorphism
snRNP	Small nuclear ribonucleoprotein
SOCS	Suppressor of cytokine signaling
SOX2	SRY-box transcription factor 2
SR	Serine and arginine-rich
SREBP	Sterol regulatory element binding protein
SRSF	Serine and arginine-rich splicing factor
STAT	Signal transducers and activation of transcription
STAU1	Staufen double-stranded RNA binding protein 1
STING	Stimulator of interferon response cGAMP interactor 1
SU	Short 3’-UTR
SYMPK	Symplekin
TAB	TAK1-binding protein
TAK1	TGF-β-activated-kinase
TBK1	TANK-binding kinase 1

TCA cycle	Tricarboxylic acid cycle
TDP43	TAR DNA-binding protein 43
TGEV	Transmissible gastroenteritis coronavirus
TGF-β	Transforming growth factor beta
TIAR1	RRM domain-containing protein
TIMM44	Translocase of inner mitochondrial membrane 44
TIR domain	Toll/Interleukin-1 receptor domain
TIS11B	Butyrate response factor 1
TLR	Toll-like receptor
TNFα	Tumor necrosis factor alpha
TOM70A	Translocase of outer membrane 70A
TOP	Terminal oligopyrimidine
TRAF	TNF receptor-associated factor
TRAM	TRIF-related adaptor molecule
TRIF	TIR-domain-containing adaptor inducing IFNβ
TRIM	Tripartite motif-containing
tRNA	Transfer RNA
TSC	Tuberous sclerosis complex
TSPAN13	Tetraspanin 13
TYK2	Tyrosine kinase 2
U1A	U1 small nuclear ribonucleoprotein A
UBXN1	UBX domain protein 1
UDP-GlcNAc	Uridine diphosphate N-acetylglucosamine
ULK1	Unc-51-like autophagy activating kinase 1
UNC93B1	Unc-93 homolog B1
USP18	Ubiquitin-specific peptidase 18
UTR	Untranslated region
VHL	Von Hippel-Lindau disease tumor suppressor
WDR33	WD repeat domain 33

List of Tables

List of Figures

Abstract

Interferon signaling is one of the most important mechanisms shaping innate immune responses and needs to be tightly regulated to successfully fight infections and modulate immune responses while avoiding toxicity.

Type I interferons (IFNs) have been shown to induce multiple transcriptional, translational and metabolic changes. The global response of murine and human macrophages to IFNβ stimulation was characterized in this study using multi-omics strategies. These analyses gave insight into a complex regulatory network of transcripts, proteins and metabolites that results in global reprogramming of the cell.

Post-transcriptional gene regulation is an important component of this network and is centered around 3'-untranslated regions (3'-UTRs), regions heavily targeted by miRNAs and harboring binding sites for many RNA-binding proteins. Poly-A-tail sequencing (PAT-seq) experiments revealed that many transcripts expressed shortened 3'-UTRs in response to IFNβ, a result of changed alternative polyadenylation (APA) patterns.

APA and changed 3'-UTR lengths are emerging fields of broad importance in physiological and pathological processes that are only starting to be explored. Differences in APA patterns and their regulation have not previously been studied in context of IFN.

Recent publications have described a scaffold-like role for 3'-UTRs that facilitates the formation of different protein complexes depending on 3'-UTR length, which can affect localization and function. This unique regulatory mechanism was investigated for two IFNβ-regulated transcripts with shortened 3'-UTRs, *EIF4EBP2* and *MAVS*. 3'-UTR-dependent protein-protein interactions were identified by mass spectrometry using tagged overexpression constructs encoding the different transcript isoforms.

This study describes a new aspect of IFN signaling and a novel layer of regulation through genes that are not part of the typical and well-characterized IFN transcriptional response. It shows how differential expression of distinct 3'-UTR transcript isoforms influences macrophage innate immune responses.

Declaration

The work that is presented in this thesis was conducted at The University of Melbourne and The Rheinische Friedrich-Wilhelms-Universität Bonn and in the laboratories of Professor Paul Hertzog (Hudson Institute of Medical Research, Melbourne) and Professor Eicke Latz (Institute of Innate Immunity, Bonn). I was was supported by the Melbourne International Research Scholarship and the Melbourne International Fee Remission Scholarship.

This is to certify that

I. the thesis comprises only my original work towards the PhD except where indicated in the Preface,
II. due acknowledgement has been made in the text to all other material used,
III. the thesis is less than 100,000 words in length, exclusive of tables, maps, bibliographies and appendices.

Sarah Straub

Preface

I acknowledge the important contributions of others to experiments presented herein.

Chapter 3

PAT-seq library preparation and analysis with the tail tools pipeline was performed by Dr Paul Harrison and Dr Angavai Swaminathan from A/Prof. Traude Beilharz's group.

Metabolite sample measurement and analysis in IDEOM was performed by Dr Dovile Anderson and A/Prof. Darren Creek from the Monash Proteomics & Metabolomics Facility.

Proteomics and HITS-CLIP data was generated and analyzed by A/Prof. Michelle Tate, Dr Sam Forster, Dr Jamie Gearing, Dr Nathan Croft and A/Prof. Kate Jeffrey prior to this thesis.

Chapter 4

The plasmid containing the MAVS 3'-UTR used to clone constructs for this project was a kind gift from Prof. Yong-Gang Yao's group.

Co-IP sample measurement and MaxQuant analysis was performed by Iresha Hanchapola and A/Prof. Ralf Schittenhelm from the Monash Proteomics & Metabolomics Facility.

Acknowledgements

Many people have supported me over the course of my PhD and contributed to its completion. I want to thank you wholeheartedly; this would not have been possible without your advice, assistance and the time you took to listen!

I am very grateful to my supervisors Prof. Paul Hertzog and Prof. Eicke Latz for giving me the opportunity to work in their labs and for the freedom to pursue the aspects of the project that most interested me. Thank you for your positivity, patience and encouragement, your enthusiasm for research is contagious!

I would like to thank Dr Jamie Gearing, who has helped with almost all aspects of my PhD and became a good friend in the process. Thank you for spending much of your time at the beginning of my PhD teaching me Bioinformatics and improving many a script. Your attention to detail, suggestions and feedback on experimental plans were really important. I am very grateful that you always made time for me whenever I needed it and supported me throughout everything!

Thank you to A/Prof Sammy Bedoui and Dr Dominic De Nardo. Your advice and assistance as well as your help with administrative aspects of my PhD completion at the University of Melbourne were vital.

Navigating the PhD requirements of two Universities and two countries is exceptionally challenging and would not have been possible without the support and immense organizational work done by Dr Marie Greyer in Melbourne and Lucie Delforge and Sandra Rathmann in Bonn. I am incredibly grateful for your assistance!

Moving my project from Australia to Germany and back was quite challenging and I am very thankful to Fraser Duthie, Rainer Stahl and Dr James Stunden, who have helped me tremendously with their expertise in molecular cloning and NanoString sample preparations, and by showing me my way around a new lab.

Having access to different technologies and methods was essential for the completion of my project, and I am very grateful to all my collaborators for lending me their expertise and helping me with specialized aspects of sample preparation, measurements and data analysis. Dr Dovile Anderson, A/Prof. Darren Creek, Iresha Hanchapola and A/Prof. Ralf Schittenhelm are metabolomics and proteomics experts and assisted me with sample measurements and data analysis. Dr Angavai Swaminathan, Dr Paul Harrison and A/Prof. Traude Beilharz developed and performed a specialized RNA-sequencing technique on my samples that was essential to the investigations of 3'-UTRs. Lastly, having access to previous work by A/Prof. Michelle Tate, Dr Sam Forster, Dr Nathan Croft and A/Prof. Kate Jeffrey was another important aspect of my analyses. A big thank you to all of you!

I am very grateful to all members of the Hertzog and Latz labs, who have always listened to the presentations of my latest results and analyses, made helpful suggestions and had coffee breaks with me to stay sane. I am especially thankful to Antony Matthews, who made and purified all of the recombinant mouse IFNβ used in this study and helped me with many odds and ends of experiments throughout my PhD. I would also like to thank all members of the Centre for Innate Immunity and Infectious Disease at the Hudson Institute for their support, feedback and remarkable willingness to collaborate.

Last, but certainly not least, I want to thank my family, friends and fellow PhD students. There is no way to quantify or describe your contribution to my thesis. Without your encouragement and support, I could not have moved my life across the world a few times and finished my PhD without losing every last bit of my sanity.

An meine Familie und Freunde in Deutschland, die trotz Zeitverschiebung zu jeder Zeit immer nur einen Anruf entfernt waren und mich ohne Einwände unterstützt haben. Ohne euch hätte ich das nicht geschafft!

To all of the amazing people I have met in Australia, thank you for going on adventures with me, whether it was to the local café or far-away places. Here is to many more! Thank you for making me fall in love with rock climbing and showing me many amazing and hidden places around Australia. A special thank you to Nathan, who gifted me his climbing rope a few years ago: it has quite literally become my lifeline.

Thank you to everyone for making my life full and exciting and balancing the time spent on my PhD!

Publications

Alharbi, AS, Garcin, AJ, Lennox, KA, Pradeloux, S, Wong, C, **Straub, S**, Valentin, R, Pepin, G, Li, HM, Nold, MF, Nold-Petry, CA, Behlke, MA & Gantier, MP 2020, 'Rational design of antisense oligonucleotides modulating the activity of TLR7/8 agonists', *Nucleic Acids Res*, vol. 48, no. 13, pp. 7052-6 https://doi.org/10.1093/nar/gkaa523

Chapter 1: Introduction

Over the course of evolution, multicellular organisms have developed defense mechanisms against infectious agents, which evolved into the innate immune system (Buchmann 2014). The broad response of innate immune cells triggered upon detection of different pathogens is very rapid and activates cells of the adaptive immune system, which developed in higher vertebrates and is highly specific to each pathogen (Flajnik & Kasahara 2010). Innate immune cells include a large variety of cell types, such as monocytes, macrophages, dendritic cells (DCs), natural killer (NK) cells and granulocytes, which can reside in different tissues or circulate in the bloodstream (Fig. 1). Their function in immunity is dependent on communication and interaction with other tissues and cells, which is why cytokines, immunoregulatory messenger molecules such as interferons (IFNs), have evolved (Striz et al. 2014).

1.1 Macrophages

Some of the most important leukocytes in the innate immune response are macrophages, which secrete large amounts of type I IFNs and other cytokines in response to the detection of pathogens. These mononuclear phagocytes were first discovered by Élie Metchnikoff in the 19th century (Gordon 2016).

1.1.1 Macrophage Development

Macrophages are the first immune cells in developing vertebrates. They are produced during early gestation and proliferate in the embryonic yolk sac (Samokhvalov 2014) (Fig. 1). This developmental stage is called primitive hematopoiesis and gives rise to hematopoietic stem cells (HSCs), which function

as a “hematopoietic organ” in the fetal liver and initiate immune cell lineages until traditional bone marrow HSCs develop during the perinatal period (Orkin & Zon 2008).

Macrophages derived from the yolk sac and fetal liver HSCs have distinct surface-marker expression patterns, which allow differentiation of the two populations, but is largely lost during later development (Schulz et al. 2012; Yona et al. 2013)

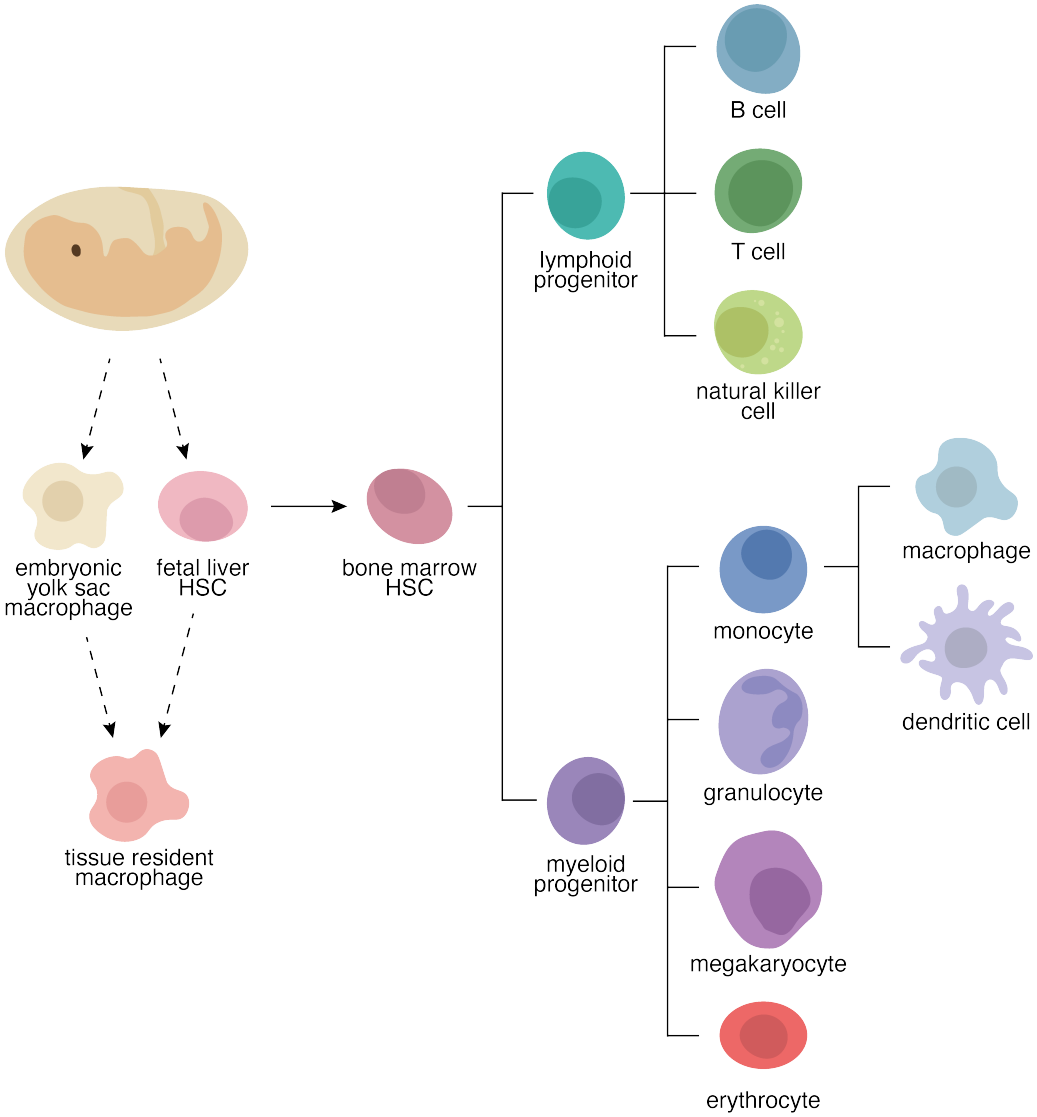

Figure 1: Immune cell lineages. Some tissue resident macrophages are derived from the yolk sac and fetal liver HSCs, while the majority of adult macrophages as well as other immune cells develop from bone marrow HSCs. Lymphoid progenitors give rise to B, T and NK cells, while myeloid progenitors differentiate into erythrocytes, megakaryocytes, granulocytes, macrophages and DCs (HSC: hematopoietic stem cell; NK cell: natural killer cell; DC: dendritic cell).

Most tissue-resident macrophages in adult organisms are derived from the embryonic yolk sac and self-renew independently of circulating monocytes (Hashimoto et al. 2013; Yona et al. 2013). They are seeded before birth and adopt tissue-specific functions during development of the corresponding organ (Gautier et al. 2012; Gosselin et al. 2014). Monocytes, on the other hand, are derived from myeloid progenitor cells, which stem from bone marrow HSCs (Fogg et al. 2006). These monocytes can circulate and differentiate into dendritic cells and macrophages that can settle in different tissues alongside embryo-derived macrophages and mirror their phenotype (van de Laar et al. 2016; Varol et al. 2015). Restricted sets of transcription factors and signaling pathways, such as nuclear factor of activated T cells 1 (NFATC1) in osteoclast differentiation and transforming growth factor beta (TGF-β) signaling in Langerhans cells, are crucial in deciding tissue macrophage fates by inducing expression of specific effector proteins (Kaplan et al. 2007; Takayanagi et al. 2002). Tissue macrophage differentiation is further influenced by exposure to characteristic metabolites in the tissue microenvironment, like heme or retinoic acid, as well as interactions with other cells (Buechler et al. 2019; Haldar et al. 2014). All of these factors lead to the development of a diverse repertoire of macrophages, restricted to different organs and tissues, that have well-known specialized and optimized functions, which contribute to pathogen clearance.

1.1.2 Macrophage Function

Sensing of molecular patterns associated with pathogens (PAMPs) or cellular damage (DAMPs) by pattern recognition receptors (PRRs), a diverse family of receptors expressed across different cellular compartments, is one of the main mechanisms initiating macrophage activity (Herre et al. 2004; Ishikawa et al. 2009; Kobayashi et al. 2007; Taylor et al. 2005; van Liempt et al. 2006). PRR families include toll-like receptors (TLRs), NOD-like receptors (NLRs), cyclic GMP-AMP synthase (cGAS) and RIG-I-like receptors (RLRs) (Amarante-Mendes et al. 2018; Taylor et al. 2005).

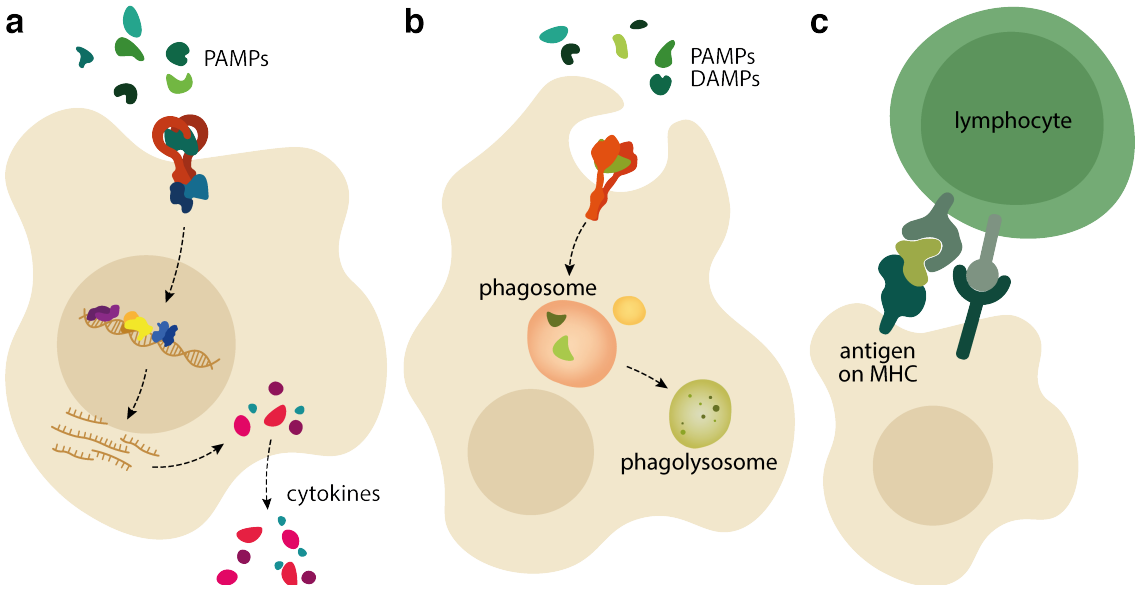

Figure 2: Common macrophage functions. Macrophages can a) produce a variety of cytokines in response to different PAMPs b) phagocytose and degrade different PAMPs and DAMPs and c) present antigens on MHC molecules to lymphocytes.

Ligand binding leads to a variety of downstream effects like phagocytic clearance of pathogens and of infected or dead cells and debris, to the presentation of antigens on major histocompatibility complex (MHC) molecules, which activate lymphocytes, or to the expression and release of different cytokines, as seen in Figure 2 (Gordon & Martinez-Pomares 2017; Muntjewerff et al. 2020; Uribe-Querol & Rosales 2020).

1.1.2.1 Cytokine Production

Cytokines and chemokines are key effectors produced upon PRR stimulation (Fig. 2a). They are small molecules that spread important messages between cells to induce local and systemic responses, like tissue repair and inflammation, by modulating recipient cells' proliferative, inflammatory and migratory potential (Dinarello 2007). Different cytokines are produced in response to different stimuli and vary between macrophage subtypes (Arango Duque & Descoteaux 2014). Some of the more prominent cytokines released by pro-inflammatory macrophages are tumor necrosis factor alpha (TNFα), interleukin 1β (IL1β), IL6, IL12 and type I IFNs. TNFα signaling activates nuclear factor kappa B (NFκB),

which leads to the secretion of chemokines that attract cells to sites of inflammation and initiates acute phase responses (Carswell et al. 1975; Griffin et al. 2012). IL1β has similar functions and also acts on cluster of differentiation 4+ (CD4+) T cells to induce their expansion and differentiation (Ben-Sasson et al. 2009; Carmi et al. 2009). IL6 attracts monocytes to sites of inflammation and induces differentiation of B and CD8+ T cells. IL12 can activate CD8+ cells and promotes IFNγ production (Dorman & Holland 2000; Hurst et al. 2001; Nishimoto & Kishimoto 2004). IFNs are important regulators of the innate immune response and the expression and function of one IFN family, type I IFNs, is discussed in more detail below.

The two key cytokines released by anti-inflammatory macrophages, IL10 and TGF-β, suppress the production and effects of pro-inflammatory molecules (Defrance et al. 1992). TGF-β also inhibits CD4+ and CD8+ T cell activation and instead promotes regulatory T cells functions, while IL10 prevents macrophage antigen presentation and subsequent lymphocyte activation (Chadban et al. 1998; Fiorentino et al. 1991; Travis & Sheppard 2014). Many other cytokines can be produced by different macrophage subtypes depending on their activation status, biological niche and repertoire of PRRs, but all of them are tightly regulated to clear infections while preventing chronic inflammation and tissue damage (Arango Duque & Descoteaux 2014).

1.1.2.2 Phagocytosis

Phagocytosis describes the recognition of different molecules by phagocytic receptors, another family of PRRs, subsequent particle internalization and enzymatic degradation in a newly formed phagolysosome (Fig. 2b) (Herre et al. 2004; Ishikawa et al. 2009; Kobayashi et al. 2007; Levin et al. 2016; Li & Underhill 2020; van Liempt et al. 2006). Recent research showed that TLRs can promote phagocytosis through physical interaction with phagocytic receptors and by enhancing their affinity for different ligands (Caron et al. 2000; Doyle et al. 2004). One of the first receptors to be investigated in detail was the macrophage mannose receptor, which is located on the cell surface and recognizes different

glycoproteins (Ezekowitz et al. 1990; Stahl et al. 1978). It is a C-type lectin, which make up the non-opsonic class of receptors along with lectin-like recognition molecules and scavenger receptor (Canton et al. 2013; Li & Underhill 2020). Non-opsonic receptors can recognize patterns on particles to be engulfed directly, while opsonic receptors, such as Fc and complement receptors, recognize objects bound by opsonins, cellular proteins like antibodies and fibronectin (Dustin 2016; Flannagan et al. 2012; Nimmerjahn & Ravetch 2010). Ligand binding activates signaling cascades that lead to remodelling of membrane lipids and the actin cytoskeleton to surround the particle and form a phagosome (Freeman et al. 2016; Freeman & Grinstein 2014; Scott et al. 2005). The phagosome matures to a phagolysosome through fusion and fission with endosomes and lysosomes (Fig. 2b) (Christoforidis et al. 1999; Desjardins 1995; Rink et al. 2005). These phagolysosomes produce reactive oxygen species (ROS), which can form microbicidal substances like hypochlorous acid, and they contain enzymes with hydrolase activity, such as proteases, lysozymes and lipases, that contribute to the degradation of the ingested particle (Kinchen & Ravichandran 2008; Minakami & Sumimotoa 2006). Other cells can inhibit phagocytosis through expression of molecular surface markers such as CD47 (Morrissey et al. 2020). CD47 interacts with the receptor signal-regulatory protein alpha (SIRPα) on phagocytic cells to block their activity and will be discussed in more detail in later parts of this study (Morrissey et al. 2020).

1.1.2.3 Antigen Presentation

Specific macrophage subtypes can cross-present antigens derived from phagocytosed particles to activate adaptive immune responses (Fig. 2c). Proteins can be processed via a cytosolic or a vacuolar pathway. Cytosolic processing requires export of the phagocytosed material to the cytoplasm, its proteasomal degradation and transport to the endoplasmic reticulum (ER) or endosomes to be loaded onto MHC-I molecules (Cruz et al. 2017). The cytosolic antigen presentation pathway is used by splenic red pulp macrophages, while the majority of other macrophage subtypes use the vacuolar pathway (Asano et al.

2011; Enders et al. 2020; Norbury et al. 1995; Schliehe et al. 2011; Soudja et al. 2012; Tang-Huau et al. 2018; Thornley et al. 2014). During the vacuolar antigen processing pathway, antigens and proteins particles are degraded by proteases in the phagolysosome and the resulting peptides directly loaded onto MHC-I (Blander 2016). These MHC complexes can activate adaptive immune responses upon interaction with a T cell receptor and promote pathogen clearance (Fig. 2c).

1.1.3 Macrophage Activation

Historically, macrophages were thought to be polarized into two phenotypes, pro- or anti-inflammatory, mainly as a result of stimulation with cytokines and other components like lipopolysaccharide (LPS) and IFNγ or IL4 respectively (Xue et al. 2014). However, growing investigations of different macrophages have shown that many other factors in their respective cellular and metabolic microenvironment influence their activation phenotype, such as metabolites, PRR ligands, cytokines and interactions with other cells. Researchers concluded that inflammatory potential is a spectrum from pro- to anti-inflammatory, which is part of a multidimensional macrophage activation phenotype (Fig. 3). The position of different macrophages on this spectrum is determined by their transcription factor activity and resulting gene expression profile, cytokine and chemokine secretion, as well as their use of metabolic processes (Ginhoux et al. 2016). The previously used M1 and M2 nomenclature describes two of many macrophage activation phenotypes in this spectrum model, which sit on the pro- and anti-inflammatory ends of the spectrum respectively (Fig. 3).

The development of pro-inflammatory characteristics in macrophages has been shown to be dependent on signal transducers and activation of transcription 1 (STAT1) and interferon regulatory factor 5 (IRF5) (Krausgruber et al. 2011; Varinou et al. 2003). On the other hand, anti-inflammatory macrophage polarization relies on STAT6 and IRF4 activity (El Chartouni et al. 2010; Satoh et al. 2010; Takeda et al. 1996). The transcriptional programs induced by these and other transcriptional regulators include gene sets related to IFN signaling,

inducible nitric oxide synthase (iNOS) signaling and apoptosis in pro-inflammatory macrophages, while ontologies in anti-inflammatory macrophages relate to fatty acid and serine biosynthesis and integrin signaling (Orecchioni et al. 2019).

These differences in gene expression profiles reflect the functional differences between macrophages at opposite ends of the polarization spectrum and heavily influence the composition of cytokines that are secreted (Anderson & Mosser 2002; Herbst et al. 2011). They also show variation in genes related to metabolic pathways, changes to which are crucial for specific macrophage function and are discussed in more detail below.

Macrophages can be activated by many other cytokines and cytokine combinations that have not been characterized as well as classical pro- and anti-inflammatory phenotypes, including type I IFNs. Current and future research will likely focus on investigating the influence of other factors on macrophage phenotypes, such as the tissue environment, interactions with other immune cells or the extracellular metabolite composition, in order to define aspects of macrophage activation other than inflammatory potential.

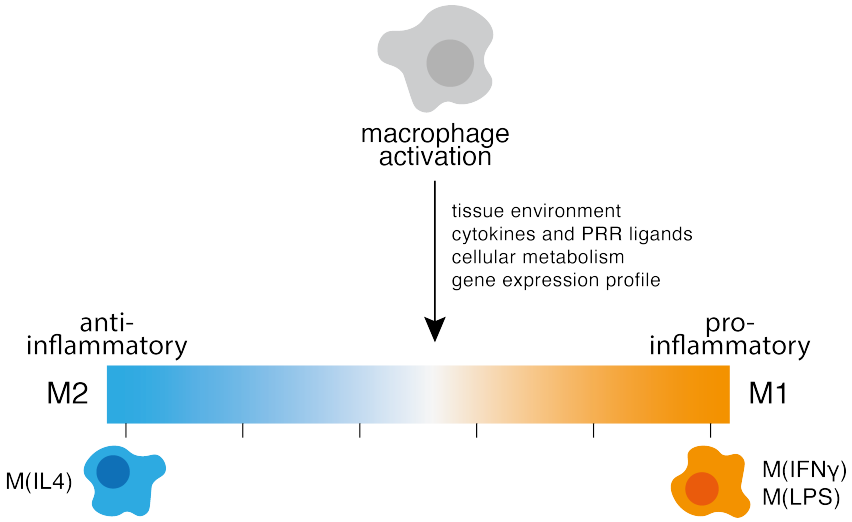

Figure 3: Macrophage activation spectrum. Macrophages can be activated and polarized by cytokines and other environmental stimuli to show varying amounts of inflammatory potential. Pro- (M1) and anti-inflammatory (M2) macrophages polarized by IFNγ and LPS or IL4 respectively sit at the ends of the spectrum.

1.2 Immunometabolism

Immunometabolism is a field of study that has gained momentum over the last 10 years. It followed some early research focusing on the utilization of different metabolic pathways by immune cells to satisfy their high demand for energy and biosynthetic intermediates (Fukuzumi et al. 1996; Newsholme et al. 1986; Oren et al. 1963). Changes to the metabolism can be regulated by extra- and intracellular cues, such as cytokines and signaling pathways, and influence different aspects like cell survival, proliferation and inflammatory properties (Mathis & Shoelson 2011).

The metabolites and pathways described below are examples of metabolic changes induced by pathogens and other stimuli, but also show that the cellular metabolism can influence and mediate functional responses. Many other pathways play similar roles in different settings and their functions in specific immune settings are areas of current research (Fig. 4).

1.2.1 Tricarboxylic Acid Cycle

The tricarboxylic acid (TCA) cycle, sometimes referred to as the Krebs or citric acid cycle, is heavily used by non-proliferative cells. Its components are located in the mitochondrial matrix and produce nicotinamide adenine dinucleotide (NADH) and flavin adenine dinucleotide ($FADH_2$), which can transfer electrons to the electron transport chain for efficient generation of adenosine triphosphate (ATP) and increased oxidative phosphorylation (Martinez-Reyes & Chandel 2020). This pathway is well characterized in macrophages and has been established as one of the key traits distinguishing pro- M1 and anti-inflammatory M2 macrophages (Jha et al. 2015).

The TCA cycle in M1 macrophages on the other hand is impaired, as shown by the accumulation of the intermediates citrate and succinate (Tannahill et al. 2013). The first break in the TCA cycle leading to the accumulation of citrate was shown to be the result of isocitrate dehydrogenase (IDH) downregulation in LPS-

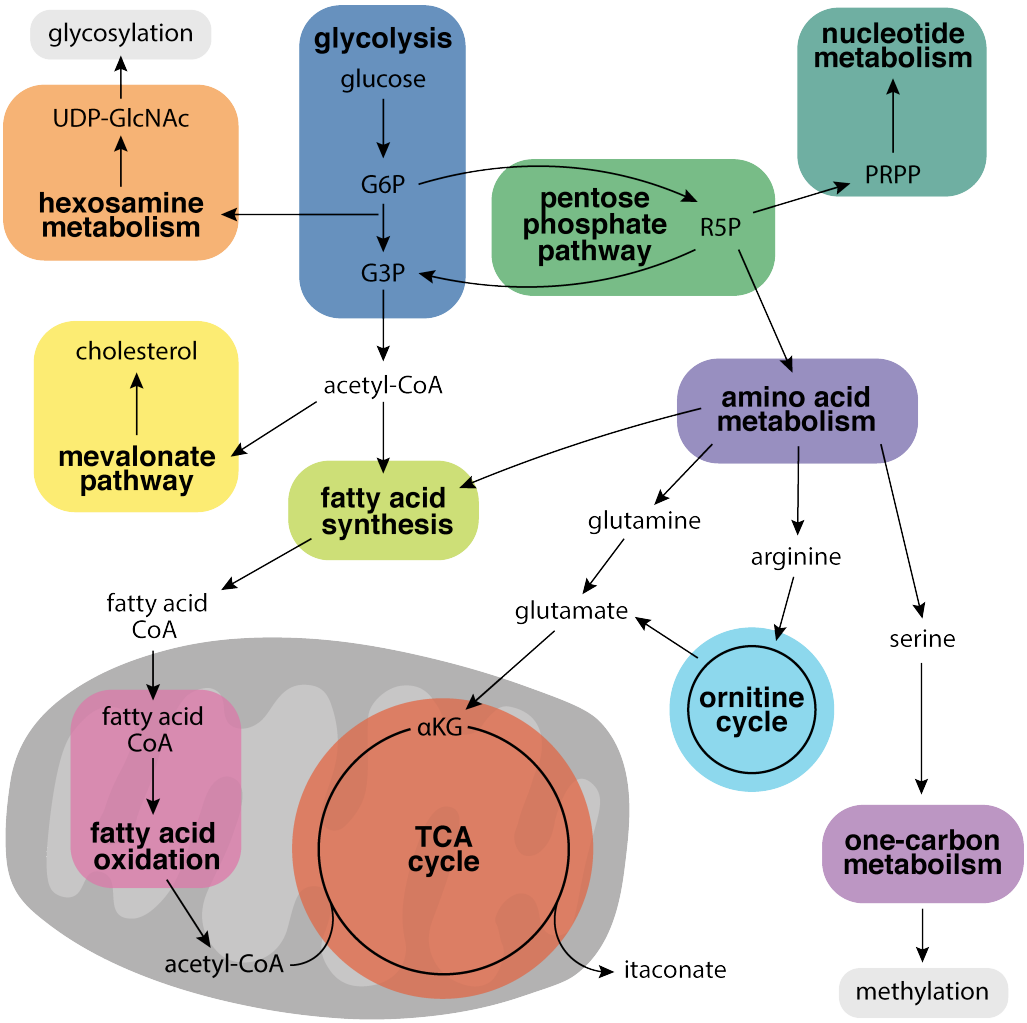

Figure 4: Overview of cellular metabolism. TCA: tricarboxylic acid; PRPP: phosphoribosyl pyrophosphate; G6P: glucose-6-phosphate; G3P: glycerol-3-phosphate; R5P: ribose-5-phosphate; αKG: α-ketoglutarate; CoA: coenzyme A; UDP-GlcNAc: UDP-N-acetyl-galactosamine.

activated macrophages (De Souza et al. 2019). Accumulated citrate can be transported to the cytoplasm by capicua transcriptional repressor (CIC), where it can promote fatty acid synthesis by activating acetyl-coenzyme A (CoA) carboxylase (ACC) and inhibit glycolysis via pyruvate kinase M2 (PKM2) and phosphofructokinase (PFK) 1 and 2 (Infantino et al. 2011; Infantino et al. 2014; Palmieri 2004; Yalcin et al. 2009). It can also be converted to malate and transported back to the mitochondria where it can lead to nitric oxide (NO) generation, described in more detail in a following passage, via an argininosuccinate shunt that is enhanced in M1 macrophages (Hou et al. 2017;

Iacobazzi et al. 2017; Jha et al. 2015; Palmieri 2004). Macrophages activated with LPS, different TLR ligands or IFNs also show increased expression of cis-aconitate decarboxylase (ACOD1; formerly IRG1), an enzyme that converts cis-aconitate, a citrate-isomer, to itaconate (Michelucci et al. 2013; Shin et al. 2011; Strelko et al. 2011).

Itaconate is an immunomodulatory molecule with pro- and anti-inflammatory properties that influences macrophage inflammation through interaction with different enzymes and regulatory proteins. Its anti-inflammatory effects are mediated through NLR family pyrin domain-containing 3 (NLRP3) modification and subsequent inhibition of inflammasome activation as well as activation of the transcriptional regulator nuclear factor erythroid 2-related factor 2 (NRF2), which limits inflammatory responses in macrophages (Hooftman et al. 2020; Mills et al. 2018). NRF2 increases expression of proteins like heme oxygenase 1 (HO1) and enzymes involved in glutathione synthesis, which protect cells from oxidative stress, while inhibiting transcription of pro-inflammatory cytokines like IL6 and IL1β (Hayes & Dinkova-Kostova 2014; Kobayashi et al. 2016). The activation of the transcription factor activating transcription factor 3 (ATF3) by itaconate, on the other hand, promotes the expression of pro-inflammatory cytokines like TNFα, IL6 and IL1β and suppresses type I IFNs (Bambouskova et al. 2018; Gilchrist et al. 2006; Labzin et al. 2015; Zmuda et al. 2010). Itaconate can also inhibit the expression of type I IFNs in response to viral infection, LPS, polyinosinic-polycytidylic acid (poly I:C) and stimulator of interferon response cGAMP interactor 1 (STING) activators in an NRF2-dependent manner (Mills et al. 2018; Olagnier et al. 2018). This may form a regulatory feedback loop, since the induction of ACOD1 expression by LPS and poly I:C can be mediated by IFNs (De Souza et al. 2019; Mills et al. 2018; Naujoks et al. 2016).

Lastly, itaconate has been shown to inhibit succinate dehydrogenase (SDH), which results in a second break in the TCA cycle as mentioned above and leads to the accumulation of succinate (Cordes et al. 2016; Lampropoulou et al. 2016). Accumulated succinate can stabilize hypoxia-inducible factor 1 subunit alpha (HIF1α) through inhibition of prolyl hydroxylase domain proteins (PHD), which increases IL1β production (Tannahill et al. 2013).

1.2.2 Glycolysis

Glycolysis describes processing of glucose taken up by the cell to generate ATP and produce important intermediates, such as NADH, a critical enzyme cofactor. These intermediates feed other pathways such as nucleotide, amino acid and fatty acid synthesis, making glycolysis an important process for cellular growth and increasing cell mass (Fig. 4). Generation of ATP by glycolysis is very inefficient compared to other pathways such as mitochondrial respiration, but it is a pathway that can be very rapidly enhanced through the induction of key enzymes to meet the high energy demands of newly activated immune cells (Jones & Bianchi 2015). Early research has shown that both macrophages and T cells metabolize a lot of glucose and that inhibiting its uptake significantly impairs cellular function, for example phagocytosis in macrophages (Alonso & Nungester 1956; Hamilton et al. 1986; Michl et al. 1976; Newsholme et al. 1986). More recent research revealed that enhanced glycolysis, also called the Warburg effect, is a hallmark of many rapidly activated immune cells, including LPS-activated DCs and macrophages, activated NK cells, B cells and effector T cells (Donnelly et al. 2014; Doughty et al. 2006; Krawczyk et al. 2010; Michalek et al. 2011; Rodriguez-Prados et al. 2010; Vander Heiden et al. 2009). It also showed that this is crucial for cytokine production and phagocytic activity in macrophages and antigen presentation in DCs (Everts et al. 2014; Michl et al. 1976; Shi et al. 2011). It is correlated with increased mechanistic target of rapamycin kinase (mTOR) signaling and negatively affects regulatory T cell homeostasis and lineage stability (Huynh et al. 2015; Wei et al. 2016).

Many cellular signaling pathways can influence glycolysis. The LPS-activated transcription factors HIF1α and NFκB can induce expression of PFK2, a crucial regulator of the pathway (Rodriguez-Prados et al. 2010; Tannahill et al. 2013). Other glycolytic enzymes influenced by LPS activation of DCs and macrophages are hexokinase (HK) 2, which phosphorylates hexoses such as glucose, and PKM2, an enzyme that regulates glycolytic flux and diverts intermediates to other metabolic pathways (Everts et al. 2014; Palsson-McDermott et al. 2015). Other functions of PKM2, independent of its enzymatic activity, include a transcription

factor-like role dependent on interaction with HIF1α, which subsequently induces the expression of other glycolytic enzymes and inflammatory genes like IL1β (Luo et al. 2011; Palsson-McDermott et al. 2015). This HIF1α-induced increase in glycolytic activity is essential for M1 macrophage activation, while it is negligible for M2 polarization (Wang F et al. 2018; Wang et al. 2017). Further connecting glycolysis to macrophage polarization is HK1, an enzyme induced by mTOR signaling (Moon et al. 2015a). It favors M1 polarization through interaction with NLRP3, an inflammasome component that regulates caspase 1 activity and subsequent maturation of the inflammatory cytokine IL1β and induces pyroptotic cell death.

1.2.3 Pentose Phosphate Pathway

The pentose phosphate pathway is heavily used in proliferating cells and shuttles glycolysis intermediates to nucleotide and amino acid biosynthesis pathways (Fig. 4). It also promotes fatty acid synthesis and maintains cellular redox levels through generation of nicotinamide adenine dinucleotide phosphate (NADPH). NADPH processing influences the cellular redox levels: it can be used to generate antioxidants, which prevent excessive tissue damage, and it can be used for ROS production, which help clear infectious agents (Stincone et al. 2015).

The pentose phosphate pathway is crucial for M1 macrophages and its activity is dependent on phosphogluconate dehydrogenase (PGD) (Baardman et al. 2018). Another key enzyme is carbohydrate kinase-like (CARKL), a sedoheptulose kinase that activates the non-oxidative part of the pentose phosphate pathway. CARKL is suppressed in M1 and induced in M2 macrophages and its overexpression impairs M1 polarization (Baardman et al. 2018; Haschemi et al. 2012). Consistent with these findings, other researchers reported that activation of macrophages with LPS leads to elevated flux through the pentose phosphate pathway and interestingly a downstream increase in nucleotide biosynthesis, despite the low proliferation rate of LPS-activated cells (Tannahill et al. 2013).

1.2.4 Fatty Acid Oxidation

The oxidation of fatty acids is an efficient way to produce energy and is mainly used by anti-inflammatory cells like M2 macrophages and cells with an extended life span, such as regulatory and memory T cells. Fatty acids are activated in the cytosol and translocated to the mitochondria, where they are broken down to produce NADH, $FADH_2$ and acetyl-CoA, which promote cellular respiration and other pathways (Fritzen et al. 2020).

In M2 macrophages, fatty acid oxidation is induced by STAT6 and peroxisome proliferator-activated receptor gamma coactivator 1 beta (PGC1β) activity and limits inflammation (Vats et al. 2006). It also suppresses effector T cell polarization and instead increases regulatory T cell generation (Michalek et al. 2011). Consistent with this, fatty acid oxidation is downregulated during effector T cells activation and increased upon programmed cell death 1 (PD1) ligand binding and antigen recognition in memory T cells (Patsoukis et al. 2015; van der Windt et al. 2013; Wang et al. 2011).

Fatty acid oxidation is also needed for type I IFN-induced antiviral responses in plasmacytoid DCs (pDCs) (Wu et al. 2016). Both IFN-activated pDCs and memory T cells take up glucose to synthesize fatty acids and sustain the oxidation pathway, while M2 macrophages rely on the uptake of lipids (Huang et al. 2014; O'Sullivan et al. 2014; Wu et al. 2016).

1.2.5 Fatty Acid Synthesis

The generation of fatty acids used for proliferation and cell growth can be initiated by mTOR-mediated expression of key enzymes, such as fatty acid synthase (FASN) and sterol regulatory element-binding proteins (SREBP) (Porstmann et al. 2008; Yan et al. 2014). Metabolic intermediates from the TCA cycle, glycolysis and the pentose phosphate pathway are used for straight-chain fatty acid synthesis in the cytosol, while additional amino acids with branched chains are

needed for their elongation to branched-chain fatty acids (Rohrig & Schulze 2016).

Fatty acids are synthesized at high rates in response to inflammatory signals like cytokines and LPS (Feingold et al. 2012; Posokhova et al. 2008). They are crucial for phagocytic differentiation of monocytes induced by macrophage colony-stimulating factor (M-CSF) and support the development of pro-inflammatory phenotypes, for example through NLRP3 inflammasome activation (Ecker et al. 2010; Moon et al. 2015b). The accumulation of unsaturated fatty acids like linoleic acid, arachidonic acid or oleic acid in the cytoplasm has also been connected to the formation of foam cells, a specific type of lipid-laden macrophage, and their increased production of IL1α (Carpenter et al. 1995; Freigang et al. 2013). In accordance with this, preventing accumulation of fatty acids in the cytoplasm through increased expression of the mitochondrial transport protein carnitine palmitoyltransferase 1A (CPT1A) lowers the inflammatory potential and cytokine production of macrophage cell lines (Malandrino et al. 2015).

Similarly, fatty acids are essential for proliferation and activation of T and B cells in response to antigen binding, as well as subsequent development of some antigen-specific T cell subtypes (Berod et al. 2014; Chen et al. 1975; Dufort et al. 2014; Lee et al. 2014).

1.2.6 Amino Acid Metabolism

Amino acids are a diverse class of molecules with functions in many metabolic pathways like the TCA cycle of fatty acid synthesis. Since they are protein building blocks, they are closely linked to anabolic growth and proliferation, which is driven by mTOR in response to amino acid level sensing (Takahara et al. 2020). The amino acids glutamine and arginine have been shown to be especially important during macrophage polarization; both have very distinct roles in M1 and M2 metabolism and are crucial contributors to either phenotype (Rath et al. 2014). Arginine can be directed to the nitric oxide synthesis or arginase pathway, which contributes to the development of an M1 or M2 phenotype in macrophages respectively (Rath et al. 2014). The breakdown of arginine to polyamines initiated

by arginase 1 (ARG1), an enzyme overexpressed in M2 macrophages, and ornithine decarboxylase (ODC) promotes tissue repair and cell growth (Albina et al. 1988; Takele et al. 2013). The anti-inflammatory environment also leads to a more reduced inflammatory potential of T cells, which is associated with impaired pathogen clearance (Pesce et al. 2009). Furthermore, ODC has been shown to modify chromatin, which impairs M1 polarization and inflammatory responses (Hardbower et al. 2017).

On the other hand, conversion of arginine to NO by the enzyme iNOS potentiates inflammatory responses in macrophages. NO reacts with ROS to produce different antimicrobial species, which are needed for pathogen clearance (MacMicking et al. 1997; MacMicking et al. 1995; Schairer et al. 2012). Increased NO production also leads to mitochondrial dysfunction, which prevents repolarization of M1 to M2 phenotypes when exposed to IL4 (Clementi et al. 1998; Van den Bossche et al. 2016). More recent research has shown that NO accumulation in M1 macrophages ultimately leads to the arrest of mitochondrial respiration through the loss of electron transport chain complexes (Palmieri et al. 2020).

Interestingly, NO levels can also suppress NLRP3-mediated release of IL1β and downregulate systemic inflammation, a process influenced by type I IFN-induced iNOS expression (Mao et al. 2013; Mishra et al. 2013).

Another amino acid that serves different purposes in differentially activated macrophages is glutamine. It has been shown to promote arginine synthesis and influence nitric oxide levels, as well as induce production of IL1β in LPS-activated macrophages (Bellows & Jaffe 1999; Murphy & Newsholme 1998; Wallace & Keast 1992). Further research showed that glutamine is dispensable for the development of M1 phenotypes, while its flux into the TCA cycle and catabolism to α-ketoglutarate is required for M2 polarization (Jha et al. 2015; Nelson et al. 2018). Glutamine-derived α-ketoglutarate contributes to the development of an M2 phenotype in macrophages by demethylating lysine 27 of histone 3 (H3K27) in specific promotor regions, which activates gene expression and can alter the cellular chromatin structure and influence epigenetic reprogramming (Liu PS et al. 2017).

Many other amino acids can influence cellular function and modulate immune response (Andreou et al. 2020; Boulland et al. 2007; Hoffman & Han 2020; Jain et al. 2012; Ma et al. 2017; Wu Q et al. 2020; Yu et al. 2019). Their roles in immunometabolism and interactions with key pathways is only starting to be explored and is likely variable across cell types and activation stimuli.

Metabolic pathways are highly interconnected and their role in antiviral immune response is a rapidly growing field in medical research (Fig. 4). Only a selection of metabolic processes that are most relevant to macrophage activation and type I IFNs have been discussed here, but many different aspects more relevant to other cell types of different physiological contexts have been described in literature (Chapman et al. 2020; Jellusova 2020; Kumar & Dikshit 2019). A crucial element of current investigations is the connection between metabolic processes and well-characterized mechanisms in immune responses, such as transcriptional activation and cytokine release.

1.3 Interferons

IFNs are important signaling molecules mediating innate immune responses and can be produced by almost all cell types (McNab et al. 2015). The first mention of an inhibitory factor, which was later reported to be an IFN, was made in 1954 by Nagano and Kojima (Nagano & Kojima 1954; Watanabe 2004). However, the first to isolate and characterize IFNs in 1957 were Isaacs and Lindemann, who discovered them in chick chorio-allantoic membrane fragments in response to incubation with heat-inactivated influenza virus (Isaacs & Lindenmann 1957). From there, many other IFN proteins were discovered and have been classified into type I, type II and type III IFNs based on their structural differences and respective receptors (Ealick et al. 1991; Gad et al. 2009; Karpusas et al. 1997; Randal & Kossiakoff 2001).

Type I IFNs are the largest of the groups and to date include various IFNα subtypes, IFNβ, IFNε, IFNκ and IFNω, as well as additional subtypes restricted to different species. They signal through IFN alpha receptor (IFNAR), a heterodimer composed of IFNAR1 and IFNAR2 (de Weerd et al. 2007). The only

type II IFN is the structurally distinct IFNγ, which signals through IFN gamma receptor (IFNGR), which is also made up of two subunits (Farrar & Schreiber 1993). Four IFNλ molecules have been identified more recently and were classified as type III IFNs. They share structural similarities with IL10 and signal through a complex formed by IFN lamba receptor 1 (IFNLR1) and IL10 receptor subunit beta (IL10RB) (Gad et al. 2009; Kotenko et al. 2003; Prokunina-Olsson et al. 2013). The expression of hundreds or thousands of genes is regulated by IFNs and while some are common among all types of IFNs, others are distinct to one type or even one IFN (Hertzog & Williams 2013; Schoggins et al. 2011).

1.3.1 Type I IFNs

Type I and type III IFNs can induce related cellular responses, likely due to the similarity in their signaling pathways. Both IFNAR2 and IFNLR1 interact with Janus kinase 1 (JAK1), while IFNAR1 and IL10RB associate with tyrosine kinase 2 (TYK2) (Ferrao & Lupardus 2017; Mendoza et al. 2017). Subsequently, both receptor complexes activate JAK-STAT signaling, which includes the formation of the IFN-stimulated gene factor 3 (ISGF3) complex, mitogen-activated protein (MAP) kinase signaling and phosphoinositide 3-kinase (PI3K)-mediated responses (Fig. 6) (Prokunina-Olsson 2019; Zhou et al. 2007). However, type I and III IFNs appear to play different physiological roles, since IFNλ signaling is mostly restricted to epithelial cells, like those in the gut and lung, and some hematopoietic cells, such as DCs, likely due to limited expression of IFNLR1 (Coccia et al. 2004; Mordstein et al. 2010; Sommereyns et al. 2008).

The expression of some type I IFNs is restricted to specific tissues as well. IFNε and IFNκ are mainly expressed in the female reproductive tract and the skin respectively (Fung et al. 2013; LaFleur et al. 2001). Unlike most type I IFNs, which are produced in response to infection, IFNε is constitutively expressed in the female reproductive tract and is crucial for local protection from viral and bacterial infection (Couret et al. 2017; Stifter et al. 2018). The other type I IFNs are not restricted to different tissues and interestingly have a much higher receptor

affinity than IFNε, IFNκ and the IFNλs (Harris et al. 2018; Lavoie et al. 2011; Mendoza et al. 2017). IFNα and IFNβ are the most extensively studied type I IFNs to date and while their physiological roles appear redundant, structural analyses have highlighted important differences. IFNβ but not IFNα can induce a distinct response via its receptor subunit IFNAR1 independently of IFNAR2, a mechanism that has initially been observed in murine cells (de Weerd et al. 2013) and is currently under investigation in human cells (de Weerd et al. unpublished). Type I IFN responses are highly conserved across species, yet different affinities of murine and human IFNβ for IFNAR1 and IFNAR2 suggest there may be species-specific responses. Murine IFNβ has a ~100-fold higher affinity for IFNAR1 than for IFNAR2, while human IFNβ shows the reverse, with a ~500-fold higher affinity for IFNAR2 (Jaks et al. 2007; Stifter et al. 2018). This is likely the result of structural differences between human and murine IFNβ, and similar structural differences have been observed for most type I IFNs across different mammalian species (de Weerd et al. 2013; Hughes 1995). Responses to IFNβ in murine and human macrophages are the focus of this study.

1.4 Type I IFN Expression

Type I IFNs are produced by most cell types, usually in response to PRR activation by PAMPs (Fig. 5). As mentioned previously, this class of receptors consists of multiple families that are expressed in different cellular compartments and recognize different types of ligands to match the location of pathogens throughout their life cycle (Amarante-Mendes et al. 2018).

1.4.1 TLR-Mediated Type I IFN Expression

TLRs are located on the cell surface and in endosomes where they recognize a large variety of PAMPs, such as lipids and foreign nucleic acids, including LPS, as well as synthetic ligands like poly I:C, a mimic of viral ribonucleic acid (RNA). Different TLRs recognize different types of ligands, but share many intracellular

signaling components (Kawasaki & Kawai 2014). All known hetero- and homodimeric TLRs, except TLR3 homodimers, interact with the adaptor myeloid differentiation factor 88 (MYD88), which can recruit IL1 receptor-associated kinase 1 (IRAK1) and 4 (Cao et al. 1996; Li et al. 2002; Medzhitov et al. 1998). Upon phosphorylation, IRAK1 dissociates and activates TNF receptor-associated factor 6 (TRAF6), which activates the NFκB and MAP kinase signaling cascades as described below. TRAF6 as well as TRAF3 can also be activated by TIR-domain-containing adaptor inducing IFNβ (TRIF). TRIF can interact with TLR3 directly and indirectly with TLR4 via the adaptor protein TRIF-related adaptor molecule (TRAM) and activates IRFs and subsequent type I IFN expression as described below. (Hacker et al. 2006; Oshiumi et al. 2003a; Oshiumi et al. 2003b).

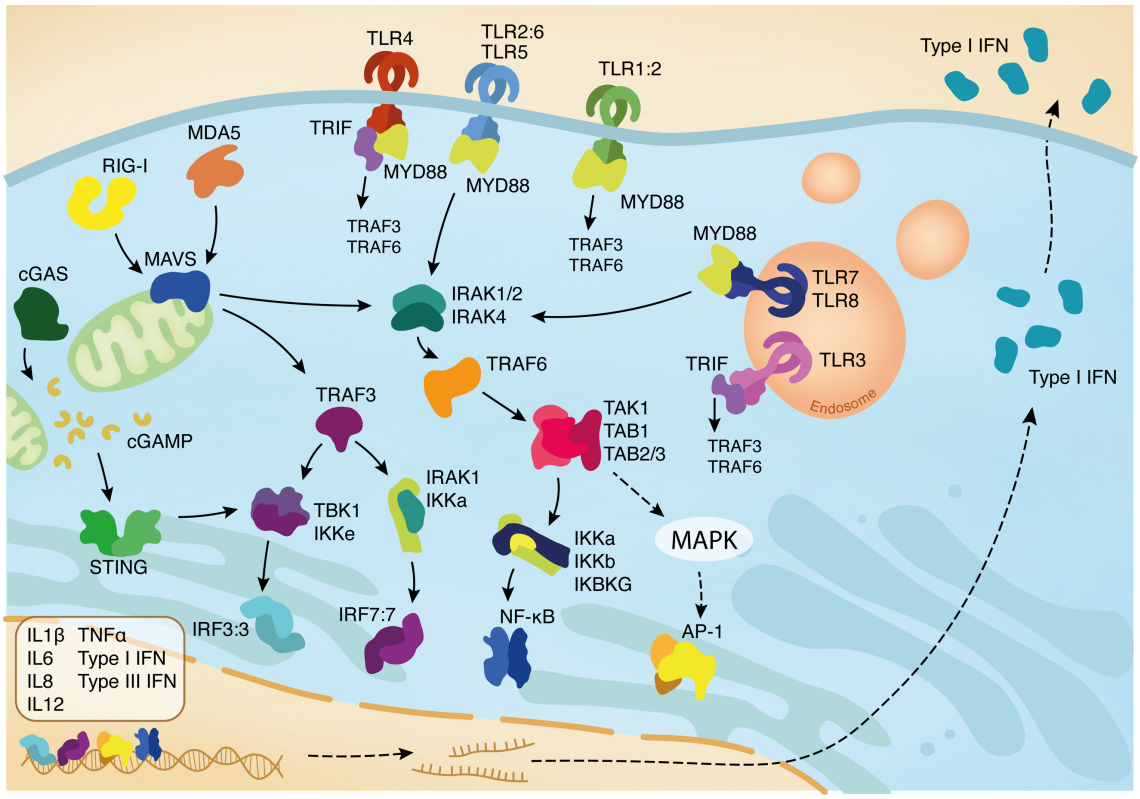

Figure 5: TLR, RLR and cGAS signaling. These PRRs activate type I and type III IFN expression via IRFs and pro-inflammatory cytokine production via NFκB and AP1.

1.4.2 RLR-Mediated Type I IFN Expression

RLRs are important cytosolic receptors that induce type I IFN expression upon binding of double-stranded RNA (Gitlin et al. 2006; Yoneyama et al. 2004). Three RLRs have been identified to date, but only two, retinoic acid-inducible gene I (RIG-I) and melanoma differentiation-associated gene 5 (MDA5), contain caspase recruitment domains (CARDs), which are crucial for signal transduction upon RNA binding (Kowalinski et al. 2011). The third RLR family member lacking these domains, laboratory of genetics and physiology 2 (LGP2), regulates signaling activity of RIG-I and MDA5: sensing of viral RNA by RIG-I is inhibited, while MDA5 activity is promoted (Bruns et al. 2014; Rothenfusser et al. 2005). Ligand binding to RLRs induces a conformational change, which exposes their CARDs and enables their oligomerization (Kowalinski et al. 2011). CARD oligomerization can occur in a spontaneous, concentration-dependent manner, after their activation by K63-linked ubiquitin or after ATP-dependent RNA-binding domain filament formation (Gack et al. 2007; Patel et al. 2013; Peisley et al. 2013; Wu et al. 2013). RLR-CARD oligomers can directly interact with the CARD of mitochondrial antiviral-signaling protein (MAVS) (Peisley et al. 2013; Wu et al. 2013).

MAVS is a membrane-anchored protein, reported to localize to the outer mitochondrial membrane, mitochondrial-associated endoplasmic reticulum membranes (MAMs) and peroxisomes, that aggregates and forms filaments upon interaction with RLR-CARDs (Dixit et al. 2010; Horner et al. 2011; Hou et al. 2011; Meylan et al. 2005; Seth et al. 2005). Subsequent MAVS signaling is highly influenced by its ubiquitination and phosphorylation status, which is regulated by a large number of enzymes and may be influenced by its subcellular location (Dixit et al. 2010; Odendall et al. 2014; Ren et al. 2020). Aggregated MAVS can interact with different TRAFs, which mediate downstream signaling. Interaction with TRAF6 promotes activation of the TANK-binding kinase 1 (TBK1) - inhibitor of κB kinase (IKKε) complex and subsequent IRF7 activation, a key transcription factor that dimerizes and translocates to the nucleus to initiate type I IFN expression (Konno et al. 2009; Liu et al. 2013). Similar roles have been described

in studies examining TRAF2-, 3- and 5- deficient cells (Fang et al. 2017; Liu et al. 2013; Saha & Cheng 2006; Tang & Wang 2010). Direct interaction between MAVS and TRAF3 has also been shown to lead to IRF3 activation downstream of TBK1-IKKε (Saha et al. 2006; Tseng et al. 2010). Additionally, TRAFs interact with the TGF-β-activated-kinase (TAK1)-TAK1-binding protein (TAB) 1-TAB2/3 complex, which initiates MAP kinase signaling cascades and activates the IKKα-IKKβ-NFκB essential modulator (NEMO)-complex, which in turn leads to the release of NFκB (Kobayashi et al. 2004; Mikkelsen et al. 2009; Shi & Sun 2018; Walsh et al. 2015; Wang et al. 2001; Yoshida et al. 2008).

Type I IFN expression downstream of MAVS is also driven by IRF5, which can act independently of IRF3 and IRF7 (Lazear et al. 2013). The exact mechanism behind IRF5 activation is not yet known, but its activity is dependent on IKKβ and likely involves TRAF6, which has been shown to activate IRF5 downstream of TLR7 (Ren et al. 2014; Schoenemeyer et al. 2005). Additionally, recent research has reported IRF1 as a downstream MAVS effector under certain conditions, which promotes type III, but not type I IFN expression (Odendall et al. 2014).

Protein modifications, such as ubiquitination and phosphorylation, of many of the signaling components, including MAVS and the RLRs, heavily influence MAVS-mediated responses. For example, tripartite motif-containing 31 (TRIM31)-induced K63-linked ubiquitination of MAVS promotes its aggregation, while K48-linked ubiquitination resolves it (Liu B et al. 2017; Yoo et al. 2015). TRIM25- and itchy E3 ubiquitin protein ligase (AIP4)-mediated K48-linked ubiquitination induces proteasomal degradation (Castanier et al. 2012; You et al. 2009). Similarly affecting RLR-signaling is ubiquitination of NEMO, which disrupts the interaction between MAVS and TRAF3, and deubiquitination of TRAF3 and 6 by ovarian tumor deubiquitinase (OTUB) 1 and 2 (Belgnaoui et al. 2012; Li et al. 2010). The list of modifications and mediating proteins in RLR-induced type I IFN production is extensive and highlights the importance of considering the cellular context that dictates their expression and activity (Dhillon et al. 2019; Ren et al. 2020).

1.4.3 cGAS-Mediated Type I IFN Expression

RLRs and TLRs are not the only receptors whose activation induces type I IFN expression; cGAS-STING are important contributors as well. Recent research suggests that the deoxyribonucleic acid (DNA) sensor cGAS is predominantly located in the nucleus, not the cytoplasm as previously thought (Sun et al. 2013; Volkman et al. 2019). Binding of double-stranded DNA to cGAS induces a conformational change that allows the production of cyclic GMP-AMP (cGAMP) from ATP and GTP, which activates STING, a sensor of cyclic dinucleotides (Ablasser et al. 2013; Burdette et al. 2011; Gao P et al. 2013). Active STING translocates to the Golgi, where it can interact with TBK1 and activate the transcription factor IRF3 (Liu et al. 2015; Shang et al. 2012; Zhang C et al. 2019).

The list of receptors and signals inducing type I IFN expression is still growing and includes some C-type lectins, the NLRs nucleotide oligomerization domain (NOD) 1 and 2 as well as the inflammasome-forming absent in melanoma 2 (AIM2), which highlights the universal role of type I IFNs in the innate immune response (Dutta et al. 2020; Rathinam et al. 2010; Sabbah et al. 2009; Watanabe et al. 2010).

1.5 Type I IFN Signaling

Type I IFNs can initiate several different signaling cascades as a result of binding to their heterodimeric receptor complex formed by IFNAR1 and IFNAR2 (Fig. 6). The most important ones are the JAK-STAT, the MAP kinase and the AKT-mTOR signaling pathways, which are all mediated by cross-phosphorylation of the JAK kinases JAK1 and TYK2, which are associated with IFNAR2 and IFNAR1 respectively (Prchal-Murphy et al. 2012; Velazquez et al. 1992; Wilks et al. 1991).

1.5.1 JAK-STAT Signaling

The JAK-STAT signaling is considered to be the canonical IFN signaling pathway and was the first to be discovered (Darnell et al. 1994). Activated JAK1 and TYK2 can phosphorylate different STAT proteins, a mechanism that was initially determined for STAT1 and 2 but applies to all 7 members of the family (Muller et al. 1993; Schindler et al. 1992b; Velazquez et al. 1992). STAT1 and 2 can form a complex with IRF9 called ISGF3, which translocates to the nucleus and binds to IFN-stimulated response elements (ISREs) in gene promotors to induce their transcription (Levy et al. 1989; Schindler et al. 1992a).

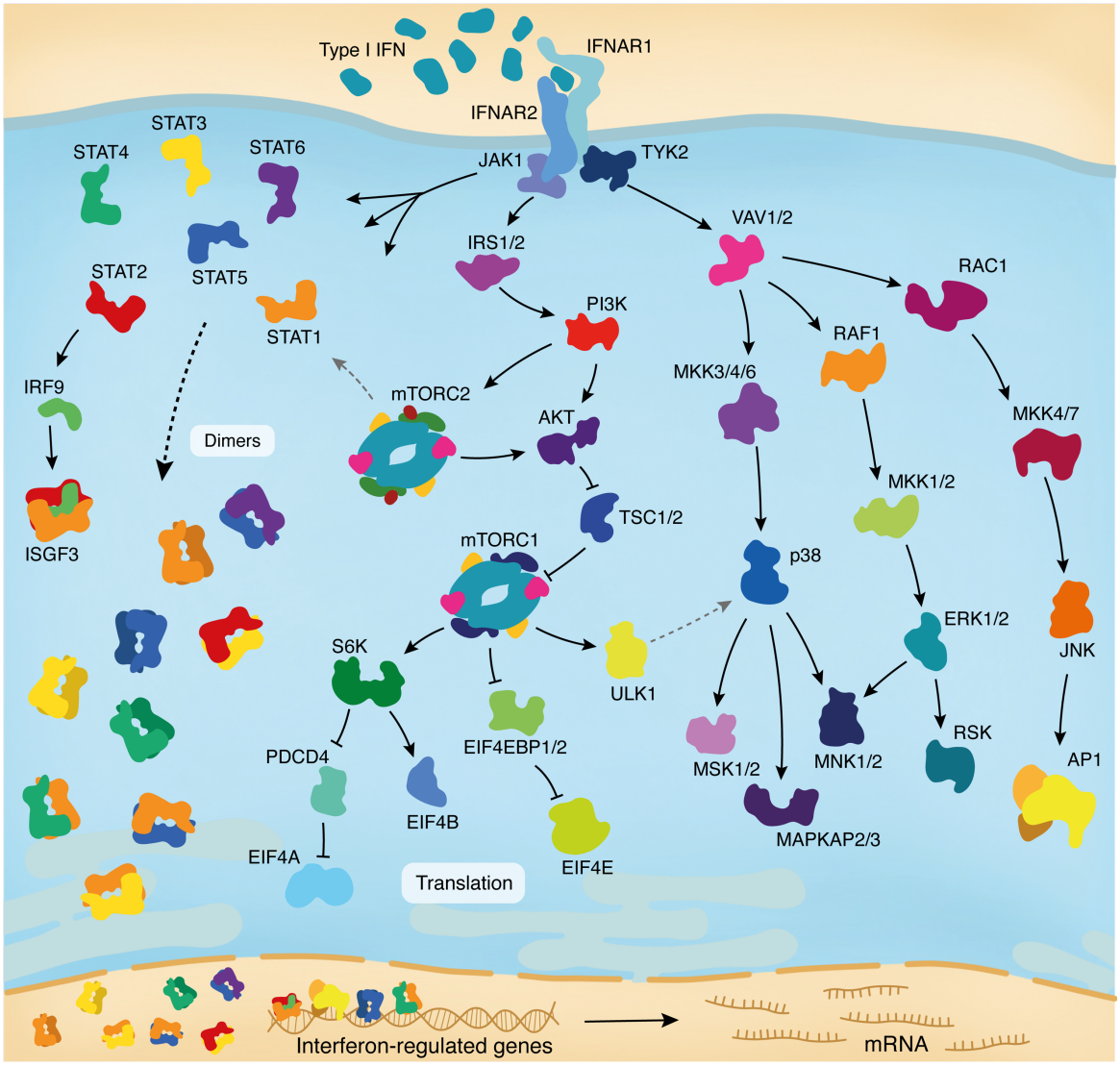

Figure 6: Type I IFN signaling. Type I IFNs can activate JAK-STAT, MAP kinase and mTOR-AKT signaling pathways and induce the expression of IRGs.

STATs also have transcription factor activities independent of ISGF3. Depending on cell type and receptor occupancy, STAT proteins form a variety of different hetero- and homodimers, although only a small number of them have been observed in response to type I IFN signaling. They include STAT1, 3, 4, 5 and 6 homodimers and heterodimers composed of STAT1:2, STAT1:3, STAT1:4, STAT1:5, STAT2:3 and STAT5:6 (Delgoffe & Vignali 2013; Levy & Darnell 2002; Platanias 2005). These STAT dimers also translocate to the nucleus, but they bind to different promotor elements, gamma-activated sequences (GASs), and induce transcription of additional genes (Decker et al. 1991; Ghislain et al. 2001). Literature suggests different STATs may induce distinct responses, such as IFNγ production by type I IFN-activated STAT4 in response to viral infection, but this mechanism is not yet well understood (Nguyen et al. 2002).

1.5.2 MAP Kinase Signaling

Type I IFN signaling also activates several MAP kinases, including the well-characterized c-Jun N-terminal kinase (JNK), p38 and extracellular signal-regulated kinase (ERK1/2), which have been shown to contribute to ISRE- and GAS-mediated gene expression (Li Y et al. 2004; Uddin et al. 2000; Uddin et al. 1999).

These signaling cascades are initiated by phosphorylation of VAV1/2 by TYK2 (Platanias & Sweet 1994; Uddin et al. 1997). VAV1/2 then phosphorylates RAF1, which subsequently activates MAP kinase kinase 1/2 (MKK1/2), which in turn can activate ERK1/2 (Kyriakis et al. 1992; Marais & Marshall 1996; Song et al. 1996). Among the ERK1/2 substrates are p90 ribosomal S6 kinase (RSK), which can regulate different transcription factors like NFκB, and MAP kinase-interacting kinase 1/2 (MNK1/2), which can influence the cellular translational activity through phosphorylation of eukaryotic initiation factor 4E (EIF4E) (Frodin & Gammeltoft 1999; Joshi & Platanias 2014; Waskiewicz et al. 1997). VAV1/2 phosphorylation of Rac family small GTPase 1 (RAC1) leads to the activation of several MKKs (Li et al. 2005; Whitmarsh & Davis 1996). MKK3 and 6 can

phosphorylate the MAP kinase p38, MKK7 activates the MAP kinase JNK and MKK4 phosphorylates both (Moriguchi et al. 1996; Raingeaud et al. 1996; Wang et al. 2007a). Among the p38 targets are mitogen- and stress-activated protein kinase 1/2 (MSK1/2), enzymes that can phosphorylate histone 3 enabling stress-related gene expression, MAP kinase-activated protein kinase 2/3 (MAPKAP2/3), kinases involved in expression of cytokines, and MNK1/2 (Clayton & Mahadevan 2003; Deak et al. 1998; Kotlyarov & Gaestel 2002; Soloaga et al. 2003; Uddin et al. 1999).

The role of activated JNK in response to type I IFN signaling is not as well studied. Literature suggests involvement in an apoptotic signaling pathway via activation of activator protein 1 (AP1), potentially eliminating virus-infected cells (Li G et al. 2004; Papachristou et al. 2003).

1.5.3 AKT-mTOR Signaling

AKT-mTOR signaling is initiated by IRS1/2 phosphorylation by receptor-associated JAKs and its subsequent association and interaction with PI3K (Platanias et al. 1996; Uddin et al. 1995). PI3K activates AKT, a central kinase in the mTOR pathway, that can also phosphorylate the p65 subunit of NFκB and a serine residue on STAT1 (Nguyen et al. 2001; Rani et al. 2002). Activation of the two functionally distinct mTOR complexes mTORC1 and mTORC2 by AKT is mediated by tuberous sclerosis complex 1/2 (TSC1/2) (Manning et al. 2002). TSC1/2 promote mTORC2 activity, but have an inhibitory effect on mTORC1, which is alleviated upon phosphorylation by AKT (Huang et al. 2008; Inoki et al. 2002). AKT is also an mTORC2 target, in addition to different members of the protein kinase C (PKC) family that regulate cell migration and the cytoskeleton, and serum- and glucocorticoid-regulated kinase 1 (SGK1), a regulator of cell survival (Gan et al. 2012; Garcia-Martinez & Alessi 2008; Jacinto et al. 2004; Li & Gao 2014; Sarbassov et al. 2005).

Functional roles of mTORC1, on the other hand, are related to cellular growth and translational activity. Additionally, mTORC1 has been shown to activate the

MAP kinase p38 via phosphorylation of Unc-51-like autophagy activating kinase 1 (ULK1) (Kim et al. 2011; Saleiro et al. 2015). Ribosomal protein S6 kinase 1 (S6K1) is one of the key mTORC1 targets, a kinase that activates EIF4B and EIF4A through direct phosphorylation and through degradation of the inhibitor programmed cell death 4 (PDCD4) respectively, which promotes activity of the mRNA 5'-cap-binding EIF4F complex (Dorrello et al. 2006; Holz et al. 2005).
EIF4E-binding protein (EIF4EBP) 1 and 2 are some other important mTORC1 targets (Brunn et al. 1997). They inhibit the interaction between EIF4E and EIF4G1, two key components of the EIF4F complex (Thoreen et al. 2012). Upon phosphorylation they release EIF4E, which allows enhanced translation of mRNAs with a 5'-terminal oligopyrimidine (5'-TOP), a motif that many genes related to protein synthesis encode (Hsieh et al. 2012; Thoreen et al. 2012). These mTOR-mediated changes to the translational activity in a type I IFN-activated cell combined with the transcriptional response induced by the JAK-STAT and MAP kinase signaling pathways lead to the induction of a large number of IFN-regulated genes (IRGs), whose functions are crucial for immune cell regulation and pathogen clearance (Schoggins et al. 2011).

1.6 IFN-Regulated Genes

IRGs encode the effector proteins that carry out type I IFN-attributed functions, such as antiviral or antibacterial defense, activation of adaptive immune cells or antiproliferative activities (Schoggins 2019). The first IRGs were identified in the 1970s and 80s, a discovery that was expanded upon in the following decades (Knight & Korant 1979; Larner et al. 1984). RNA-sequencing techniques have allowed a genome-scale assessment of IFN-induced transcriptional responses, which revealed thousands of potential IRGs, about 10% of the human genome (Shaw et al. 2017). They also showed that IRG compositions induced by different type I IFN subtypes across species and tissues vary a lot and that only a small subset is conserved in most of them (Rusinova et al. 2013; Shaw et al. 2017). Gene promotors generally contain multiple regulatory elements for different

transcription factors that are activated by type I IFNs. Some of these induced genes encode other transcriptional regulators that can further influence gene expression, which makes additional classifications of IRGs by IFN subtype or transcription factor challenging (Bluyssen et al. 1994; Platanitis & Decker 2018; Rubio et al. 2013). IRGs have instead been grouped by their ability to inhibit replication of different viruses or interference with particular steps in viral life cycles (Schoggins 2019; Schoggins et al. 2011).

Investigations of functional roles have so far mostly been restricted to common IRGs, but emerging clustered regularly interspaced short palindromic repeats (CRISPR)/Cas9-based screening approaches allow much broader assessments (Roesch et al. 2018). Utilization of these methods has revealed that only a small group of genes is involved in IFN-mediated suppression of different viruses, despite the induction of hundreds or thousands of genes, and that the composition of crucial IRGs varies between viruses and even their respective strains (OhAinle et al. 2018; Richardson et al. 2018). Similar screens also identified a large number of cellular proteins that are not IFN-inducible, but mediate antiviral responses, sometimes through direct interaction with IRGs (Fusco et al. 2013; Hubel et al. 2019; Zhao H et al. 2012).

1.6.1 Antiviral Function of IRGs

Type I IFNs are responders to both viral and bacterial infections. The role of type I IFN signaling in the context of bacterial infections is not as well studied as in viral infections, but research has shown it has ambivalent consequences. Antibacterial IRG activity is an important protective mechanism, for example during *Legionella pneumophila* and *Helicobacter pylori* infections, but can also have harmful effects, as seen during *Myobacterium tuberculosis* and *Listeria monocytogenes* infections (O'Connell et al. 2004; Plumlee et al. 2009; Stanley et al. 2007; Watanabe et al. 2010). Protective IRG-mediated antiviral activity is much more extensively studied and has been shown in response to infection by most viruses. Many of these bacteria and viruses have subsequently developed

escape mechanisms, such as repurposing of host proteins or pathogen encoded antagonistic proteins (Wang & Fish 2019). Pathogens and host organisms are therefore in a constant arms race to stay on top.

1.6.2 IRGs in HIV Infection

The role of IRGs in human immunodeficiency virus (HIV) infections is an example of their antiviral potential and interactions with viral proteins. The two known HIV species are retroviruses that can cause acquired immunodeficiency syndrome and an infection elicits an innate immune response including type I IFN expression downstream of cGAS-STING and TLR7 (Cohen et al. 2015; Gao D et al. 2013; Poli et al. 1989).

A small panel of IRGs that restrict HIV infection has been described to date and a recent screening approach revealed the composition differs between HIV strains (OhAinle et al. 2018). Interferon-induced transmembrane (IFITM) proteins suppress viral entry, TRIM5 promotes the disassembly of the viral capsid and exposure of the nucleoprotein complex and TRIM22 inhibits long terminal repeat (LTR) expression (Barr et al. 2008; Lu et al. 2011; Stremlau et al. 2004; Tissot & Mechti 1995). Reverse transcription is suppressed indirectly by different apolipoprotein B mRNA editing enzyme catalytic subunit 3 (APOBEC3) proteins and SAM and HD domain-containing deoxynucleoside triphosphate triphosphohydrolase 1 (SAMHD1), which deaminate cytosines that cause hypermutations and degrade nucleotides respectively (Hultquist et al. 2011; Laguette et al. 2011; Sheehy et al. 2002; Zheng et al. 2004). APOBEC3s and SAMHD1 are targeted by virally encoded proteins: HIV Vif inhibits translation of APOBEC3s and HIV Vpx antagonizes SAMHD1 (Hrecka et al. 2011; Stopak et al. 2003; Wiegand et al. 2004). The IRG MX dynamin-like GTPase 2 (MX2) inhibits translocation of the reverse transcribed genome to the nucleus and schlafen 11 (SLN11), guanylate binding protein 5 (GBP5) and Mac-2-binding protein (M2BP) prevent translation and processing of viral proteins (Goujon et al. 2013; Kane et al. 2013; Krapp et al. 2016; Li M et al. 2012; Wang Q et al. 2016). Lastly, budding of viral particles is inhibited by Viperin and Tetherin, which is

prevented by HIV-1 Vpu and HIV-2 Env proteins (Le Tortorec & Neil 2009; Nasr et al. 2012; Perez-Caballero et al. 2009; Swiecki et al. 2013; Wang et al. 2007b). These examples show how critical localized IFN responses are to antagonize different stages of viral infection, which are spread across different subcellular locations. The list of IRGs that restrict infection of HIV and other viruses is constantly expanded and modified and is an important avenue to therapeutic strategies.

1.6.3 Type I IFN Feedback Regulation by IRGs and miRNAs

Another important aspect of IRG function is the formation of regulatory feedback loops, which can positively and negatively affect type I IFN expression and signaling. They are formed by IRGs as well as IFN-inducible microRNAs (miRNAs) and complement the tight regulatory network that is crucial to prevent inflammation and tissue damage.

Many components involved in type I IFN expression and signaling are IFN inducible, among them RLRs and IRFs, which potentiate IFN responses (Sato et al. 1998; Xu L et al. 2017). Other IRGs promote IFN signaling by activating transcription factors, such as protein kinase R (PKR) and interferon-stimulated gene 15 (ISG15), which activate and stabilize IRF3 respectively (Shi et al. 2010; Zhang & Samuel 2008). IRF3 stabilization is the result of HECT and RLD domain-containing E3 ubiquitin protein ligase 5 (HERC5)-mediated ISGylation, the addition of the ubiquitin-like protein ISG15. ISG15 is an IRG with many diverse functions; some others include the inhibition of exosome secretion and a cytokine-like role (Bogunovic et al. 2012; Dos Santos & Mansur 2017; Villarroya-Beltri et al. 2016). Some ISG15 effects are counteracted by other IRGs. ISGylation of IRF3 can be removed by ubiquitin-specific peptidase 18 (USP18), another IRG that negatively influences IFN signaling (Malakhov et al. 2002). It can also bind to the receptor subunit IFNAR2 and prevent its association with JAK1, which prevents further signaling, with the exception of murine IFNβ (Francois-Newton et al. 2011; Makowska et al. 2011; Malakhova et al. 2006). Other negative feedback regulators are suppressor of cytokine signaling (SOCS)

1 and 3, which dephosphorylate and inactivate JAKs, and adenosine deaminase RNA specific (ADAR1), an RNA-editing enzyme whose binding activity limits RIG-I-mediated RNA sensing and subsequent IFN expression (Dalpke et al. 2001; Endo et al. 1997; Pfaller et al. 2018; Yang et al. 2014).

Type I IFN signaling can induce the expression of several miRNAs in addition to IRGs (Ohno et al. 2009; Pedersen et al. 2007). miRNAs are small, non-coding RNAs processed from primary RNA that bind complementary target sequences, which are often located in 3'-untranslated regions (3'-UTRs) of mature transcripts. miRNA binding inhibits target RNA translation or leads to its cleavage and degradation (Ha & Kim 2014).

Several mediators of type I IFN expression and signaling are targeted by IFN-inducible miRNAs. *IFNAR1* and *STAT1* are bound by miR499a-5p and miR146 respectively, which leads to a substantial protein decrease and negatively affects IFN responses (Bruni et al. 2011; Jarret et al. 2016; Papadopoulou et al. 2011; Xu D et al. 2017; Yan et al. 2017). Other miR146 targets include the PRR signaling components *TRAF6*, *IRAK1* and *IRAK2* (Ho et al. 2014). The miRNAs let7b and miR34a target *IFNB1* directly, while miR122 and miR155 target the negative feedback regulator *SOCS1*, which effectively enhances the IFN response (Cheng et al. 2013; Fiorucci et al. 2015; He et al. 2014; Ho et al. 2014; Yao R et al. 2012). Many other miRNAs that are not IFN-inducible contribute to the complex regulatory network that controls the type I IFN response.

Another layer of regulation has been added to this network after recent research revealed that the length of 3'-UTRs, the main binding area for miRNAs and RNA-binding proteins (RBPs), is variable across cell types and cellular context (Cheng et al. 2020; Elkon et al. 2012; Flavell et al. 2008; Fu et al. 2011; Hoque et al. 2013; Ji et al. 2021; Ji et al. 2009; Ji & Tian 2009; Li et al. 2016; Lin et al. 2012; Mayr & Bartel 2009; Miura et al. 2013; Sandberg et al. 2008; Ulitsky et al. 2012). Additionally, 3'-UTR-length-dependent interactions with RBPs have been shown to influence protein-protein complex formation and cellular function, highlighting the significance of post-transcriptional regulation, which may also play a role in type I IFN responses (An et al. 2008; Berkovits & Mayr 2015; Lau et al. 2010; Lee & Mayr 2019).

1.7 3'-UTR-Mediated Post-Transcriptional Regulation

3'-UTRs are important sites of post-transcriptional regulation that can influence localization of mRNA and protein, their abundance and functionality. The length of 3'-UTRs is defined through cleavage and polyadenylation of pre-mRNAs by a machinery of different protein complexes seen in Figure 7 (Moore & Sharp 1985; Wahle & Kuhn 1997). 3'-end formation occurs co-transcriptionally and protein interactions link it closely to the splicing of introns, another RNA processing mechanism (Proudfoot et al. 2002; Zhao et al. 1999). The resulting poly-A tail is a critical structure for efficient translation of mature mRNAs (Sachs et al. 1997).

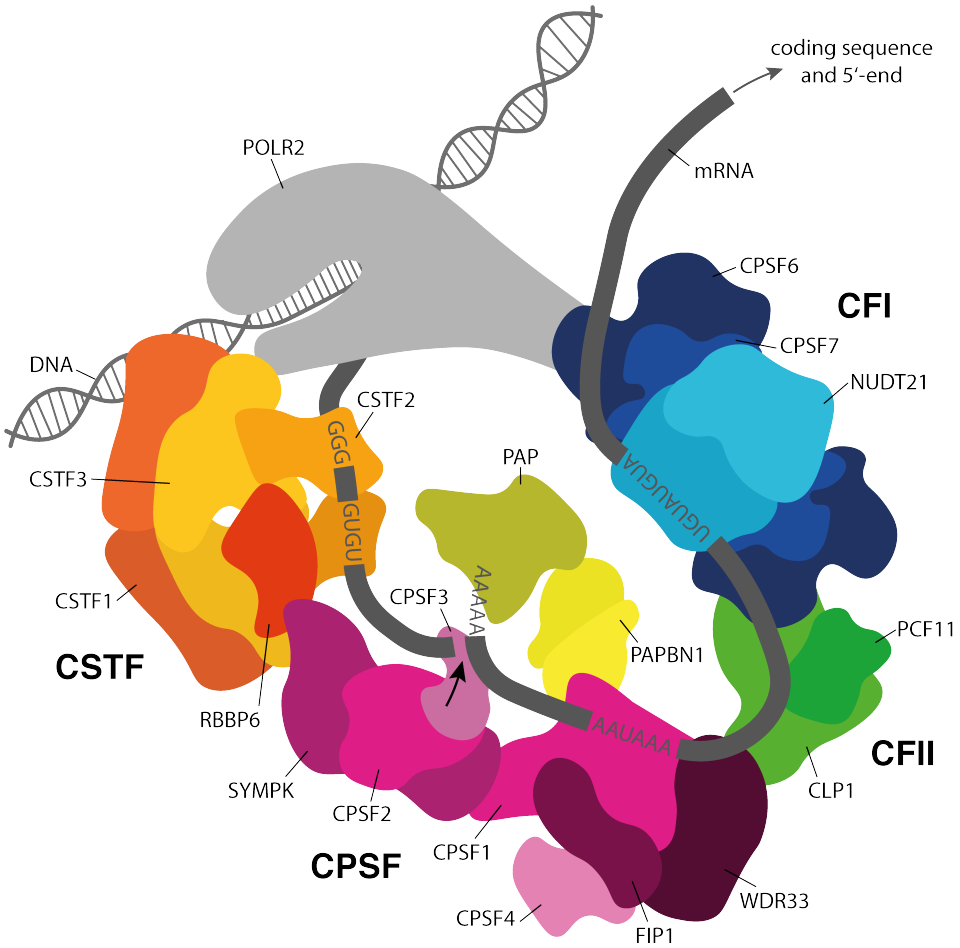

Figure 7: The cleavage and polyadenylation machinery. The cleavage and polyadenylation machinery consists of four large protein complexes that interact with RNA polymerase 2 (POLR2) and other related proteins. The CSTF, CPSF and CFI complexes bind different motifs in the pre-mRNA and mediate its cleavage by CPSF3, indicated by the arrow. Poly-A polymerase (PAP) polyadenylates the cleaved transcript.

1.7.1 Cleavage and Polyadenylation

Cleavage and polyadenylation of transcripts is initiated co-transcriptionally upon recognition of a polyadenylation sites (PASs) (Fig. 7). These processes involve the concerted action of more than 80 proteins, some of which contribute to the assembly of four core protein complexes called cleavage and polyadenylation specificity factor (CPSF), cleavage stimulation factor (CSTF) and cleavage factors I (CFI) and II (CFII) (Shi et al. 2009). Individual components will be referred to by their gene names.

1.7.1.1 The CPSF Complex

The CPSF complex, consisting of CPSF1, 2, 3 and 4, WD repeat domain 33 (WDR33), factor interacting with poly-A polymerase (FIP1) and Symplekin (SYMPK), has nuclease activity, associates with the poly-A polymerase and recognizes a hexanucleotide sequence in the PAS (Schonemann et al. 2014). The most common sequence of this motif is AAUAAA, but to date 12 variations have been identified (Gruber et al. 2016; Hu et al. 2005). CPSF1, CPSF4, WDR33 and FIP1 are involved in recognition of this motif, while cleavage is mediated by CPSF3 in tight association with CPSF2 and the scaffold protein SYMPK (Clerici et al. 2018; Mandel et al. 2006; Sullivan et al. 2009). The RNA is cleaved 10 to 30 nucleotides downstream of the PAS motif; the exact location is determined by recognition and binding of up- and downstream sequences by CFI and CSTF respectively (Chan et al. 2014; Schonemann et al. 2014; Takagaki & Manley 1997; Xiang et al. 2014).

1.7.1.2 The CSTF Complex

The CSTF complex is made up of two copies of CSTF1, 2 and 3 and binds downstream of the PAS motif in cooperation with CPSF (Bai et al. 2007; Gilmartin

& Nevins 1991; Takagaki et al. 1990; Wilusz et al. 1990). CSTF associates with GU- and U-rich sequences, which are recognized by its subunit CSTF2, and interacts with RNA polymerase 2 (POLR2) to couple transcription elongation and 3'-end processing (Hu et al. 2005; MacDonald et al. 1994; McCracken et al. 1997; Perez Canadillas & Varani 2003; Takagaki & Manley 1997). CSTF3 functions as a bridging protein that connects CSTF1 and 2, but it is in competition with the scaffold protein SYMPK, which binds to the same region on CSTF2. Its interaction with CSTF2 is not needed for polyadenylation, but is essential for histone pre-mRNA processing, the only eukaryotic mRNAs that are not polyadenylated (Marzluff 2005; Ruepp et al. 2011; Takagaki & Manley 2000). RB-binding protein 6 (RBBP6) is another CSTF2-interacting protein that was recently discovered. It is an essential protein mediating RNA cleavage, but the mechanism and exact interaction sites are not known (Di Giammartino et al. 2014).

1.7.1.3 The CF Complexes

The CFI complex is associated with the transcription elongation complex, like CSTF, and is assembled from a Nudix hydrolase 21 (NUDT21) dimer and two complexes of CPSF6 and 7 (Ruegsegger et al. 1996; Venkataraman et al. 2005). NUDT21 associates with UGUA-rich sequences upstream of the PAS motif and cooperative binding of CPSF6 creates an RNA loop that may contribute to PAS selection (Yang et al. 2011; Yang et al. 2010). Additionally, CPSF6 interacts with splicing factors and the poly-A polymerase, therefore linking cleavage and polyadenylation to the splicing machinery (Dettwiler et al. 2004; Millevoi et al. 2006).

The exact composition of the CFII complex is not yet known and may include more than 15 proteins, but only pre-mRNA cleavage complex 2 protein Pcf11 (PCF11) and cleavage factor polyribonucleotide kinase subunit 1 (CLP1) have been identified in connection to CFII function (de Vries et al. 2000). CFII is not as well studied as the other complexes, but knockdown studies in HeLa cells showed that PCF11 is required for RNA cleavage and degradation of the resulting 3'-fragment, termination of transcription and subsequent POLR2 dissociation

(West & Proudfoot 2008). CLP1 interactions with CPSF and CFI connect the CFII complex to the rest of the cleavage and polyadenylation machinery (de Vries et al. 2000).

The last step of 3'-end processing is the addition of a 200–300 nucleotide poly-A tail by the poly-A polymerase, which requires interactions with the CPSF complex and the poly-A-binding protein nuclear 1 (PABPN1) (Bienroth et al. 1993; Kerwitz et al. 2003; Wahle 1995).

Current research contributes to the growing number proteins associated with the core cleavage and polyadenylation components or that influence their activity. A purified human 3'-end processing complex was shown to contain over 80 proteins, which included more than 50 proteins that could mediate crosstalk with other processes and significantly contribute to the regulation of cleavage and polyadenylation (Shi et al. 2009). More recent additions are two members of the serine- and arginine-rich (SR) protein family, SR splicing factor (SRSF) 3 and 7. SRSF7 can associate with the CPSF complex protein FIP1, which is counteracted by SRSF3 (Schwich et al. 2021).

1.7.2 Functional Outcomes of 3'-UTR-Mediated Regulation

3'-UTR-mediated post-transcriptional regulation is dependent on interactions with miRNAs and RBPs, which are influenced by RNA sequence and structure (Bartel 2009; Chen & Shyu 1995; Wu & Bartel 2017). These RBPs can recruit effector proteins that can facilitate different functions, alter protein abundance and localization.

Protein abundance is affected post-transcriptionally through changes to mRNA stability and translation efficiency, as seen for *P21* mRNA, which is bound by the Musashi RNA-binding protein 1 (MSI1) resulting in repression of translation (Battelli et al. 2006; Zaessinger et al. 2006). The translation of *MYC* mRNA is regulated by competitive binding of the RBPs AU-rich element RNA-binding protein 1 (AUF1) and RRM domain-containing protein (TIAR1) (Liao et al. 2007; Mazan-Mamczarz et al. 2006).

Sorting and compartmentalization of mRNAs and subsequent local translation can be mediated by 3'-UTRs and is sometimes dependent on interactions with the cytoskeleton (Huttelmaier et al. 2001; Jansen 1999; Loya et al. 2008). For example, the *Saccharomyces cerevisiae ASH1* mRNA is transported by the motor protein Myo4p, which is associated with the 3'-UTR-bound adaptors She2p and She3p (Bohl et al. 2000; Takizawa & Vale 2000). 3'-UTR-bound She2p can also shuttle *ASH1* mRNA to the nucleus where it interacts with Loc1p and Puf6p, which in turn repress translation through association with Fun12p, the yeast homolog of EIF5B (Deng et al. 2008; Shen et al. 2009). Similar mechanisms have been described for human calmodulin-dependent protein kinase 2 alpha (*CAMK2A)* and brain-derived neurotrophic factor *(BDNF)* mRNA transport, which enables local translation and proper function of neurons (Miller et al. 2002; Severt et al. 1999; Wu H et al. 2020). Another example of a human 3'-UTR that influences protein localization has been reported by Xu and colleagues, who expressed green fluorescent protein (GFP) with the *MAVS* 3'-UTR and observed transport to the mitochondria (Xu et al. 2019).

3'-UTRs can also influence functions of their corresponding proteins, as seen for CCAAT enhancer-binding protein beta (CEBPB) (Basu et al. 2011). The 3'-UTR of *CEBPB* and the RBP Hu antigen R (HuR) have been shown to prevent CEBPB modification by RAS and subsequent cytostatic activity, without altering protein abundance. This has also been observed in connection to a lack of *CEBPB* mRNA in the perinuclear cytoplasmic region.

Effects like the ones described above may be mediated by a scaffold-like assembly of RBPs and effector proteins on the 3'-UTR, which can be co-translationally transferred to the nascent protein and modulate its function (Chartron et al. 2016; Duncan & Mata 2011; Fernandes & Buchan 2020; Ribeiro et al. 2020). A recent publication has shown that this kind of mechanism facilitates ribosomal protein S28B (RPS28B) association with enhancer of mRNA decapping 3 (EDC3), a crucial interaction driving P-body assembly (Fernandes & Buchan 2020). Similar observations have been made for CD47 and baculoviral inhibitors of apoptosis repeat-containing protein 3 (BIRC3), which are described in more detail below.

1.8 Alternative Polyadenylation Regulates Protein Function

More than 60% of human genes contain multiple PASs, which are differentially used across tissues and cell types, a process called alternative polyadenylation (APA) (Derti et al. 2012; Hoque et al. 2013; Lianoglou et al. 2013).
Transcripts with different coding sequences can be produced through usage of PASs in introns and exons, which has been associated with destabilization of transcripts and reduced protein levels (Mittleman et al. 2020). The usage of different PASs in the 3'-UTR of pre-mRNAs, on the other hand, results in the formation of transcripts with different 3'-UTR lengths that encode the same protein (Fig. 8). They are the main focus of 3'-UTR investigations in this study.
Locations of PASs in the genomes of different mammals have been collected and cataloged in different databases, such as TREND-DB and PolyA_DB (Derti et al. 2012; Hoque et al. 2013; Marini et al. 2021; Wang R et al. 2018). Global changes to polyadenylation patterns have been described in a variety of contexts, such as embryonic development, neuron function, pluripotency, cell proliferation and cancer (Cheng et al. 2020; Elkon et al. 2012; Flavell et al. 2008; Fu et al. 2011; Hoque et al. 2013; Ji et al. 2021; Ji et al. 2009; Ji & Tian 2009; Li et al. 2016; Lin et al. 2012; Mayr & Bartel 2009; Miura et al. 2013; Sandberg et al. 2008; Ulitsky et al. 2012).

1.8.1 Regulation of APA Patterns by 3'-End Processing Components

Changes to global polyadenylation patterns can be observed in response to altered abundance of components of the cleavage and polyadenylation machinery, as well as their interacting proteins.
The CPSF component FIP1 has been shown to influence APA in stem cells and can associate with SRSF7 to regulate cleavage and polyadenylation of proximal PASs, an effect that is counteracted by SRSF3 (Lackford et al. 2014; Li et al. 2015; Schwich et al. 2021). FIP1 also contributes to CFI-mediated APA through direct interactions (Zhu et al. 2018).

Two of the three CFI-forming proteins have been implicated in APA. Proximal PASs are used more frequently in NUD21- or CPSF6-depleted HEK293 cells and similar changes have been reported in NUDT21-deficient HeLa and immortalized pluripotent stem cells (Brumbaugh et al. 2018; Gruber et al. 2012; Kubo et al. 2006; Weng et al. 2020).

Involvement of the CFII component PCF11 in APA regulation has been observed in neurons and breast cancer cells, while CLP1 plays a role in APA in developing plants (Li et al. 2015; Ogorodnikov et al. 2018; Turner et al. 2020; Xing et al. 2008).

CSTF2 and 3, two core components of the CSTF complex can also regulate APA, as well as their interaction partner RBBP6. CSTF2 was first identified as a regulator of PAS selection in immunoglobulin M (*IGM)* RNA, a mechanism that is influenced by interaction with heterogeneous nuclear ribonucleoprotein (HNRNP) F and U1 small nuclear ribonucleoprotein A (U1A) binding to a downstream GU-rich region of the 3'-UTR (Phillips et al. 2004; Takagaki et al. 1996; Veraldi et al. 2001). HNRNPA1 is also involved in the regulation of APA of the hematological and neurological expressed 1 (*HN1*) mRNA (Jia et al. 2019). Global regulation of APA by CSTF2 has been seen during T cell differentiation and in macrophages (Chuvpilo et al. 1999; Shell et al. 2005). Regulation of cleavage and polyadenylation on a global scale has also been shown for CSTF3, which was dependent on U1 small nuclear ribonucleoprotein (snRNP), a ribonucleoprotein component of the splicing machinery, whose regulatory activity of mRNA 3'-end processing has been published before (Berg et al. 2012; Kaida et al. 2010; Luo et al. 2013). The CSTF2-interacting protein RBBP6 and its isoforms also influence PAS selection, especially in AU-rich 3'-UTRs (Di Giammartino et al. 2014).

Lastly, differential APA has described in connection to expression levels of the poly-A tail-binding proteins PABPN1, poly-A binding protein C (PABPC) and cytoplasmic polyadenylation element binding protein 1 (CEBP1). PABPN1 and PABPC suppress usage of proximal PASs and CEBP1 couples APA with translation initiation (Bava et al. 2013; de Klerk et al. 2012; Jenal et al. 2012; Li et al. 2015).

1.8.2 Regulation of APA by Additional Factors

A few publications have described regulation of APA by factors unrelated to the cleavage and polyadenylation machinery. mTORC1, a protein complex that activates gene expression and alters cellular translation efficiency, can mediate global shortening of 3'-UTRs in mouse embryonic fibroblasts (MEFs) (Chang et al. 2015). TAR DNA-binding protein 43 (TDP43) is a transcriptional repressor that is involved in 3'-UTR length changes of nuclear paraspeckle assembly transcript 1 (*NEAT1)*. Lastly, SRY-box transcription factor 2 (*SOX2)* and the transcription factor E2F altered global APA patterns in proliferating cells (Elkon et al. 2012; Modic et al. 2019).

These observations are especially interesting in the context of a recent publication that showed a dependency of PAS selection on transcription factor binding to promotor regions of genes with multiple PASs in the breast cancer cell line MCF7 (Kwon et al. 2021). Binding of the phosphatase and tensin homolog (*PTEN)* promotor by 10 transcription factors, including MYC and RELA, resulted in altered cleavage and polyadenylation without changing RNA expression by more than 1.7-fold (Kwon et al. 2021).

1.8.3 Sequence-Independent Multi-Functionality of Proteins

In-depth investigations of PASs have shown that 3'-UTR length increases with organism complexity and that APA is a mechanism conserved across many higher species (Chen et al. 2012; Derti et al. 2012; Tian et al. 2005; Ulitsky et al. 2012).

Altering 3'-UTR length will lead to loss or gain of sequence and structural features that substantially contribute to post-transcriptional gene regulation and influence protein function. APA could be one of the mechanisms developed by complex organisms to meet their need for a more diverse repertoire of protein functions, since an increase in protein abundance is limited by evolutionary constraints (Gupta et al. 2014; Levy et al. 2012; Weiss et al. 2010). This matches results from genome-wide studies showing that 3'-UTR length isoform choice has limited

effects on protein abundance (Gruber et al. 2014; Spies et al. 2013). *In silico* analyses also showed that the number of PASs in mammalian genes negatively correlates with abundance of the corresponding proteins, which was interpreted as a sign of purifying selection against alternative polyadenylation (Xu & Zhang 2018). However, protein abundance is also negatively correlated with the number of its protein interaction partners (Levy et al. 2012). This supports the hypothesis that APA is a mechanism enabling protein multi-functionality independent of amino acid sequence variations, which has recently been described for a few different candidates (Berkovits & Mayr 2015; Boutet et al. 2012; Lee & Mayr 2019; Ribeiro et al. 2020; Wong et al. 2008).

1.8.4 APA-Mediated Regulation of Protein Function

Research has shown that APA produces transcripts with short (SU) and long 3'-UTRs (LU) that can be differentially bound and targeted by miRNAs and RBPs (Fig. 8). Polyadenylation patterns differ across tissues and cell types, which can result in tissue-specific gene regulation, as reported for paired box 3 (PAX3) (Boutet et al. 2012; Lianoglou et al. 2013).

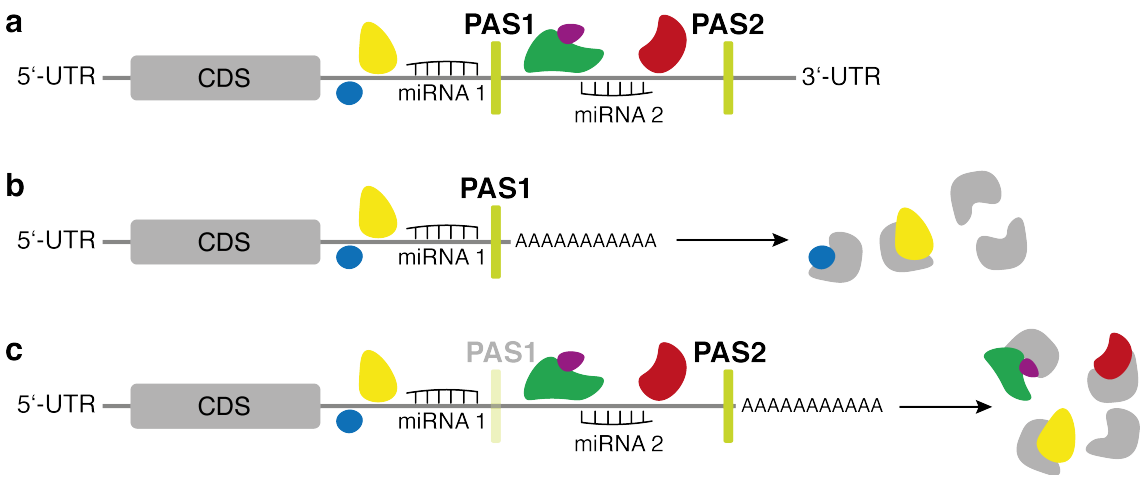

Figure 8: APA-mediated differences in protein function. a) Many transcripts contain multiple PASs. Their usage leads to the formation of transcripts with b) short or c) long 3'-UTRs, which encode different binding motifs for RBPs and miRNAs that can influence subsequent interactions with the nascent protein (grey).

PAX3 LU contains a miR206 binding site, which regulates transcript stability and represses translation in most tissues. However, muscle stem cells preferentially express *PAX3 SU*, which escapes regulation by miR206, and results in increased PAX3 protein compared to other tissues. Researchers estimated that 10% of all miRNA binding sites are located in alternative 3'-UTRs (Agarwal et al. 2015; Grimson et al. 2007). This should heavily influence the abundance of corresponding proteins, but closer investigations showed that LU transcripts are generally less responsive to miRNA regulation, a likely result of the formation of complex RNA structures in LUs that obstruct regulatory elements (Hoffman et al. 2016; Nam et al. 2014; Wu & Bartel 2017).

SU- and LU-specific protein function can also be the result of differential RNA transport and translation, as described for BDNF and CD47. BDNF is a neurotransmitter that is expressed with a short and long 3'-UTR in neurons (Miranda et al. 2019). *BDNF SU* is retained in the soma and translated in resting cells, while *BDNF LU* mRNA is transported to the dendrites and only translated in response to synapse activation and subsequent membrane depolarization. (An et al. 2008; Bauer et al. 2019; Lau et al. 2010).

CD47, a plasma membrane protein that inhibits phagocytosis of healthy cells, can also be expressed from transcripts with a short and long 3'-UTR (Oldenborg et al. 2000). *CD47 LU* is bound by the RBP HuR, which recruits SET and facilitates formation of CD47-SET-RAC1 complex (Berkovits & Mayr 2015). This complex is translocated to the plasma membrane where hyperactivated RAC1 can enable lamellipodium-mediated cell migration (ten Klooster et al. 2007). The same HuR-SET-mediated localization mechanism specific to proteins expressed from LU transcripts was shown for CD44, integrin subunit alpha 1 (ITGA1), tetraspanin 13 (TSPAN13) and B-cell-activating factor receptor (BAFFR) (Berkovits & Mayr 2015). CD47 SU on the other hand is retained in the ER and is a potential mediator of γ-irradiation-induced apoptosis (Berkovits & Mayr 2015).

CD47 LU functions have also been shown to be dependent on interaction with butyrate response factor 1 (TIS11B), an AU-rich sequence binding RBP, that can form granular structures close to the ER, subsequently named TIS granules (Ma & Mayr 2018). *CD47 LU*, but not *SU*, mRNA is associated with the TIS granule

and locally translated. The granule microenvironment proved to be crucial for CD47 protein interaction with SET, since increasing concentration of the granule-forming TIS11B, but not SET, could enhance it.

Preliminary research suggests that the TIS granule is formed through extensive interactions of large, intrinsically disordered regions in 3'-UTRs (Ma et al. 2020). This is consistent with previous reports that discovered LUs are preferentially found in lipid droplets, not the cytoplasm like SUs, and that RNA granules contain 3'-UTRs that are five times longer than average (Han et al. 2012; Kato et al. 2012). The TIS granule contains many different mRNAs, but the formation of similar, smaller granules in the cytoplasm by individual RNAs has also been reported, which could also factor into differential protein complex formation by distinct 3'-UTR transcript isoforms (Mateu-Regue et al. 2019).

Another published example of APA-regulated protein multi-functionality is BIRC3-mediated migration of B cells (Lee & Mayr 2019). BIRC3 LU forms a protein complex with IQ motif-containing GTPase activating protein 1 (IQGAP1) and RAS like proto-oncogene A (RALA), a process dependent on the RBPs staufen double-stranded RNA binding protein 1 (STAU1) and HuR. The complex regulates C-X-C motif chemokine receptor 4 (CXCR4) trafficking and cell surface expression and loss of one of its components affects B cell migration. Further investigations showed that CD27 was similarly affected by knockdown of IQGAP1, RALA or BIRC3 LU (Lee & Mayr 2019). The study also showed that many other proteins were specifically associated with BIRC3 LU, including translocase of inner mitochondrial membrane 44 (TIMM44), heat shock protein family A (HSPA9) and SWI/SNF-related matrix-associated actin-dependent regulator of chromatin subfamily A member 4 (SMARCA4), which may link BIRC3 function to chromatin regulation and mitochondrial biology, ontologies it was previously not associated with (Lee & Mayr 2019).

1.8.5 APA in Hereditary Disorders

A growing number of mutations that contribute to hereditary monogenic disorders are reported in the literature that result in heightened susceptibility to infectious

diseases (Casanova 2015). Initial investigations focused on mutations and single nucleotide polymorphisms (SNPs) in gene coding regions, including many components involved in type I IFN expression and signaling, which resulted in no protein production or the expression of defective proteins (Cotsapas et al. 2021). However, SNPs in PASs can cause severe hereditary disorders, as seen from mutations in hemoglobin subunit alpha 2 (*HBA2*) and beta (*HBB*) PASs that cause thalassemia and the development of immunodysregulation polyendocrinopathy enteropathy X-linked (IPEX) syndrome as a result of a mutation in a forkhead box P3 (*FOXP3*) PAS (Bennett et al. 2001; Higgs et al. 1983; Orkin et al. 1985).

Conversely, mutations in PASs can also have protective effects. A mutation in the arylsulfatase A (*ARSA*) gene, for example, inhibits the development of metachromatic leukodystrophy, a neurodegenerative disorder caused by null mutations of the same gene (Barth et al. 1993; Harvey et al. 1998).

Recent research suggests that genetic variants change PAS usage of target genes, which alters 3'-UTR length and contributes to complex hereditary traits and disorders (Li L et al. 2021; Mariella et al. 2019; Mittleman et al. 2020). A large number of PASs are interrupted by SNPs, which inhibit their usage by the 3'-end processing machinery and impair regulatory functions mediated by alternative polyadenylation (Shulman & Elkon 2020). This is especially critical since proteins with important roles in host defenses against pathogens are directly or indirectly regulated by alternative polyadenylation, such as CD47 and CXCR4 respectively. Therefore, investigating 3'-UTRs and their regulation in the innate immune response may increase our understanding of their role in disease.

1.9 Thesis Aims

Type I IFNs are crucial components of the innate immune response, predominantly produced by immune cells, that can induce antiviral states in almost all cell types (Colonna et al. 2002; McNab et al. 2015). They were subject to extensive investigations following their discovery in the 1950s and have been characterized as potent antiviral factors that activate many cellular pathways, including JAK-STAT signaling. Considerable progress has been made in recent years after the development of omics technologies, which established that more than 10% of human genome can be regulated by type I IFNs (Rusinova et al. 2013; Shaw et al. 2017). These technological advancements also allowed investigations of other aspects on a global scale, such as chromatin structure, protein abundance and modifications, and cellular metabolism. Research has shown that changes to any one of these structures or processes can affect others, which leads to complex responses and cellular phenotypes (De Souza et al. 2019; Mills et al. 2018). The importance of type I IFN-induced changes to many of these features has been demonstrated in literature; however, their relationship and connection to one another has not been extensively addressed.

The first aim of this study is the characterization of the global response of macrophages to IFNβ, as well as the investigation of changes across different levels of the response. These analyses will show how transcriptional changes relate to the corresponding protein levels and explore their correlation with metabolic changes.

Post-transcriptional and post-translational mechanisms are crucial aspects of the regulatory network formed by these multi-level changes, which have not been extensively studied in context of type I IFNs. Alternative polyadenylation of transcripts and the resulting difference in 3'-UTR length is one of these mechanisms and recent research has attributed it with a role in coordinating protein function (Berkovits & Mayr 2015). 3'-UTRs can have scaffold-like properties and facilitate the assembly of protein complexes that enable diverse functions of the protein encoded in the mRNA (Miller et al. 2002; Severt et al. 1999; Wu H et al. 2020). Changing 3'-UTR length can affect the formation of

these complexes and therefore regulate different protein functions. The consequences of this mechanism were discovered very recently and have so far only been described for a small number of proteins, such as CD47 and BIRC3 (Berkovits & Mayr 2015; Lee & Mayr 2019).

The second aim of this study will investigate the effect of type I IFNs on alternative polyadenylation, which has not been addressed in literature to date. A potential scaffold-like role for IFN-regulated 3'-UTRs will also be explored, since many IRG functions are heavily reliant on interactions with additional proteins and other cellular components. Activation of macrophages by IFNβ will likely alter the length of many 3'-UTRs, which would represent a new layer of regulation in the IFN response independent of differential expression of IRGs.

Chapter 2: Materials and Methods

2.1 Materials

2.1.1 Chemicals

Table 1: Chemicals

Name	Supplier
Agar	ChemSupply, Australia
Agarose	Meridian Bioscience, UK
β-Mercaptoethanol	Sigma-Aldrich, USA
BSA	Sigma-Aldrich, USA
DMSO	Sigma-Aldrich, USA
EDTA disodium salt dehydrate	Sigma-Aldrich, USA
Ethanol	ChemSupply, Australia
Glycine	Sigma-Aldrich, USA
KCl	Sigma-Aldrich, USA
KH_2PO_4	Sigma-Aldrich, USA
Methanol	ChemSupply, Australia
NaCl	ChemSupply, Australia
Na_2HPO_4	ChemSupply, Australia
NaN_3	Sigma-Aldrich, USA
Nonident P40	Sigma-Aldrich, USA
PMSF	Sigma-Aldrich, USA
SDS (20 %)	Bio-Rad Laboratories, USA
Sodium deoxycholate	Sigma-Aldrich, USA
Trizma R base	Sigma-Aldrich, USA
Triton X-100	Sigma-Aldrich, USA
Tryptone	Sigma-Aldrich, USA
Tween 20	ThermoFisher Scientific, USA
Yeast extract	Sigma-Aldrich, USA

2.1.2 Consumables

Table 2: Consumables

Name	Supplier
4–12 % Bis-Tris mini protein gel	Life Technologies, USA
Cell scrapers	Sarstedt Inc., USA
Centrifuge tubes 15/50 ml	Sigma-Aldrich, USA
Glass petri dishes 40 mm x 12 mm	Sigma-Aldrich, USA
LS columns	Miltenyi Biotec, USA
Protein standard (precision + dual color)	Bio-Rad Laboratories, USA
PVDF membrane	Merck Millipore, USA
Reaction tubes	Fisher Biotec, Australia
Syringe filters 0.45 μm	Sartorius Stedim, Australia
Tissue culture flask (T25, T75, T150)	Sigma-Aldrich, USA
Tissue Culture plates (6/12/96 wells)	Sigma-Aldrich, USA
Whatman filter paper	GE Healthcare, USA

2.1.3 Commercial Reagents

Table 3: Commercial Reagents

Name	Supplier
Ampicillin	ThermoFisher Scientific, USA
Blasticidin	Jomar Life Research, Australia
DMEM	Life Technologies, USA
dNTPs	Meridian Bioscience, UK
D-PBS	Life Technologies, USA
Fc block	BD Bioscience, USA
Fetal calf serum (FCS)	Sigma-Aldrich, USA
LDS sample buffer	ThermoFisher Scientific, USA
L-Glutamine	Life Technologies, USA
Lipofectamine 3000	ThermoFisher Scientific, USA

MES running buffer	ThermoFisher Scientific, USA
Odyssey PBS blocking buffer	LI-COR Biosciences, USA
Penicillin/Streptomycin (P/S)	Life Technologies, USA
Protease inhibitor cocktail	Sigma-Aldrich, USA
Puromycin	ThermoFisher Scientific, USA
Random hexamers	Promega, USA
RPMI	Life Technologies, USA
Power SYBR master mix	ThermoFisher Scientific, USA
Transfer buffer	Life Technologies, USA
TrypLE Express	Life Technologies, USA
Zeocin	Jomar Life Research, Australia

2.1.4 Buffers

Table 4: Buffers

Name	Composition
Dilution buffer	10 mM Tris pH 7.5, 150 mM NaCl, 0.5 mM EDTA
Elution buffer	200 mM Glycine (pH 2.5)
Extraction solvent	Chloroform-Methanol-H_2O at 1:3:1 ratio
FACS buffer	2 % FCS, 0.5 mM EDTA, 2 mM NaN_3 in D-PBS
LB agar	LB medium supplemented with 1 % (w/v) agar
LB medium	10 g tryptone, 10 g NaCl, 5 g yeast extract in 1 l H_2O
MACS buffer	0.5 % BSA, 2 mM EDTA in D-PBS
Neutralization buffer	1 M Tris buffer (pH 10.4)
PBS-Tween	137 mM NaCl, 2.7 mM KCl, 10 mM Na_2HPO_4, 1.8 mM KH_2PO_4, 0.1 % (w/v) Tween 20
RIPA buffer	10 mM Tris pH 7.5, 150 mM NaCl, 0.5 mM EDTA, 0.1 % SDS, 1 % Triton X-100, 1 % deoxycholate
TE buffer	10 mM Tris pH 8, 1 mM EDTA
TE-Tween	10 mM Tris pH 8, 1 mM EDTA, 0.1 % Tween 20

Wash buffer	10 mM Tris pH 7.5, 150 mM NaCl, 0.5 mM EDTA, 0.05 % Nonidet P40 Substitute

2.1.5 Cell Lines and Bacterial Strains

Table 5: Cell Lines and Bacterial Strains

Name	Supplier
JM109 *E. coli*	Promega, USA
HEK293T	ATCC, USA
HEK Blue IFNα/β	InvivoGen, USA
THP-1	ATCC, USA

2.1.6 Antibodies, Antibody-Conjugated Beads and Cell Stains

Table 6: Antibodies, Antibody-Conjugated Beads and Cell Stains

Name	Supplier
AF680 anti-mouse IgG	Life Technologies, USA
AF680 anti-rabbit IgG	Life Technologies, USA
Anti-AKT	Cell Signaling Technology, USA
Anti-p-AKT (Ser473)	Cell Signaling Technology, USA
Anti-p-mTOR (Ser2448)	Cell Signaling Technology, USA
Anti-p42/44	Cell Signaling Technology, USA
Anti-p-p42/44 (Thr202/Tyr204)	Cell Signaling Technology, USA
Anti-RPL18A	Abcam, UK
Anti-STAT1	Cell Signaling Technology, USA
Anti-p-STAT1 (Tyr701)	Cell Signaling Technology, USA
Anti-S6	Cell Signaling Technology, USA
Anti-p-S6 (Ser235/236)	Cell Signaling Technology, USA
MitoTracker™ Green FM	ThermoFisher Scientific, USA

Propidium iodide	Sigma-Aldrich, USA
Zombie Violet fixable viability dye	eBiosciences, USA
Anti-CD38 antibody BV421	eBiosciences, USA
Anti-CD14-conjugated beads	Miltenyi Biotec, USA
Anti-GFP-conjugated beads	ChromoTek, Germany

2.1.7 Enzymes

Table 7: Enzymes

Name	Supplier
BsmBI	NEB Biolabs, USA
FastDigest AscI	ThermoFisher Scientific, USA
FastDigest MreI	ThermoFisher Scientific, USA
FastDigest NotI	ThermoFisher Scientific, USA
FastDigest XhoI	ThermoFisher Scientific, USA
M-MLV reverse transcriptase	Promega, USA
Phu polymerase	NEB Biolabs, USA
T4 DNA ligase	Promega, USA

2.1.8 Human Primers for qPCR

Table 8: Human qPCR Primers

Name	Sequence
18S fwd	GTAACCCGTTGAACCCCATT
18S rev	CCATCCAATCGGTAGTAGCG
hCBX5 total fwd	ACCATCCCCTCCTTTAGCTC
hCBX5 total rev	GCTGACCTGGTTCTTGCAAA
hCBX5 LU fwd	CACCCAGCAGTCCATTTTCC
hCBX5 LU rev	CCAACCCCTCACTGTACCTT

hCCL7 fwd	ACCACCAGTAGCCACTGTCC
hCCL7 rev	GTCCTGGACCCACTTCTGTG
hCD47 total fwd	AGTGATGGACTCCGATTTGG
hCD47 total rev	GGGTCTCATAGGTGACAACCA
hCD47 LU fwd	AAGAGAACTCCAGTGTTGCT
hCD47 LU rev	ACGGTAACACAGCTGTAAAACA
hCLP1 fwd	TTTACCTGTTGGGCTCCTGG
hCLP1 rev	AGATGCCTCCACCTCAAAGC
hCSTF2 fwd	CCACTGGAGCACCTTGATAG
hCSTF2 rev	CCACCTGGCACTGATTTG
hCSTF3 fwd	TGTCCGAGAAACCAAGGGTA
hCSTF3 rev	CCTACAGCTTCCACGCCTTT
hCXCL10 fwd	TTCCTGCAAGCCAATTTTGT
hCXCL10 rev	TTCTTGATGGCCTTCGATTC
hCXCL11 fwd	TTGTTCAAGGCTTCCCCATGT
hCXCL11 rev	AAGCCTTGCTTGCTTCGATT
hEIF4EBP2 total fwd	CACGACAGGAAACATGCAGT
hEIF4EBP2 total rev	ATTGGCCAAATCAGGTGCAC
hEIF4EBP2 LU fwd	TTGCCCAAGTGTATCCCCTT
hEIF4EBP2 LU rev	CTCCTCCCCAGTTTCCAGTT
hG3BP1 total fwd	ACTTTGCTCATGTGCTCGTG
hG3BP1 total rev	TCCAAGTAACACCCACTGCA
hG3BP1 LU fwd	TTGAAATGTGGCCAGTGTCC
hG3BP1 LU rev	GGCAACCTTCCCCAAAAGTG
hIFIT1 fwd	GATCAGCCATATTTCATTTTGAATC
hIFIT1 rev	GAAAATTCTCTTCAGCTTTTCTGTG
hIFIT3 fwd	GGAACAGCAGAGACACAGAGG
hIFIT3 rev	ACACTGTCTTCCTTGAATAAGTTCC
hIL6 fwd	CTCCAGGAGCCCAGCTATGA
hIL6 rev	CCCAGGGAGAAGGCAACTG
hIRF7 fwd	TGTGCTGGCGAGAAGGC

hIRF7 rev	TGGAGTCCAGCATGTGTGTG
hMAVS total fwd	GTCACTTCCTGCTGAGA
hMAVS total rev	TGCTCTGAATTCTCTCCT
hMAVS LU fwd	CCTAAGGCCCTCTCTTTGCT
hMAVS LU rev	GCACCTCCAAAGAGCTTGAC
hRBBP6 fwd	ACAAGCACCACCTTTGTCCA
hRBBP6 rev	GAGCGTGAACGTGTTGAACC
hSTAT1 fwd	GTTACTTTCCCTGACATCATT
hSTAT1 rev	GAATTCTACAGAGCCCACTAT

2.1.9 Mouse Primers for qPCR

Table 9: Mouse qPCR Primers

Name	Sequence
mCXCL10 fwd	GATGACGGGCCAGTGAGAAT
mCXCL10 rev	TCAACACGTGGGCAGGATAG
mCXCL11 fwd	AGGAAGGTCACAGCCATAGC
mCXCL11 rev	CGATCTCTGCCATTTTGACG
mRSAD2 fwd	ATCGCTTCAACGTGGACGAA
mRSAD2 rev	GGAAAACCTTCCAGCGCAC
mSTAT1 fwd	TCACATTCACATGGGTGGAA
mSTAT1 rev	CGGCAGCCATGACTTTGTAG

2.1.10 Cloning Primers and Oligonucleotides

Table 10: Cloning Oligonucleotides

Name and Restriction Site	Sequence
EIF4EBP2 CDS + SU fwd – AscI	GGCGCGCCTATGTCCTCGTCAGCCGGC

EIF4EBP2 CDS + SU rev – NotI	GCGGCCGCATACAGCAAGGGCCTTCAATCTAAC
EIF4EBP2 LU fwd – NotI	GCGGCCGCTTCTGTAGAGCTAAGCAGCCCTTAG
EIF4EBP2 LU rev – MreI	CGCCGGCGTTGATACTCAAGATCTTTACTGATTTAACTATAAC
MAVS CDS fwd – AscI	AGGCGCGCCATGCCGTTTGCTGAAGACAAGAC
MAVS CDS rev – XhoI	ACGTCTCGAGTCAGTGCAGACGCCGCCG
MAVS SU fwd – XhoI	ACGTCTCGAGTGAAGCCCTGGGCTC
MAVS SU rev – NotI	AGCGGCCGCATATATACTTATCCT
sgIFNAR1 fwd	TCCCGCGGCTGCGGACAACACCCA
sgIFNAR1 rev	AAACTGGGTGTTGTCCGCAGCCGC

2.1.11 NanoString Probe Set Sequences

Table 11: NanoString Probes

Name	Sequence
ABC50	GATGTCCTCCCGCCAAGCCATGTTAGAAAATGCATCTGACATCAAGCTGGAGAAGTTCAGCATCTCCGCTCATGGCAAGGAGCTGTTCGTCAATGCAGAC
ACOX1 LU	TTGCTAAATTGTCACAGTAGTAGGAAGTATAGGGAAACCTCTCAGCTGTGGCACTGTTGTAGCTTTGGAGTGCAGAGTGTAACTCTGGGACAATCAGATT
ACOX1 Total	TCCATGGAAACATAACTCCTATCTTGGGACCTGACATAATATCTATCTATCCTGGGGAACTGGTAATATGAGACTTATAGGTTACAGCAGAAATGCTACA
AKAP13 LU	AGATAGCAAGTCAATCATGAGGATGAAGAGTGGTCAGATGTTTGCCAAGGAAGATTTGAAACGGAAGAAGCTTGTACGTGATGGGAGTGTGTTTCTGAAG

AKAP13 Total	TTCCAGCATGTTTACCCACATGTTTTGGCCATGGATAAAGTG AAGAGGCCTACTCACCATTATCCCTGCAGCGTGACACCTTT TGATTGTCACTGACCAC
ALAS3	AGTGCAACTTCTGCAGGAGGCCACTGCATTTTGAAGTGATG AGTGAAAGAGAGAAGTCCTATTTCTCAGGCTTGAGCAAGTT GGTATCTGCTCAGGCCTG
ARL8B Total	ACCATTACAAAGAATGTGGCAACTTGCTTGTGCCTAAAAGG AGGAATTGGAACTAGAATGTGTGACTCTGTGGGGACTGCAT AGGTTTGTTAATTGACCT
ARL8B LU	CCAAAATGGTCTGCAGAGAGTGAGCGGAGGCACCAGATCA ATGTTGGTTCTTTGCACTGGTGAGATTCTGCCTGATGAATAT TAAAGATATCCTGCTTTC
ATP6V1C 1 LU	AGGTCTAGCAATGTTCTTTCAGAGGACCAAGACAGTTACCT GTGTAATGTCACCTTGTTTAGGAAGGCAGTTGATGACTTCA GACACAAAGCCAGAGAAA
ATP6V1C 1 Total	GAAGTCATTGTGTCTAACATAACAACAGAGCAGTTTGTGTCA CTGAGCTCCAGTCTGTGCTGGATTATTGATATTGTTGGTGG CGGTCACCATTCCTGGA
ATXN1 LU	AGGAGCATCGTGCATCAAGTCACCAGGGTGGTCCATTCAA GCTGCAGATTTGTTTGTCATCCTTGTACAGCAATCTCCTCCT CCACTGCCACTACAGGGA
ATXN1 Total	CTGTCACCGCTTCTGTGTAGCAAACATTAACGATGACAGGG GTAGAAATTCTTCGGTGCCGTTCAGCTTACAAGGATCAGCC ATGTGCCTCTGTACTATG
C6orf90	AGAGGAAGCGACGCGAGGAGCTGTTCATCGAACAGAAGAA AAGAAAACTCCTTCCAGACACTATTTTGGAGAAGTTAACCAC AGCTTCACAGACTAACAT
C12orf49 Total	CACTCTTCCATTCTAATCTAACTGCACGATTTCTAACAGTGG GCACCATGTGCCTGCCCTCAGGTTATTTTCCAGTGGTAGTC GAATGTGCTCATATACC

C12orf49 LU	CAACGGCTGCTGCAGCGCCTATGAGTACTGTGTCTCCTGCTGCCTGCAGCCCAACAAGCAACTTCTCCTGGAGCGCTTCCTCAACCGGGCAGCCGTGGCA
CD84 LU	TCTGCTAGAACAGTGCCGTGCTTTTCCACAGAAGGTTAGACCCTGAAAGAGATGGCTCAGCACCACCTATGGATCTTGCTCCTTTGCCTGCAAACCTGGC
CD84 Total	TGTCAATTCCAACTTCTCTATATGGCTCCTCTCAGGCATGTGCCCTTAATTGGCCTAATTCTCTAATACACCTTCCCTCTACATGCTCACTCCCTCAGAT
CLN8 Total	GGCGCCAGAGCTGGGCTCTTCAACACGGCATTTAGCGCAGAAAGTCGTGGTTCAGGCAGTATGGGCCGCTGTGACAAAACACCTAAGACTGGGTAGTTTA
CLN8 LU	TATGCATCCTGGGGGATCCGCTCCACGCTGATGGTCGCTGGCTTTGTCTTCTACTTGGGCGTCTTTGTGGTCTGCCACCAGCTGTCCTCTTCCCTGAATG
CYLD Total	ATCAGAGGGAATATGAAATGTGTCCCTGCCCTACCTAGTTTTAACGACAGAATATCTATTAAAGGCTACTTAGCTGAAGGGTAAGGGTGACAGGTCTAGG
CYLD LU	CACTGACCACCGAGAACAGATTCCACTCTTTACCATTCAGTCTCACCAAGATGCCCAATACCAATGGAAGTATTGGCCACAGTCCACTTTCTCTGTCAGC
EIF4EBP2 Total	TGAGAGGGGTGGTAAGACATGGCAATTCCCAGGAGTAGTAGAAAATAATATGCCTGACTACCAACAGCTCAAGTATGCTTATTTGCACATCCTAGACTTG
EIF4EBP2 LU	CCCAGGAGTCACTAGCCCTGGCACCTTAATTGAAGACTCCAAAGTAGAAGTAAACAATTTGAACAACTTGAACAATCACGACAGGAAACATGCAGTTGGG
FAM168B Total	CTCCTCACCACAGGCTGTGCCCATGAGTCCCTGTGCAGACCAGTGGGCAAGGCAGCTGGGCCAGATCTCAGGCCAGCCGTTTGTGCTCCTAGCAGGGTTG

FAM168B LU	ATGCCAAAGGAATTGGTTATCCAGCTGGTTTTCCCATGGGC TATGCAGCAGCAGCTCCTGCCTATTCTCCTAACATGTATCCT GGAGCGAATCCTACCTT
G3BP1 LU	TTCCACCCAGTGGAGCTGTTCCAGTTACTGGGATACCACCT CATGTTGTTAAAGTACCAGCTTCACAGCCCCGTCCAGAGTC TAAGCCTGAATCTCAGAT
G3BP1 Total	TCAAAACAGAAGTTCTTCCTACTTGGAGACTTAAGGGCATTA ACTAGATGCAGCAATCCTCAGCTTGGTGTTATCACATACTA GAGGACATTTGGAAATG
GLG1 LU	CAAGGATGATTCAGAATTAGAAGGACAAGTCATCTCTTGCC TGAAGCTGAGATATGCTGACCAGCGCCTGTCTTCAGACTGT GAAGACCAGATCCGAATC
GLG1 Total	GTGTGGTTTGCAGGTAGGATGGATGTTCACTGTTTGACCGG GTGGGGTATCCTTCCTCTCTGCAGTCTCCTTCCCAGTATGC GTAAACACCCTTATAGTT
GNB4 Total	TGCCATCAGCAAGGATATCTCCTCCACTTTAATGGACAGGC CTCATTTTTGGCAGCTATGCTGTTTGAGATGTAGACTGAATA TCCAAGGTTCCTCCCTA
GNB4 LU	TAGATGACAGCCAAATTGTTACAAGTTCAGGAGATACAACTT GTGCTTTATGGGACATCGAAACTGCCCAGCAGACCACCACA TTCACTGGGCATTCTGG
GPATC3	AGTCTGGGAGCAGCAGTCTTCGTGGCTGGTTCAGGGTGTT TTGTTCCGAGCCTGCCTGCCTGCCGGTTCTATACCTCAGGG GCATTTTTACAAAAAGCCC
GU2	CCAGATATGAACAGGTTGACCTTGTTGGAAAAATGACTCAA AAGGCTGCAACTACTGTGGAACATTTGGCCATCCAGTGTCA TTGGTCTCAGAGGCCAGC
MLLT6 Total	AAGTAACCTTCAGAGATTCTTAGAAGAGTTGCTCATTCACAC CCACGCCCTTGCCCAAGGCTGGCCCACTTAGAGCGAAACT TAACTTTTGTCTGGATGG

MLLT6 LU	CTCCAGCAACTCCAGCAGCTCCTGGCCTCCCCGCAGCTGA CCCCGGAACACCAGACTGTTGTCTACCAGATGATCCAGCAG ATCCAGCAGAAACGGGAGC
MULK	GTGAGCCCGGAGGTCTGGAAAGATGTGCAGCTGTCCACCA TTGAACTGTCCATCACAACACGGAATAATCAGCTTGACCCG ACAAGCAAAGAAGATTTTC
NLN LU	CAGCTACTCCCACTGCGAACCAAGGTGGCCAAACTACTCG GTTATAGCACACATGCTGACTTCGTCCTTGAAATGAACACT GCAAAGAGCACAAGCCGCG
NLN Total	TGTCTCCCAGGAAGGTGTGACCTCTCCTTTGCCTGCATACC TCAAGGCCAGGGGAATATGCCTCAGTGATGCATTTATCTTT GTATATCAGGCCGCATGA
OGFRL1 LU	ACTTTATCTGGGGACCGCCTCGAAAAGAACAGTCGGAGGG AAGCAAAGCCCAGAAAATGTCTTCCCCTCTCGCCTCCAGTC ATAACAGTCAAACTTCTAT
OGFRL1 Total	TACAGATATCAAGGGACCACTATACACATTAGGATGATCTAT ATTGAAATCTACATGGAACAGAGTGGGACTTCTAATTGTATG ACTTCAAGATTTTGCT
PAK1 LU	TGAACCACTTCCTGTCACTCCAACTCGGGACGTGGCTACAT CTCCCATTTCACCTACTGAAAATAACACCACTCCACCAGATG CTTTGACCCGGAATACT
PAK1 Total	TTAGAGACTGCATGTTAGTTCTGGATGGATTTGGTGGCCTG ACATGATACCCTGCCAGCTGTGAGGGGACCCCGTTTTTAAG ATGCATGGCCAAGCTCTC
PANK3 LU	GGCATCCAAAGGTGATAGCACACAAGCTGACAAGCTGGTC CGTGATATTTATGGAGGAGATTATGAAAGATTTGGTTTGCCA GGTTGGGCTGTAGCATCT
PANK3 Total	AGTTAGAGGACGGTCACTTTTTCCAACAAAACCCACTCCAT AGCCATGTGGATTTTTATCCAAAGGCTCAACAACCAGAGGG AATGGTGAGACCTGATAA

PARP14 LU	TACACTGCCACAGACACAAAGGGCCACAGTTTATCTGTTCA GCGCCTCACGAAATCCAAAGTTGACATCCCTGCACACTGGA GTGATATGAAGCAGCAGA
PARP14 Total	GTCGCTGGGAGGATTAAGGGACTTAATCTGCTAGGAACACC TGTACTTGAAGTGGAGGAGGCTAGGGGGCCACAGTTGCTG CTTCATTAACATAGAGGTT
PHC3 LU	GTCTATGCAGTCTTTACAAGTGCAGCCTGAAATTCTGTCCC AGGGCCAGGTTTTGGTGCAGAATGCTTTGGTGTCAGAAGA GGAACTTCCAGCTGCAGAA
PHC3 Total	TTCCCTCTTCTTGGAATTTCAGAACACAAATACAGGCTAAGC ATTAGTAAGAGATGGCCCACAGTATGAGAGAGAGAGGTGC AACGGAAAATCTCGCCTG
PSD3 Total	GCATTAGCAGTTTTGGGTAAGCTGGCGGTACTATAACACGT ACTGGAAACCTGTTCCTCATCACCACCTACCAGATTCTGGA AATGCCGTCTTCTAGAAA
PSD3 LU	TTTTGGAAAAGGAGACCCCAGAAAATCTCAGTAATGGTACC AGCAGCAATGTGGAAGCAGCCAAAAGGTTGGCCAAACGCC TTTATCAGCTGGACAGATT
PTGFRN Total	CCCCTCCTGCCCAGACCTTCGTTTGTTTCCCCGGTGGCCCT TGCTTCTTGCTTTGCAGACTGCCTGCAGCCATGATTTTGTCA CTGACATCTGTGAGCCA
PTGFRN LU	TCTTTGCTGCCGGAAATACATTTGAGATGACTTGCAAAGTAT CTTCCAAGAATATTAAGTCGCCACGCTACTCTGTTCTCATCA TGGCTGAGAAGCCTGT
RNF217 LU	GCGAAATTGAGCATGGGCAGAGGAATGCCCAGAAGTGTCC AAAGTGCAAGATCCACATCCAGCGAACTGAAGGATGTGACC ATATGACCTGCTCACAATG
RNF217 Total	AGGAGAGACAGGAGGGGCCTAAAAACTCACTCTGGTATGT GGGAAACATTAGAATTCCTTCCTGACCTTTGTCAAATGAGG GCACATCTGCCAAGACATC

SPTLC2 LU	AAGAGTTTTGGTGCTTCTGGAGGATATATTGGAGGCAAGAA GGAGCTGATAGACTACCTGCGAACACATTCTCATAGTGCAG TGTATGCCACGTCATTGT
SPTLC2 Total	TGATAAGGATTTCTGGTTCCTAGTGATCCGGGATTGGGCAA CAGTGCAGAACTGCCAGTCATGCCGTAGGCCGTGAAGAAA GAATGTGAGTAACTGTTGT
SRF Total	GGAGGACATGCGTGTGTCAGGGATGAGTTGAGGTGATATTT TTATGTGCAGCGACCCTTGGTGTTTCCCTTCCTCGGTGGCT CTGGGGTATGTGTGTGTG
SRF LU	CCAGACTCTCCACCCCGTTCAGACCCCACAACAGACCAGA GAATGAGTGCCACTGGCTTTGAAGAGACAGATCTCACCTAC CAGGTGTCGGAGTCTGACA
TNS1 LU	GCCACCGTGGGACATCAAGTGGAAGAACTTGTTTGCTTGAA AGTATCTCAGACCCAAGGCACCTCAGGTCTCTTTGCTGTGC CTCCACTATATTGTCGTG
TNS1 Total	CCTTCCTTTGTAAATATCTCATCTCCCACTGGAGAGCCCAG GAGCCTATTCCTGGCATGGATGTTCTGTCCACACTTGAGGC TGGGCGGTGTATCAGACC
TRIM44 Total	ACAGAGACACTCCTGAGGTTGGACTTCCTTGCTTTTCTCTA CTTCCAAATCACAATTTCTTACAACCAAGCTTTGTGCTCCCG AGTAAGCAGGGATGTAC
TRIM44 LU	GATGAGGAGAGTGAAGAAGACAGCGAGGAAGAAATGGAGG ATGAGCAAGAAAGCGAGGCCGAAGAAGACAACCAAGAAGA AGGGGAATCCGAGGCGGAGG
ZC3HAV1 Total	TTGGAAAGTTTACTGAAGGAAATATAACGTACACGAGCCCT CCTCCACAGTTCGACAGCTGTGTGGATACCAGATCGAATCC CTCCGTTTTTGTCATCTT
ZC3HAV1 LU	CACGAACTCTCTGGACTGAACAAAGAGGAATTAGCAGTGCT CCTCCTCCAAAGTGATCCTTTTTTTATGCCCGAGATATGCAA AAGTTATAAGGGAGAGG

ZNF24 Total	TGGCAGTGCCAAGCAGTGGCATCGCCAGAGTATCTGTTTG GTTAGCAAATGAGCAGTCATTTTAGGTCATGCAGATTGCTG ATATCTGCCCAGTAGCCAC
ZNF24 LU	GAATCCCATGAAGTTCCTGGCACTCTCAATATGGGTGTTCC TCAAATTTTTAAATATGGAGAAACCTGTTTCCCCAAGGGCAG GTTTGAAAGAAAGAGAA

2.1.12 PrimeFlow Probes

Table 12: PrimeFlow Probes

Name/Target and Fluorochrome	ThermoFisher Scientific Assay ID
CBX5 Total – Alexa Fluor 568	VPGZE6P
CBX5 LU – Alexa Fluor 647	VPH49RM
G3BP1 Total – Alexa Fluor 568	VPEPRZV
G3BP1 LU – Alexa Fluor 647	VPFVKKT

2.1.13 Cytokines and Inhibitors

Table 13: Cytokines and Inhibitors

Name and Working Concentration	Supplier
Human M-CSF (50 mg/ml)	R & D Systems, USA
Mouse IFNβ (100 IU/ml)	Made by Antony Matthews (Hertzog group)
Human IFNβ Rebif (100 IU/ml)	Merck & Co., USA
Actinomycin D (100 ng/ml)	Sigma-Aldrich, USA
Cycloheximide (20 μg/ml)	Sigma-Aldrich, USA
Cyt387 (10 μM)	InvivoGen, USA
SB203580 (10 μM)	Cell Signaling Technology, USA
U0126 (20 μM)	Sigma-Aldrich, USA

Torin1 (250 nM)	Cell Signaling Technology, USA
Wortmannin (50 nM)	ThermoFisher Scientific, USA
PMA (100 ng/ml)	Sigma-Aldrich, USA

2.2 Molecular Cloning Methods

2.2.1 Transformation of JM109 Competent *Escherichia coli* Cells

JM109 competent cell aliquots (Promega) were thawed on ice and incubated with the plasmid DNA or ligation product that was being transformed for 20 min. The cells were heat shocked for 30 s at 40 °C and subsequently supplemented with 500 µl LB medium. The suspension was incubated at 37 °C for 30 min and 200 µl of the suspension was plated on 100 µg/ml Ampicillin-containing LB agar plates.

2.2.2 Plasmid Preparation from *Escherichia coli* Cultures

3 ml or 250 ml *E. coli* suspension cultures were used for mini- and maxi-plasmid preparations respectively. These cultures were grown overnight in LB medium supplemented with 100 µg/ml ampicillin from individual colonies picked from LB agar plates. Plasmids were extracted using PureYield Plasmid Maxiprep or Miniprep systems (Promega) according to the manufacturer's instructions.

2.2.3 Cloning of an IFNAR1 sgRNA Plasmid

Complementary oligonucleotides were hybridized in 200 µl TE buffer at a concentration of 1 µM in a heat block that was cooling down to room temperature after an initial denaturation at 95 °C for 5 min. The single guide RNA (sgRNA) backbone was digested with the restriction enzyme BsmBI (NEB Biolabs) according to the manufacturer's instructions and subsequently ligated to the annealed oligonucleotides with T4 DNA ligase (Promega).
Sanger sequencing was used to validate the base sequence of the final construct.

2.2.4 Cloning of mCitrine-Tag Constructs

Expression constructs for MAVS and 4EBP2 were cloned into the plasmid backbone pRP that encodes an mCitrine tag. Both protein coding regions and 4EBP2 3'-UTRs were amplified by PCR using Phusion polymerase (NEB Biolabs) in HF buffer according to the manufacturer's instruction. THP-1 cDNA was used as a template with primer pairs amplifying the MAVS and 4EBP2 coding sequences and 4EBP2 SU and LU as listed in the Materials section. The MAVS SU was amplified from a full-length MAVS 3'-UTR plasmid, a kind gift from the Yao lab (Xu et al. 2019). The MAVS LU was cut out of the plasmid using the restriction enzymes NotI and XhoI (ThermoFisher). The final constructs were assembled one insert at a time starting with the coding sequences at the 5'-end. The backbones and PCR products were digested with the restriction enzymes (ThermoFisher) listed with the respective primers and ligated using T4 DNA ligase (Promega) according to the manufacturer's instructions. The integrity of the final constructs was determined by Sanger sequencing.

2.3 Cell Culture Methods

2.3.1 Isolation and Differentiation of Mouse Bone Marrow-Derived Macrophages

Bone marrow was extracted from femurs of C57BL/6J mice and cultivated in RPMI medium supplemented with 1 % P/S, 1 % L-glutamine and 10 % L929-cell-conditioned media for 7 days without movement. Mouse bone marrow-derived macrophages (BMDMs) were lifted using TrypLE Express, counted and replated in RPMI supplemented with 1 % P/S solution and 1 % L-glutamine at the appropriate density for further experiments.

2.3.2 Isolation and Differentiation of Human Blood Monocyte-Derived Macrophages

Whole-blood donations were layered on top of a Histopaque-1077 (Sigma-Aldrich) gradient and centrifuged at 700 g for 20 min without brakes. Plasma was removed and mononuclear cells located in the interphase were pooled and washed with Dulbecco's phosphate buffered saline (D-PBS). After spinning for 10 min at 340 g, the cell pellet was resuspended in 1,000 µl MACS buffer and mixed with 250 µl anti-CD14 beads (Miltenyi Biotec). CD14+ cells were isolated using LS or MS columns (Milentyi Biotec) according to the manufacturer's instructions.

Monocytes were differentiated in RPMI supplemented with 1 % P/S, 1 % L-glutamate and 50 mg/ml human recombinant M-CSF (R&D Systems) for 7 days without movement. Human blood monocyte-derived macrophages (HMDMs) were lifted using TrypLE Express, counted and replated in RPMI supplemented with 1 % P/S solution and 1 % L-glutamate at the appropriate density for further experiments.

2.3.3 Thawing and Freezing of Cell Lines

Frozen cell aliquots were thawed in a 37 °C water bath with gentle agitation. The cells were transferred to a 15 ml tube containing pre-warmed growth medium and pelleted at 300 g for 5 min. The cell pellet was resuspended in 15 ml fresh medium and pelleted again. This process was repeated two more times before the cells were plated in 25 cm^2 tissue culture flasks and grown at 37 °C in 5 % CO_2.

To freeze cell aliquots, they were first harvested and pelleted by centrifugation. The cell pellet was resuspended in fetal calf serum (FCS) supplemented with 10 % dimethyl sulphoxide (DMSO) and transferred to a cryovial. The vials were placed in a freezing container and stored at −80 °C overnight. They were then transferred to long-term storage in liquid nitrogen.

2.2.4 L929-Cell Cultivation and Generation of L-Cell-Conditioned Media

L929 murine fibroblasts were cultivated in RPMI supplemented with 10 % FCS, 1 % L-glutamine and 1% P/S at 37 °C, 5 % CO_2. Cells were split 1:10 every three days by aspirating the medium, washing with D-PBS and lifting the cells with TrypLE Express. To generate L929-conditioned medium, L929 cells were grown for 10 days, then the cell culture medium was aspirated, centrifuged at 200 g and 4 °C, filtered through a 0.45 μm sterile filter and frozen at −80 °C.

2.3.5 Culture and Transfection of HEK293T and HEK Blue IFNα/β Cells

HEK293 Blue IFNα/β and HEK293T cells were cultured in DMEM supplemented with 10 % FCS, 1 % L-glutamine and 1 % P/S. HEK293 Blue IFNα/β medium was additionally supplemented with 10 μg/ml blasticidin and 100 μg/ml zeocin. The cells were split 1:5 to 1:10 every two days or 1:20 every three days.
For transfection of fluorescent constructs $5x10^6$ cells were seeded in 10 cm dishes. The next day they were transfected with Lipofectamine 3000 using a 1:1.3 Lipofectamine:DNA ratio according to manufacturer's instructions except that DMEM without supplements was used instead of OptiMEM. 10 μg of the empty vector, 15 μg of 4EBP2 SU and MAVS CDS plasmids and 22 μg of of 4EBP2 LU, MAVS SU and MAVS LU constructs were used for transfection to ensure highest efficiency.

2.3.6 THP-1 Cultivation

THP-1 cells were cultivated in RPMI supplemented with 10 % FCS, 1 % L-glutamate and 1% P/S at 37 °C in 5 % CO_2. They are split 1:5 every two days or 1:10 every three days. Differentiation to a macrophage-like phenotype was done overnight by supplementing the growth medium with 100 ng/ml PMA. The

supernatant was replaced with PMA-free medium the next day and cells used for further analyses.

2.3.7 Lentiviral Transduction of THP-1 Cells

1.5 x 10^6 HEK293T cells were transfected with the lentiviral packaging plasmids pMDL (5 μg), RSV-REV (2.5 μg) and VSVg (3 μg) in addition to a Cas9 or sgRNA expression plasmid (10 μg). The supernatant was replaced with fresh medium on day two and on day three the supernatant containing viral particles was filtered through a 0.45 μm syringe filter. 2–3 ml supernatant was added to 1 x 10^6 THP-1 cells, which were grown overnight. The medium was replaced the following day and marker expression was monitored. The growth medium for the new cell pool was supplemented with the respective selection marker two days later.

2.4 Metabolite Methods

2.4.1 Extraction of Metabolites

6.5 x 10^5 BMDMs were plated on fibronectin-coated glass dishes (Sigma Aldrich) and treated with 100 IU/ml recombinant mouse IFNβ for the indicated times. Metabolite extraction was performed at 4 °C. Culture medium was washed off with ice cold D-PBS and cells were lysed using extraction solvent. Cell lysates were mixed thoroughly for 30 min and subsequently centrifuged at 20,000 g for 10 min. The supernatant was transferred to a new tube and dried by evaporating the solvents in a Biotage Nitrogen dryer at 37 °C.

2.4.2 Acquisition of Metabolites by Quantitative Mass Spectrometry

Further sample processing and acquisition was done in collaboration with Dovile Anderson and Darren Creek from the Monash Proteomics & Metabolomics Facility. Samples were reconstituted in extraction solvent (chloroform-methanol-water at 1:3:1 ratio), supplemented with metabolite standards and analyzed on a Q-Exactive Orbitrap mass spectrometer (Thermo Fisher) using a ZIC-pHILIC column (Merck Sequant) coupled to U3000 RSLC HPLC (Thermo Fisher).
The data was processed using the IDEOM workflow, which is initiated by peak picking and annotation using XCMS and mzMatch (Creek et al. 2012; Scheltema et al. 2011; Smith et al. 2006). Further identification of metabolites through mass and retention times and the determination of statistical significance using t-tests was performed in the IDEOM Excel interface (Creek et al. 2012).

2.5 RNA Methods

2.5.1 RNA Extraction Protocol

Cells were washed with D-PBS and harvested in RLT buffer supplemented with 1 % β-mercaptoethanol. RNA was extracted by following the manufacturer's instructions using the RNeasy Mini Spin Column kit (Promega) and included an on-column DNase digest. Elution was performed in a total volume of 50 µl of H_2O.

2.5.2 Reverse Transcription and qPCR

Reverse transcription was performed using M-MLV reverse transcriptase and random hexamer primers (Promega), according to the manufacturer's instructions.
Synthesized cDNA was diluted 1:5 and 2 µl was used with 5 µl Power SYBR mix and 0.2 µl of 10 µM reverse and forward primer each in a total volume of 10 µl to

perform quantitative PCR using a QuantStudio 6 machine (Thermo Fisher). All samples were tested in technical triplicates and all experiments included a melt curve analysis as a quality control. The average of the technical replicates excluding outliers were normalized using the housekeeping gene 18S in each sample. Statistical significance of expression and 3'-UTR ratio fold changes (FCs) were tested using a one-way analysis of variance (ANOVA) with Geisser-Greenhouse correction for paired data and Tukey's multiple comparisons tests in GraphPad Prism.

2.5.3 Poly-A-Tail-Sequencing Library Preparation

Poly-A-tail-sequencing (PAT-seq) requires specialized processing of RNA, which was done in collaboration with Angavai Swaminathan from Traude Beilharz's lab at Monash University, who has published a detailed protocol for this method (Swaminathan et al. 2019). A biotin-tag was added to the 3'-end of polyadenylated RNA followed by a limited digest and enrichment of 3'-ends using streptavidin-conjugated beads. A library was generated from the enriched fragments by reverse transcription, barcoding and PCR amplification. The libraries were sequenced on an Illumina HiSeq 1500 instrument at the Monash Health & Translational Precinct Medical Genomics Facility.

2.5.4 Poly-A-Tail-Sequencing Data Analysis

The sequencing data generated from PAT-seq libraries was analyzed in collaboration with Paul Harrison, who developed an open-source processing pipeline called tail-tools for this purpose (Harrison et al. 2015; Swaminathan et al. 2019). The initial processing steps included clipping of adaptor and poly-A sequences and alignments to the reference genomes using Bowtie 2 (Langmead & Salzberg 2012). Sequencing data from BMDM was aligned to the *Mus musculus* genome assembly GRCm38 (mm10) and HMDM sequencing data was

aligned to the *Homo sapiens* genome assembly GRCh38 (hg38). Sequencing reads were assigned to a gene if they aligned between the 5'-end of a gene and 200 base pairs (bp) downstream of its annotated 3'-end. The number of reads for each gene was determined and cleavage and polyadenylation sites were called. The number of $\log_2$ reads per million for each gene was calculated and normalized between samples using the TMM method described in the Bioconductor package edgeR (Robinson & Oshlack 2010). Differential testing was performed on features with at least 10 reads in a sample using moderated t-statistics described in the Bioconductor package limma (Smyth 2004). The genes were then ranked by confident effect size (confect) (Harrison et al. 2019).
Subsequent analysis of statistical overrepresentation of gene ontologies was done using the PANTHER Classification System (PANTHERV14.0) (Mi et al. 2019). *De novo* motif enrichment analyses were performed using HOMER with default settings (Heinz et al. 2010).

2.5.5 NanoString nCounter Sample Preparation

NanoString probe A and B master stocks for the custom 3'-UTR array were prepared in TE buffer to a final concentration of 5 nM and 25 nM respectively, then working pools were made by 8.3-fold dilution with TE-Tween. A master mix for 12 reactions was made by combining 7 μl of probe A and B working pools with 70 μl hybridization buffer and a TagSet aliquot. 8 μl of this master mix was added to 100 ng RNA in a volume of 7 μl, thoroughly mixed by inverting the tubes and incubated at 67 °C for 16 h to allow hybridization of RNA and probe sets. Samples were hybridized to a cartridge and analyzed on a NanoString nCounter with a fields of view count of 555.

2.5.6 NanoString nCounter Data Analysis

NanoString count data was analyzed using different Bioconductor packages in R. Data was imported and probes were annotated using the package NanoStringDiff (Wang H et al. 2016). Counts were normalized across samples using the TMM method described in the package edgeR (Robinson & Oshlack 2010). Subsequent linear modelling and statistical differential expression testing using moderated t-statistics were performed using the Bioconductor package limma (Smyth 2004). Further investigations of transcript isoform fold changes were done with the limma function diffSplice.

2.5.7 PrimeFlow Staining of RNA

5 x 10^6 cells per sample were stained using the PrimeFlow™ RNA Assay Kit (Thermo Fisher) with custom probes to detect different transcript variants. Cells were harvested with TrypLE Express and washed three times with D-PBS. Staining was done according to the manufacturer's instructions for 96-well plates with a few exceptions. ZombieViolet (Biolegend) was used at a 1:200 dilution in 100 µl FACS buffer to stain dead cells for 30 min prior to fixing and permeabilizing the cells. The permeabilization step was extended to 20 min and a hybridization oven was used for the probe hybridization and signal amplification steps. The cells were measured on a BD LSR Fortessa and data of single viable cells were shown.

2.6 Protein Methods

2.6.1 CD38 detection by Flow Cytometry

Cells were harvested and washed with D-PBS. On ice and in the dark, cells were stained with Zombie Violet (Biolegend) in a 1:200 dilution for 30 min. After

washing with D-PBS, unspecific binding sites were blocked using Fc block (Biolegend) for 15 min and subsequently stained using an anti-CD38 antibody (Biolegend) at a 1:100 dilution for 30 min. After a final washing step with D-PBS cells were analyzed using a BD LSR Fortessa. The mean fluorescence intensity of the CD38 conjugate of single viable cells was recorded and plotted using GraphPad Prism. Statistical analysis was done using a one-way ANOVA with Geisser-Greenhouse correction and Šídák's multiple comparisons test.

2.6.2 Detection of Mitochondrial Mass

Mitochondrial mass of HMDMs was determined by staining of live cells with MitoTracker Green FM (Thermo Fisher). The MitoTracker stain was diluted to a 100 nM in cell culture medium and prewarmed to 37 °C. HMDM medium was aspirated and replaced with the staining solution and cells were grown for another 30 min at 37 °C, 5 % CO_2. HMDMs were harvested with TrypLE Express and pelleted by centrifugation. Following a washing step with D-PBS, HMDMs were resuspended in FACS buffer supplemented with 1 μg/ml propidium iodide to stain dead cells. Cells were analyzed using a BD LSR Fortessa and the MitoTracker™ stain mean fluorescence intensity of single, viable cells was recorded. Statistical analysis was done in GraphPad Prism using a one-way ANOVA with Geisser-Greenhouse correction and Šídák's multiple comparisons test.

2.6.3 Protein Extraction

Whole protein was extracted from 1 x 10^6 THP-1 and 5 x 10^6 HEK Blue IFNα/β cells using 200 μl ice cold RIPA buffer supplemented with 1 mM PMSF and a protease inhibitor cocktail. Cell lysis was performed for 30 min on ice followed by a 10 min centrifugation step at 17,000 g and 4 °C. The protein-containing supernatant was transferred to a new tube and the protein concentration was

determined using absorbance at 280 nm measured on a NanoDrop Spectrophotometer.

2.6.4 Detection of Proteins by Western Blot

Equal amounts of protein were mixed with 4x Bolt LDS sample buffer (Thermo Fisher) in a total volume of 20 µl and denatured at 95 °C for 5 min. The denatured samples were loaded on a 4–12 % Bis-Tris gel in MES running buffer (Thermo Fisher) along with a protein size standard. Proteins were separated at 200 V for 30 min and subsequently blotted onto a PVDF membrane activated in methanol. Protein blotting was done in a Mini Blot Module (Invitrogen) in transfer buffer at 20 V for 60 min, with gel and membrane sandwiched between filter paper and sponges.

Unspecific binding sites on the membrane were subsequently blocked using Odyssey PBS blocking buffer (LI-COR), followed by overnight incubation at 4 °C with primary antibodies diluted 1:1,000 in the same buffer. The primary antibody was removed, and the membrane was washed with PBS-Tween three times for 5 min at room temperature, before a secondary antibody conjugated to a fluorochrome was added at a 1:5,000 dilution in Odyssey PBS blocking buffer for 60 min in the dark. The secondary antibody was removed, and the membrane was washed again as previously, before detection of a fluorescent signal using an Odyssey imaging system.

2.6.5 Immunoprecipitation of Protein Complexes

Protein extracted from cell lysates as described previously was diluted with 300 µl dilution buffer supplemented with 1 mM PMSF and a protease inhibitor cocktail. This diluted lysate was incubated with equilibrated magnetic anti-GFP beads for 60 min at 4 °C and rotated end-over-end. Bead equilibration was achieved by washing of 25 µl bead slurry with 500 µl ice cold dilution buffer.

After protein binding, beads were separated with a magnet and the supernatant was removed. The beads were washed with wash buffer three times and transferred to a new tube. Protein was eluted from the beads with 100 µl elution buffer, which was transferred to a new tube after separation of the beads. The eluate was neutralized with 10 µl neutralization buffer.

2.6.6 Immunoprecipitation Sample Processing for Mass Spectrometry

Further processing and quantification of proteins by mass spectrometry was done in collaboration with Iresha Hanchapola and Ralf Schittenhelm from the Monash Proteomics & Metabolomics Facility. Proteins were subjected to a tryptic digest and the peptide composition was acquired using the Dionex Ultimate 3000 RSLCnano Liquid Chromatography system and the QExactive Plus2 (Thermo Scientific) mass spectrometer using the analytical and trap columns Acclaim PepMap RSLC and 100 (Thermo Scientific).

2.6.7 Analysis of Mass Spectrometry Data

The data was processed using MaxQuant (MaxQuant v1.6.5.0) and peptides were annotated using the RS Human SwissProt Jun2020 iRT database (Cox & Mann 2008). Normalization was based on library size, which is appropriate under the assumption that the abundance of the majority of proteins is consistent between samples. Statistical analysis and data visualization were performed using LFQ-Analyst (Shah et al. 2020). The initial pipeline step removed potential contaminant or reverse sequences and proteins that were identified by a single peptide or were not consistently identified within a sample group. Missing values were imputed using the missing not at random (MNAR) method after conversion of the data to a $\log_2$ scale. Differential expression analysis was done using the Bioconductor package limma and adjusted p-values were calculated using the Benjamini-Hochberg method (Smyth 2004). Protein-protein interaction networks were generated using STRING, only including highest confidence interactions

(Szklarczyk et al. 2015). Clustering was performed using the Markov Cluster algorithm with the inflation parameter setting 1.5. Cluster annotations including ontologies were researched and added manually.

3. Characterizing the Global Response of Macrophages to IFNβ

3.1 Introduction

A comprehensive understanding of changes induced by type I IFNs is fundamental to deciphering the many complex biological contexts in which they operate. Type I IFNs are key components of the innate immune response to many different pathogens, commensals and other stressors, but current research rarely focuses on the effects of IFNs alone (Stetson & Medzhitov 2006). Understanding the direct effects of IFN signaling is key to deciphering observations in complex infection scenarios and, more importantly, to translating their use therapeutically against new emerging pathogens and the diseases they cause.

An increased understanding of IFN signaling would play an equally important role in addressing auto-immune diseases caused by type I IFN dysregulation (Emamian et al. 2009; Javed & Reder 2006; Ko et al. 2012) or hereditary monogenic disorders caused by mutations in some of the genes associated with type I IFN production and signaling (Hernandez et al. 2019; Zhang et al. 2020).

Type I IFNs are conserved among vertebrates and many studies use mice as a convenient model for *in vivo* studies (Stetson & Medzhitov 2006). Interactions with the receptor subunits IFNAR1 and 2 are conserved across species for IFNα and IFNε, but interestingly not IFNβ. Recombinant human IFNβ interacts more strongly with IFNAR2 than IFNAR1, whereas the reverse is true for recombinant mouse IFNβ (Stifter et al. 2018). This is especially interesting in the context of non-canonical signaling by IFNβ independently of IFNAR2 (de Weerd et al. 2013). Since the ultimate goal of medical research is to develop treatments for humans, it is important to compare responses in both species to determine when the use of a mouse model is appropriate.

Type I IFNs can act on almost all tissues and cell types, including epithelial cells, different parenchymal and stromal cells of organs, tissues and blood vessels, as well as immune cells (Colonna et al. 2002; McNab et al. 2015). These immune cells include macrophages, which play a central role in many innate immune

responses and are the subject of this study (Gordon & Martinez-Pomares 2017; Muntjewerff et al. 2020; Uribe-Querol & Rosales 2020). Type I IFNs activate several signaling cascades upon receptor binding, such as the JAK-STAT pathway, which initiates the expression of IRGs (Prchal-Murphy et al. 2012; Velazquez et al. 1992; Wilks et al. 1991). Studies of the Interferome database, a manually curated collection of hundreds of publicly available datasets of IFN-treated cells, have shown that type I IFNs can induce transcription of about 10% of the human genome (Rusinova et al. 2013). The most commonly induced genes encode proteins that can interfere with different stages of cellular processes and viral infection, mediate specialized functions of immune cells, stimulate the adaptive immune response or have anti-proliferative properties (Schoggins 2019).

Recent global analyses of RNA and protein levels in different biological contexts have established that many transcripts correlate with translated protein levels, but a large fraction does not (Liu et al. 2016). Considerable progress has been made in understanding the regulatory mechanisms of the transcriptional response in the IFN field since their discovery, but post-transcriptional regulation, a key contributor to discrepancies between transcript and protein levels, has not been as extensively studied (Shaw et al. 2017). The 3'-UTR is the main site of the post-transcriptional regulation mechanisms mediated by RBPs and miRNAs. Its length is determined during pre-mRNA processing and can vary depending on the cells' biological context (Mayr & Bartel 2009; Miura et al. 2013). Recent investigations have shown that this can affect post-transcriptional regulatory mechanisms and alter protein function (An et al. 2008; Lau et al. 2010).

Many functional changes induced by type I IFNs are dependent on reprogramming of the cellular metabolism (Wu et al. 2016). For example, nucleotide and amino acid biosynthesis pathways affect transcriptional and translational activities and can be altered by changed expression levels of key metabolic enzymes (Rath et al. 2014). Investigations of metabolic pathways of immune cells (immunometabolism) is a field of research that has been growing rapidly in recent years as a result of the development of unbiased mass spectrometry approaches, which allow assessments of global metabolite profiles

(Mathis & Shoelson 2011). Metabolic reprogramming during pro- and anti-inflammatory macrophage activation has already been heavily investigated, but changes induced by type I IFNs are only starting to be addressed (De Souza et al. 2019; Michelucci et al. 2013; Strelko et al. 2011; Viola et al. 2019; Wu et al. 2016).

3.2 Study Aims

Global changes to RNA, protein and metabolite levels in BMDMs in response to IFNβ will be examined in this study. Transcriptional changes will be investigated using PAT-seq, a specialized sequencing technique that yields information on transcript 3'-ends in addition to gene expression levels, in collaboration with Traude Beilharz's lab, who developed the technique (Harrison et al. 2015; Swaminathan et al. 2019). These changes will be compared to their corresponding protein levels, which were measured in a proteomics dataset of BMDMs treated with IFNβ by Michelle Tate, Nathan Croft and Jamie Gearing prior to this study (unpublished). RNA and protein level changes will be compared to metabolic profiles of IFNβ-treated BMDMs, which were determined in this study using quantitative mass spectrometry, in collaboration with Darren Creek from the Monash Proteomics & Metabolomics Facility.

IFNβ-induced changes to 3'-UTR lengths will be investigated and compared to RNA and protein expression levels, as well as miRNA-binding sites, whose location in IFNβ-treated BMDMs was determined by our lab previously (Sam Forster, Kate Jeffrey et al.) by high-throughput sequencing of RNA isolated by crosslinking immunoprecipitation (HITS-CLIP).

Taken together, these datasets and analyses will give an overview of the regulatory network across RNA, protein and metabolites and can be used to assess the global reprogramming process in IFNβ-treated macrophages.

3.3 Results

Despite its prevalence in the innate immune response, changes induced by type I IFNs alone are rarely investigated and are instead often described indirectly through receptor knockout models or in experiments involving a preceding stimulus that induces IFNs amidst other cytokines. The direct effects of IFNβ treatment on transcript, protein and metabolite levels and their relationship will be investigated in the following chapter.

3.3.1 Transcriptomic Changes in BMDMs Induced by IFNβ

BMDMs were treated with 100 IU/ml IFNβ for 3 h and 12 h, RNA was extracted, processed and sequenced using the PAT-seq protocol to assess transcriptional changes.

The results revealed vast changes in gene expression levels at both time points compared to untreated cells (Fig. 9a and b). 1,673 and 3,044 genes were significantly upregulated after 3 h and 12 h respectively. The number of significantly downregulated genes at either time point was slightly smaller: 1,393 and 2,817 at 3 h and 12 h respectively. The numbers decrease significantly when the common fold change cutoff for differential expression of 2 is used. The number of upregulated genes is reduced to 455 and 657 and the number of downregulated genes to 44 and 203 at 3 h and 12 h respectively.

The highlighted genes *Rsad2*, *Stat1*, *Cxcl10* and *Cxcl11* are IRGs whose induction by type I IFNs has been reported in many settings (Rusinova et al. 2013). Their expression changes in BMDMs treated with 100 IU/ml IFNβ were further validated by qPCR over a period of 12 h (Fig. 9c–f). The qPCR results agree with the changes measured by PAT-seq after 3 h and 12 h and extend the sequencing data by showing differences in the expression kinetics between the different genes. *Rsad2*, *Cxcl10* and *Cxcl11* are induced very rapidly and decrease again after 5–12 h, while *Stat1* expression increases at these later time points.

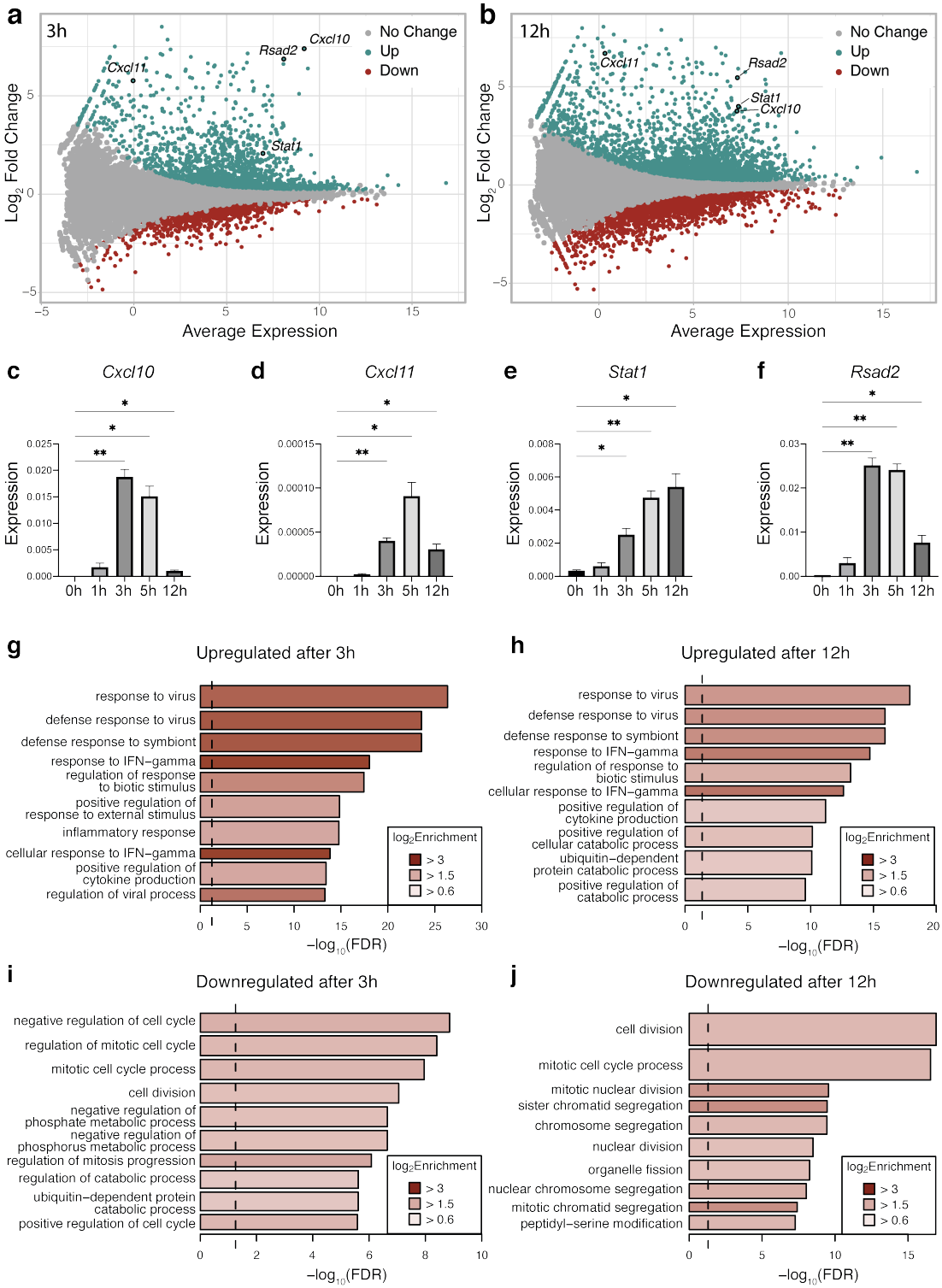
a
3h
No Change
Up
Down
Cxcl11
Rsad2
Cxcl10
Stat1
Log2 Fold Change
Average Expression
b
12h
No Change
Up
Down
Cxcl11
Rsad2
Stat1
Cxcl10
Log2 Fold Change
Average Expression
c
Cxcl10
d
Cxcl11
e
Stat1
f
Rsad2
Expression
0h 1h 3h 5h 12h
g
Upregulated after 3h
response to virus
defense response to virus
defense response to symbiont
response to IFN−gamma
regulation of response to biotic stimulus
positive regulation of response to external stimulus
inflammatory response
cellular response to IFN−gamma
positive regulation of cytokine production
regulation of viral process
log2Enrichment
> 3
> 1.5
> 0.6
−log10(FDR)
h
Upregulated after 12h
response to virus
defense response to virus
defense response to symbiont
response to IFN−gamma
regulation of response to biotic stimulus
cellular response to IFN−gamma
positive regulation of cytokine production
positive regulation of cellular catabolic process
ubiquitin−dependent protein catabolic process
positive regulation of catabolic process
log2Enrichment
> 3
> 1.5
> 0.6
−log10(FDR)
i
Downregulated after 3h
negative regulation of cell cycle
regulation of mitotic cell cycle
mitotic cell cycle process
cell division
negative regulation of phosphate metabolic process
negative regulation of phosphorus metabolic process
regulation of mitosis progression
regulation of catabolic process
ubiquitin−dependent protein catabolic process
positive regulation of cell cycle
log2Enrichment
> 3
> 1.5
> 0.6
−log10(FDR)
j
Downregulated after 12h
cell division
mitotic cell cycle process
mitotic nuclear division
sister chromatid segregation
chromosome segregation
nuclear division
organelle fission
nuclear chromosome segregation
mitotic chromatid segregation
peptidyl−serine modification
log2Enrichment
> 3
> 1.5
> 0.6
−log10(FDR)

Figure 9: Differential gene expression in BMDMs in response to treatment with 100 IU/ml IFNβ. Scatter plot of $\log_2$ fold change of up- and downregulated genes with an FDR < 0.05 after a) 3 h and b) 12 h of treatment with 100 IU/ml IFNβ over average expression in all samples are shown in green and red respectively. Validation of *Cxcl11* c), *Cxcl10* d), *Stat1* e) and *Rsad2* f) gene expression via qPCR (n = 3, asterisks indicate significance using a one-way ANOVA, * $p < 0.05$, ** $p < 0.01$). g) – j) Bar graphs of most significantly overrepresented gene sets among up- and downregulated genes after 3 h and 12 h. Analysis was done using PANTHER. The bar width represents the size of the gene set, the length its $-\log_{10}$FDR and the color its $\log_2$ enrichment value. The dashed line at 1.3 (equivalent to an FDR value of 0.05) indicates the threshold for statistical significance.

Statistical gene set overrepresentation analyses on up- and downregulated genes were done using PANTHER to characterize these IRGs. Among the most significant results of upregulated genes after 3 h and 12 h (Fig. 9g and h) are gene sets associated with viral infection, responses to treatment with IFNγ and positive regulation of cytokine production.

IRGs induced by type I and II IFNs overlap substantially, which is reflected and confirmed by the presence of the IFNγ response gene set in this analysis. Gene sets from different catabolic processes were significantly overrepresented in the analysis of upregulated genes after 12 h, but not 3 h. Some of the most highly overrepresented gene sets in downregulated genes at both time points are associated with cell division and cell cycle regulation (Fig. 9i and j). Related gene sets on chromosome and chromatid segregation and organelle fission as well as a peptidyl-serine modification gene set are overrepresented among genes downregulated after 12 h, while the top results of the 3 h analysis include gene sets with distinct ontologies related to phosphorus metabolism and catabolic processes.

3.3.2 Metabolic Reprogramming of BMDMs by IFNβ

Investigations of transcript levels in BMDMs in response to IFNβ have shown altered expression levels of genes related to different metabolic pathways.

Therefore, changes to the global metabolic profile of BMDMs treated with 100 IU/ml IFNβ were measured, to study the connection between these transcripts and the cellular metabolism.

BMDMs were treated for 1 h and 3 h to observe very rapid and direct changes on metabolite levels induced by the IFNβ signaling cascade, as well as 16 h and 24 h to assess the later or secondary effect of proteins expressed in response to IFNβ. 348 metabolites were detected and putatively identified; 129 were significantly changed during one of more of the selected time points compared to untreated cells as determined by a moderated t-test (Fig. 10a–d). The number of changed metabolites varies across investigated time points. After just 1 h of IFNβ treatment, the levels of 29 metabolites are significantly altered, but mostly return to the levels detected in untreated samples after 3 h; 9 metabolites show changed

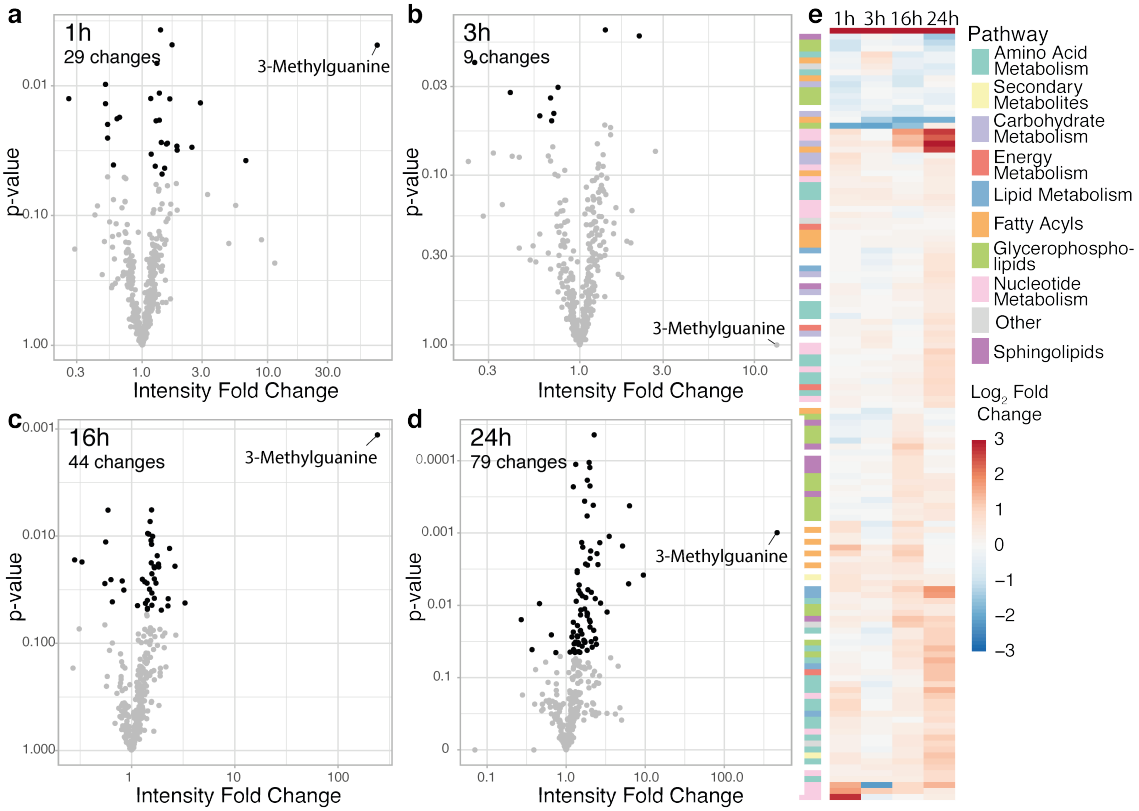

Figure 10: Quantitative metabolomics analysis of IFNβ-treated BMDMs. Volcano plots highlighting significantly changed (moderated t-test; adjusted p-value < 0.05) metabolites in black after 1 h a), 3 h b), 16 h c) and 24 h d) of 100 IU/ml IFNβ treatment. The metabolite 3-methylguanine is labelled. e) Heat map showing $\log_2$ fold changes (truncated to ±3) of significantly changed metabolites including pathway annotation.

levels at this time point. After 16 h of IFNβ treatment, 44 of the detected metabolites are significantly changed compared to their level in untreated cells. This number increases to 79 in the samples harvested after 24 h of IFNβ treatment.

The heat map shown in Figure 10e highlights the differences and fluctuations of the levels of these metabolites across all time points. Notably, a large number of upregulated metabolites are a part of the nucleotide, amino acid or carbohydrate metabolism pathways. The most highly upregulated metabolite across all time points was putatively identified as 3-methylguanine. 3-methylguanine is released by DNA-3-methyladenine glycosylase (MPG), the only known mammalian DNA glycosylase that excises alkylated purines (Robertson et al. 2009).

3.3.3 IFNβ-Induced Changes to the Purine Metabolism

A group of metabolites belonging to the purine pathway was notably upregulated at the early time points of this experiment (Fig. 11). Purines can be synthesized through two pathways (Pareek et al. 2021). The first is salvage pathway, in which enzymes add recovered purine bases to phosphoribosyl pyrophosphate (PRPP) to form guanosine, adenosine or inosine monophosphate (GMP, AMP or IMP). The second more complex pathway is *de novo* synthesis, a snapshot of which is shown in Figure 11a. During this more energy-efficient approach, PRPP is converted to IMP through a number of different enzymatic reactions (Pareek et al. 2021). IMP in turn can be converted to inosine and hypoxanthine; hypoxanthine can then either be reverted back to IMP or converted to xanthine and excreted in the form of uric acid. GMP and AMP can be derived from IMP as well and AMP in turn is part of the inosine conversion cycle via adenosine (Pareek et al. 2021).

In this dataset, adenosine, IMP and hypoxanthine are significantly upregulated 1 h after IFN treatment but revert to untreated level at the later time points. The other metabolites mentioned in the diagram in Figure 11a (GMP, AMP, xanthine and uric acid) were not reliably identifiable in the data. In the literature, changes

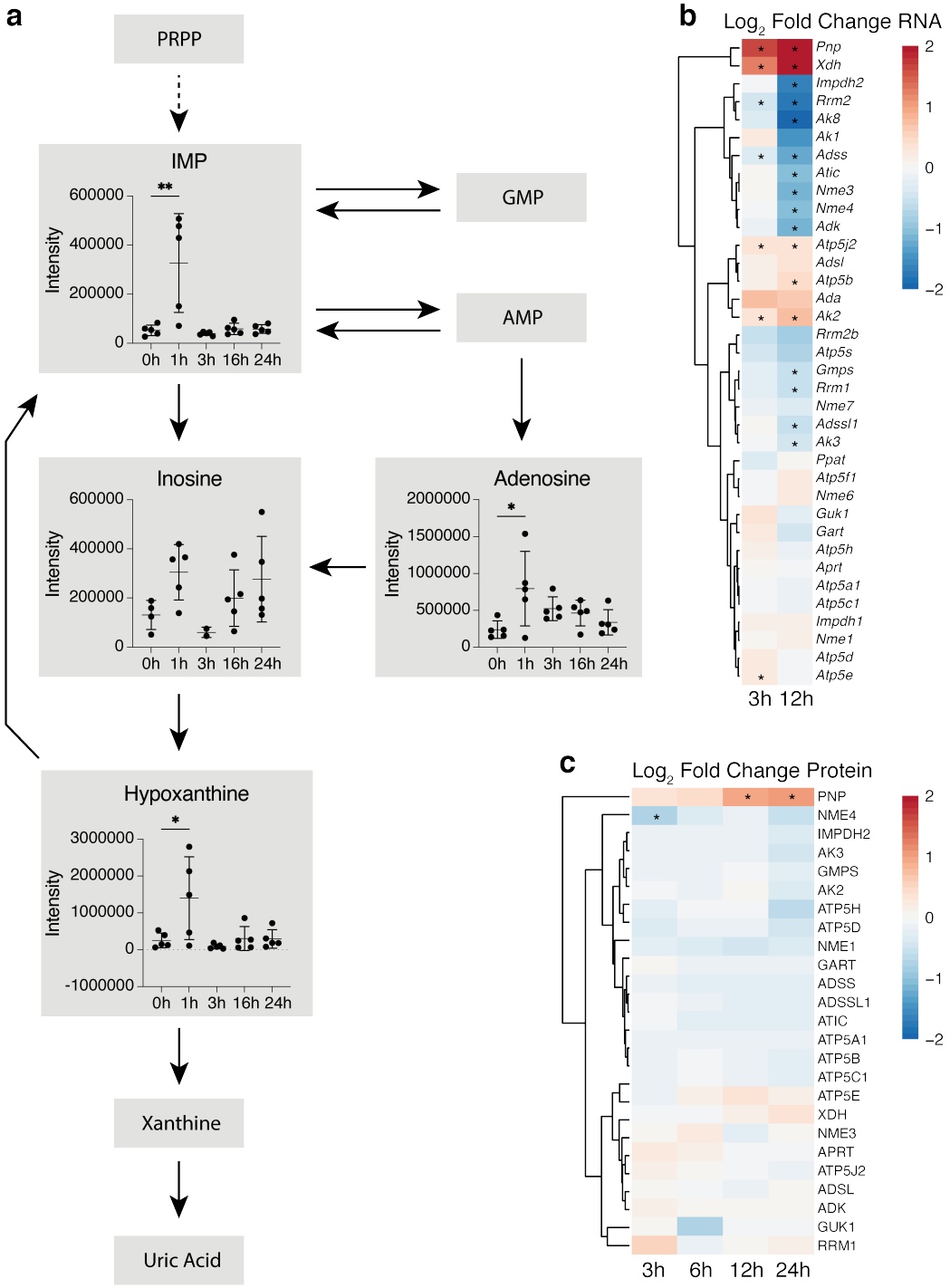

Figure 11: Rapid changes to metabolite levels in the purine metabolism pathway in response to IFNβ treatment. a) Diagram of part of the purine metabolism pathway (PRPP: phosphoribosyl pyrophosphate). Intensities of all detected metabolites are shown across all time points (n = 5, asterisks indicate significance using a one-way ANOVA, * $p < 0.05$, ** $p < 0.01$). b) Heat map of RNA $\log_2$ fold changes of enzymes involved in the purine metabolism pathway as determined by PAT-seq (n = 3, * FDR < 0.05). c) Heat map of protein $\log_2$ fold changes of enzymes involved in the purine metabolism pathway measured prior to this thesis by quantitative mass spectrometry (n = 3, * FDR < 0.05).

on metabolic level have sometimes been described as a result of differential gene expression (Cordes et al. 2016; De Souza et al. 2019). However, very few of the purine metabolic enzymes are differentially expressed on RNA (Fig. 11b) or protein level (Fig. 11c) after 3 h of IFN treatment, making this an unlikely mechanism in this study.

3.3.4 Changes to TCA Cycle Metabolite Levels in IFNβ-Activated BMDMs

The carbohydrate metabolism pathway, especially the TCA cycle, has been well described in different macrophage polarization studies (Ryan & O'Neill 2020). In accordance with the M1 polarization phenotype, the metabolite itaconate was significantly upregulated after 24 h of IFNβ treatment (De Souza et al. 2019; Strelko et al. 2011). Itaconate is derived from the citrate isomerization intermediate cis-aconitate and is described as one of the key results of a break in the TCA cycle. Figure 12 shows part of the cycle; intensity values for each time point are shown for metabolites putatively identified in this dataset. Previously, pro-inflammatory M1 macrophages have been characterized by accumulation of citrate and itaconate, as well as succinate as a downstream effect of elevated itaconate levels (Lampropoulou et al. 2016). In this dataset, a significant increase of itaconate was observed, as well as a trend towards increased levels of other metabolites, at 24 h. Elevation of itaconate levels were shown to be the product of increased ACOD1 expression and decreased IDH activity (De Souza et al. 2019; Mills et al. 2018).

Acod1 and *Idh1* transcript levels changed correspondingly in this study, but the ACOD1 protein levels only showed a slight trend towards upregulation up to 24 h post-treatment that is not statistically significant and IDH1 protein levels were not altered (Fig. 12), indicating that the mechanism underlying itaconate accumulation might be different in IFNβ-activated macrophages, as opposed to LPS-treated macrophages (De Souza et al. 2019).

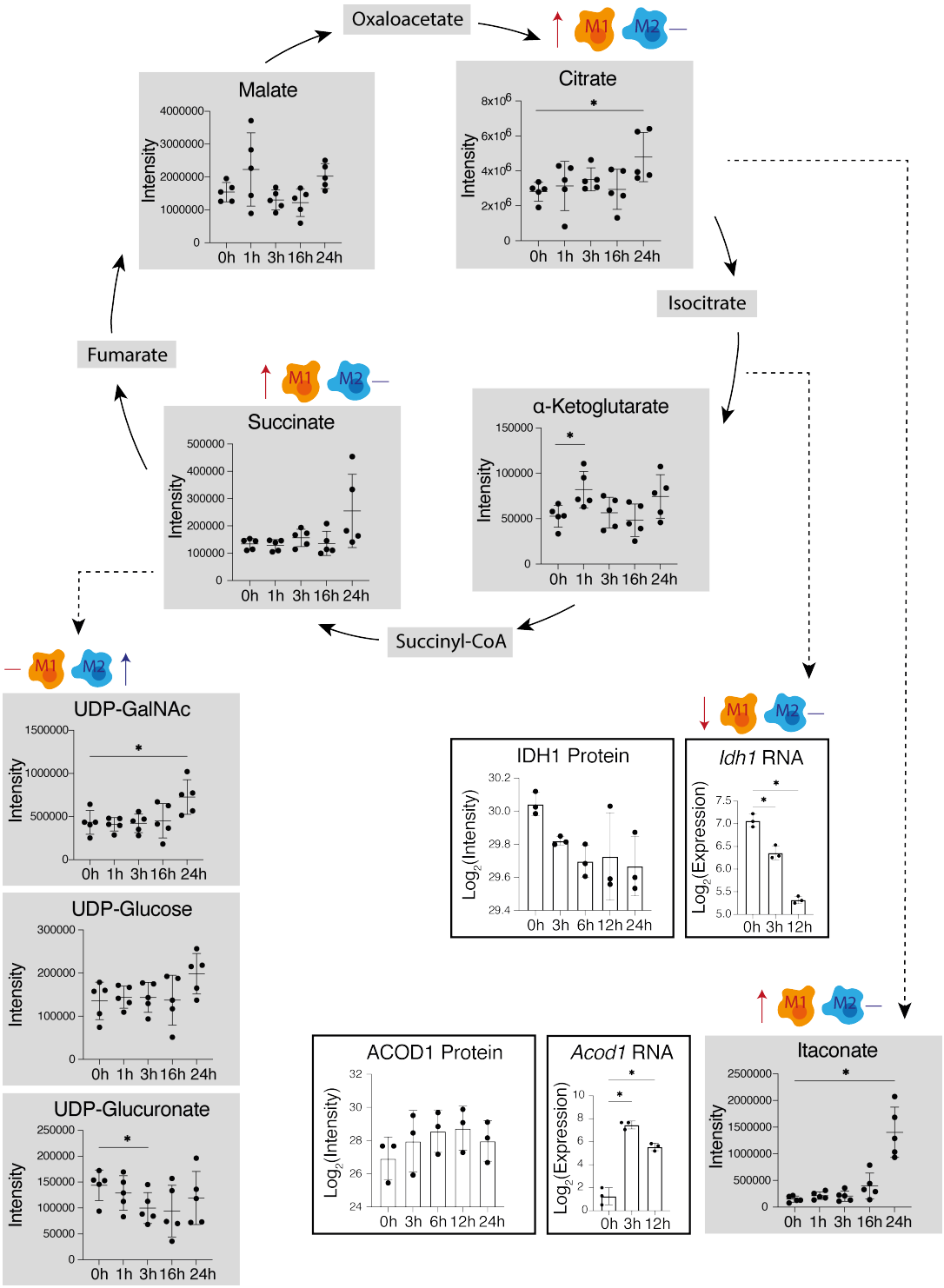

Figure 12: Schematic diagram of the TCA cycle and associated metabolites and enzymes in BMDMs treated with 100 IU/ml IFNβ. Intensity values of metabolites (n = 5) putatively identified using quantitative mass spectrometry are shown on a light grey background. ACOD1 and IDH1 RNA (n = 3; PAT-seq) and protein levels (n = 3; identified by quantitative mass spectrometry in previous work) are shown (statistical significance determined by moderated t-tests, * adjusted $p < 0.05$).

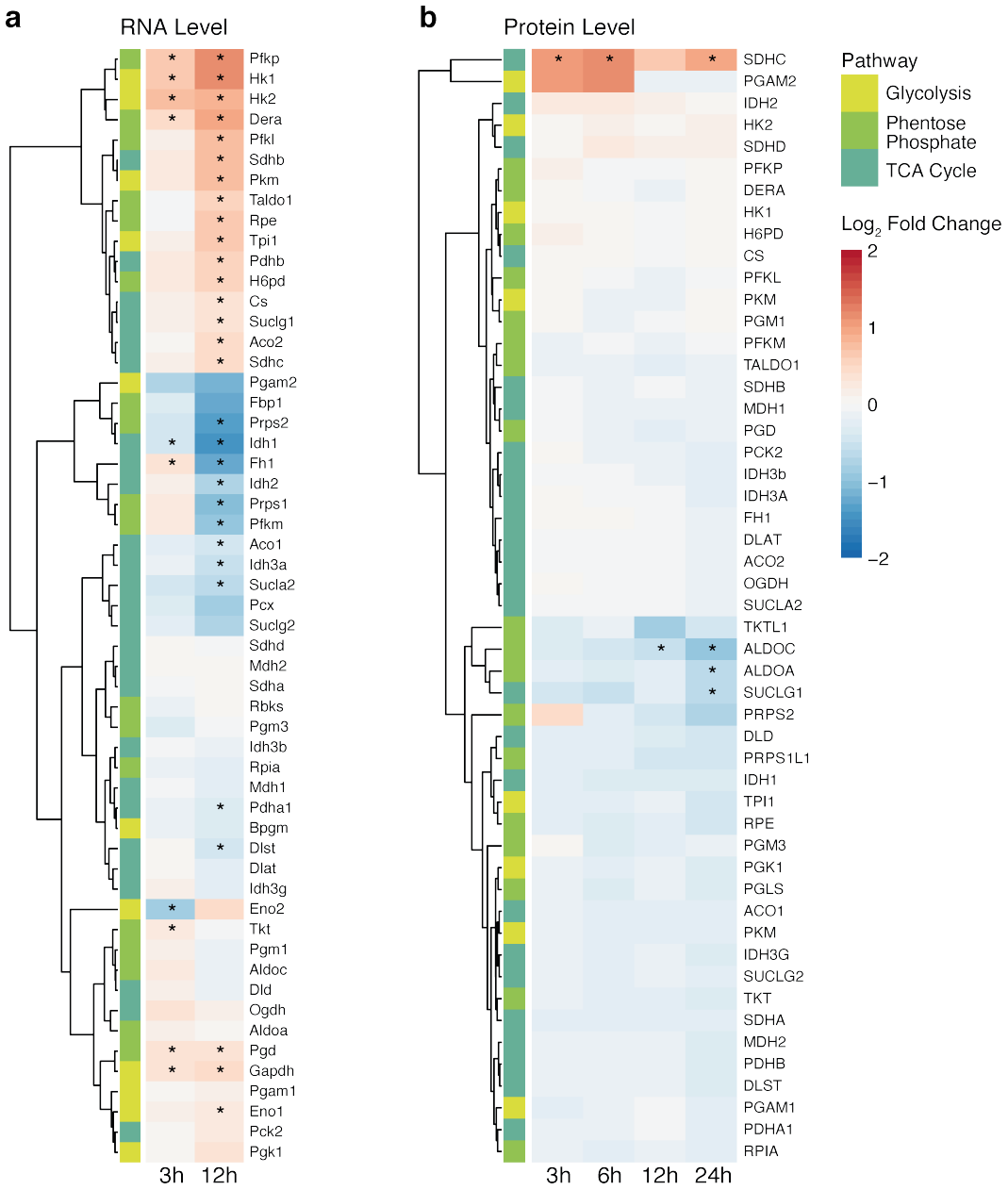

Figure 13: Expression levels of enzymes involved in glycolysis, the pentose phosphate pathway and the TCA cycle. Heat map of a) RNA and b) protein $\log_2$ fold changes in BMDMs treated with 100 IU/ml IFNβ. RNA expression was determined by PAT-seq (n = 3, * FDR < 0.05), protein levels were measured prior to this thesis by quantitative mass spectrometry (n = 3, * FDR < 0.05).

One of the defining features of anti-inflammatory M2 macrophages is an increased metabolism of amino and nucleotide sugars, which requires an intact TCA cycle and leads to elevated levels of UDP-GlcNAc derivates (Jha et al. 2015). In this dataset, UDP-N-acetyl-D-galactosamine levels are significantly

elevated after 24 h of IFNβ treatment, UDP-glucose shows a slight upward trend, and UDP-glucuronate a significant reduction after 3 h (Fig. 12).
Most of these changes associated with the TCA cycle occurred in the late stages of IFNβ signaling from about 24 h, much in contrast to the rapid changes observed in the purine metabolism pathway.
Similarly, gene expression levels of about half of the enzymes involved in different carbohydrate metabolism pathways changed after 12 h of IFN treatment (Fig. 13a). However, only a small number of them translated to protein level at 12 h or 24 h (Fig. 13b), suggesting that changes to the total protein level might not be the sole cause for metabolic changes. The only significantly upregulated protein is SDHC, one of four components that make up the succinate dehydrogenase complex in the electron transport chain at the mitochondrial membrane, which converts succinate to fumarate and can lead to increased production of ROS (Ryan & O'Neill 2020).

3.3.5 Integration of Protein Expression Changes in IFNβ-Activated BMDMs

To assess the relationship between RNA and protein changes globally, BMDM PAT-seq data was correlated with protein expression changes of BMDMs treated with 100 IU/ml IFNβ for 3 h, 6 h, 12 h and 12 h, which was generated by Michelle Tate and analyzed by Nathan Croft and Jamie Gearing.
When comparing RNA and protein expression level changes for all detected genes, it is very clear that the lack of correlation is not specific to enzymes of the carbohydrate metabolism (Fig. 14). Only a small number of the changes observed at the RNA level after 3 h of treatment with IFNβ were also detected at the protein level after 3 h (Fig. 14a).
Throughout the next 21 h, more of the 3 h transcriptional changes are detected on protein level, along with a general increase in differentially expressed proteins (Fig. 14b–d). However, the number of differentially expressed transcripts after 12 h is also increased compared to 3 h, and only a fraction of them were translated after 12 h and 24 h (Fig. 14e and f). Additionally, a very small number

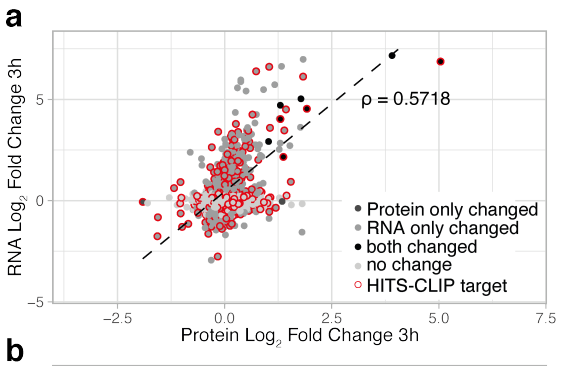

3h RNA - Protein Correlation

	3h	6h	12h	24h
Protein only changed	2	3	7	31
RNA only changed	1408	1387	1348	1321
both changed	8	29	68	95
no change	3207	3206	3202	3178

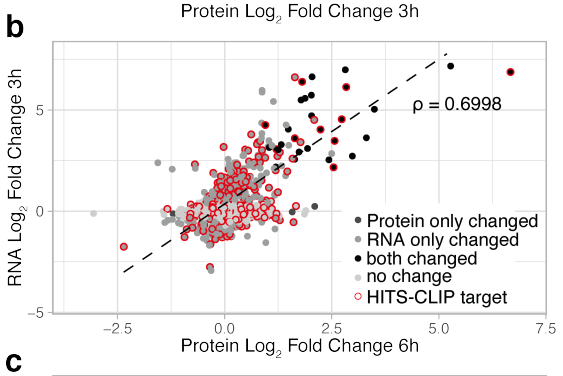

12h RNA - Protein Correlation

	12h	24h
Protein only changed	3	12
RNA only changed	2446	2404
both changed	72	114
no change	2104	2095

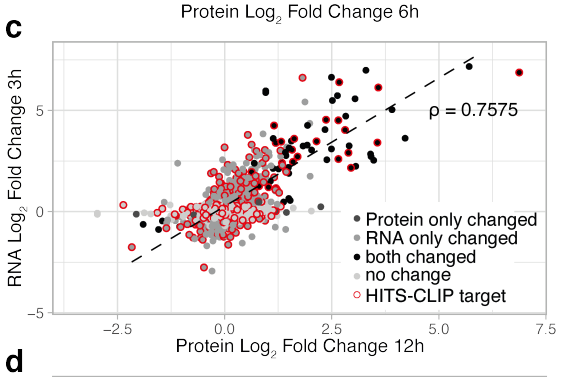

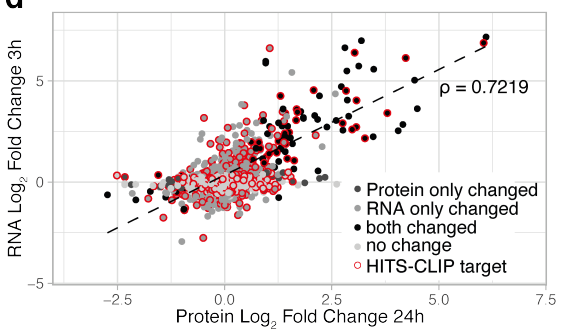

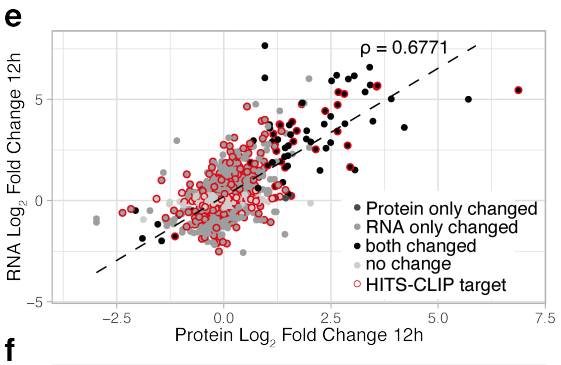

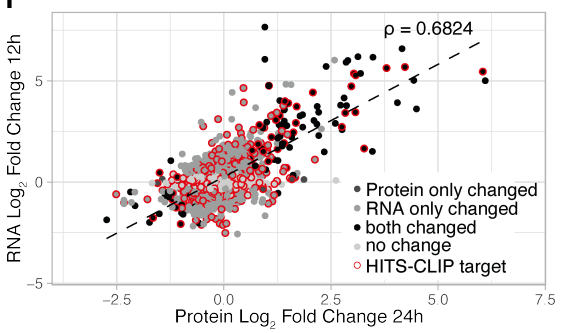

Figure 14: Correlation of RNA and protein level changes in BMDMs treated with 100 IU/ml IFNβ. Correlation of 3 h RNA log_2 fold changes and protein log_2 fold changes after a) 3 h, b) 6 h, c) 12 h and d) 24 h. RNA log_2 fold changes after 12 h were plotted over protein log_2 fold changes after e) 12 h and f) 24 h. RNA expression was determined by PAT-seq (n = 3, FDR < 0.05), protein levels were measured prior to this thesis by quantitative mass spectrometry (n = 3, FDR < 0.05). Genes targeted by miRNAs as determined by HITS-CLIP prior to this thesis are highlighted with a red outline (n=3, FDR< 0.05). The correlation coefficient of a Pearson correlation test on changed genes is shown in each graph. The number of genes in each category are listed in the tables.

of proteins were differentially expressed while their transcript levels stay constant. This strongly suggests that many genes are regulated post-transcriptionally, which can be mediated by many factors.

One example of post-transcriptional regulation highlighted in Figure 14 is miRNA binding, which can lead to degradation of complementary RNA. Some of these miRNA targeting events were detected in a HITS-CLIP experiment in BMDMs treated with 100 IU/ml IFNβ for 3 h, which was performed and analyzed by Sam Forster and Kate Jeffrey. This HITS-CLIP dataset contains sequences of both miRNAs and target RNAs that were crosslinked to argonaute 2 (AGO2), a protein that binds miRNAs and enables recognition and degradation of complementary target RNA (Darnell 2010).

Genes targeted by miRNAs are highlighted with a red circle in all graphs in Figure 14. A large number of genes with changes on RNA, but not protein level, fall into this category, but the majority does not. Additionally, genes whose RNA and protein expression correlates are targeted to a similar extent, which shows that miRNA binding is only one of many mechanisms that can contribute to the final picture.

3.3.6 Alternative Polyadenylation in IFNβ-Treated BMDMs

Another mechanism that diversifies transcriptional responses was detected through the PAT-seq approach. Since the poly-A tail was used during the library preparation, it is possible to determine the exact 3'-end of each sequenced transcript and therefore the length of the 3'-UTR.

Multiple transcripts per gene were detected this way, which were generated through APA, and had been combined for the previous gene expression analysis. However, not all transcripts per gene responded to IFNβ treatment in the same way. To assess this further, the ratio of expression levels was calculated for the two most highly abundant transcripts per gene and plotted in Figure 15a and b.

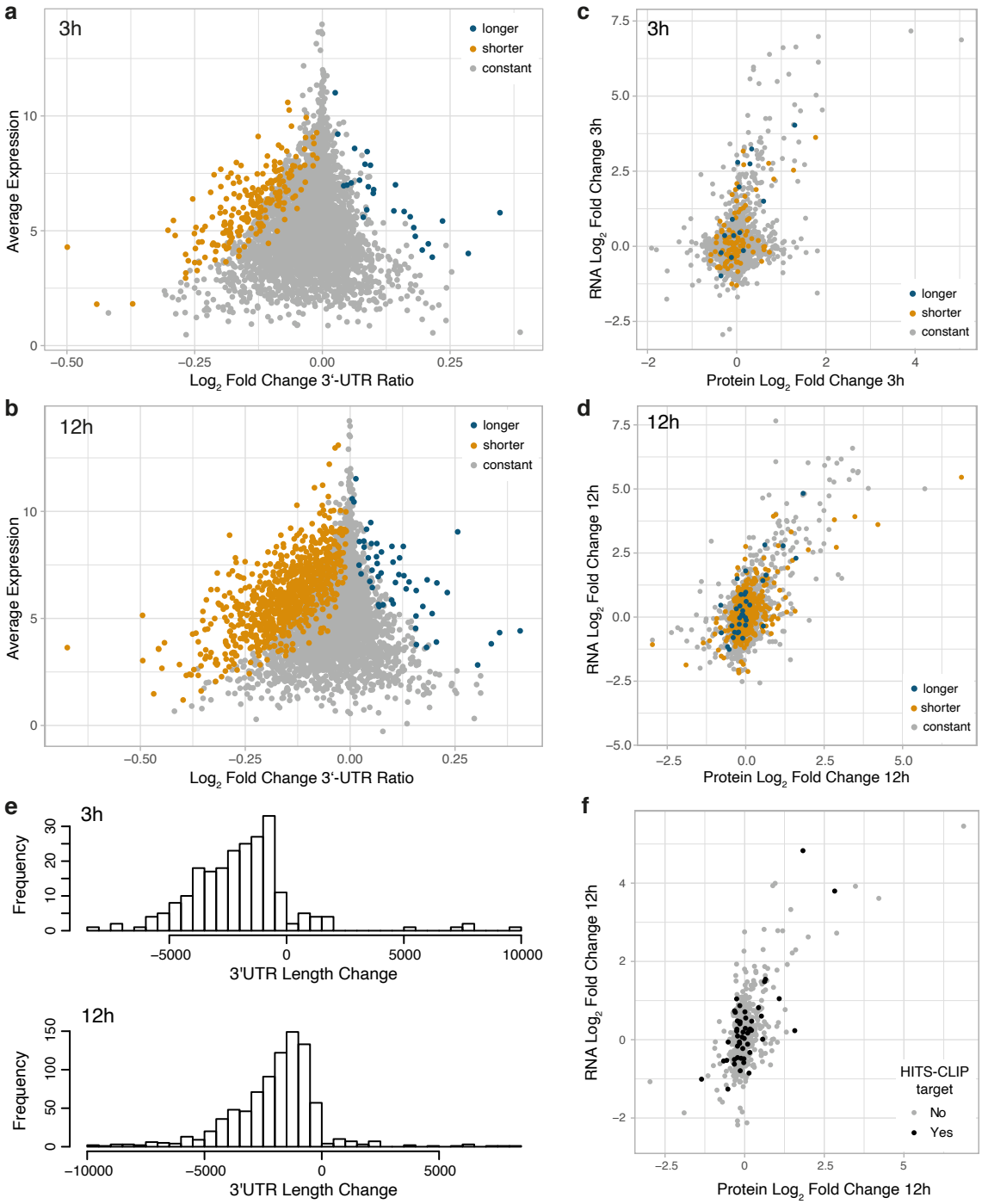

Figure 15: 3'-UTR length changes in BMDMs in response to IFNβ. Average gene expression plotted over $\log_2$ fold changes of 3'-UTR isoform ratios in BMDMs after a) 3 h and b) 12 h of treatment with 100 IU/ml IFNβ (n=3, FDR < 0.05). Changes summarized at the gene level are plotted over protein changes after c) 3 h and d) 12 h. Shortened and lengthened genes are highlighted. e) Histogram of 3'-UTR length changes after 3 h and 12 h. f) Protein changes of shortened and lengthened genes after 12 h plotted over gene-wise RNA changes; genes containing miRNA binding sites in the dynamic 3'-UTR are highlighted in black (HITS-CLIP; n=3, FDR < 0.05, measured prior to this thesis).

Ratios shifted towards the transcript with a longer 3'-UTR were plotted in blue and called "longer"; ratios shifted towards the shorter transcripts were called "shorter" and plotted in orange. A total of 204 and 831 genes were shortened after 3 h and 12 h respectively, and 27 and 51 genes were lengthened.

Lengthening and shortening of transcripts did not appear to influence or be influenced by overall transcript or protein changes at either time point (Fig. 15c and d), since changes in transcript lengths were observed regardless of the degree of change in overall transcript levels.

The distribution of length differences between the two investigated transcripts per gene spanned more than 10,000 bases, but the majority were seen within 0 and 5,000 bases (Fig. 15e). The changes in 3'-UTR length for each gene observed after 3 h were dispersed across this range with an increasing trend in frequency around 1,000 bases, whereas the changes in 3'-UTR length for each gene recorded after 12 h are more focused around 2,000 bases.

The incorporation of miRNA binding events within these dynamically expressed 3'-UTRs, as identified in the previously mentioned HITS-CLIP dataset, shows that 51 of the shortened and lengthened genes after 12 h were targeted (Fig. 15f).

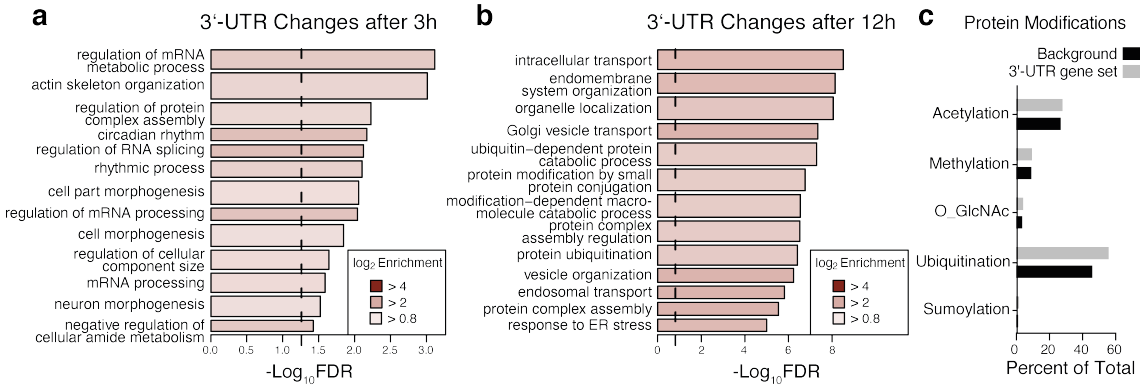

Figure 16: *In silico* characterization of BMDM 3'-UTR gene sets. Top results of a statistical gene set overrepresentation test of lengthened and shortened genes after a) 3 h and b) 12 h of 100 IU/ml IFNβ treatment in BMDMs (PAT-seq; n=3, FDR < 0.05) performed using PANTHER. The bar width represents the size of the gene set, the length its $-\log_{10}$FDR and the color its $\log_2$ enrichment value. The dashed line at 1.3 (equivalent to an FDR value of 0.05) indicates the threshold for statistical significance. c) Potential protein modifications of shortened and lengthened genes after 12 h compared to a background gene set consisting of all differentially expressed genes.

This illustrates how selective induction or repression of different 3'-UTR transcript isoforms could affect regulation of the corresponding protein level. Binding sites for miRNAs are only one example of post-transcriptional regulation mechanisms that are influenced by dynamic 3'-UTRs. Many others, such as recognition motifs of RNA-binding proteins, will be affected in a similar way.

Many genes with shortened or lengthened 3'-UTRs in response to IFNβ treatment are not among the well-described IRGs. *In silico* analyses proved inconclusive and revealed little to no shared ontology between them. A gene set overrepresentation analysis on shortened and lengthened transcripts at 3 h resulted in a few significant ontologies connected to RNA processing and cellular morphogenesis (Fig. 16a). However, the false discovery rate (FDR) values are very high, suggesting potential false positive results, which makes further investigation of biological relevance difficult without more information. FDR values of the 12 h time point analysis are much lower (Fig. 16b). The top results show various gene sets connected to intracellular protein transport, localization and metabolism, as well as vesicles. Determining the relationship between 3'-UTRs and nascent protein localization proved challenging, however.

De novo motif analyses led to no significant results (data not shown), suggesting there is no specific signaling or binding sequence associated with 3'-UTR length change, and the subcellular localization of the proteins encoded by the changed transcripts as described in the Human Cell Atlas was similar to that of all differentially expressed genes (data not shown). The extent of potential post-translational protein modifications of the changed transcripts was also comparable to that of all differentially expressed genes used as a background dataset (Fig. 16c). Overall, no shared characteristics other than dynamic 3'-UTR length in response to IFNβ treatment could be identified at this stage.

3.3.7 Transcriptomic Changes in IFNβ-Activated HMDMs and Comparison to BMDMs

To get an indication of the level of cross-species conservation of IFNβ signaling, the previous PAT-seq experiment (Fig. 9 and 15) was repeated in HMDMs. Five

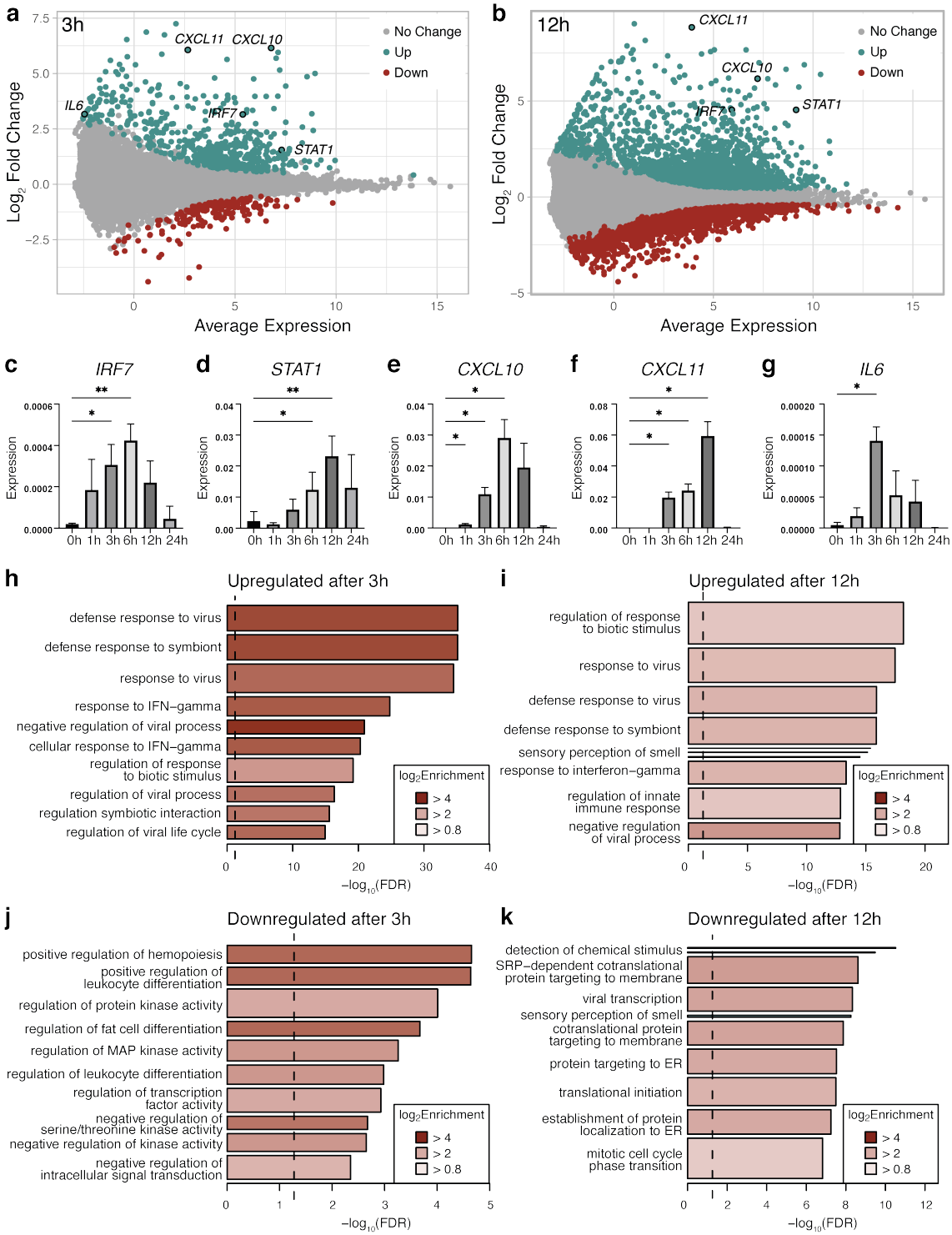
a
3h
CXCL11
CXCL10
IL6
IRF7
STAT1
No Change
Up
Down
Log2 Fold Change
Average Expression
b
12h
CXCL11
CXCL10
IRF7
STAT1
No Change
Up
Down
Log2 Fold Change
Average Expression
c
IRF7
d
STAT1
e
CXCL10
f
CXCL11
g
IL6
Expression
0h 1h 3h 6h 12h 24h
h
Upregulated after 3h
defense response to virus
defense response to symbiont
response to virus
response to IFN−gamma
negative regulation of viral process
cellular response to IFN−gamma
regulation of response to biotic stimulus
regulation of viral process
regulation symbiotic interaction
regulation of viral life cycle
log2Enrichment
> 4
> 2
> 0.8
−log10(FDR)
i
Upregulated after 12h
regulation of response to biotic stimulus
response to virus
defense response to virus
defense response to symbiont
sensory perception of smell
response to interferon−gamma
regulation of innate immune response
negative regulation of viral process
log2Enrichment
> 4
> 2
> 0.8
−log10(FDR)
j
Downregulated after 3h
positive regulation of hemopoiesis
positive regulation of leukocyte differentiation
regulation of protein kinase activity
regulation of fat cell differentiation
regulation of MAP kinase activity
regulation of leukocyte differentiation
regulation of transcription factor activity
negative regulation of serine/threonine kinase activity
negative regulation of kinase activity
negative regulation of intracellular signal transduction
log2Enrichment
> 4
> 2
> 0.8
−log10(FDR)
k
Downregulated after 12h
detection of chemical stimulus
SRP−dependent cotranslational protein targeting to membrane
viral transcription
sensory perception of smell
cotranslational protein targeting to membrane
protein targeting to ER
translational initiation
establishment of protein localization to ER
mitotic cell cycle phase transition
log2Enrichment
> 4
> 2
> 0.8
−log10(FDR)

Figure 17: Differential gene expression in HMDMs in response to treatment with 100 IU/ml IFNβ. Log_2 fold change of up- and downregulated genes with FDR < 0.05 after a) 3 h and b) 12 h of treatment over average expression in all samples are shown in green and red respectively. Validation of *IRF7* c), *STAT1* d), *CXCL10* e), *CXCL11* f) and *IL6* g) gene expression via qPCR (n = 5, asterisks indicate significance using a one-way ANOVA, * $p < 0.05$, ** $p < 0.01$). h) – k) Top results of statistical gene set overrepresentation tests performed using PANTHER are shown for both time points for up- and downregulated genes. The bar width represents the size of the gene set, the length its $-\log_{10}$FDR and the color its log_2 enrichment value. The dashed line at 1.3 (equivalent to an FDR value of 0.05) indicates the threshold for statistical significance.

instead of three replicates were used to control for potential inter-individual variability.

As seen in the mouse data, the expression level of a very large number of genes is changed in response to IFNβ: 539 and 2,109 are upregulated after 3 h and 12 h respectively; 192 and 1,611 are downregulated (Fig. 17a and b). Some of these changes can also be seen in the qPCR results derived from HMDMs of five independent donors (Fig. 17c–g). The fold changes of *IRF7*, *STAT1*, *CXCL10* and *CXCL11* reflect the sequencing results at the 3 h time point, and with the exception of IL6, also the results after 12 h; *IL6* transcript levels were below the analysis threshold after 12 h. The additional treatment times in these experiments extend the PAT-seq data and reveal distinct expression kinetics, which show how differently IRGs are affected by the complex regulatory mechanisms controlling the global cellular response.

The results of a statistical gene set overrepresentation test showed similar ontologies to the mouse experiment in upregulated genes after 3 h (Fig. 17h): responses and regulation of viral infections and cellular IFN responses. The gene sets associated with downregulated genes (Fig. 17j), however, were quite different to the response in mouse cells. Instead of cell cycle-associated ontologies, this analysis resulted in gene sets connected to regulation of cell signaling, in particular kinase activity, as well as regulation of leukocyte differentiation and transcription factor activity.

More differences in the IFNβ response of BMDMs and HMDMs can be observed in the 12 h up- and downregulated genes. The results of upregulated genes are

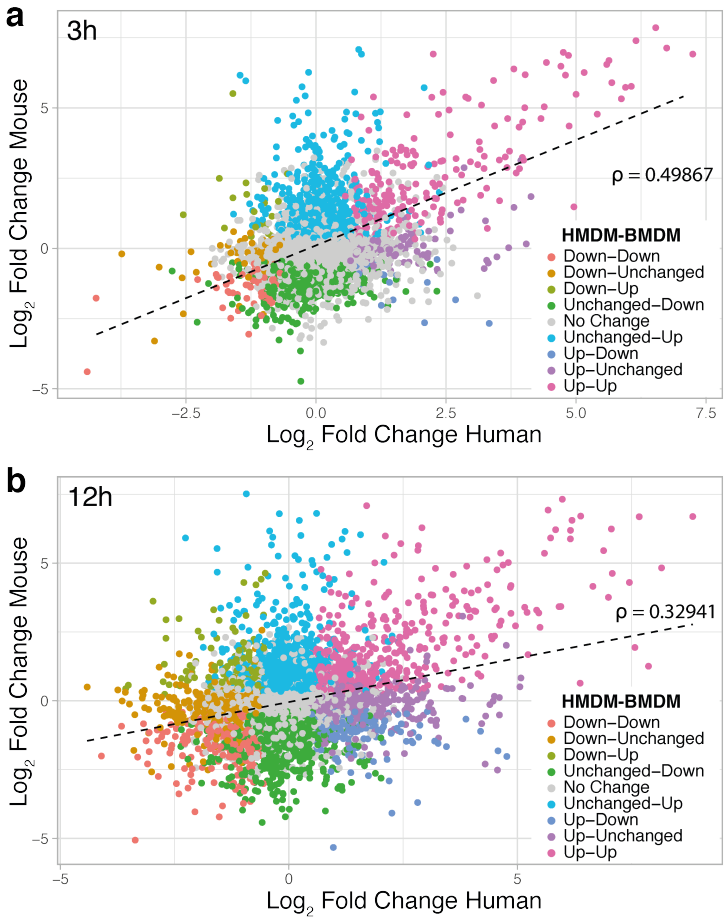

HMDM - BMDM	3h	12h
Down - Down	68	430
Down - Unchanged	59	536
Down - Up	20	174
Unchanged - Down	1094	1637
No Change	7277	4093
Unchanged - Up	992	1550
Up - Down	22	283
Up - Unchanged	142	643
Up - Up	206	559

Figure 18: Correlation of gene log_2 fold changes in BMDMs and HMDMs treated with 100 IU/ml IFNβ. Correlations shown after a) 3 h and b) 12 h (PAT-seq; n=3, FDR < 0.05). Genes are colored depending on up- and downregulation in either species. The Pearson correlation coefficient of changed genes is shown in each graph. The number of genes in each category is listed in the table.

similar to 3 h, showing regulation and responses to viral infection and IFN treatment (Fig. 17i). In comparison, the protein catabolic process and cytokine production ontologies seen in the mouse data are not among the top results.

As seen at the 3 h timepoint, the top gene sets of the downregulated genes after 12 h (Fig. 17k) are very different from the mouse data. The main ontologies are associated with protein localization and translation initiation and cell cycle progression.

These differences between species become more apparent when the log_2 fold changes of orthologous genes are correlated after 3 h and 12 h of IFN treatment (Fig. 18). The most highly upregulated genes show similar induction levels in both

species (pink dots) suggesting a similar core response. However, most of the other induced or repressed genes are specific to only one species, highlighting the differences already seen in the gene set overrepresentation analysis. This is made even clearer by the low correlation coefficients of 0.499 and 0.329 for changes detected after 3 h (Fig. 18a) and 12 h, respectively (Fig. 18b).

3.3.8 Alternative Polyadenylation in IFNβ-Treated HMDMs

In this PAT-seq dataset, we can again detect multiple transcripts of different lengths per gene, a result of APA. When observing the ratios of the two most highly expressed transcripts per gene as before, no significant changes were detected after 3 h of IFNβ treatment (Fig. 19a). After 12 h, the 3'-UTRs of 12 genes were shown to lengthen and those of 311 genes shortened (Fig. 19b).
When comparing shortened and lengthened genes to the other differentially expressed genes after 12 h, it is clear that they show no association with fold change or average expression, as was the case for the mouse genes (Fig. 19c).
The majority of transcripts are shortened by up to 5,000 bp after 12 h of IFN treatment (Fig. 19d), a similar range but different distribution compared to the mouse data. When comparing the $\log_2$ fold change of ratios of the 88 genes that showed altered 3'-UTR lengths in both species after 12 h of IFNβ treatment, however, it is very apparent that the 3'-UTR shift is not highly conserved. The correlation coefficient is 0.185, and even the genes with very similar transcript length changes highlighted in black show a lot of variation. This reflects the differences seen in the total gene differential expression results.
Validating some of the changes seen in the sequencing results and investigating expression levels of individual transcripts is technically challenging, because the shorter transcript cannot be uniquely detected by a qPCR. Instead, the total gene level and LU transcripts were measured using two primer pairs. One primer pair targets the coding region or 5'-end of the 3'-UTR to detect the total gene level and another primer pair targets the distal 3'-UTR and was designed to measure only the longer transcript variant.

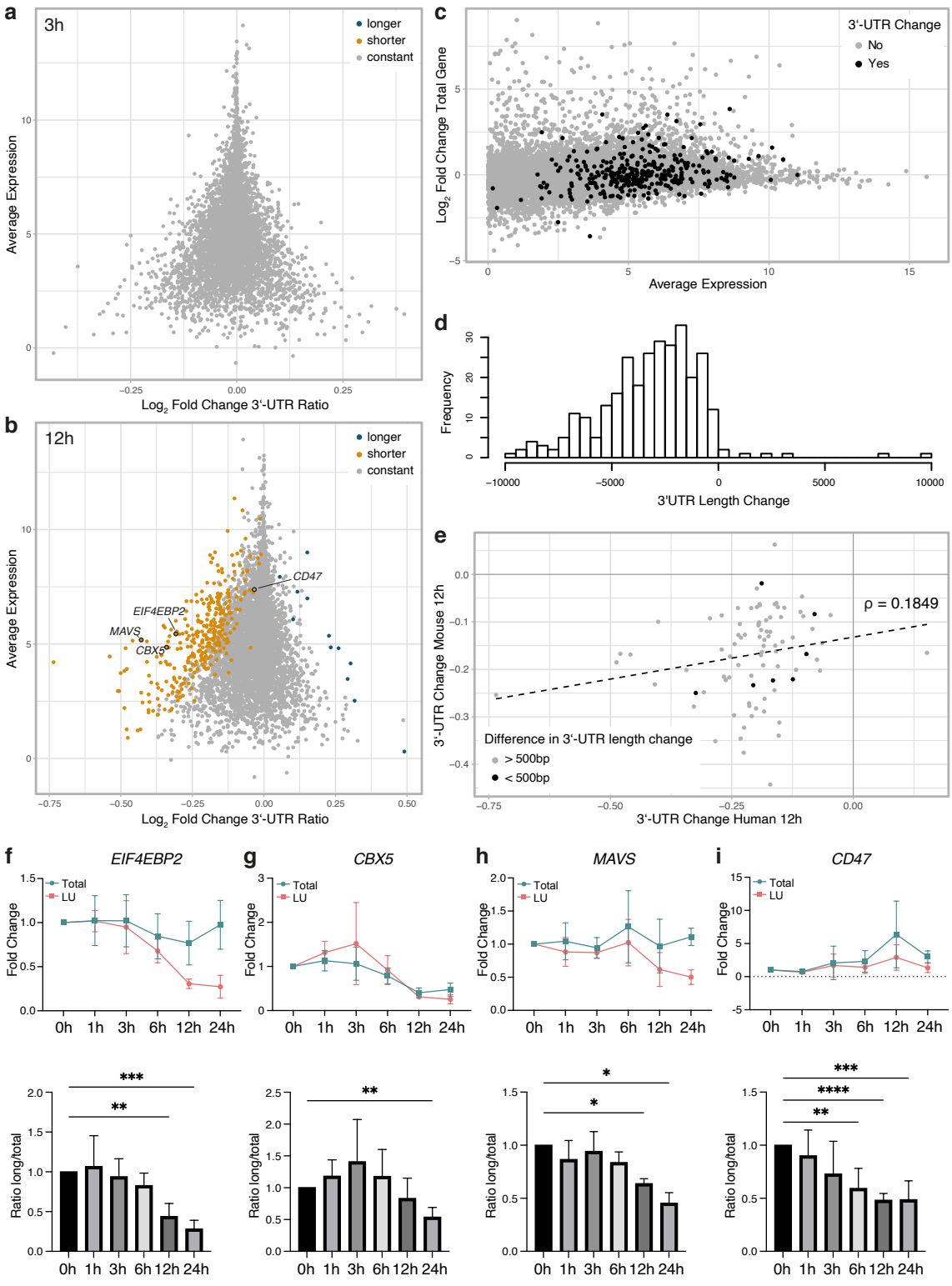
a
3h
longer
shorter
constant
Average Expression
Log2 Fold Change 3'-UTR Ratio
b
12h
longer
shorter
constant
CD47
EIF4EBP2
MAVS
CBX5
Average Expression
Log2 Fold Change 3'-UTR Ratio
c
3'-UTR Change
No
Yes
Log2 Fold Change Total Gene
Average Expression
d
Frequency
3'UTR Length Change
e
ρ = 0.1849
Difference in 3'-UTR length change
> 500bp
< 500bp
3'-UTR Change Mouse 12h
3'-UTR Change Human 12h
f
EIF4EBP2
g
CBX5
h
MAVS
i
CD47
Total
LU
Fold Change
0h 1h 3h 6h 12h 24h
Ratio long/total
***
**
*
****

Figure 19: 3'-UTR length changes in HMDMs in response to 100 IU/ml IFNβ. Average gene expression plotted over log_2 fold changes of 3'-UTR isoform ratios after a) 3 h and b) 12 h (PAT-seq; n=3, FDR < 0.05). c) Log_2 fold changes after 12 h plotted over average expression, lengthened and shortened genes are highlighted in black. d) Histogram of 3'-UTR length changes after 12 h. e) Correlation of log_2 fold changes of 3'-UTR isoform ratios after 12 h in mouse plotted over human. qPCR analysis results of different 3'-UTR isoforms of f) *EIF4EBP2*, g) *CBX5*, h) *MAVS* and i) *CD47*. Fold changes are of each are shown in the top row, a ratio is in the bottom (n = 5, asterisks indicate significance tested by a one-way ANOVA, * $p < 0.05$, ** $p < 0.01$, *** $p < 0.001$, **** $p < 0.0001$).

Changes to the 3'-UTR length of *EIF4EBP2*, chromobox 5 (*CBX5)*, *MAVS* and *CD47* (Fig. 19f–i) by 100 IU/ml IFNβ were investigated over a 24 h time period in HMDMs derived from five independent donors. Individual expression levels measured with both primer pairs are shown in the top row; a ratio of the two, similar to the sequencing results, is shown in the bottom row. All genes were significantly shortened when depicted as a ratio of LU/total, but the changes to the individual expression levels contributing to this observation are different. The *EIF4EBP2* and *MAVS* total gene levels remained unchanged across the measured time period, whereas the LU-specific transcript levels decreased (Fig. 19f and h). Both CBX5 transcript measurements decreased over time; however, the ratio plot below shows that there is a significant difference by 24 h, roughly half the expression of the total (Fig. 19g). Lastly, the *CD47* total gene expression increased over time, whereas the LU transcript remained constant (Fig. 19i).
The qPCR results could only be indirectly compared to the sequencing data, since the short transcript was not measured specifically. The *MAVS*, *CBX5* and *EIF4EBP2* results reflect the ratio log_2 fold changes highlighted in in Figure 19b, *CD47* total and LU transcript measurements by qPCR show a higher degree of shortening than the PAT-seq data.

3.3.9 Ontology Analyses of Transcripts with Changed 3'-UTR Lengths in IFNβ-Activated HMDMs

Identifying a shared ontology between the shortened and lengthened transcripts with different *in silico* approaches proved just as challenging as for the mouse

analysis. A statistical gene set overrepresentation test resulted in a very small number of significant changes, which are associated with serine modifications, intracellular transport, translation, amide metabolism and WNT signaling (Fig. 20a). However, the FDR values are very high, suggesting the results may not be biologically relevant. Potential modifications of the corresponding proteins of changed genes were similar to that of all differentially expressed genes used as a background set (Fig. 20c). The *de novo* motif enrichment led to no significant results and protein localization of changed genes was comparable to that of the background genes (data not shown).

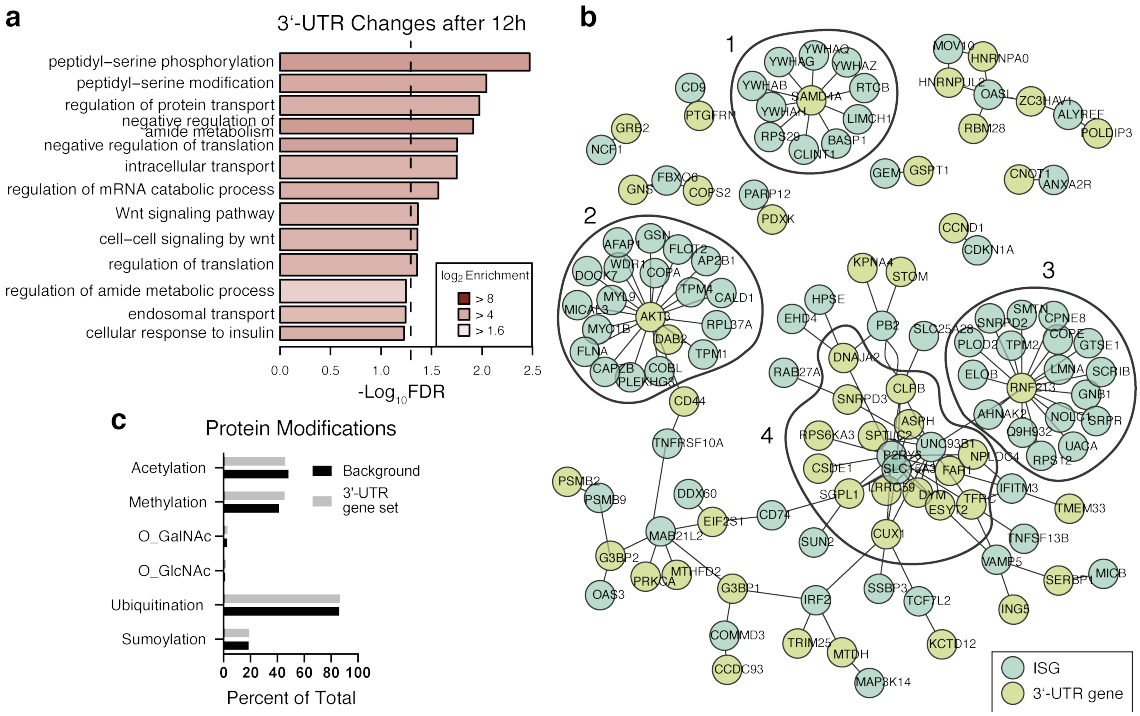

Figure 20: *In silico* characterization of the 12 h HMDM 3'-UTR gene set. a) Top results of a statistical gene set overrepresentation test of lengthened and shortened genes after 12 h of 100 IU/ml IFNβ treatment (PAT-seq; n=3, FDR < 0.05) performed using PANTHER. The bar width represents the size of the gene set, the length its $-\log_{10}$FDR and the color its $\log_2$ enrichment value. The dashed line at 1.3 (equivalent to an FDR value of 0.05) indicates the threshold for statistical significance. b) Protein interaction network of interactions described by Hubel et al. that involve a lengthened or shortened gene (Hubel et al. 2019). c) Potential protein modifications of shortened and lengthened genes after 12 h compared to a background gene set.

3’-UTRs can facilitate the formation of protein complexes through a scaffold-like function, and protein-protein interactions are an important aspect of IRG function (Lee & Mayr 2019). Some of these IRG interactions with non IFN-regulated proteins have been described Hubel and colleagues, which were compared to the list of genes with changed 3’-UTRs in this study (Hubel et al. 2019). Interactions that involve one of these genes were plotted in Figure 20b.

Three clusters of IRGs around changed genes were formed: the first around sterile alpha motif domain-containing 4A (SAMD4A), an RNA-binding protein involved in translational repression; the second around AKT3, a kinase involved in cell signaling; and the third around ring finger protein 213 (RNF213), an E3 ubiquitin ligase that is known to mediate protein-protein interactions (Ahel et al. 2020; Baez & Boccaccio 2005). A fourth cluster was formed by changed genes around three IRGs: solute carrier family 15 member 3 (SLC15A3), a transporter protein thought to be involved in TLR and NOD-signaling; Unc-93 homolog B1 (UNC93B1), a TLR-trafficking protein; and pyrimidinergic receptor P2Y6 (P2RY6), a UDP-sensing receptor that may be involved in inflammatory responses (Hao et al. 2014; Pelka et al. 2018; Song et al. 2018). Translational repression and protein transport are ontologies also represented in the gene set enrichment result, as is phosphorylation of peptidyl-serine, one of the targets of AKT signaling.

The results overall suggest that changing transcript lengths is a regulatory mechanism of very diverse genes and can therefore be involved in many different functions. They would be ideally investigated on an individual basis.

3.4 Discussion

In this study, properties of IFNβ-treated BMDMs and HMDMs were investigated by creating and integrating large datasets at different molecular levels. This work contributes to the understanding of the molecular mechanisms underlying functional reprogramming of macrophages in response to IFNβ.

3.4.1 RNA Expression Changes in BMDMs and HMDMs Treated with IFNβ

Assessing transcriptomic changes is the obvious starting point of the analysis, because IFN signaling is well known to activate a signaling cascade, culminating in transcriptional activation of certain IRGs. The expression level of a few thousand genes in BMDMs was altered in the PAT-seq experiment in response to IFNβ treatment. This number is comparable to previously published literature when a commonly used fold change cut-off value of 2 was considered (Rusinova et al. 2013; Shaw et al. 2017). Expression levels of some core IRGs were further validated, such as the antiviral chemokines *Cxcl10* and *Cxcl11* and the transcription factor *Stat1* (Trifilo et al. 2004; Wuest & Carr 2008).

The gene set analysis results showed that the identified IRGs were representative of IFNγ and viral infection. The detected gene sets in up- and downregulated genes at both time points also reflect well-known IRG functions like production of cytokines that have antiviral properties and changes to proliferation through effects on chromosome segregation and cell cycle inhibition respectively (Bekisz et al. 2010; Tsuno et al. 2009). Additionally, changes to phosphorus metabolism were suggested in the early time point, which are potentially reflective of various kinase signaling cascades activated upon receptor binding (Wang & Fish 2019). Gene sets associated with catabolic processes were overrepresented among downregulated genes after 12 h. This has previously been shown to be dependent on NFκB, one of the transcription factors activated in response to IFNβ (Pijet et al. 2013).

While similar numbers and ontologies overall were seen in human cells as well, a direct comparison between species shows many differences in gene induction. Although both experiments were performed in comparable cell types, BMDMs and HMDMs are extracted from distinct tissues and are differentiated following different protocols. Some differences especially in metabolic pathways have been described before (Ahmed et al. 2018). Another paper has compared the effects of type I IFN induction across ten different species and cell types and found a core response of only 62 genes (Shaw et al. 2017). This clearly shows the importance of key IFNβ-mediated antiviral effects, while highlighting the specificity depending on cell type and species (Rusinova et al. 2013).

The effects of the main ontologies observed in the statistical gene set overrepresentation tests in BMDMs have been well published. However, not all transcripts contributing to the results of this analysis are reflective of their corresponding protein level within 24 h, as seen through comparison with proteomics data. It may take longer for these transcripts to be translated, which could be investigated with a more extensive time course. It is also possible that the corresponding proteins half-life is shortened in response to IFNβ, and a larger amount of transcript or faster rate of translation is needed to keep the protein level consistent. Lastly, the changed RNA level may serve a function that is independent of immediate translation, such as miRNA sinks. The contribution of miRNAs to regulation of type I IFN signaling has already been extensively described and the global scope of targeted genes could be assessed in this study using HITS-CLIP data (Forster et al. 2015). Transcripts can be targeted in multiple positions by the same or different miRNAs, scenarios that were not considered here (Li et al. 2013; Wang et al. 2010). Different binding events can result in different effects, adding another dimension to an already complex system. These effects cannot be assessed accurately using current omics approaches and are much better investigated on an individual basis.

3.4.2 Rapid Changes to the Purine Metabolism Pathway in BMDMs by IFNβ

A class of compounds that reflects functional changes directly are metabolites. Among the most rapidly changing metabolites in response to IFN stimulation at 1 h and 3 h in this study were those involved in purine metabolism pathways. Purine metabolism was among the most highly enriched metabolic gene sets in an analysis on M2 macrophages performed by Hörhold and colleagues based on transcriptomic changes (Horhold et al. 2020). Conversely, the transcriptomic changes of genes in this pathway observed in this study did not translate to protein level. Instead, these nucleic acid metabolism changes precede transcriptomic changes. Therefore, it seems unlikely that the observed metabolite changes are the result of differential enzyme expression levels. They may instead be the result of altered enzymatic activity, for example through post-translational modifications like phosphorylation. Additionally, rapid changes to the purine biosynthesis pathways could contribute to the regulation of a subsequent transcriptional response by supplying or removing nucleotide substrates.
IMP biosynthesis is the rate-limiting step during *de novo* purine biosynthesis, hence its rapid accumulation suggests a catabolic pathway (Pareek et al. 2021). However, since this study only provides a snapshot of metabolite levels at certain time points and under certain conditions, it is not possible to determine if nucleotides were synthesized or degraded following IFNβ treatment. In a more detailed follow-up experiment, use of labelled media substrates could distinguish between these possibilities. Fluctuations in the purine metabolism pathway have also previously been reported in anti-inflammatory macrophages, therefore IFNβ-activated BMDMs might also have anti-inflammatory potential (Horhold et al. 2020).

3.4.3 IFNβ-Induced Changes to Metabolites of the TCA Cycle of BMDMs

Another metabolic pathway central to macrophage polarization is the TCA cycle (De Souza et al. 2019; Horhold et al. 2020; Jha et al. 2015; Michelucci et al. 2013;

Mills et al. 2018; Ryan & O'Neill 2020; Strelko et al. 2011; Viola et al. 2019). Four key intermediates were identified in this experiment and were shown to only vary slightly upon IFNβ treatment, suggesting that the pathway is intact and functional, again supporting an anti-inflammatory phenotype seen in M2 macrophages. This observation seems to be further supported by UDP-GlcNAc, a metabolite belonging to the UDP amino sugar group involved in protein glycosylation, an important mechanism in M2 macrophages (Jha et al. 2015). However, only two other members of this class were identified and were not significantly upregulated.

Additionally, itaconate, a metabolite with pro-inflammatory properties, is significantly upregulated in BMDMs after 24 h of IFNβ treatment. Elevated itaconate levels have previously been shown in M1 macrophages and are the result of a break in the TCA cycle. Current literature describes the involvement of two enzymes, ACOD1 and IDH1 (Cordes et al. 2016; De Souza et al. 2019). ACOD1 catalyzes the conversion of a citrate isomerization intermediate to itaconate; its transcript levels were upregulated in pro-inflammatory macrophages (Michelucci et al. 2013; Strelko et al. 2011). IDH1 is one of three isozymes that catalyze the conversion of isocitrate to α-ketoglutarate. Its transcript and protein levels were downregulated in an IFN-dependent manner in M1 macrophages (De Souza et al. 2019). Transcript levels of both *Acod1* and *Idh1* were altered by IFNβ treatment in this study, but protein levels remained constant, suggesting an alternative regulatory mechanism in IFNβ-treated macrophages, which likely does not involve a break in the TCA cycle.

Only one of the identified enzymes involved in the TCA cycle, glycolysis and the pentose phosphate pathway was upregulated by IFNβ treatment of macrophages in this study. SDHC is part of the SDH protein complex that makes up part of the respiratory chain in the outer mitochondrial membrane that converts succinate to fumarate (Lampropoulou et al. 2016). Interestingly, its expression is inhibited by LPS treatment, which contributes to succinate accumulation (Dominguez-Andres et al. 2019). Increased succinate turnover would lead to increased production of ROS through reverse electron transfer, resulting in many pro-inflammatory effects downstream, such as HIF1α inhibition and increased IL1β production

(Ryan & O'Neill 2020). This is another aspect that would have to be explored in a more detailed secondary analysis, since SDHC is only one of four proteins that make up the SDH complex and enzyme activity is not just influenced by the amount of available enzyme, but also through availability of substrate, cofactors or inhibitors and sometimes also through post-translational modifications.
The differences in metabolite level fluctuations in the TCA cycle and closely related pathways in comparison to descriptions of M1 and M2 macrophages in the literature again highlights the ambivalence of IFNβ-activated macrophages.

3.4.4 IFNβ-Induced Increase in 3-Methylguanine Levels in BMDMs

Another metabolite that showed strong, rapid and sustained induction in this study was 3-methylguanine. Methylation of DNA is a well-known mechanism modulating transcriptional activity and replication (Wyatt et al. 1999). CpG methylation is most commonly associated with transcriptional silencing and is often linked to modification of histones, such as acetylation, and chromatin structure (Wood et al. 2016). One example of this is the activity of a reader of CpG methylation, methyl-CpG binding domain protein 2 (MBD2), which recognizes and binds methylated CpG sites and has histone-deacetylase and ATP-dependent nucleosome remodelling activity when associated with the nucleosome remodeling and deacetylase (NuRD) complex (Wood et al. 2016). Methylation patterns can be highly regulated, as shown for the *IFITM3* gene. The promotor of *IFITM3* is demethylated in response to type I IFN treatment, which results in enhanced transcription. It is methylated again shortly after, resulting in the same methylation pattern as before (Scott et al. 2011).
Free methylated purines, such as 3-methylguanine, are the product of DNA glycosylases (Sedgwick et al. 2007). While their substrate specificity overlaps significantly in different species, the only enzyme capable of excising alkylated bases identified to date in mammals is MPG (Hans et al. 2020; Robertson et al. 2009). Transcript levels of *Mpg* were not significantly changed in the PAT-seq data generated in this study and the protein was not identified in the proteomics data, likely due to technical limitations. MPG is a very slow-working enzyme, but

its activity can be boosted through association with different proteins, such as UV excision repair protein (RAD23) A and B, or phosphorylation, for example by the serine/threonine protein kinase ATM after exposure to oxidative stress or alkylating agents (Agnihotri et al. 2014; Miao et al. 2000). Additional phosphorylation sites on MPG were discovered in several high-throughput phosphoproteomics studies. The two most prevalent sites were identified using an antibody specific to phospho-MAP kinase and cyclin-dependent kinase (CDK) phosphorylation (Gu et al. 2011; Mertins et al. 2013; Moritz et al. 2010). Many MAP kinases are rapidly activated upon IFNβ treatment and can could potentially regulate MPG activity (Wang & Fish 2019). MPG activity should be assessed in future studies, in combination with experiments addressing changes to DNA methylation patterns and chromatin structure in response to IFNβ signaling in BMDMs.

3.4.5 Other Metabolic Changes in IFNβ-Activated BMDMs

Many other interesting pathways and metabolites were identified in this dataset, both novel and previously described in the literature, that can be explored further. Some examples are changes to the choline metabolism, which has been associated with inflammation, or the oxidation of fatty acids.

The changes observed in the dataset seem to constitute two waves of responses. The first wave occurs before transcriptomic and proteomic changes are observed. The second wave is detected at the same time or following these changes. Investigating these changes in more detail in the future will help to further connect the different stages that macrophages undergo following IFNβ stimulation.

Additionally, the macrophages show both pro- and anti-inflammatory properties that fluctuate over the 24 h time period investigated here. It is possible that the changes observed after 16 h and 24 h form the starting point for a sustained response in these cells, which poises them for a future stimulus or contributes to the development of a trained immune response (Cheon et al. 2013; Cheon & Stark 2009).

3.4.5 IFNβ-Induced Alternative Polyadenylation Pattern Changes in HMDMs and BMDMs

The development of inflammatory properties is likely not just the response of transcriptional changes. It is fine-tuned through various regulatory mechanisms on protein and RNA level, for example through the expression of different splice variants of transcripts. In the current study, differential expression of specific splice variants, transcripts with different 3'-UTRs, was measured in response to IFNβ treatment. Expression was shifted towards shorter 3'-UTR isoforms after 3 h and 12 h in BMDMs and is the result of APA, something that is regulated independently of the protein-coding sequence. This type of global scale shift has been previously described in various other biological circumstances, but no conserved mechanism or function has been identified to date (Jia et al. 2017; Li Y et al. 2012; Mayr & Bartel 2009; Miura et al. 2013). In some cases, differential expression of components of the polyadenylation machinery have been associated with global 3'-UTR shortening or lengthening; in others, activation of a specific signaling protein was involved, such as mTORC1 (Chang et al. 2015; Miles et al. 2016; Zhang S et al. 2019). The effect of IFNβ on these components and their involvement in the context of global shortening in macrophages has yet to be investigated.

The function of dynamic 3'-UTRs has also not been extensively explored; in the literature they have only been studied on an individual basis. Specific transcripts have been shown to act as scaffolds, leading to differential localization of the encoded protein or resulting in protein modifications (Berkovits & Mayr 2015; Lee & Mayr 2019). They diversify the function of the encoded protein without changing its coding sequence.

In this study, no clear shared ontology between genes that have varying 3'-UTR lengths has been found. Some of the significantly overrepresented gene sets after 12 h reflect the published roles of protein localization and protein complex formation, something that is best explored for individual candidates. Very similar observations were made in the HMDM dataset. Global shortening of transcripts was detected after 12 h of IFN treatment, but the overlap and conservation of the

identified genes between species was small. The degree of conservation is consistent with observations made on gene expression level in BMDMs and HMDMs discussed above, as well as the findings in literature on cross-species conservation of the type 1 IFN response by Shaw and colleagues described in this thesis previously (Shaw et al. 2017). Gene ontology analyses on this dataset lead to equally ambiguous results, similar to the BMDM data. The ontologies of protein complex formation and localization appear in both the gene set enrichment and protein interaction network analysis. They were also detected in the mouse analysis, suggesting an overarching theme that should be explored in future studies.

3.5 Conclusion

Overall, this study assessed the global reprogramming of mouse BMDMs by IFNβ, which has previously not been extensively described. Type I IFN responses are generally investigated as part of a more complex experiment, which is affected by secondary and sometimes tertiary stimuli, such as viral infection or immunostimulants.

First, extensive changes to transcript levels in IFNβ-treated BMDMs were described and compared to current literature, confirming the antiviral and antiproliferative nature of induced genes. After comparing transcript levels to protein expression, it became apparent that only a fraction of the elevated transcript levels is translated to protein. This opens up a discussion around the role of transcriptomic data and post-transcriptional regulation, such as the newly discovered field of dynamic 3'-UTRs, which will be explored further in the next chapter. Some areas of immunometabolism are likely highly affected by post-transcriptional gene regulation as well. The fluctuations in metabolite levels highlighted two waves of responses in BMDMs. The first is very rapid: it shows changes preceding the transcriptional response, such as in the purine biosynthesis pathway and the release of 3-methylguanine. These changes could be essential to initiate the transcriptional response mediated by the various

transcription factors activated by IFNβ. The second wave of metabolic changes is observed after 16 h and 24 h. The ambivalence of macrophage polarization by IFNβ becomes very apparent in the context of the scientific literature. Both pro- and anti-inflammatory properties can be seen in different metabolic pathways related to the TCA cycle, which places IFNβ-activated macrophages somewhere in the middle of the macrophage activation spectrum. Lastly, a comparison of transcriptional response in BMDMs and HMDMs emphasized the differences between species and cell types. Only the core IFNβ-induced IRGs and likely functions are conserved; many other aspects, including metabolic reprogramming, appear cell type- or species-specific and should be explored separately. Further metabolomics analyses on HMDMs could be used to characterize these differences and investigate potential rapid metabolic changes preceding the transcriptional response to IFNβ as seen in BMDMs. The effects highlighted in this study represent only a small selection of the global restructuring IFNβ induces. Many more can be investigated using this data as a starting point for a larger, more detailed project.

4. Characterizing the Effect of IFNβ on Alternative Polyadenylation

4.1 Introduction

Investigations of the global reprogramming of IFNβ-activated macrophages gave insight into a complex regulatory network across different stages of gene expression, protein function and cellular metabolism. Post-transcriptional regulation was shown to be a crucial component of this network, which is centered around 3'-UTRs harboring binding sites of miRNAs and RBPs. This study has shown that IFNβ treatment leads to shortening and lengthening of 3'-UTRs, a result of changed APA patterns, which can fine-tune post-transcriptional gene regulation.

70–80 % of human mRNAs contain multiple PASs with different usage preferences, which can be altered during development of an organism, during cellular differentiation or activation by an outside stimulus (Derti et al. 2012; Hoque et al. 2013). Proliferating cells and cancer cells have been shown to express more transcripts with a SU, while development and differentiation are often characterized by usage of more distal PASs and longer 3'-UTRs (Elkon et al. 2012; Fu et al. 2011; Hoque et al. 2013; Li Y et al. 2012; Lianoglou et al. 2013; Mayr & Bartel 2009; Miura et al. 2013; Sandberg et al. 2008; Ulitsky et al. 2012). The formation and function of the cleavage and polyadenylation machinery is dependent on interactions between more than 50 core proteins, as well as their association with other components depending on physiological context (Shi et al. 2009). The cleavage and polyadenylation protein complexes are intricately connected to DNA structures, such as the chromatin, DNA methylation and histone modifications, as well as other pre-mRNA processing mechanisms (Huang et al. 2013; Jiao et al. 2013; Li et al. 2016; Mansfield & Keene 2012; Proudfoot et al. 2002). These related ontologies involve an equally large number of components that differ depending on the cellular physiological context, which makes mechanistic studies of APA very challenging. Over the last decades, many

researchers have identified differential expression and interactions of some components of the cleavage and polyadenylation machinery, such as RBBP6, CSTF2, CSTF3, CLP1, FIP1, NUDT21 and PCF11, as regulators of APA, as well as some unrelated proteins, like E2F, TDP43, mTORC1 and some transcription factors (Beaudoing et al. 2000; Brumbaugh et al. 2018; Chan et al. 2011; Chang et al. 2015; Di Giammartino et al. 2014; Elkon et al. 2012; Gruber et al. 2012; Isobe et al. 2020; Kwon et al. 2021; Lackford et al. 2014; Li et al. 2015; Luo et al. 2013; Martin et al. 2012; Modic et al. 2019; Rappsilber et al. 2002; Takagaki et al. 1996; Turner et al. 2020; Wang et al. 2019; Xing et al. 2008; Yao et al. 2013; Zhu et al. 2018). The expression level of some of these proteins can be altered in response to type I IFNs and they could therefore play a role in the context of this study as well (Rusinova et al. 2013).

Functional consequences of PAS usage in intronic and exonic regions, resulting in different protein splice variants, have been described in the literature, but differential effects of 3'-UTR transcript isoforms encoding the same protein have only been investigated in a small number of publications involving PAX3, BDNF, BIRC3 and CD47 (An et al. 2008; Berkovits & Mayr 2015; Boutet et al. 2012; Lau et al. 2010; Lee & Mayr 2019). *CD47* can be expressed with a short and long 3'-UTR. The LU of *CD47* acts as a scaffold and binds HuR, a protein that interacts with the effector SET (Berkovits & Mayr 2015). This allows interaction of the newly translated CD47 with SET, which results in translocation of the complex to the plasma membrane via RAC1. CD47 protein translated from a SU transcript primarily localizes to the ER. This kind of scaffold function has also been described for the LU of *BIRC3* in B cell lymphoma (Lee & Mayr 2019). A protein complex containing IQGAP1 and RALA is assembled in the *BIRC3 LU* and is transferred onto the nascent BIRC3. This complex interacts with CXCR4 and regulates its trafficking to the cell surface, which is essential for its function as a cytokine receptor mediating B cell migration. Upregulation of CXCR4 surface expression and subsequent changes to migration efficiency is specific to BIRC3 translated from the LU transcript.

More than 70 % of the human proteome can be translated from more than one 3'-UTR transcript variant and could therefore have similar 3'-UTR-dependent

functions (Hoque et al. 2013). Since many ubiquitously expressed genes show a tissue- and cell type-specific preference for one variant, 3'-UTR switching may be a crucial mechanism for regulation of diverse protein function relevant in different biological settings and needs to be explored further (Lianoglou et al. 2013).

4.2 Study Aims

APA and resulting 3'-UTR shifts are fields previously not investigated in the context of type I IFNs. This study will investigate both the mechanism behind global 3'-UTR shortening activated by IFNβ in macrophages, as well as its effect on two selected proteins.

Genes, whose expression is altered in favor of shorter transcripts, are for the most part not core IRGs. They represent a novel set of IRGs, which are influenced through post-transcriptional regulation, not induction or repression of transcription, and whose subsequent role has not been characterized. The choice of isoform expression can be influenced by genetic variants that contribute to hereditary disorders; therefore, it is possible that these previously overlooked IRGs play a role in IFN-related diseases (Li L et al. 2021).

Understanding how IFNβ activation alters transcript isoform expression and what other cellular components are involved is crucial to characterize this novel gene set. However, measuring expression of distinct 3'-UTRs is challenging using standard established methods in molecular biology. Considerable effort was therefore spent on adapting and optimizing different approaches in this study that were used to identify essential components mediating 3'-UTR shortening.

The two IRGs *EIF4EBP2* and *MAVS* are expressed with a shortened 3'-UTR in IFNβ-treated HMDMs and were investigated in more detail in this study. Neither of them has been described as an IRG in the literature, which is reflected by data deposited in the Interferome database (Rusinova et al. 2013). *EIF4EBP2* and *MAVS* are listed as downregulated IRGs in just one and two microarray datasets involving type I IFN stimulation respectively. However, this information is based on two microarray probes each, all hybridizing to regions determined to be LU-specific in this study, which means this result is not representative of all transcripts of these genes.

EIF4EBP2 is a translational repressor protein that strongly binds and thereby inhibits EIF4E, a key component of translation initiation. EIF4E is released upon phosphorylation of EIF4EBP2 by mTORC1, a process initiated by type I IFN

signaling, among many others, resulting in altered translational activity (Burnett et al. 1998; Livingstone et al. 2015).

MAVS is a well-characterized scaffold protein involved in signal transduction of RNA sensing, leading to activation of transcription factors and cytokine production (Kawai et al. 2005). It has been observed in a variety of cellular organelles, but the distal region of its 3'-UTR has been connected to preferential mitochondrial localization (Xu et al. 2019). Organelle-specific functions of MAVS connected to differential type I and III IFN production have been subject to controversy in recent publications and still need to be clarified (Bender et al. 2015; Dixit et al. 2010; Odendall et al. 2014).

In this study, protein interaction partners of EIF4EBP2 and MAVS expressed from SU and LU transcripts will be identified and characterized, to investigate potential functions dependent on 3'-UTR length.

The results of this study will expand current understanding of the regulatory pathways activated or altered by IFNβ in macrophages and the effect on a new class of IRGs and their functions.

4.3 Results

4.3.1 PMA-Activated THP-1 Cells as a Model for HMDMs

THP-1 cells are a monocytic cell model frequently used in research, which can be activated by PMA to develop a macrophage-like phenotype (Chanput et al. 2014). 3'-UTR shifts in response to IFNβ were first investigated on a small subset of genes to test the suitability of THP-1 cells as a model for APA pattern changes in HMDMs.

THP-1 cells were activated with PMA overnight (from here on, referred to just as THP-1 cells) and treated with 100 IU/ml IFNβ for up to 24 h. Expression levels of all transcripts (total) and the LU transcript specifically were investigated by qPCR for each gene. The total transcript is detected with a primer pair binding the SU or coding region of a gene, while the LU transcript is detected with a primer pair amplifying the distal 3'-UTR not included in the shorter transcripts (Fig. 21a). The relative expression levels for *MAVS* and *EIF4EBP2* total and LU transcripts in THP-1 cells are comparable to the relative expression levels in HMDMs (Fig. 21b–e). The total transcript measurements remain mostly unchanged across the 24 h time frame, while the LU transcripts are downregulated. The ratio of changes for both genes in both cell models decrease significantly after 12–24 h.

A custom NanoString array was used to assess the similarity of 3'-UTR changes after 24 h of IFNβ treatment on a larger scale. It was also used for further experiments described in later sections. 30 genes with a range of 3'-UTR ratio fold changes were manually selected from the sequencing data. Two probes were designed for each gene to detect the total and LU transcript respectively, analogous to the qPCR primers, and were included on the array, as well as individual probes for six housekeeping genes from a commercial NanoString panel.

In a NanoString experiment, RNA molecules are directly bound by probes coupled to fluorescent barcodes, which are counted after immobilization on a flat surface. This method allows comparisons between total and LU transcripts, since qPCR biases introduced by primer composition, secondary structure as well as

amplicon length and sequence are not an issue. This allows an indirect assessment of SU transcript levels, by subtracting LU from total transcript expression and an estimation of the distribution of SU and LU per gene.

Expression of stress granule assembly factor 1 (*G3BP1*) and *EIF4EBP2* total and LU transcripts are shown in Figure 21f and g. LU expression is significantly downregulated in both cell types in response to IFNβ treatment, as are the total transcript levels in THP-1 cells.

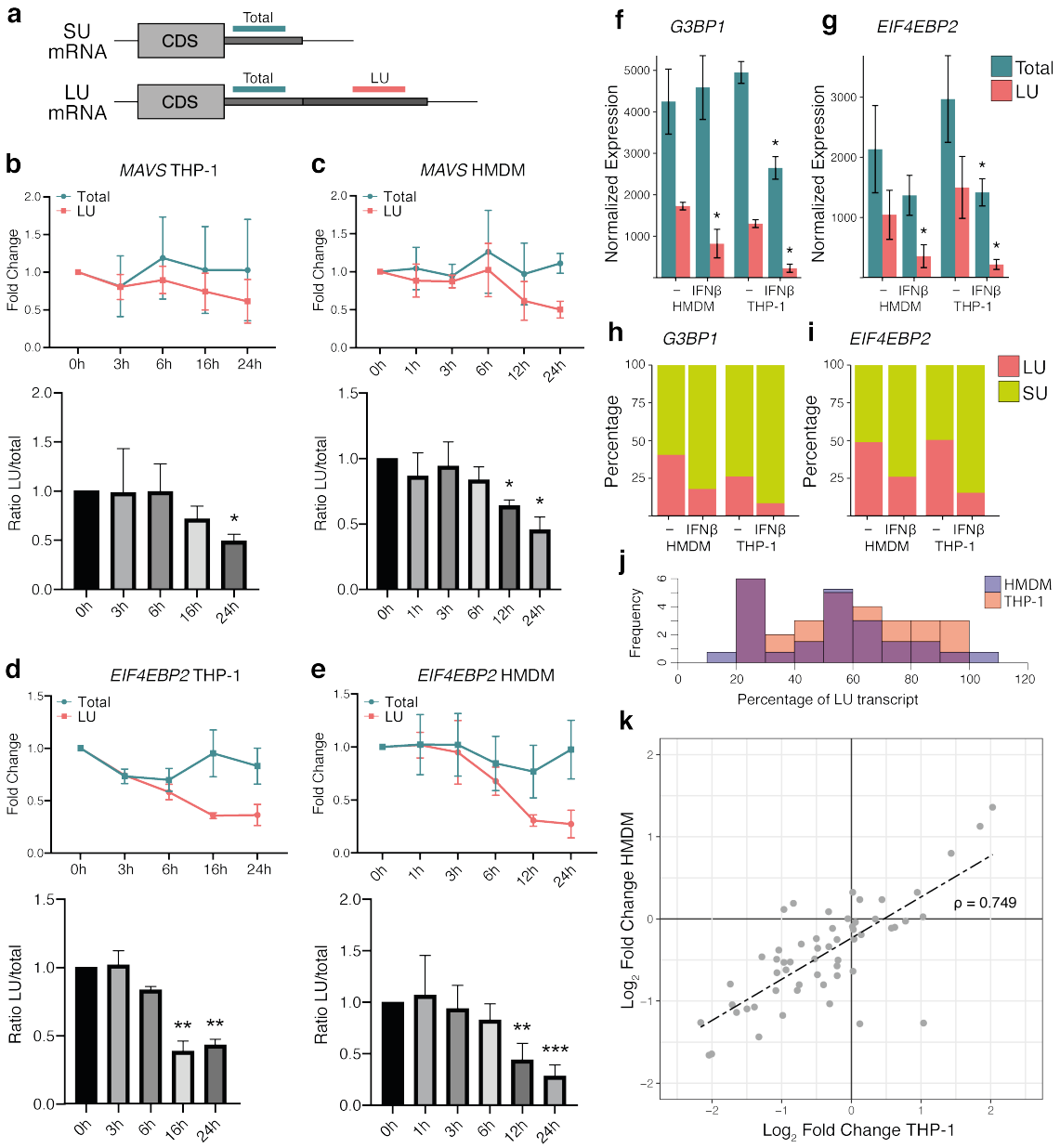

Figure 21: qPCR and NanoString measurements of 3'-UTR changes in THP-1 cells and HMDMs treated with 100 IU/ml IFNβ. a) Diagram showing qPCR primer and NanoString probe binding sites detecting total (teal) and LU transcripts (red). *MAVS* transcript expression changes following IFNβ stimulation in b) THP-1 cells (n = 3) and c) HMDMs (n = 5) measured by qPCR. *EIF4EBP2* transcript expression changes following IFNβ stimulation in d) THP-1 cells (n = 3) and e) HMDMs (n = 5) measured by qPCR. The top graphs show expression fold changes compared to untreated cells (0 h); the bottom ones show the averaged ratios of LU/total normalized to untreated cells (asterisks indicate significance using a one-way ANOVA, * $p < 0.05$, ** $p < 0.01$, *** $p < 0.001$, error bars represent the standard deviation of the mean). Expression of f) *G3BP1* and g) *EIF4EBP2* measured using a NanoString array (n = 3, asterisks indicate FDR < 0.05). The same expression data for h) *G3BP1* and i) *EIF4EBP2* is shown as a percentage of total. j) Histogram showing the percentage of LU transcripts per gene in untreated HMDMs (purple) and THP-1 cells (orange). k) The $\log_2$ fold changes of all target probes in the NanoString array after IFNβ treatment in HMDMs and THP-1 cells were correlated; the Pearson correlation coefficient is shown on the graph. CDS: cDNA sequence, SU: short 3'-UTR, LU: long 3'-UTR.

About 40 % of the *G3BP1* transcripts measured in untreated HMDMs and about 25 % of transcripts in THP-1s are LU transcripts, which decreased to about 20 % and 10 % respectively with IFNβ treatment (Fig. 21h). *EIF4EBP2* LU transcripts make up about 50 % of the total in both cell types, which reduces to 25 % and about 15 % in HMDMs and THP-1s with IFNβ treatment (Fig. 21i). This reduction of LU transcript proportion by about half was also observed in the LU/total fold change calculated from the qPCR results at 24 h (Fig. 21b–e). Overall, the percentage of LU transcript varies greatly across the tested genes and ranges from 10–100 % in untreated HMDMs and THP-1s (Fig. 21j).

The general similarity of THP-1 and HMDM 3'-UTR shifts across the 30 genes on the NanoString array was estimated using the $\log_2$ fold changes of all probes after IFNβ treatment (Fig. 21k). The Pearson correlation coefficient of 0.749 summarizes how comparable the 3'-UTR responses for this gene subset in HMDMs and THP-1 cells are and validates their use as a primary macrophage model.

4.3.2 A Method for Flow Cytometric Measurements of 3'-UTR Changes

Following the validation of 3'-UTR changes and assessment of THP-1 cells as a model, investigation of the underlying IFN-inducible mechanism was started. Since the previously used techniques are not suited to high-throughput assays and screening approaches, another probe-based method, called PrimeFlow, was adapted to measure the distribution of IFNβ-induced changes to LU transcript expression across a pool of cells. Target-bound probes are labelled with fluorochromes, whose signals are measures by flow cytometry.

Cells were treated with 100 IU/ml IFNβ for 24 h and stained with two probe sets detecting total and LU transcripts of a gene, analogous to the qPCR primer and NanoString probe designs. A reduction of LU signal in response to IFNβ treatment is expected based on previous results; therefore, the LU gate was drawn to exclude the majority of cells in IFNβ-treated samples and then applied to the untreated samples. Two cell populations with different signal intensities for total and LU transcripts were observed in *CBX5*-stained samples of untreated HMDMs and THP-1 cells (Fig. 22a and b). The populations with a higher LU signal disappear with IFNβ treatment. A similar effect can be seen in untreated HMDMs stained for total and LU *G3BP1* transcripts, but it is less clear in THP-1 cells (Fig. 22c and d).

Exemplary mean fluorescence intensity (MFI) histograms of HMDMs stained with *G3BP1* an *CBX5* LU probes visualize the shift in a different way (Fig. 22e). The LU positive populations from different experiments were quantified to show the negative shift following IFNβ treatment (Fig. 22f).

Lastly, the IFNβ dependency of the observed population shift was investigated using IFNAR1 (AR1) knockout THP-1 cells, generated through CRISPR/Cas9 genome editing. As expected, no change in *CBX5* or *G3BP1* total and LU transcript intensity was observed after 24 of IFNβ treatment, as the percentage of cells in the LU positive gate stayed roughly the same (Fig. 22g and h). Overall, these two sets of experiments show that THP-1 cells reflect HMDM 3'-UTR responses and are an adequate, but much more malleable, experimental model.

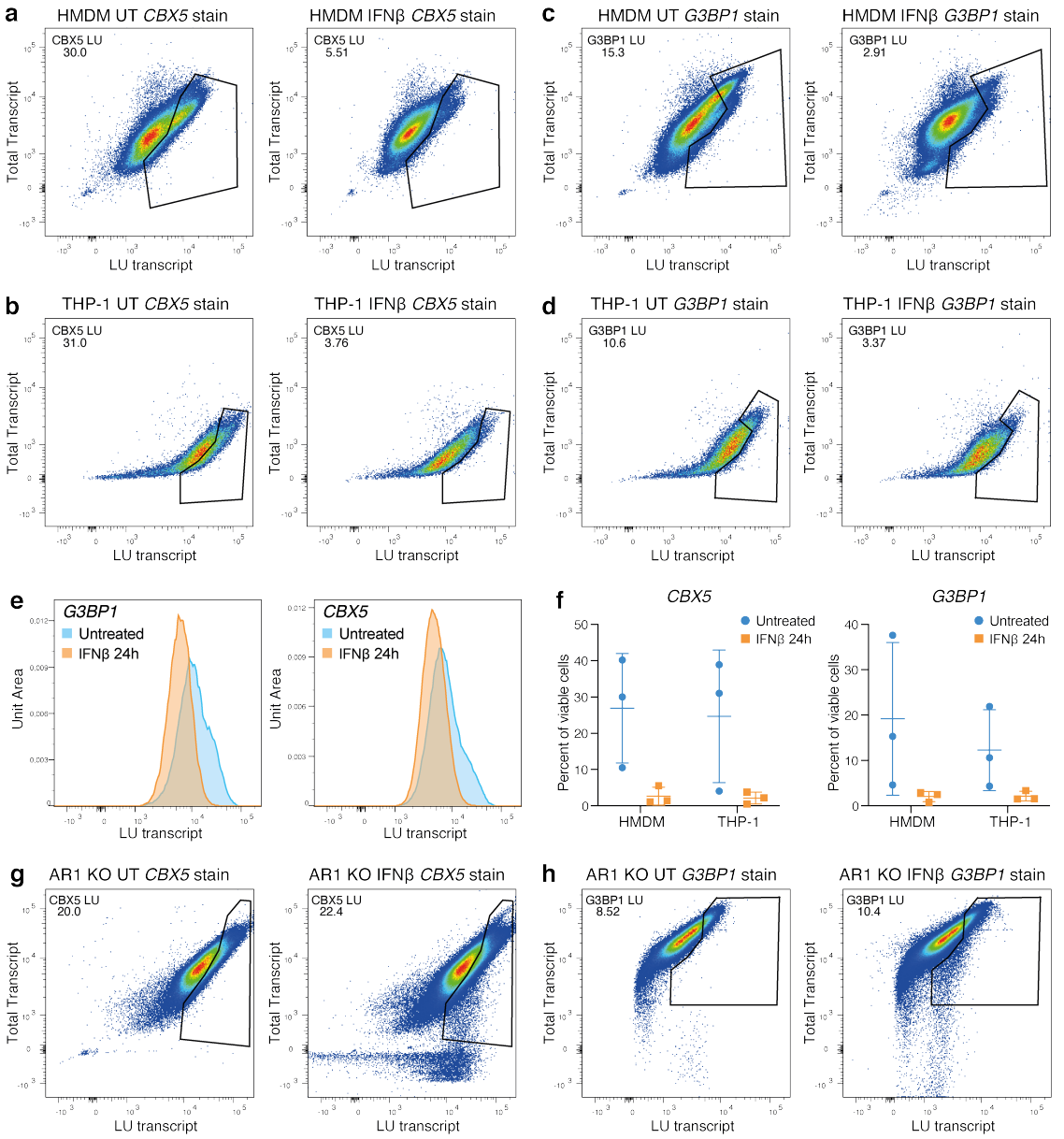

Figure 22: PrimeFlow-based investigation of 3'-UTR changes in THP-1 cells and HMDMs. Untreated and 100 IU/ml IFNβ-treated viable, single HMDMs a) or THP-1 cells b) stained for *CBX5* transcript variants are shown (representative of n = 3). The percentage of cells in the LU gate is shown on the graphs. Untreated and IFNβ-treated viable, single HMDMs c) or THP-1 cells d) stained for *G3BP1* transcript variants are shown. The percentage of cells in the LU gate is shown on the graphs. e) A histogram of LU transcript stain intensities in HMDMs f) The percentage of cells in the LU transcript gate for *CBX5* and *G3BP1* in three replicates of HMDM and THP-1 cells, error bars indicate the standard deviation of the mean. Untreated and IFNβ-treated viable, single THP-1 *IFNAR1* (AR1) knockout cells stained for g) *CBX5* and h) *G3BP1* transcript variants (n = 1). The percentage of cells in the LU gate is shown on the graphs.

4.3.3 Measurement of 3'-UTR Isoform Transcript Stability

Many of the IFNβ-induced shifts investigated so far are the result of downregulation of LU transcripts. Half-lives of RNAs vary across genes and transcripts, so 3'-UTR shifts could be the result of different rates of degradation of long and short mRNAs. To investigate this, THP-1 cells were treated with the transcriptional inhibitor actinomycin D (used at 100 ng/ml). Estimates of RNA half-lives can be made from decreasing transcript levels, since they directly relate to transcript stability in the absence of new RNA transcription.

Transcript levels were determined by qPCR within a period of 8 h. An exemplary graph of total and LU transcript levels normalized to untreated cells in one replicate are shown for each gene; the transcript half-lives were determined with a one-phase decay fit (Fig. 23). No significant differences were observed between the half-lives of total and LU transcripts of each gene across three replicates, indicating that they are degraded at a similar rate in untreated cells.

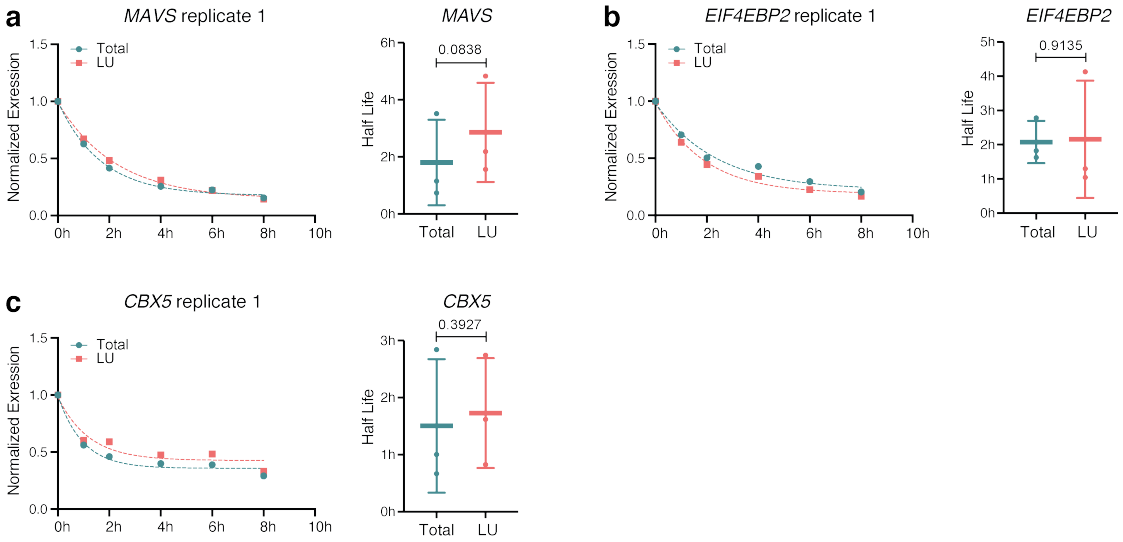

Figure 23: Investigation of mRNA half-lives of 3'-UTR transcript isoforms. Representative expression values of total and LU transcripts normalized to untreated cells of a) *MAVS*, b) *EIF4EBP2* and c) *CBX5* in 100 ng/ml actinomycin D-treated THP-1 cells are shown. The plotted one-phase decay fits (dashed lines) were used to determine mRNA half-lives. The results of three biological replicates are shown, with p-values determined using a one-way ANOVA test; error bars show the standard deviation of the mean.

4.3.4 The Role of IRG Translation in IFNβ-Induced 3'-UTR Shifts

IFNβ treatment induces hundreds of IRGs in macrophages. These IRGs globally reprogram the cells and are one of the most likely factors influencing 3'-UTR shifts. To determine if one or multiple IRGs are crucial for changes in 3'-UTR expression, protein translation can be inhibited with cycloheximide (CHX). CHX inhibits one of the crucial steps during protein translation: translocation and dissociation of transfer RNA (tRNA), whose amino acid has been added to the growing peptide. This prevents binding of new amino acid-coupled tRNAs and hence further elongation of the peptide (Fig. 24a).

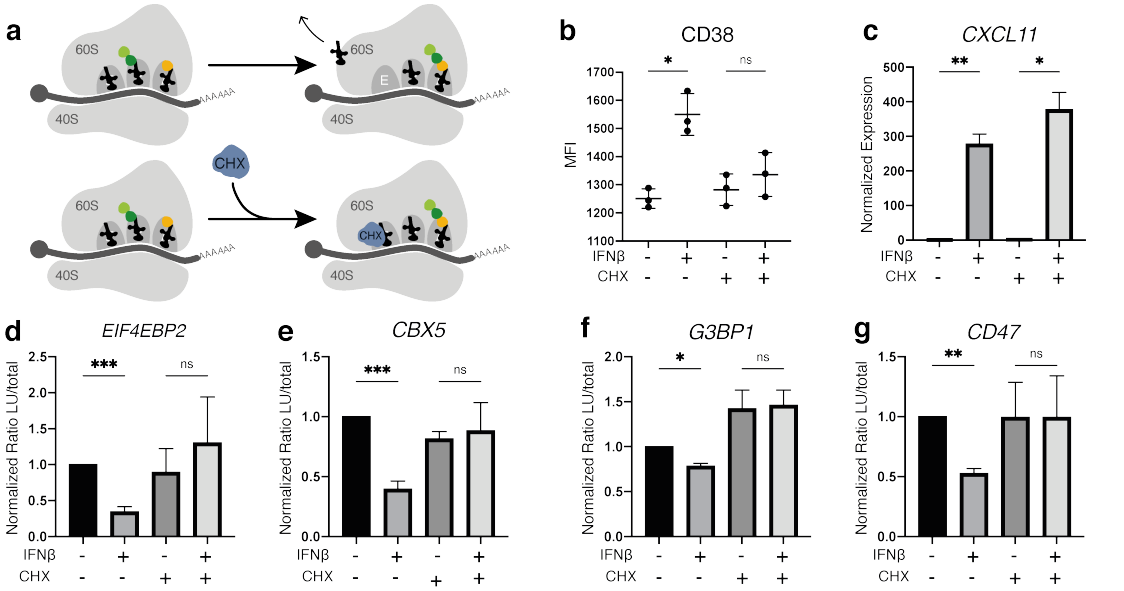

Figure 24: The role of IRG induction in 3'-UTR shifts. a) Diagram of the translation inhibition mechanism of CHX. Amino acid-conjugated tRNAs bind the ribosomal A-site and a peptide bond is formed to connect the amino acid to the growing peptide. Cycloheximide blocks the next step, the shift of the ribosome to the next codon and dissociation of the empty tRNA from the E-site. b) MFI of CD38 measure by flow cytometry (n=3) and c) *CXCL11* mRNA expression values measured by qPCR (n=3) normalized to untreated cells in THP-1 cells treated with IFNβ for 24 following CHX pretreatment for 30 min. Ratio of LU/total transcript measure by qPCR normalized to untreated cells of d) *EIF4EBP2*, e) *CBX5*, f) *G3BP1*, and g) *CD47* in THP-1 cells treated with 100 IU/ml IFNβ for 24 following CHX pretreatment for 30 min (n=3). Asterisks indicate significance using a one-way ANOVA, * $p < 0.05$, ** $p < 0.01$, *** $p < 0.001$, ns $p \geq 0.05$; error bars show the standard deviation of the mean.

In this study, THP-1 cells were treated with 20 mM CHX for 30 min followed by 100 IU/ml IFNβ for 24 h. Assessment of the mean fluorescence intensity of CD38 by flow cytometry shows that the increase of protein in response to IFNβ is inhibited by CHX (Fig. 24b). Induction of transcription of the IRG *CXCL11* by IFNβ is unaffected by CHX pretreatment (Fig. 24c). LU/total transcript ratio changes for *EIF4EBP2*, *CBX5*, *G3BP1* and *CD47* were determined by qPCR. The ratio reduction observed in response to IFNβ treatment for all of the genes is inhibited by CHX pretreatment, indicating that translation of IRGs is essential for this response (Fig. 24d–g).

4.3.5 The Role of mTORC1 in IFNβ-Induced Changes of APA Patterns

One of the many proteins activated in response to IFNβ that leads to IRG induction downstream is mTORC1. Upon activation by phospho-AKT it can alter the cell's transcriptional and translational activity through inhibition of EIF4BP1 or activation of S6K1 (Fig. 25a). Its inhibition by Torin1 has previously been shown to stop a shift towards shorter 3'-UTRs in TSC1 knockout mouse embryonic fibroblasts (Chang et al. 2015).

To determine its role in this context, THP-1 cells were treated with 250 nM Torin1 for 30 min followed by 1 h with 100 IU/ml IFNβ. The activation status of different signaling components was assessed by Western blot (Fig. 25b). Phosphorylation of S6 and AKT was inhibited, while STAT1 phosphorylation was not affected. Some phosphorylation of mTOR was still detected in pretreated cells, possibly due to mTORC2 phosphorylation, which is not inhibited by Torin1 but detected by the anti-mTOR antibody. Increased transcription of C-C chemokine ligand 7 *(CCL7)*, a gene whose induction was previously described as mTORC1 dependent (Ai et al. 2014), after 24 h of IFNβ treatment was also inhibited by Torin1 (Fig. 25c). However, the reduction in LU/total transcript ratios of *EIF4EBP2*, *CBX5* and *G3BP1* seen after 24 h of IFNβ treatment was not affected by Torin1 pretreatment, suggesting mTORC1 is not a key mediator of IFNβ-induced 3'-UTR shifts (Fig. 25d–f).

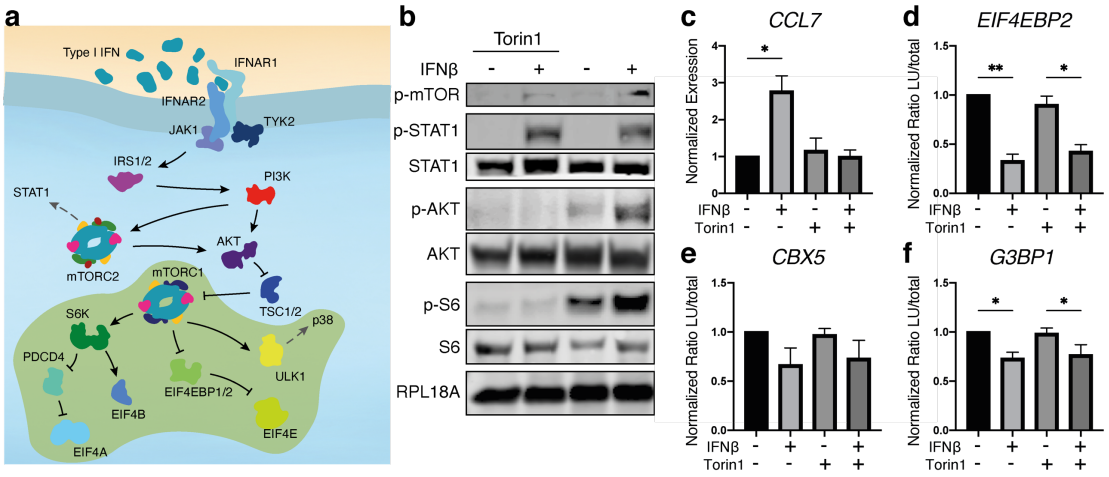

Figure 25: The role of mTORC1 in IFNβ-induced 3'-UTR shifts. a) Diagram of AKT/mTOR activation by type I IFNs and the inhibitory effect of Torin1 (green). b) Western blot showing the phosphorylation status of IFNβ signaling components in PMA-activated THP-1 cells after 1 h of 100 IU/ml IFNβ with and without 30 min 250 nM Torin1 pretreatment; RPL18A serves as a loading control (representative of n=3). c) *CCL7* expression fold change in 100 IU/ml IFNβ treated THP-1 cells after 24 h with and without 30 min 250 nM Torin1 pretreatment measure by qPCR (n=3). Ratio of LU/total transcript of d) *EIF4EBP2*, e) *CBX5* and f) *G3BP1* normalized to untreated cells in THP-1 cells treated with IFNβ and Torin1 as in c) (n = 3). Asterisks indicate significance using a one-way ANOVA, * $p < 0.05$, ** $p < 0.01$; error bars show the standard deviation of the mean.

4.3.6 The Effect of Selective Inhibition of IFNβ Signaling Pathways

To further characterize which of the many IFNβ-activated signal transduction pathways are involved in mediating 3'-UTR changes, a panel of inhibitors was used to block individual upstream signaling components (Fig. 26a). Torin1 and the PI3K inhibitor Wortmannin (from now referred to as mTOR inhibitors, used at 250 nM and 50 nM respectively) were used in combination to prevent AKT-mTOR signaling. SB203580 and U0126 selectively inhibit signaling through the MAP kinases p38 and MKK1/2 (from now referred to as mapK inhibitors, used at 10 μM and 20 μM respectively), and the pan-JAK inhibitor CYT387 blocks all signaling dependent on JAK1, JAK2 and TYK2 (from now referred to as JAK inhibitor, used at 10 μM).

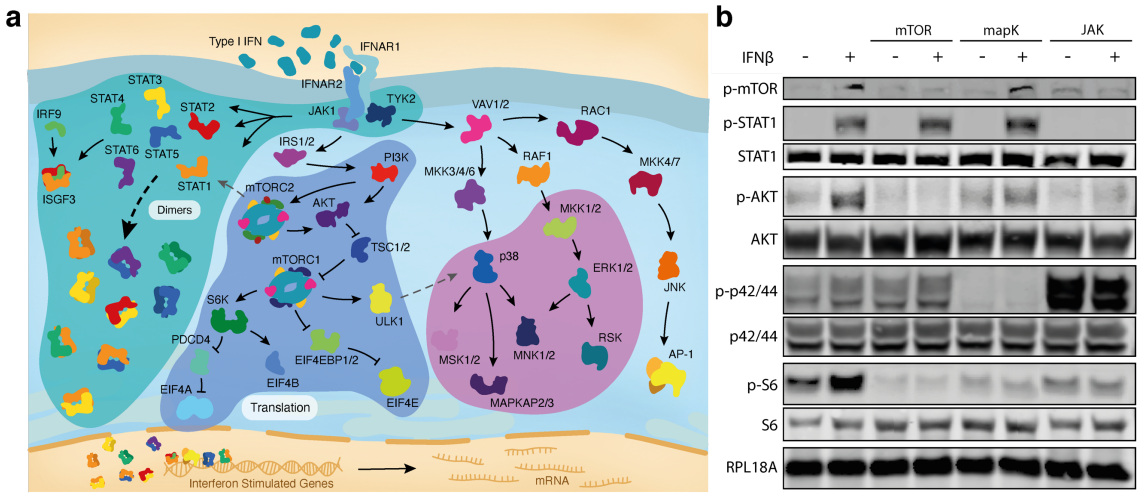

Figure 26: Selective inhibition of IFNβ signaling by a panel of inhibitors. a) Diagram of IFNβ signaling pathways and their inhibition by JAK (teal), mTOR (blue) and mapK (pink) inhibitors. b) Western blot showing the phosphorylation status of IFNβ signaling components in PMA-activated THP-1 cells after 24 h of 100 IU/ml IFNβ treatment with and without inhibitor pretreatment for 30 min (representative of n = 3).

THP-1 cells were treated with the inhibitor panel for 30 min followed by 100 IU/ml IFNβ for another 30 min. The activation status of different signaling molecules was assessed by Western blotting (Fig. 26b). The JAK and mTOR inhibitors block mTOR, AKT and S6 phosphorylation; the mapK inhibitors prevent p42/44 phosphorylation. The JAK inhibitor is the only one inhibiting STAT1 phosphorylation and also appears to increase basal p42/44 phosphorylation, independent of IFNβ treatment.

The effect of the inhibitor panel on 3'-UTR shifts was assessed using the previously described NanoString array, after THP-1 cells were treated with CHX, JAK, mTOR or mapK inhibitors for 30 min, followed by 100 IU/ml IFNβ for 24 h (Fig. 27 and Supplementary Fig. 1).

The normalized expression values of total and LU transcripts for *EIF4EBP2* and *ACOX1* across all THP-1 cell samples are shown in Figure 27a and b. IFNβ treatment leads to a significant reduction of both total and LU transcripts compared to untreated cells in both genes. This effect is reduced by CHX and inhibited by JAK pretreatment. The mapK or mTOR inhibitors do not affect the reduction of total and LU transcript levels in either gene.

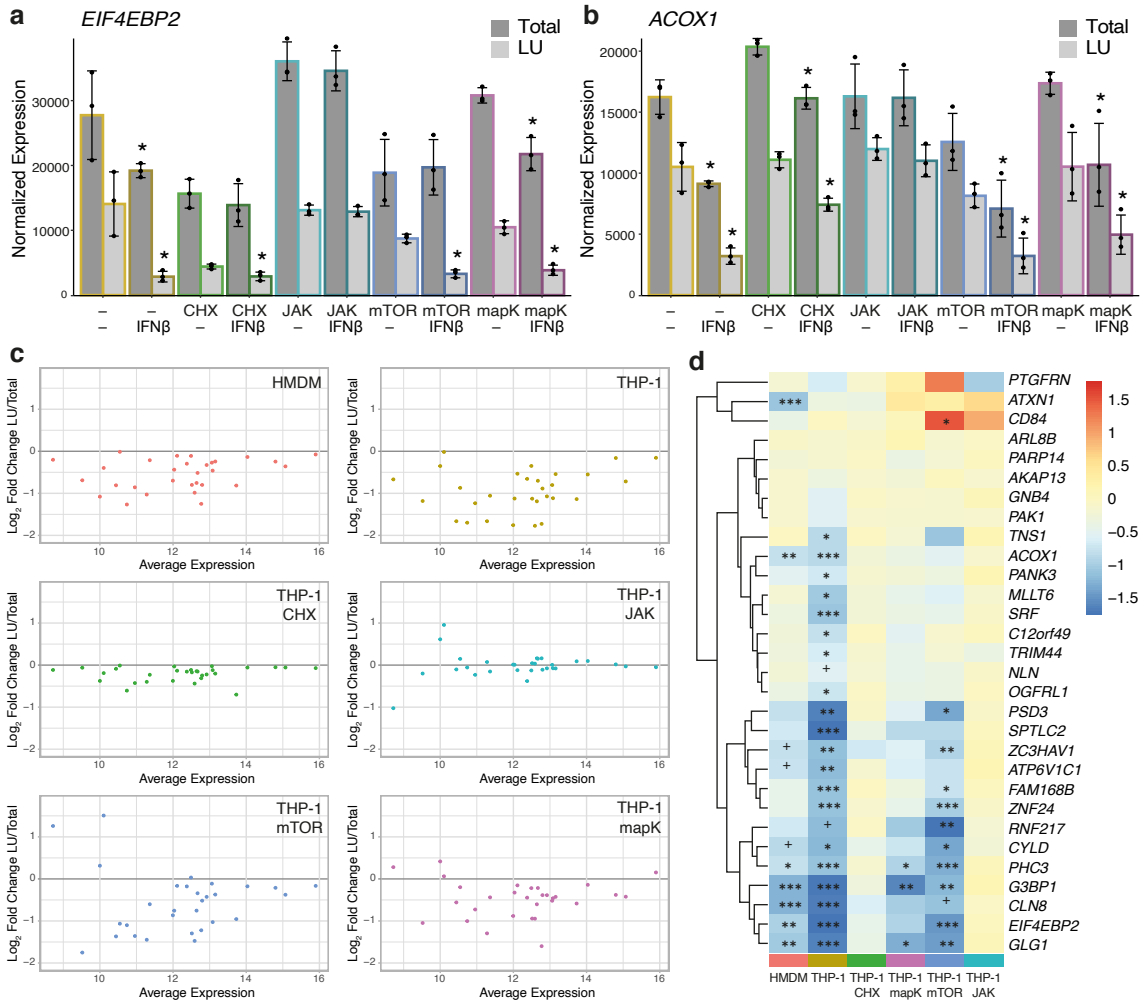

Figure 27: The effect of selective inhibition of different IFNβ signaling pathways on 3'-UTR shifts. Expression of a) *EIF4EBP2* and b) *ACOX1* total and LU transcript in 100 IU/ml IFNβ-treated THP-1 cells after 24 h with and without inhibitor pretreatment, determined using a NanoString array (n = 3, asterisks indicate an FDR < 0.05 on statistical tests between IFNb-treated and untreated samples within each sample group (colored outlines), error bars show the standard deviation of the mean). c) Log_2 fold changes of LU/total transcripts of all genes on the array in all samples over average expression. d) Heat map of log_2 fold changes of LU/total transcripts (symbols represent statistical significance, + FDR < 0.1, * FDR < 0.05, ** FDR < 0.01, *** FDR < 0.001).

The log_2 fold changes of LU/Total induced by IFNβ were calculated for every gene and sample and plotted over average expression and as a heat map (Fig. 27c and d). No changes with an FDR value below 0.05 are seen in CHX and JAK pretreated cells, which is very different from the result in untreated THP-1s and HMDMs. Pretreatment with mTOR and mapK inhibitors, on the other hand,

results in a spread that is more similar. These results confirm the CHX effect observed by qPCR analyses on a larger scale and show the change in 3'-UTR ratios is dependent on JAK activity. The kinases associated with the IFN receptor, TYK2 and JAK1, both belong to this group of kinases and initiate a large number of signaling cascades upon binding of IFNβ. These experiments have thus identified that translation is necessary for IFNβ-induced 3'UTR changes and they depend on JAK activity.

4.3.7 Expression Changes of Select Components of the Cleavage and Polyadenylation Machinery and Associated Proteins

Subsequently, expression levels of some candidate IRGs were investigated in response to IFNβ and the inhibitor panel. Since the cleavage and polyadenylation machinery has previously been associated with changes in APA patterns, candidate IRGs were selected that are either components of (RBBP6, CSTF2, CSTF3 and CLP1) or have been associated with (interferon induced protein with tetratricopeptide repeats (IFIT) 1 and 3) these complexes. Their expression levels in THP-1 cells and HMDMs treated with 100 IU/ml IFNβ for up to 24 h were investigated by qPCR (Fig 28 and 29).

The effect of the previously used inhibitor panel on the expression of these genes in THP-1 cells was determined through 30 min pretreatment with each inhibitor followed by 24 h treatment with 100 IU/ml IFNβ. *RBBP6* is upregulated most highly after 3 h in HMDMs and returns to the expression level of untreated cells after about 12 h, while it remains slightly elevated in THP-1 cells (Fig. 28a). 30 min pretreatment with all but the JAK inhibitor followed by 24 h IFNβ treatment show a similar but very small trend towards increased expression. *CSTF2* expression is upregulated in IFNβ-treated HMDMs after about 12 h, whereas it is downregulated in THP-1 cells after 3 h and then returns to untreated expression levels (Fig. 28b). In the follow-up experiment with the inhibitor panel, untreated THP-1s show reduced transcript levels with IFNβ treatment, while it remains unchanged in the other sample groups.

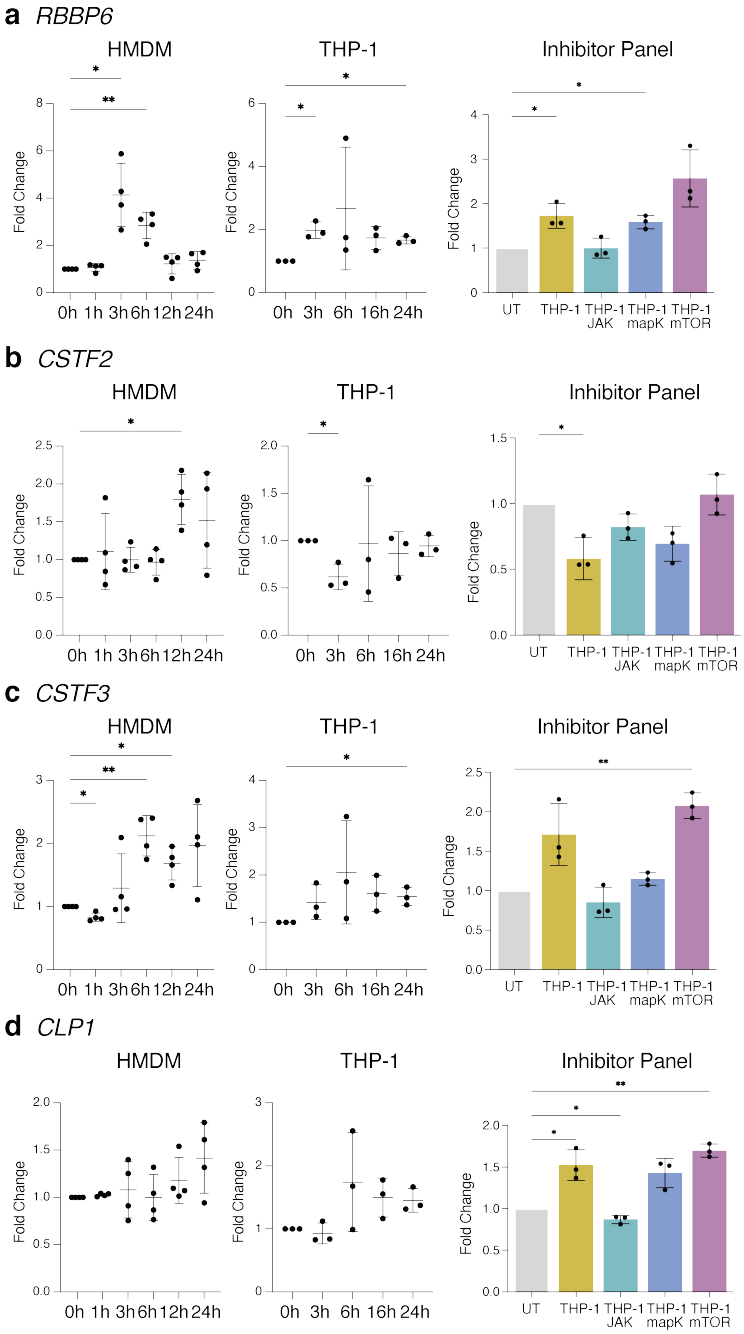

Figure 28: qPCR-based investigation of components of the cleavage and polyadenylation machinery. Expression fold changes of a) *RBBP6*, b) *CSTF2*, c) *CSTF3* and d) *CLP1* in HMDMs (n = 3–4) and THP-1 cells (n = 3) in response to IFNβ treatment compared to untreated cells and after 24 h of IFNβ treatment following 30 min pretreatment with the inhibitor panel (JAK: Cyt387, mapK: SB203580 + U0126, mTOR: Torin1 + Wortmannin). Asterisks indicate significance using a one-way ANOVA, * $p < 0.05$, ** $p < 0.01$, error bars show the standard deviation of the mean.

Expression of *CSTF3* is significantly upregulated in IFNβ-treated HMDMs after 6 h; THP-1 cells show a similar trend, while pretreatment with JAK and mTOR inhibitors prevents it (Fig. 28c). *CLP1* expression shows an upregulation trend in both IFNβ-treated HMDM and THP-1, which is also seen after mapK and mTOR inhibitor pretreatment, while JAK pretreatment reverses that effect (Fig. 28d). Lastly, both *IFIT1* and *IFIT3* are highly upregulated from 3 h onwards in IFNβ-treated HMDM and THP-1 cells, an effect that is not prevented by any of the tested inhibitors (Fig. 29a and b).

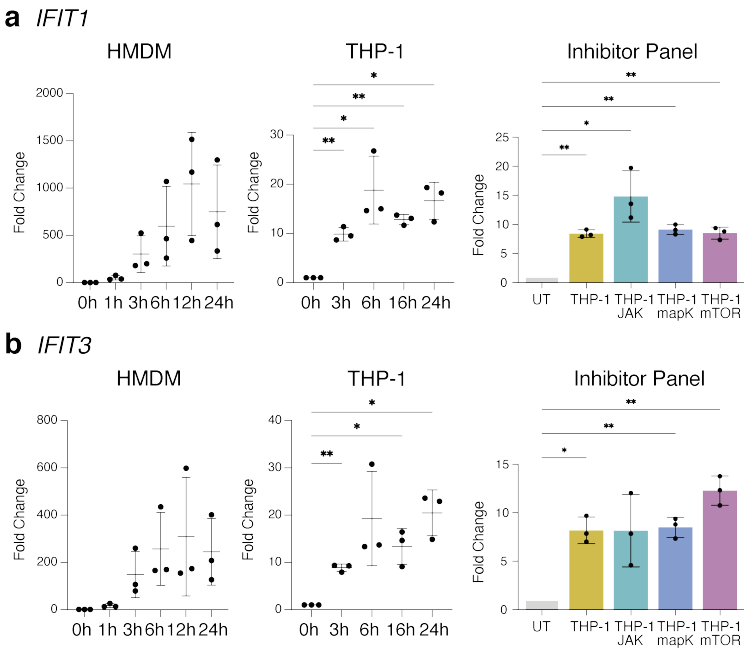

Figure 29: qPCR-based investigation of the IRGs *IFIT1* and *IFIT3*. Expression fold changes of a) *IFIT1* and b) *IFIT3* in HMDMs (n = 3–4) and THP-1 cells (n = 3) in response to IFNβ treatment compared to untreated cells and after 24 of IFNβ treatment following 30 min pretreatment with the inhibitor panel (JAK: Cyt387, mapK: SB203580 + U0126, mTOR: Torin1 + Wortmannin). Asterisks indicate significance using a one-way ANOVA, * $p < 0.05$, ** $p < 0.01$, error bars show the standard deviation of the mean.

All observed IFNβ-induced changes are either very small or are not inhibited by the JAK inhibitor that prevents 3'-UTR shifts, making it unlikely they alone are causing the change in polyadenylation pattern. Further experiments are needed to shed light on the components and mechanisms involved in IFNβ-induced 3'-UTR changes, but the experimental data in this study so far can be used as a point of reference in future.

4.3.8 Identification of 3'-UTR-Dependent Protein Interactors of MAVS and EIF4EBP2

Understanding functional implications of changing polyadenylation patterns in response to IFNβ is just as important as understanding the mechanism behind them. A scaffold-like function has been attributed to 3'-UTRs in recent publications. Transcript 3'-ends contain binding sites for various proteins and protein complexes, which can be transferred to the nascent protein encoded by the mRNA as it is being translated. Different 3'-UTRs, such as SU and LU, contain different binding sites and can hence lead to the formation of different protein complexes (Fig. 30a).

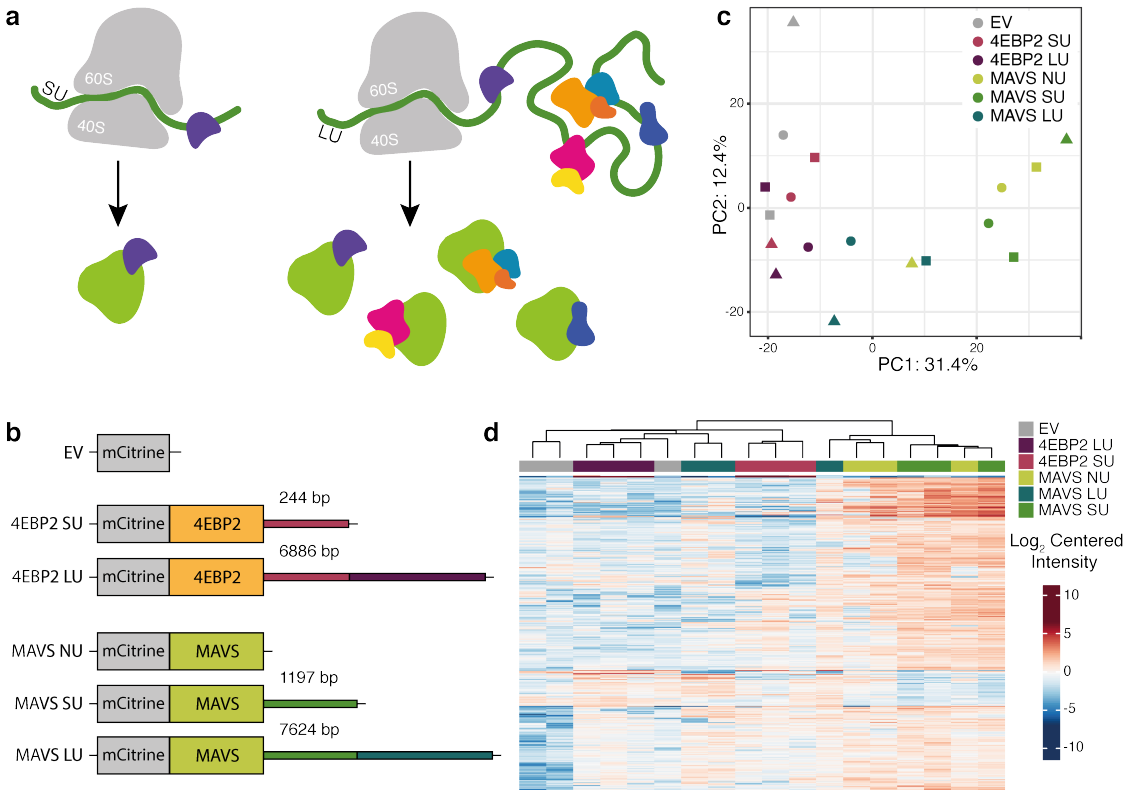

Figure 30: Co-IP of protein-protein interactors of MAVS and 4EBP2 in HEK-Blue IFNα/β cells. a) A diagram of 3'-UTR scaffold function and protein complex formation, whose composition may be influenced by different 3'-UTR lengths. b) Diagrams of mCitrine-fusion constructs used in the experiment. Lengths of 3'-UTRs encoded on the plasmids are shown in base pairs (bp). c) PCA plot and d) heat map of centered log_2 intensities of identified proteins in HEK293 Blue IFNα/β cells following transfection with the respective constructs, co-IP and identification of proteins using mass spectrometry (technical replicates).

In this study, the composition of these protein complexes was investigated via co-immunoprecipitation (IP) of the mCitrine-tagged candidate proteins MAVS and EIF4EBP2 (4EBP2) expressed from constructs with different 3'-UTRs. The interacting proteins were subsequently identified by quantitative mass spectrometry. 4EBP2 and MAVS coding regions were cloned to the C-terminal end of mCitrine encoded in a plasmid backbone (empty vector; EV), followed by their respective short and long 3'-UTRs (Fig. 30b). The full set of constructs also includes an mCitrine-MAVS construct without a 3'-UTR (no 3'-UTR; NU).

HEK-Blue IFNα/β cells, a modified HEK293T cell line expressing a type I IFNβ reporter, were transfected with the different expression constructs and protein was extracted 48 h later. The abundance and sequence of associated proteins were measured by quantitative mass spectrometry after co-IP of the mCitrine-fusion proteins using an anti-GFP antibody. Between 500 and 1,200 proteins were detected in each sample (Supplementary Fig. 2). The replicates of each sample group on a principal component analysis (PCA) plot do not form separate, distinct clusters, which is an indicator of the degree of variance between replicates as well as similarity between different sample groups (Fig. 30c). This is also reflected in the coefficients of variation per protein (Supplementary Fig. 2). A heat map of $\log_2$ centered intensities, a measure to quantify protein abundance compared to the average across samples, shows MAVS constructs bind more protein than 4EBP2 and the EV control (Fig. 30d). It further separates MAVS NU and SU from the MAVS LU samples and 4EBP2 SU from LU. One cluster of proteins that has negative $\log_2$ centered intensities in MAVS NU and SU and positive ones in MAVS LU samples stands out in particular. Empty vector samples show negative $\log_2$ centered intensities for a large proportion of proteins suggesting lower binding of proteins compared to the other groups.

When looking at intensities of individual proteins that are different between the sample groups, mCitrine stands out immediately (Fig. 31a). Its intensity is significantly lower in MAVS LU compared to the other samples, which suggests normalization of the data was not ideal, since interactions of proteins to equal amounts of the different fusion-proteins should be investigated. Positive control

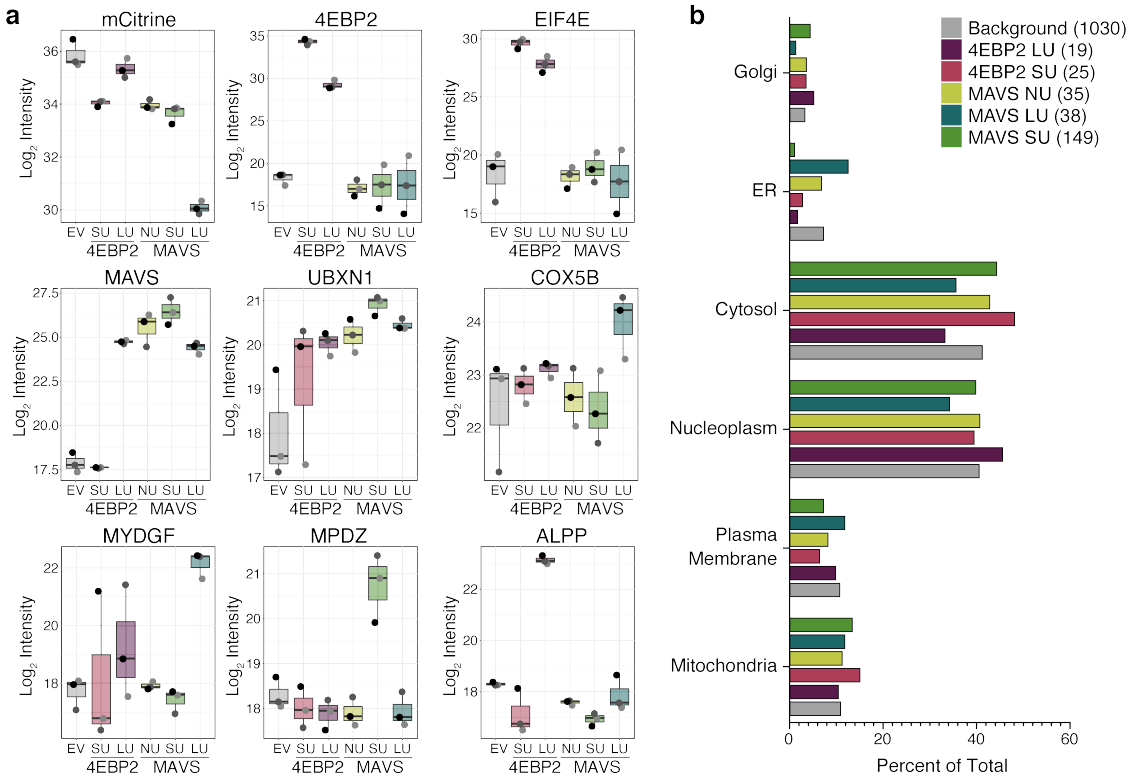

Figure 31: Analysis of protein-protein interactors detected in the MAVS and 4EBP2 Co-IP. a) Box plots of log_2 intensities of selected proteins identified by mass spectrometry following co-IP of HEK293 IFNα/β cells transfected with the respective constructs (technical replicates). b) Graph showing subcellular localization of transcript-specific interacting proteins as described in The Human Protein Atlas as percentage of total per sample.

measures are the intensities of the overexpressed proteins MAVS and 4EBP2, which are very high in their respective samples. The interaction of UBX domain protein 1 (UBXN1) and EIF4E with MAVS and 4EBP2 respectively has been described in literature, and their detection in the respective samples is an indicator that associated proteins were precipitated alongside the mCitrine-fusion proteins (Fletcher et al. 1998; Wang et al. 2013).

Some proteins show very different log_2 intensities between SU and LU samples. cytochrome C oxidase subunit 5B (COX5B) and myeloid-derived growth factor (MYDGF) are detected in much higher amounts in MAVS LU samples compared to SU, while alkaline phosphatase, placental (ALPP) and MAVS are measured in higher abundance in 4EBP2 LU compared to SU. Multiple PDZ domain protein (MPDZ) appears to bind MAVS SU specifically, but not LU and NU. The selected

proteins exclusively interact with MAVS and 4EBP2 derived from constructs that include specific (or no) 3'-UTRs while encoding the same proteins. This proves 3'-UTRs can affect association of 4EBP2 and MAVS with different proteins, which may have functional consequences.

Different 3'-UTRs have previously also been associated with a change in protein localization. To investigate this, the detected proteins were categorized by interaction with one of the constructs and information on their subcellular localization incorporated from The Human Protein Atlas. To be sorted into a category, proteins had to be enriched 1.5-fold in one sample group compared to the groups belonging to the same gene and the empty vector. For example, MAVS LU interactors are proteins with a fold change higher than 1.5 in comparison to MAVS SU, MAVS NU and EV. 4EBP2 LU interactors are enriched 1.5-fold compared to 4EBP2 SU and EV. Proteins that did not fall into any of the categories were classified as background. Protein localization was expressed as a percentage of total to account for the difference in numbers across the categories (Fig. 31b). A slightly larger proportion of MAVS LU-interacting proteins localizes to the ER compared to MAVS SU, but the difference is small. Overall, there is no obvious difference in potential localization of interacting proteins.

4.3.9 Investigation of Proteins Interacting with 4EBP2

4EBP2 does not bind a lot of proteins overall as seen in the 4EBP2 LU and SU comparison to EV. Ten proteins are significantly enriched in 4EBP2 SU compared to EV and five are significantly enriched in 4EBP2 LU compared to EV (Fig. 32a and b). 4EBP2 itself and EIF4E, one of its well described interactors, are in these groups in both comparisons, showing expression and precipitation of the fusion-protein and its binding partners was successful. Other proteins such as dynactin subunit 1 (DCTN1), ALPP and MAVS are unique to either comparison and appear in the direct comparison of 4EBP2 SU and LU (Fig. 32c). Just 6 and 2 proteins with an FDR less than 0.05 are enriched more than two-fold in 4EBP2 LU or SU respectively.

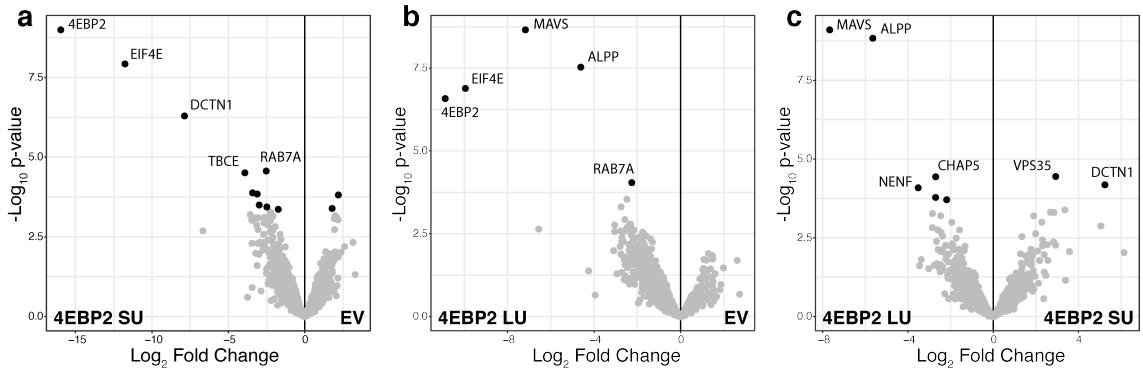

Figure 32: Pairwise comparison of 4EBP2 and EV samples. Volcano plots showing $-\log_{10}$ p-values versus $\log_2$ fold changes of proteins bound to a) EV compared to 4EBP2 SU, b) EV compared to 4EBP2 LU and c) 4EBP2 SU compared to 4EBP2 LU. Proteins with an adjusted p-value below 0.05 are highlighted in black (transiently transfected HEK293 IFNα/β cells, technical replicates: 3).

Further characterization of functional differences between the protein complexes derived from SU and LU transcripts was done by plotting interaction networks using STRING, a database for protein-protein interactions (Szklarczyk et al. 2021). The networks include SU- or LU-dependent interactors with a fold change of 1.5 or higher compared to EV as well as one another. Only proteins connected to others with the highest confidence limit are plotted and colored by clusters determined through the Markov Cluster (MCL) algorithm (Fig. 33). The three largest clusters stand out in SU-dependent interactions. They were manually annotated and highlighted in the graph. The 1st cluster contains proteins associated with RNA splicing and export and protein folding and transport activity. The 2nd contains a large number of ribosomal proteins and proteins involved in ubiquitination and proteasome activity. Lastly, proteins that facilitate vesicular protein transport or are associated with tubulin and cytoplasmic dynein are connected in the 3rd cluster (Fig. 33a).

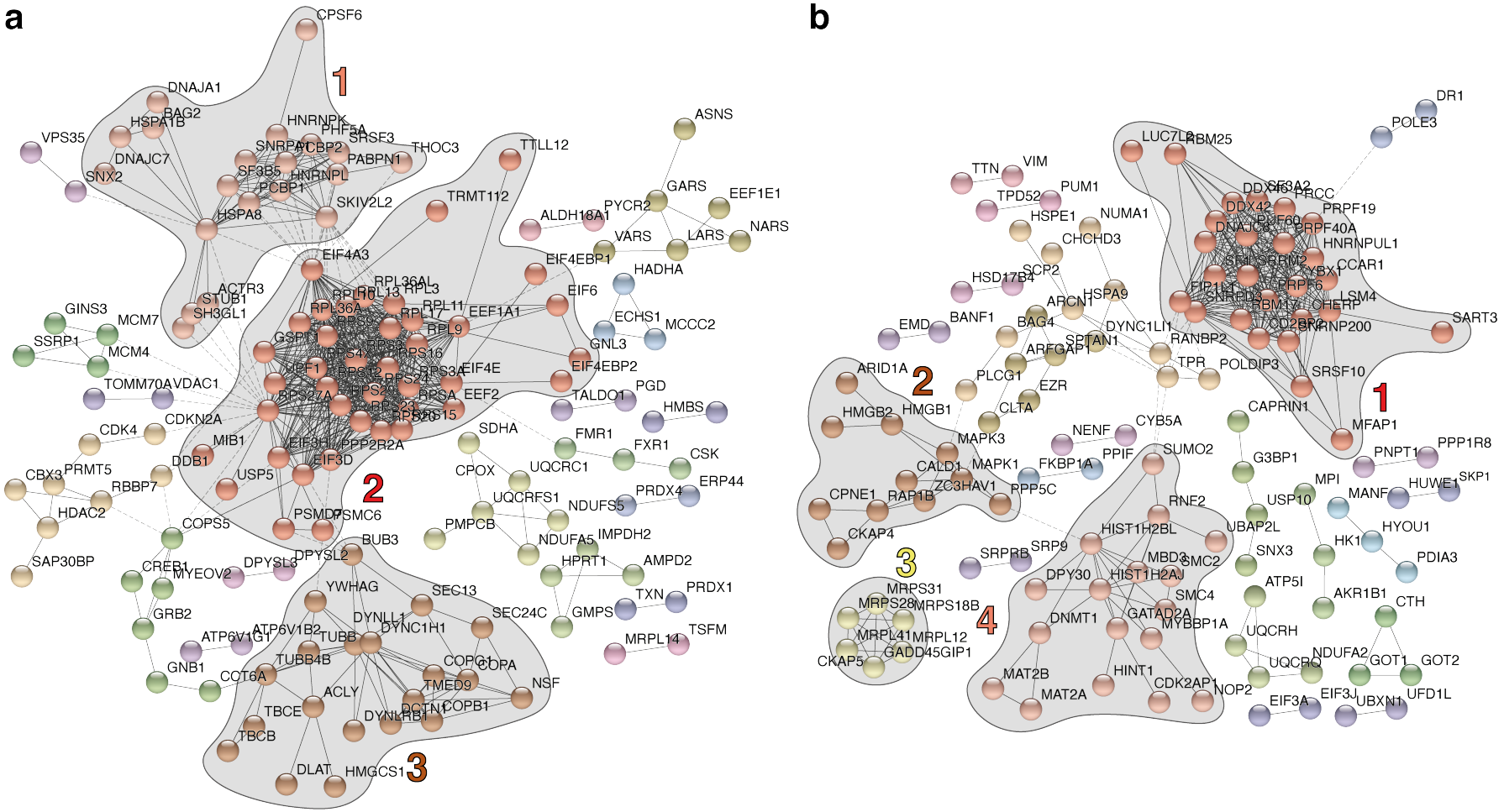

Figure 33: Investigation of proteins interacting with 4EBP2 translated from different 3'-UTR isoforms. Interaction networks of a) SU-dependent and b) LU-dependent interactors based on information from STRING database are colored by clusters determined through the MCL algorithm (inflation parameter 1.5). A subset of clusters was manually selected, numbered and highlighted in grey. SU network annotation: 1 – Protein and RNA transport, 2 – Ribosomal proteins, 3 – Cytoskeleton. LU network annotation: 1 – Splicing factors, 2 – Signaling, 3 – Mitochondrial splicing proteins, 4 – Transcriptional repression.

Four clusters were highlighted and annotated in the network derived from LU-dependent interactors. Like in the SU-dependent interaction network, the 1st is connected to spliceosome activity, but interestingly also contains SNRNPs and proteins associated with apoptosis and cell cycle progression. Proteins in the 2nd cluster are part of the MAP kinase signaling pathway and regulate transcriptional activity. Some are also connected to the cytoskeleton. The 3rd cluster is a bit smaller and related to the 1st. It consists of mitochondrial splicing proteins and proteins involved in cell cycle arrest. The 4th cluster also contains proteins connected to cell cycle arrest, as well as histones, ubiquitin ligases and proteins associated with DNA methylation and transcriptional repression (Fig. 33b).
While there is overlap between the clusters of SU- and LU-dependent 4EBP2 interactors, some pathway ontologies seem to be restricted to one or the other, suggesting different functional nuances.

4.3.10 Investigation of Proteins Interacting with MAVS

The same approach was used to characterize interactors and potential functions of the MAVS 3'-UTR. Volcano plots for the relevant sample group comparisons are shown in Figure 34. MAVS interacts with a much larger number of proteins than 4EBP2. The comparison between EV and MAVS NU interactors show that MAVS is bound by 134 proteins with an FDR less than 0.05 (Fig. 34a).
Despite encoding a 3'-UTR of roughly 2,500 bp, MAVS SU interactions appear very similar to NU (Fig. 34b). MPDZ is the only protein with an FDR smaller than 0.05 that is enriched more than twofold in MAVS SU. MAVS LU and MAVS SU, however, seem to bind proteins differentially. 12 proteins with an FDR of 0.05 or lower are more than twofold enriched in MAVS LU and 36 proteins in MAVS SU (Fig. 34c). The suboptimal normalization is again very apparent in this plot, since both mCitrine and MAVS are among the proteins enriched in MAVS SU, which should ideally have roughly equal levels across all samples.

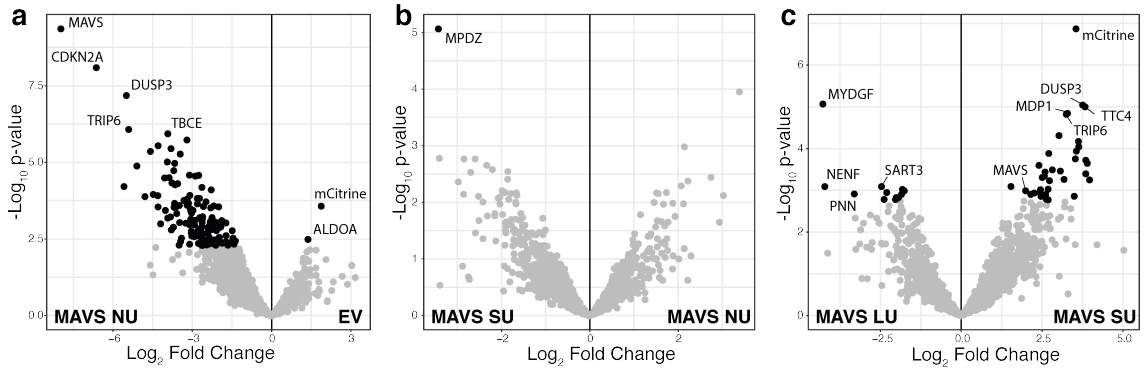

Figure 34: Pairwise comparisons of select MAVS sample groups. Volcano plots showing $-\log_{10}$ p-values versus $\log_2$ fold changes of proteins bound to a) EV compared to MAVS NU, b) MAVS NU compared to MAVS SU and c) MAVS SU compared to MAVS LU. Proteins with an adjusted p-value below 0.05 are highlighted in black (transiently transfected HEK293 IFNα/β cells, technical replicates: 3).

Nevertheless, network analyses were used to investigate functional ontologies of MAVS SU- and MAVS LU-specific interactors. Detected proteins were classified as described previously and highest confidence interactions were plotted using STRING, followed by coloring through MCL clustering (Szklarczyk et al. 2021). Nine of the largest clusters with shared ontologies between proteins were manually selected annotated and highlighted further in the SU-dependent interaction network (Fig. 35a). The 1st cluster contains proteins mediating tRNA ligation, the 2nd consists of mitochondrial import and respiration proteins localized in the mitochondrial matrix. The 3rd cluster is made up of enzymes from the purine biosynthesis and related pathways. The 4th cluster is connected to translational activity. Proteins from the 5th cluster mediate RNA splicing and transport and regulate transcriptional activity, while proteins in the 6th relate to DNA replication, cell cycle progression and remodeling of the cytoskeleton. Proteins from the 7th and 8th cluster are related: they are involved in vesicular transport and are associated with the cytoskeleton; in particular, proteins from the 7th cluster are involved in actin filament nucleation and microtubule-bundle formation. The 9th cluster is made up of proteins mediating MAP kinase and AKT1 signaling as well as chaperone activity and cell cycle progression.

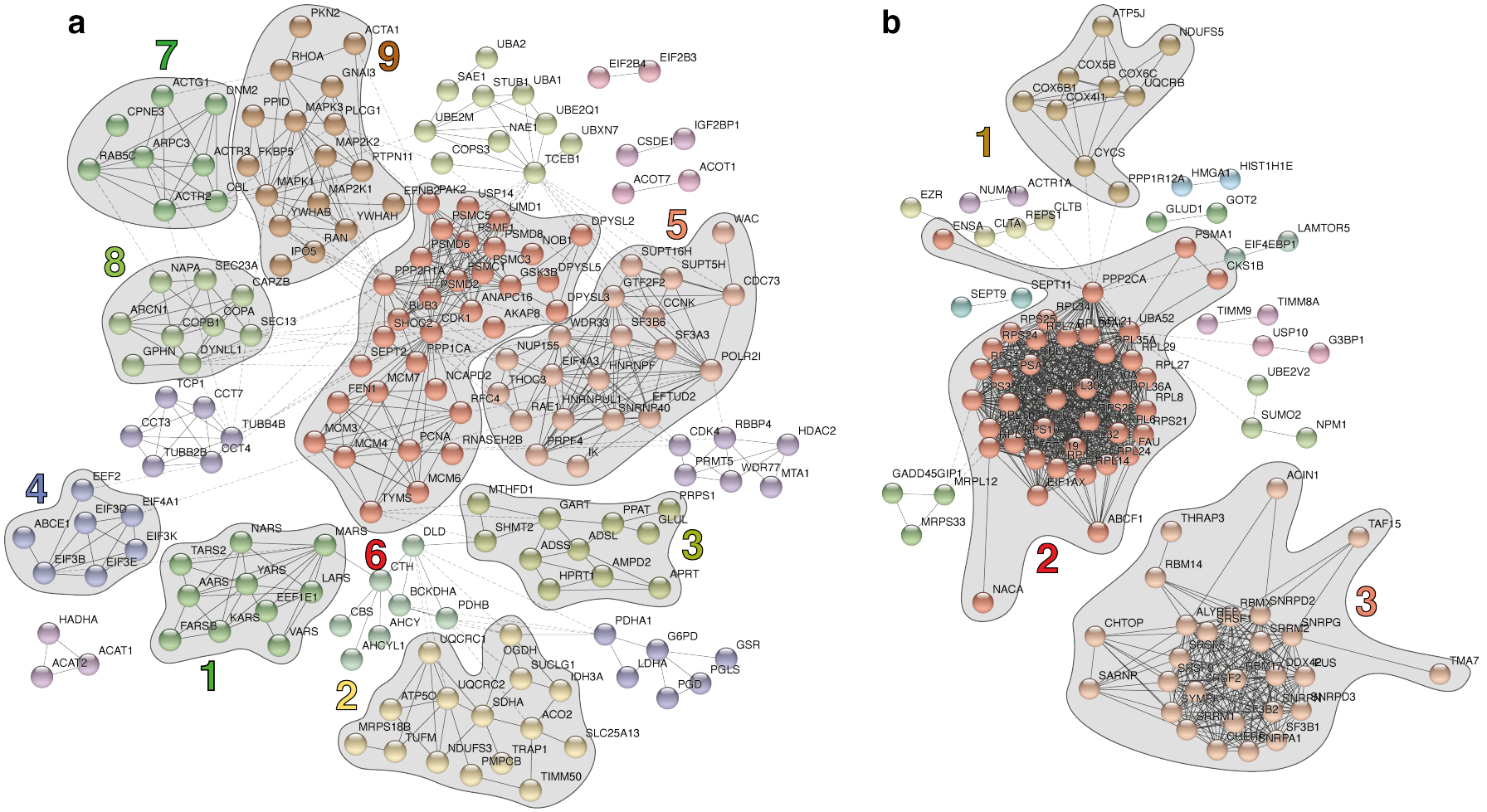

Figure 35: Investigation of proteins interacting with MAVS translated from different 3'-UTR isoforms. Interaction networks of a) SU-dependent and b) LU-dependent interactors based on information from STRING database are colored by clusters determined through the MCL algorithm (inflation parameter 1.5). A subset of clusters was manually selected, numbered and highlighted in grey. SU-network annotation: 1 – tRNA ligases, 2 – Mitochondrial import, 3 – Purine biosynthesis, 4 – Translation, 5 – RNA splicing, 6 – Proliferation, 7 – Cytoskeleton, 8 – Vesicular traffic, 9 – Signaling. LU-network annotation: 1 – Mitochondrial respiration, 2 – Ribosomal proteins, 3 – RNA splicing.

A second network was plotted with MAVS LU-dependent interactors, which form only three obvious clusters, two of which contain a large number of proteins that are more highly interconnected than the clusters seen in the MAVS SU network (Fig. 35b). They were highlighted and annotated as before. Cluster 1 is the smallest of the three and consists of proteins of the mitochondrial respiratory chain, which mostly sit in the mitochondrial membrane. The 2nd cluster contains mostly ribosomal proteins as well as proteins associated with translation initiation or ubiquitination and the proteasome. The 3rd cluster consist of proteins similar in function to cluster 5 in the SU dependent network. They are involved in transcriptional regulation as well as RNA transport, splicing and polyadenylation. The number, size and function of protein clusters in MAVS SU- compared to MAVS LU-dependent interactors are related, but still distinct. Association with different components of the cytoskeleton and vesicular transport as well as cell cycle progression and signaling activity is distinct to MAVS SU-dependent interacting proteins, whereas MAVS LU-dependent interactors show a clear ontology around ribosomal activity and potentially suggest preferential localization to the mitochondrial membrane. Many of these are good leads for further investigations into differential activity of MAVS translated from short and long 3'-UTR transcripts.

4.4 Discussion

This study investigated the mechanism and function of IFNβ-induced changes to APA patterns and the resulting changes in 3'-UTR length in HMDMs and THP-1 cells. The majority of human genes contains more than one PAS that can be used for 3'-end processing (Derti et al. 2012). Changes to PAS usage results in altered 3'-UTR lengths, which can affect post-transcriptional gene regulation and 3'-UTR-dependent protein functions.

4.4.1 PMA-Activated THP-1 Cells as a Model for IFNβ-Induced 3'-UTR Shortening

HMDMs were used in the initial sequencing experiment that led to the discovery of 3'-UTR changes in IFNβ-treated human macrophages. These primary cells are derived from independent human donors; they are inherently variable and challenging to work with. Hence, 3'-UTR dynamics in PMA-activated THP-1 cells, a well-established cell model allowing more flexible experimental designs, were investigated. THP-1 is a monocytic lineage cell line isolated from peripheral blood of a 1-year-old male acute monocytic leukemia patient. They can be differentiated to adopt a macrophage-like state using PMA or M-CSF and further polarized to display M1 and M2-like phenotypes through stimulation with different cytokines. However, in both their monocytic and macrophage states they show differences in baseline gene expression, in the degree of gene induction and cytokine secretion in response to different stimuli compared to HMDMs (Chanput et al. 2013; Chanput et al. 2014). Therefore, their suitability in context of IFNβ-induced changes in APA patterns needed to be investigated.

3'-UTR changes were measured and compared using a few different methods, to determine the suitability of THP-1 cells as a model for HMDMs. qPCRs are the most flexible and cost-effective option, but results are biased by sequence composition and length of primers and amplicons and are limited to a small set of genes. The custom NanoString array is one of two probe-based systems used

instead in this study. It measures individual RNA molecule numbers by counting fluorescent barcodes attached to complementary target probes. The barcode signal is not influenced by the composition of the probe target sequence therefore allows comparisons of different transcripts and genes, as well as estimations of the proportion of transcripts expressed with a LU.

The IFNβ-induced changes of total and LU transcripts of the 30 tested genes in HMDMs and THP-1 cells correlate very well, despite small differences in their baseline expression. This suggests that THP-1 cells are a suitable model for further *in vitro* investigations, such as a CRISPR/Cas9-based high-throughput knockout screen to identify proteins essential for IFNβ-induced 3'-UTR shifts. The screen will be based on the second probe-based system employed in this study, called PrimeFlow, which allows a flow cytometric readout of transcript abundance. A scalable cell model that can be genetically engineered, such as THP-1 cells, is essential for high-throughput approaches.

Additionally, the existence of two cell populations was observed in untreated HMDMs stained for different *CBX5* and *G3BP1* transcripts, which are separated by their abundance of LU transcript. These populations may express different levels of key factors mediating APA patterns, which would result in varying levels of LU transcripts. Combining stains for different genes in one sample could help to determine if this is a general observation or specific to *CBX5* and *G3BP1*. Further characterization of the differences between these populations will follow in future, for example through bulk RNA-sequencing or quantitative proteomics on the sorted populations or through single-cell investigations. Although PrimeFlow is less sensitive than the other two methods used in this study and the 3'-UTR shifts separating treated and untreated cell populations appear small, its dependency on IFNβ signaling has been shown through the generation and staining of IFNAR1 knockout THP-1 cells.

4.4.2 Characterizing Processes Involved in IFNβ-Induced 3'-UTR Shortening

Experiments with actinomycin D also showed that total and LU transcript half-lives of selected genes are similar in untreated THP-1 cells. Therefore, IFNβ treatment differentially affects the rate of synthesis or decay of LU and SU transcripts leading to a changed ratio in activated cells. While half-lives were only determined for transcripts from a small number of genes in this study, the results match previously published data from mouse fibroblasts, which showed little influence of 3'-UTR length on global transcript stability or translational efficiency (Gruber et al. 2014; Spies et al. 2013).

Treatments with the translational inhibitor cycloheximide revealed that IFNβ-induced 3'-UTR shifts of all investigated genes in this study are dependent on IRG induction. This is in line with the late onset of the observed 3'-UTR shifts compared to other IFNβ-induced transcriptional changes; it appears to be a secondary response and IRGs have to be expressed to mediate it. These IRGs may affect different stages of the RNA life cycle. They could direct the cleavage and polyadenylation machinery to alternative, more proximal processing sites or alter transcript stabilities of long and short 3'-UTR isoforms differently. Further experiments with a panel of inhibitors revealed that JAK activity is needed for the induction of these IRGs, while AKT/mTOR and MAPK pathways have very little effect on 3'-UTR length.

Contrary to this, previous research in TSC1 knockout MEFs showed mTORC1-dependent 3'-UTR shortening (Chang et al. 2015). TSC1 is a negative regulator of mTORC1, one of two mTOR complexes that modulate protein synthesis and cell proliferation through inhibition of the EIF4EBP translational repressors and activation of the kinase S6K1 (Dowling et al. 2010; Lekmine et al. 2003). Loss of TSC1 leads to hyperactivation of mTOR and expression of transcripts with SUs, an effect that was counteracted by the mTORC1-specific inhibitor Torin1. In this study, however, neither partial inhibition of IFNβ-dependent mTOR activation with Torin1 nor complete inhibition with a combination of Wortmannin and Torin1 affected 3'-UTR shortening, suggesting an alternative mechanism in IFNβ-treated HMDMs. A potential explanation for this is the broad activation of different

signaling cascades in response to IFNβ. Recent studies have shown that p38 and STAT1 are downstream targets of mTOR and they could therefore play a role in 3'-UTR shortening in MEFs (He et al. 2020; Kristof et al. 2003). Their activation would be prevented through mTORC1 inhibition by Torin1 in TSC1 knockout MEFs. In IFNβ-activated THP-1 cells, however, MAPK and STAT pathways are activated through signaling cascades initiated at the IFN receptor and inhibiting crossregulation via mTOR has little to no effect. Additional cell type-specific signaling could also play a role. Extending the panel of inhibitors to block multiple pathways at once or knocking out key components further downstream to prevent cross-activation may be options to address some of this in future.

4.4.3 Expression Levels of Components of the Cleavage and Polyadenylation Machinery

A potential group of proteins that may be affected by IFNβ signaling are components of the cleavage and polyadenylation machinery (Fig. 7). Differential expression of some of them has previously been linked to changes in 3'-UTR length. Therefore, changes to the expression level of selected components, *CSTF2, CSTF3, RBBP6* and *CLP1*, in response to IFNβ was investigated in this study.

Initially, increased CSTF2 expression was shown to result in preferential use of proximal poly-A site of *IGM* during B-cell differentiation and of *NFATC1* in effector T-cells (Chuvpilo et al. 1999; Takagaki et al. 1996). Subsequently the global effect of CSTF2 upregulation on APA has been described. Knockdown of CSTF2 in combination with its paralog CSTF2T results in use of more distal PASs (Yao C et al. 2012; Yao et al. 2013). In this study, regulation of *CSTF2* in HMDMs and THP-1 cells in response to IFNβ was not consistent and the different inhibitor treatments showed few differences, making CSTF2 an unlikely candidate to pursue further. However, the expression level of another component of the CSTF complex, *CSTF3*, is showing an upwards trend in both HMDMs and THP-1 cells treated with IFNβ, as well as in mapK- and mTOR-, but not JAK-inhibitor-treated

cells. CSTF3 is the second of three core proteins of the CSTF complex and changes to its expression level have been linked to global APA pattern changes (Luo et al. 2013). Its role in 3'-UTR changes in macrophages should be explored further.

RBBP6 is a similar candidate: its expression is increased in HMDMs and THP-1 cells, mapK and mTOR inhibition only have a small effect, while JAK inhibition prevents it. A ubiquitin-like domain enables RBBP6 interactions with other polyadenylation factors and a knockdown of RBBP6 leads to preferential use of distal poly-A-sites (Di Giammartino et al. 2014).

The last protein investigated in this study is CLP1, a component of the CFII complex. A combined knockdown of the two CFII components CLP1 and PCF11 led to preferential selection of proximal PASs in human breast cancer cells, while downregulation of just PCF11 results in suppression of intronic polyadenylation of specific subsets of genes in differentiating cells (Li et al. 2015; Turner et al. 2020). The *Arabidopsis thaliana* homolog of CLP1 has been shown to control poly-A-site selection of a subset of genes in developing plants (Xing et al. 2008). The trend towards upregulation of *CLP1* in response to IFNβ in this data in all but the JAK-inhibitor treated samples suggest CFII may contribute to differential PAS selection in this context as well.

Lastly, components of the CFI complex have recently been connected to regulation of APA. Suppression of NUDT21 was reported to change APA patterns in HeLa cells and in induced pluripotent stem cells (iPSCs) (Brumbaugh et al. 2018; Kubo et al. 2006). Interestingly, this led to an increased rate of differentiation in iPSCs and chromatin regulators were enriched among the affected transcripts. Similarly, another two-part study suggests CFI subunits control 3'-UTR length after showing an increase in proximal poly-A-site usage in response to loss of NUDT21 or CPSF6 but not CPSF7 function in HEK293 cells (Gruber et al. 2012; Martin et al. 2012). Interaction of CFI with the FIP1 arginine-serine-repeat-like domain has equally been showing to affect APA patterns (Zhu et al. 2018). FIP1-RNA interactions are also a key mediator of an embryonic stem cell (ES) cell-specific polyadenylation pattern, which changes during differentiation (Lackford et al. 2014).

4.4.4 Expression Levels of the IRGs IFIT1 and IFIT3

In addition to the core components, other proteins may be associated with the cleavage and polyadenylation machinery and influence PAS selection, such as SRSF3 and SRSF7 and the well-known IRGs IFIT1 and IFIT3, which were identified in pull-down experiments in HeLa cells (Schwich et al. 2021; Shi et al. 2009). IFIT proteins have been shown to facilitate different antiviral processes by mediating protein-protein interactions via their tetratricopeptide repeat motifs, but have to date not been described in context of polyadenylation (Pidugu et al. 2019). *IFIT1* and *IFIT3* were highly upregulated in both HMDMs and THP-1 cells upon IFNβ treatment. Induction of their expression was dampened in inhibitor pretreated samples, but still significantly increased compared to untreated cells. There was little difference between cells treated with the JAK-inhibitor, which abolishes 3'-UTR shifts, and the mapK and mTOR inhibitors. The role of IFIT1 and IFIT3 in 3'-UTR shortening in this context therefore remains unclear and needs to be investigated further.

The list of proteins contributing to changes to polyadenylation patterns in the literature is steadily growing. Many of the interactions between components of the cleavage and polyadenylation machinery are essential for its function, so knockdowns and altered expression levels are expected to affect polyadenylation patterns. Additionally, other IRGs and components specific to a particular cellular context may interact with parts of the machinery and alter their function. The IRGs IFIT1 and IFIT3 were associated with the cleavage and polyadenylation machinery in a pull-down experiment in HeLa cells, without any IFN stimulation.

It is likely that more proteins can interact with core components of the cleavage and polyadenylation machinery in IFNβ-activated macrophages, which induce the expression of hundreds of additional IRGs, as seen in this study. The number of potential regulators of IFNβ-mediated 3'-UTR shortening is therefore very large. Different techniques were established in this study to perform further experiments, such as an unbiased CRISPR/Cas9-based knockout screen based on detection of RNA using PrimeFlow. Results of these experiments will help

reduce potential protein mediators to a number that can be investigated using individual candidate approaches.

4.4.5 3'-UTRs as Scaffolds Mediating Protein-Protein Interactions

3'-UTRs contribute to degradation, localization and translation of mRNAs and have been shown to act like small RNAs or long noncoding RNAs. More recent publications have also described a scaffold function for 3'-UTRs, which can mediate protein-protein interactions (Berkovits & Mayr 2015; Lee & Mayr 2019). Early research suggested a change in 3'-UTR length is an additional mechanism that controls protein abundance through altering transcript stability and translational rates. However, this observation was not consistent with later research as well as the results of this study (Brumbaugh et al. 2018; Gruber et al. 2014). Instead, more recent investigations suggest genes with changing 3'-UTRs could be involved in different forms of intracellular protein transport and trafficking (Li et al. 2015). Another study showed transport of CD47 protein is influenced by the length of its 3'-UTR, a mechanism dependent on protein-protein interactions facilitated by the RBP SET (Berkovits & Mayr 2015).

In silico predictions of interactions like these are very challenging due to RNA secondary structures and limited availability of data. Hence the 3'-UTRs of two proteins, MAVS and 4EBP2, were examined using a wet-lab approach. Protein-protein interactions of LU- and SU-proteins were investigated in HEK293T cells. Constructs encoding LUs are very large and challenging to work with, hence this easily transfectable cell line was chosen in lieu of a more accurate model, such as THP-1 cells. A large number of proteins was measured in each sample and each sample group showed an increase in abundance of specific interactors.

The results of an initial analysis did not reveal any obvious difference in protein localization, one of the key roles of 3'-UTRs suggested in the literature among LU- and SU-specific interactors. However, it is possible that including all potential locations recorded in The Human Protein Atlas for every protein regardless of abundance and cellular context masked subtle differences in this analysis.

Additionally, interaction network plots revealed SU- and LU-proteins are predicted to be bound by different proteins associated with microtubule and actin filaments, along which protein complexes can be transported, and showed a subtler association with ontologies connected to different organelles. Subcellular location and abundance of SU- and LU-proteins should be confirmed by microscopy in future.

4.4.6 4EBP2 Interactions Mediated by Long and Short 3'-UTRs

Only a small number of 4EBP2-interacting proteins were identified in this study regardless of transcript 3'-UTR length. 4EBP2 is a small 27 kDa protein that contains intrinsically disordered domains in an unphosphorylated state, which likely do not facilitate interactions with many other proteins (Fletcher et al. 1998). It is one of three mammalian paralogs (4EBP1, 4EBP2 and 4EBP3) whose expression varies depending on tissue and cell type (Banko et al. 2005; Grolleau et al. 1999; Poulin et al. 1998; So et al. 2016; Tsukiyama-Kohara et al. 1996). 4EBPs inhibit translation by competing with EIF4G1 for the same binding motif on EIF4E. This interaction prevents formation of the 5'-cap binding protein complex EIF4F, which promotes translation initiation (Banko et al. 2005; Dawson et al. 2020; Fukuyo et al. 2011; Thoreen et al. 2012). The interaction of EIF4E with EIF4G1 influences the translational rate of most mRNAs, but especially 5'-TOP-containing mRNAs (Signer et al. 2016; Thoreen et al. 2012). This translation inhibition mechanism is likely not 3'-UTR dependent and not LU-specific, since both 4EBP2 SU and LU interacted with EIF4E in this study. It is therefore possible that overexpressing 4EBP2 in HEK293T cells negatively affected the rate of translation and led to a reduction of the overall amount of protein in the cell, which would also affect the number and abundance of interacting proteins detected in the subsequent IP.

4EBP2 and its paralogs can be phosphorylated by mTORC1, which results in restructuring of its disordered domains, release of EIF4E and increased translational efficiency (Blandino-Rosano et al. 2016; Dawson et al. 2020; So et

al. 2016). This mechanism is a crucial component of the signaling pathways activated in response to IFNβ signaling in macrophages. It is therefore possible that the dynamic 3'-UTR of 4EBP2 contributes to a regulatory loop.

It has been reported previously that translation of different types of mRNAs can be spatially distinct. For example, viral infections often lead to the 4EBP2-dependent formation of stress granules that inhibit translation of the accumulating mRNAs (McCormick & Khaperskyy 2017). Another example from a recent publication is the TIS granule, a membraneless organelle with a mesh-like structure formed through interactions between mRNAs with LUs (Ma & Mayr 2018). The directed transport and local translation of these mRNAs, as well as a distinct protein composition in the organelle, facilitates the formation of specific protein complexes. If expression of the distal 3'-UTR region of 4EBP2 is subjected to the same localization mechanism, it is possible that translation rates of only specific subcellular compartments are affected. Hence, IFNβ could regulate spatially restricted mRNAs specifically through altering the 3'-UTR length of 4EBP2.

Some recent publications have already shown that the spatial distribution of 4EBPs and their phosphorylation status are dynamic and can be regulated by different factors. Protrusions formed during mammary gland development require accumulation of phosphorylated 4EBP1 to remain stable, a process that is controlled by the phosphorylated protein BCL2-associated agonist of cell death (BAD) (Githaka et al. 2021). Susor and colleagues reported spatial regulation of translation of a subset of mRNAs in the nucleus during mammalian oocyte development, which is dependent on mTOR and EIF4F activity (Susor et al. 2015). Another study connected deamidation of 4EBP2, a modification sometimes induced in cellular proteins during viral evasion strategies, to a change in subcellular location (Kouloulia et al. 2019). Deamidated 4EBP2 was more susceptible to proteasomal degradation, an ontology connected to a cluster of 4EBP2 SU-specific interacting proteins in this study, and to NFκB activity, a transcription factor that can be activated by MAP kinase signaling cascades, an ontology exclusively detected in a 4EBP2-LU cluster. Additionally, MAP kinases activate MNK1, an enzyme that can phosphorylate EIF4E (Wang et al. 2007c).

EIF4E phosphorylation is another mechanism associated with this protein that controls translational rates and currently thought to be independent of 4EBP2 binding (Herdy et al. 2012; Joshi et al. 2009). However, the results of this study suggest that this could be regulated by 4EBP2 in a 3'-UTR-dependent manner.

4EBP2 LU-specific interacting proteins are also connected to DNA methylation, transcriptional repression and cell cycle arrest, processes that 4EBPs have been linked to in literature before. As mentioned previously, a recent study reported that 4EBP1 phosphorylation, and hence activity, is controlled by the pro-apoptotic BCL2-family member BAD and another publication showed that 4EBP2 mediates p53-dependent senescence through translational control of the p53-stablizing protein growth arrest specific 2 (GAS2) (Githaka et al. 2021; He et al. 2020; Petroulakis et al. 2009).

Lastly, 4EBP2-LU specific interactors include mitochondrial proteins, a class of proteins that has previously been mentioned as being preferentially translated in response to mTORC1 activation (Morita et al. 2013).

Among them is the protein mitochondrial fission process 1 (MTFP1), which can recruit dynamin-related protein 1 (DRP1) to the mitochondria and induce mitochondrial fission (Morita et al. 2017). Interestingly, IFNβ signaling leads to a

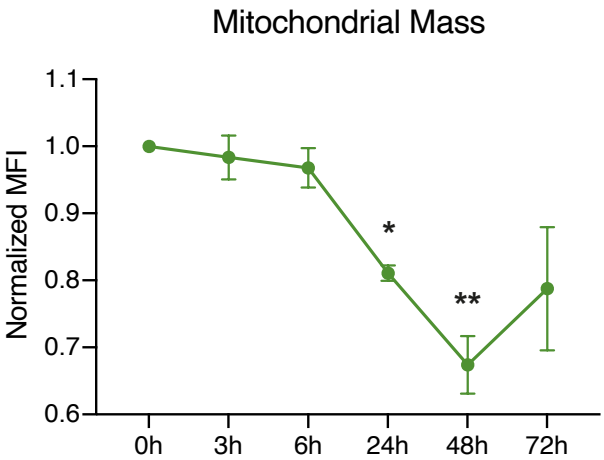

Figure 36: IFNβ-induced changes to mitochondrial mass in HMDMs. MFI of MitoTracker Green FM in single, viable HMDMs treated with 100 IU/ml IFNβ for the indicated periods normalized to untreated cells (n = 4, except 24 h: n = 2; asterisks indicate significance using a one-way ANOVA, * $p < 0.05$, ** $p < 0.01$; error bars represent the standard deviation of the mean).

significant reduction of mitochondrial mass in HMDMs after 24–48 h, even though mTORC1 is rapidly activated (Fig. 36). This suggests that the translational rate of mitochondrial genes connected to mitochondrial fission might be dependent on 4EBP2 3'-UTR length.

Overall, the number of proteins detected to be specifically associated with 4EBP2 is small compared to non-specific interactions with mCitrine in the EV samples, irrespective of its 3'-UTR length. The abundance of EIF4E among both 4EBP2-SU and 4EBP2-LU suggests that its role as a translational inhibitor through competitive binding is 3'-UTR independent. Many of the other ontologies among SU- and LU-specific interactors have been connected to 4EBPs in different studies. However, none of these studies considered the role of spatial separation of specific mRNA subsets during translation as part of those processes or whether the investigated 4EBP was translated from a SU or LU mRNA. Determining the location of 4EBP2 SU and LU transcripts and proteins within the cell is a crucial next step for further study and exploring effects on translational rates of different mRNA classes by 4EBP2 SU and LU should follow. IFNβ-mediated changes to 4EBP2 3'-UTR length could be a key mechanism to regulate translational rates of distinct mRNAs, potentially through spatial separation.

4.4.7 3'-UTR-Dependent MAVS Protein-Protein Interactions

The second protein investigated in this experiment is MAVS, a mitochondrial antiviral signaling protein. It is activated by the RLRs RIG-I and MDA5, which undergo conformational changes upon sensing viral RNA, that expose a CARD domain, which mediates interaction with an equivalent domain on MAVS (Brisse & Ly 2019; Kowalinski et al. 2011). Subsequently, MAVS oligomerizes and forms aggregates, which allow recruitment of adapter proteins such as TRAFs that mediate downstream signaling (Hou et al. 2011; Tang & Wang 2009). TRAF proteins can initiate phosphorylation and activation of different IRFs by TBKI-IKKε and lead to downstream type I and type III IFN production (Liu et al. 2013). They

can also mediate phosphorylation of NFκB via IKKα/β/γ, which results in the expression of inflammatory genes (Liu et al. 2013). Since MAVS 3'-UTR shortening was observed in response to IFNβ signaling in this study, functional consequences may relate to or affect the formation of regulatory feedback loops to control the expression of IFNs and other cytokines.

One of the proteins that prevents MAVS aggregation and subsequent interactions with the adaptor proteins TRAF3 and TRAF6 is UBXN1 (Wang et al. 2013). It was detected in all MAVS sample groups in this experiment, indicating that the proteins expressed from these constructs have formed secondary and tertiary structures similar to that of the endogenous protein, which enable interactions with other components. Translocase of outer membrane 70A (TOM70A), a scaffold protein that enables MAVS association with IRF3 and TBK1 in connection with HSP90 and allows downstream signaling, was detected as well (Liu et al. 2010).

Several MAVS interactors that have been described in the literature were not measured at all in this experiment, likely either because their interaction is too transient to be measure in an IP or because they are not expressed at a sufficient level in HEK293T cells.

In addition to known MAVS interactors such as UBXN1 and TOM70A that may bind to MAVS independent of a 3'-UTR, network analyses of 3'-UTR-length-specific interactors revealed some ontologies that could be influenced by APA.

4.4.8 MAVS Interactions Mediated by its Long 3'-UTR

Three clusters were formed by MAVS LU interactors, the smallest of which contains proteins from the outer mitochondrial membrane, one of the most prominent subcellular MAVS locations (Seth et al. 2005). It is a central point of RLR signaling to which RIG-I and MDA5 are transported by a mitochondria-targeting chaperone to activate MAVS (Liu et al. 2013). The LU-specificity of this network suggests MAVS LU could be more abundant in mitochondria than other organelles, which is discussed in more detail in a following paragraph. One of the

interactors in this cluster is COX5B, a component of the mitochondrial respiratory chain, which can suppress mitochondrial MAVS activity by binding MAVS in cooperation with the autophagy protein 5 (ATG5) and by reducing the level of ROS (Zhao Y et al. 2012).

The two other LU-specific clusters are much bigger and contain proteins involved in the protein synthesis and degradation, such as ribosomal proteins and ubiquitin ligases, and transcriptional regulator and RNA processing factors. Clusters with similar ontologies were found in the SU-specific network analysis, but they were much smaller.

Of the ontologies in this second LU-specific cluster, no connection has previously been described between MAVS and ribosomal proteins; however, ubiquitin ligases are prominent interactors of MAVS and can modify different lysine residues. Ubiquitination can act as a regulatory signal as well as a marker for degradation by the ubiquitin-proteasome, both of which are essential to avoid excessive inflammation in a cell. Its function mainly depends on which lysine residue serves as a linker in the polyubiquitin chain (Komander & Rape 2012). membrane-associated ring-CH-type finger (MARCH) 5, TRIM25, RNF5, AIP4 and von Hippel-Lindau disease tumor suppressor (VHL) can all mark MAVS for proteasomal degradation through K48-linked ubiquitination (Castanier et al. 2012; Du et al. 2018; Yoo et al. 2015; You et al. 2009; Zhong et al. 2010). MAVS is similarly marked for proteasomal degradation by K11-linked ubiquitination through TRIM29 (Xing et al. 2018). Nuclear dot protein 52 (NDP52)-dependent autophagic degradation can be induced by a K27- and K27/K29-linked polyubiquitin chain added by MARCH8 and RNF34 respectively (He et al. 2019; Jin et al. 2017). This effect is dependent on the lysine residue the polyubiquitin chain is added to, since K27-linked ubiquitination mediated by TRIM21 promotes antiviral signaling by enhancing MAVS association with TBK1 (Xue et al. 2018). K63-linked polyubiquitination by TRIM31 has an equally positive effect on MAVS signaling through promoting aggregate formation (Liu B et al. 2017). Interestingly, K63-linkage is stimulated by MAVS O-GlcNAcetylation (Li et al. 2018; Song et al. 2019), and the O-GlcNAc metabolism is altered in response to IFNβ in BMDMs, as shown in this study previously.

The third LU-specific cluster contains proteins that are connected to RNA processing and transcriptional responses. The transcriptional responses activated by MAVS signaling through IRFs and NFκB have been well described in the literature, but their connection to the mRNA processing machinery has only been mentioned in a study by Soonthornvacharin and colleagues, who identified RNA metabolism among others as a critical pathway regulating RIG-I signaling (Soonthornvacharin et al. 2017). However, another study has shown that the RNA editing enzyme ADAR1 can lead to enhanced degradation of MAVS through deamination of adenosine, which reduces the antiviral response (Li T et al. 2021). The editing site described in this study is located in the distal 3'-UTR, so only MAVS LU is subject to this regulatory mechanism. ADAR1 is also induced by IFNβ treatment in HMDMs, which suggests a potential escape from targeted degradation through 3'-UTR shortening.

4.4.9 MAVS Interactions Mediated by its Short 3'-UTR

In addition to these MAVS LU-specific interactions, a lot of ontologies unique to MAVS SU interactors were revealed in the MAVS SU network analysis. Although MAVS LU contains all MAVS SU sequence information and more, it is possible for proteins to uniquely interact with MAVS SU due to the complex RNA secondary structures formed through intramolecular interactions. These structures can mask and reveal certain regions and motifs.

The number of clusters in the MAVS SU network was much bigger and were therefore associated with much more diverse ontologies, but each cluster contained a significantly smaller number of proteins compared to MAVS LU.

The ontologies of a few of the clusters were related, showing a connection to MAP kinase signaling, transcriptional activation and cell cycle progression. MAVS-mediated type I IFN induction in response to viral infection has been shown to be dependent on the MAP kinases p38 and ERK. If these kinases play a similar role in the context of this study, they could be part of a regulatory feedback loop (Odendall et al. 2014).

Another, more distinct cluster contains a variety of tRNA-amino acid-ligases, a class of enzymes whose role in immune regulation has also been connected to MAP kinase activity. Lysine-tRNA ligase (KARS1), a cytoplasmic-tRNA- amino acid -ligase, is released from multi-synthase-complex (MSC) in response to HIV infection, a process dependent on MEK activity. Proteins from this free pool of KARS1 are transported into the nucleus and facilitate incorporation of lysine-conjugated tRNAs into HIV particles (Cen et al. 2001; Duchon et al. 2017). Cellular tRNAs can serve as primers to initiate reverse transcription at the start of the viral replication cycle and their loss can lead to reduced infectivity of viral progeny (Guo et al. 2003; Mak & Kleiman 1997; Wakefield et al. 1995). Another example of involvement of this class of enzymes in antiviral immunity has been published by Marquez-Jurado and colleagues. Arginyl-tRNA synthetase (RRS) and glutamyl-prolyl-tRNA synthetase (EPRS) can interact with a 3'-motif on the transmissible gastroenteritis coronavirus (TGEV) genome and block MDA5 activation (Marquez-Jurado et al. 2015). This prevents subsequent antiviral signaling, which is mediated by MAVS. A last example highlights the role of these enzymes in starting an immune response. EPRS can be phosphorylated and dissociates from the MSC in response to viral infection (Lee et al. 2016). It can then bind the ubiquitin ligase poly rC-binding protein 2 (PCBP2), which usually mediates MAVS ubiquitination and degradation via AIP4, and stabilize and enhance antiviral signaling.

The last distinct SU-specific cluster contains proteins associated with the cytoskeleton, some of which have regulatory effects on MAVS signaling. The microtubule-associated proteins GEF-H1 and HAUS augmin-like complex subunit 1 (HAUS1), for example, stimulate MAVS ubiquitination and TBK1 activity, which alters IRF activation and subsequently IFN induction (Chiang et al. 2014; He et al. 2018). The focal adhesion kinase (FAK), on the other hand, is associated with actin filaments and can interact with and potentiate MAVS signaling in response to viral infection (Bozym et al. 2012). The connection between the cytoskeleton and MAVS is not extensively researched yet and similar roles for other proteins associated with microtubule or actin filaments are plausible. A key role of these filaments, however, is in transport of protein

complexes and organelles (Hirokawa et al. 2009). The MAVS SU specificity of this ontology again suggests protein localization and transport could be affected by 3'-UTR length. This argument is supported by a recent publication investigating MAVS 3'-UTR function (Xu et al. 2019). It showed that expression of a specific section of the 3'-UTR leads to mitochondrial localization of a GFP reporter. This region is located in the distal part of the 3'-UTR, which was defined as MAVS LU-specific in the PAT-seq results of this study and aligns with the mitochondrial association of cluster 1 of the MAVS LU-interactor network described above. The MAVS transport mechanism is currently not known, but these results strongly suggest it may be dependent on the length of its 3'-UTR. Transport of MAVS protein by co-translationally formed RBP-dependent protein complexes as seen for CD47 and other cell surface proteins translated from LU transcript is plausible (Berkovits & Mayr 2015; Ma & Mayr 2018). Another possibility is transport and local translation of *MAVS LU* at the mitochondria, a mechanism that has been described for *BDNF LU* in neurons (An et al. 2008; Lau et al. 2010).

Studies have shown that MAVS can localize to different subcellular structures, the ER, MAMs, mitochondria and peroxisomes, but little is known about location-specific functions (Dixit et al. 2010; Horner et al. 2011; Seth et al. 2005). A group of researchers reported differential type I and type III IFN induction by peroxisomal and mitochondrial MAVS, an effect that was dependent on IRF1 activation, exclusively mediated by the peroxisomal variant (Dixit et al. 2010; Odendall et al. 2014). However, this observation was not consistent with findings of another group and are generally challenging to investigate, due to the dynamic interactions of the involved organelles during viral infections and their differences across cell types and species (Bender et al. 2015; Horner et al. 2011). This is additionally complicated by the ability of IRF1 to block the interaction between IRF3 and the protein phosphatase 2A (PP2A), which enables phosphorylation and activation of IRF3 (Wang et al. 2020). Although the results in this experiment do not suggest distinct type I and type III IFN production by MAVS SU and LU, their ability to activate IRFs and other transcription factors will be investigated in

future experiments, since they could have effects on regulatory feedback loops initiated by IFNβ.

Overall, many MAVS-related ontologies were detected among all MAVS-specific interactors, suggesting a successful experimental setup. As expected, many proteins interact with MAVS independently of its 3'-UTR, and many interactors described in literature could not be detected, likely due to the experimental setup. However, investigation of MAVS LU-specific interactions showed a clear bias towards proteins in the outer mitochondrial membrane, consistent with recent findings in literature, which suggest the distal 3'-UTR plays a role in protein localization. Other ontologies connected to MAVS LU such as ribosomal proteins and RNA processing are not well described and their role in antiviral signaling should be investigated. MAVS SU-specific interactor showed equally distinct ontologies. Most of them have already been connected to antiviral signaling, but the results of this experiment suggest they might play more significant roles than previously thought. It seems plausible, for example, that additional tRNA- amino acid -ligases can regulate RLR-signaling and their roles should be investigated. Similarly, MAP kinase signaling contributed to type I and type III IFN induction in different studies, but the MAP kinase activation pathway in connection to MAVS has not been described (Jiang et al. 2015; McGuire et al. 2017). The results of this experiment suggest MAVS SU and LU signaling might be differentially regulated and, consistent with current literature, indicate that protein localization could be dependent on 3'-UTR-length.

4.5 Conclusion

The experiments in this study showed that IFNβ treatment in THP-1 cells and HMDMs led to a global change to the cellular polyadenylation pattern, with a shift towards the use of more proximal cleavage sites, which produces shorter 3'-UTRs. Inhibitor experiments showed that this effect is mediated by JAK-dependent IRG expression and is therefore a secondary response in IFNβ-treated macrophages. The set-up of additional experimental approaches, such as a PrimeFlow-based unbiased screen, will allow further characterization of the IRGs involved in 3'-UTR shortening.

Investigation of MAVS and 4EBP2 3'-UTR-dependent protein complex formation revealed a scaffold-like function in line with recent reports in literature. These 3'-UTR-isoform-specific protein complexes may have diverse functions that are differentially regulated by IFNβ. The results also suggest a potential role for 3'-UTR length in RNA and protein localization, which could further specify their function.

In conclusion, findings in this study describe a new mechanism of post-transcriptional gene regulation by IFNβ, which may diversify protein functions and expand the current understanding of IRGs.

4.6 Supplementary Figures

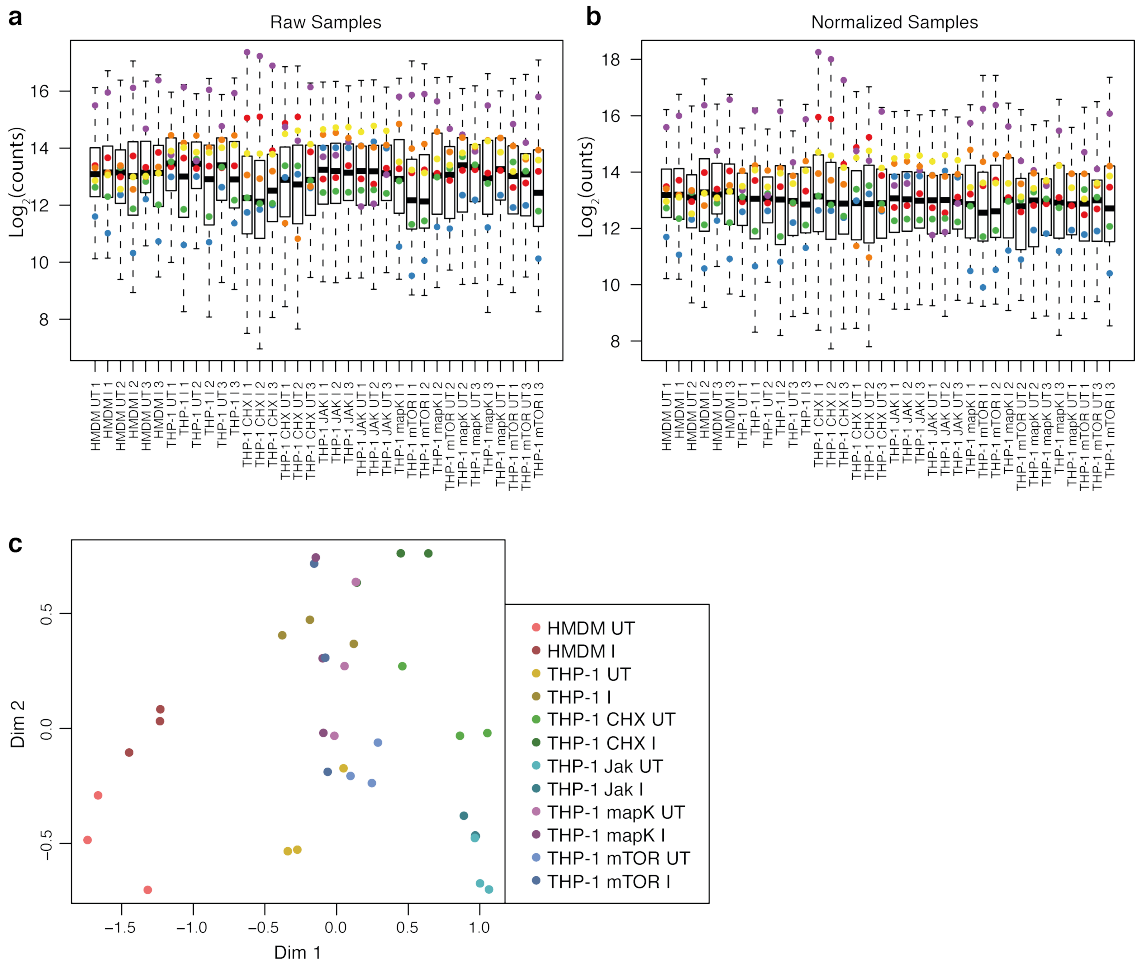

Supplementary Figure 1: NanoString analysis quality control plots. Probe counts before (a) and after (b) normalization using the R package limma are shown across samples. Counts of housekeeping genes are highlighted by color. c) MDS plot of all samples.

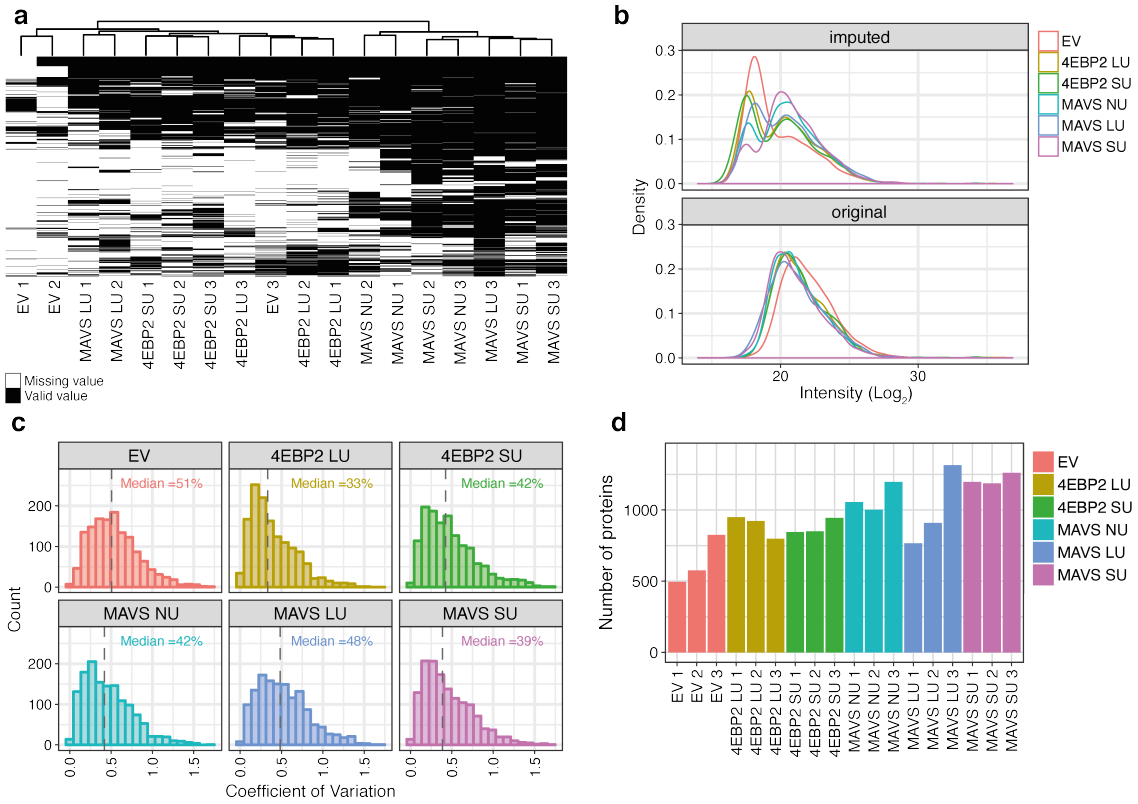

Supplementary Figure 2: Co-IP analysis quality control plots. a) Heat map showing undetected proteins (missing values) across samples. b) Density of log_2 intensities before and after imputation of missing values. c) Plots showing the coefficients of variation across sample groups. Median values are shown. d) Plot showing the number of proteins detected per sample.

5. Discussion and Future Directions

5.1 Cellular Metabolism

The global reprogramming of IFNβ-activated macrophages was investigated in this study by looking at changes on transcript, protein and metabolite levels and their relationship to one another.

The metabolic profile of IFNβ-activated BMDMs shared similarities with both M1 and M2 macrophages and showed a dynamic response over a 24 h time period. The cellular inflammatory potential changed from showing M2-like characteristics after 1–3 h of IFNβ treatment to a phenotype more similar to M1 macrophages after 16 h. The initial anti-inflammatory properties of BMDMs could be a combined effect of IFNβ treatment and their differentiation with L929-conditioned medium, which contains high levels of M-CSF, a cytokine that has previously been shown to induce a transcriptional profile similar to that of M2 macrophages (Jaguin et al. 2013). Although the experimental setup in this study did not include additional stimuli, it is likely that cytokines, newly expressed in response to IFNβ, were secreted and auto-activated the BMDMs, as they would in physiological settings, and therefore contributed to metabolic profiles observed after 16 h and 24 h (Goritzka et al. 2014). Taken together, these changes to metabolite levels highlight the dynamic nature of macrophage polarization, which has not been extensively described in literature to date. A recent publication has described the loss of electron transport chain complexes as a result of NO accumulation in M1 macrophages in an extended experiment, which emphasizes the importance of temporal control of inflammation (Palmieri et al. 2020). Future investigations should examine the secreted cytokine profile in response to IFN at different times to investigate their potential impact and interactions. Further studies could also address responses at much later time points, which would relate to the development of an innate immune memory. Additional experiments should also include the use of isotopically labelled substrate supplements in cell culture media, which would allow characterization of the direction of metabolic

conversion reactions. This could, for example, help to determine what function purine and amino acid metabolism intermediates have in the rapid response to IFNβ.

The changes to these intermediates observed after 1 h of IFNβ treatment in this experiment preceded alterations of corresponding enzymes on protein level, which suggests they could be regulated post-translationally. Modifications such as phosphorylation, ubiquitination and glycosylation are important post-translational regulators of protein function, which can be measured by mass spectrometry. The extent and character of post-translational modifications of metabolic enzymes should be investigated in future in response to IFNβ, since most components of the different rapidly activated signaling cascades are kinases that phosphorylate their respective targets. Additional key aspects of protein function that could be relevant in the context of rapid changes to purine metabolism intermediates are protein-protein interactions. This is not as easily addressed as protein modifications, since it requires a targeted approach for every enzyme of interest, but it should be considered at later stages of a project investigating the purine metabolism.

Investigating IFNβ-induced changes to the cellular metabolism, their connection to RNA and protein expression and uncovering the molecular mechanisms behind these changes is crucial to understanding the role of macrophages and type 1 IFNs in the immune response. This understanding is the basis for future research into treatments and medication for many autoimmune disorders or infectious diseases that have a type 1 IFN component. The metabolic changes in the early stage of IFNβ-activation of BMDMs discovered in this study in particular are important contributions to the field, since they have not been reported in literature, but are likely important components of a potent IFN response.

5.2 3’-UTR Scaffold Function

This study has shown that IFNβ treatment changes the global APA pattern in murine and human macrophages, which resulted in changed 3’-UTR lengths of

affected transcripts. Further investigations of the proteins MAVS and 4EBP2 expressed from mRNA with a short or a long 3'-UTR showed that they interact with different proteins. 3'-UTR length-dependent differential protein complex formation is a recently discovered mechanism that can regulate diverse protein functions of CD47 and BIRC3 (Berkovits & Mayr 2015; Lee & Mayr 2019; Ma & Mayr 2018). A similar role seems likely for *MAVS* and *4EBP2* 3'-UTRs given the difference and diversity of interactors of SU and LU proteins.

3'-UTR-dependent protein complex formation is generally mediated by RBPs. These RBPs can directly associate with the nascent protein or facilitate interactions between the nascent protein and other components that are associated with these RBPs (Berkovits & Mayr 2015; Lee & Mayr 2019; Ma & Mayr 2018). Adaptor RBPs are necessarily part of the resulting protein complexes and were therefore not comprehensively measured in the experiments of this study. Interactions of RBPs with SU and LU mRNA will be investigated in future, for example through overexpression of RBPs and detection of interactions with *in vitro* transcribed SU and LU mRNA. Information on which RBPs preferentially bind SU and LU mRNA could help narrow down the list of interactors detected in this study for further validation. For example, SU- and LU-specific protein binding partners could be filtered and grouped using information on previously recorded interactions with certain RBPs, which can be found in public databases such as STRING DB.

3'-UTR length-dependent protein-protein interactions should be validated and investigated in a cell model more relevant to macrophages than the previously used HEK293T cells, which will likely involve the generation of several cell lines that only express one transcript isoform of a gene of interest. Their specific function and contribution to IFNβ-induced antiviral responses should be investigated and compared to the effects of whole gene knockouts.

Other previously described components of 3'-UTR-dependent protein function are differential transport and localization of mRNA and protein (An et al. 2008; Berkovits & Mayr 2015; Lau et al. 2010; Lee & Mayr 2019; Ma & Mayr 2018; Wu H et al. 2020). The results of this study suggest that this could also be the case

for 4EBP2 and MAVS, which will be addressed microscopically using immunofluorescence or RNA-fluorescence *in situ* hybridization (FISH).

A recent study also linked mitochondrial localization of a reporter to a motif in the distal part of the *MAVS* 3'-UTR (Xu et al. 2019). This motif is located in the LU-specific sequence described in this study, making mitochondrial MAVS function compared to MAVS in other compartments a particular focus of future experiments. The expression of type I and type III IFNs in response to mitochondrial or peroxisomal MAVS signaling is the only functional distinction in connection to localization suggested in literature so far (Dixit et al. 2010; Odendall et al. 2014). A connection to the MAP kinase ERK and the transcription factor IRF1 were suggested in a subsequent publication by the same group of researchers, while another reported opposing results, which showed no difference in cytokine expression depending on MAVS localization (Bender et al. 2015; Odendall et al. 2014).

None of the publications considered the *MAVS* 3'-UTR in this context and future studies should address the possibility of differential transcription factor activation and cytokine expression as a result of *MAVS* 3'-UTR length. These future experiments should also investigate the consequences of different APA events across species, which was shown for mouse and human macrophages in this study, since they may influence the formation of species-specific type I IFN responses.

An aspect that was not investigated in the experiments of this study is the activation status of 4EBP2 and MAVS, which affects how they interact with other proteins. 4EBP2 is bound to EIF4E and inhibits its involvement in translation initiation, but upon phosphorylation by mTORC1 it releases EIF4E and its disordered domains fold into β-sheets (Dawson et al. 2020; Fletcher et al. 1998). MAVS is activated through interaction with an RLR-CARD in response to viral infections, which leads to aggregation and MAVS filament formation, which is needed for subsequent interactions with different signal transducers (Hou et al. 2011). These signal-dependent changes to the MAVS and 4EBP2 interactomes could in future be addressed using protein tags that allow investigations of live-cell proteomics, such as apurinic/apyrimidinic endodeoxyribonuclease 2

(APEX2), a peroxidase that covalently tags molecules in close proximity with biotin-phenol (Hung et al. 2016). The role of 3'-UTR length on signal-dependent changes to protein interactions could be investigated by adding an APEX2 tag to MAVS and 4EBP2 gene loci in cell lines expressing only one 3'-UTR transcript isoform.

MAVS and 4EBP2 are just two examples of hundreds of genes that are expressed with changed 3'-UTR lengths in response to IFNβ treatment. Since they are not part of the core IRGs that are highly induced by type I IFNs, they have not been extensively studied and considered in the cellular IFN response. However, these new IRGs could be a class of genes whose role in antiviral responses and other cellular processes is dependent on protein-protein interactions that are facilitated by specific 3'-UTRs, which are preferentially expressed in response to IFNβ-induced APA. This would align with previous reports of interactions between IRGs and other cellular proteins, and the importance of proteins other than IRGs in antiviral responses (Hubel et al. 2019; OhAinle et al. 2018). Future experiments should address if this new class of IRGs is specific to macrophages and type I IFNs or part of a global phenomenon by looking at different cell types and responses to type I and III IFNs.

5.3 Regulation of APA by IFN

The results of this study showed that changes to APA patterns in response to IFNβ are mediated by one or multiple IRGs. Previous studies have reported the involvement of components of the cleavage and polyadenylation machinery in regulation of APA, but none of them are highly induced upon IFNβ treatment, making them all equally likely regulatory candidates in this study (Beaudoing et al. 2000; Brumbaugh et al. 2018; Chan et al. 2011; Chang et al. 2015; Di Giammartino et al. 2014; Elkon et al. 2012; Gruber et al. 2012; Isobe et al. 2020; Lackford et al. 2014; Li et al. 2015; Luo et al. 2013; Martin et al. 2012; Modic et al. 2019; Rappsilber et al. 2002; Takagaki et al. 1996; Turner et al. 2020; Wang et al. 2019; Xing et al. 2008; Yao et al. 2013; Zhu et al. 2018). An unbiased large-

scale screen is the most appropriate experimental approach for further investigations, given the large number of proteins constituting the cleavage and polyadenylation machinery and the hundreds of IFNβ-inducible IRGs that could associate with them in a manner similar to IFIT1 and 3 (Shi et al. 2009). The RNA-labelling technique PrimeFlow was set up for this purpose as part of this study. It will be the read out for a CRISPR/Cas9-based genome-wide knockout screen in THP-1 cells to identify IFN-inducible regulators of APA.

The expression of *CBX5* and *G3BP1* 3'-UTRs in HMDMs was investigated as part of this set-up and resulted in the discovery of two cell populations with distinct RNA expression signals, highlighting the heterogeneity of primary cell cultures. Further characterization of these populations should follow in future, for example through PAT-seq to determine the overall APA pattern to see if LU expression is conserved across multiple genes or by quantitative proteomics analyses to determine the existence of unique expression markers and potential functional differences. This is a first step towards investigations of APA patterns in single cells, a technique that has been used in recent publications and revealed the existence of subpopulations within a pool of cells with similar gene expression levels (Gao et al. 2021). This is especially important in the context of the emerging role of APA in differential regulation of protein function, which influences the cellular functional repertoire without significantly altering the abundance of proteins, including lineage markers commonly used to distinguish populations.

The findings of this study expand the current understanding of

5.4 Summary

Investigations of transcriptomic, proteomic and metabolic changes in IFNβ-activated macrophages have characterized the global response on different levels. They have contributed to the current understanding of the connection between these levels and the complex regulatory network that is formed. Transcriptional responses to IFNβ include the expression of enzymes that influence the cellular metabolic profile, such as ACOD1 and IDH, which promote

itaconate production. The resulting metabolic profile can alter protein function, such as the increase in UDP-GlcNAc levels observed after 24 h of IFNβ treatment in this study, which can drive glycosylation of macromolecules. One such protein described in the literature is MAVS, whose glycosylation promotes K63-linked ubiquitination, a key modification that regulates MAVS signaling activity, the end result of which is the activation of transcription factors (Li et al. 2018; Song et al. 2019). Protein modifications or interactions are also likely to contribute to the very rapid metabolic changes observed in response to IFNβ in this study, since they precede changes to the transcriptome. These examples highlight the complex interactions that are necessary to initiate and control the cellular responses induced by type I IFNs.

Another aspect of this network is the post-transcriptional regulation of proteins, which is centered around 3'-UTRs. Investigations in this study focused on global shortening of 3'-UTRs in response to IFNβ, which is a result of IRG-mediated differential regulation of APA. The length of 3'-UTRs influences interactions of the encoded protein, as shown for MAVS and 4EBP2 in this study, which can result in different protein localization and function.

Future investigations will focus on identifying IFN-inducible components that contribute to differential regulation of APA in this setting and on defining the functional roles of this new class of IRGs made from transcripts with different 3'-UTRs in antiviral responses. APA is a phenomenon observed in many biological contexts and the integrity of different PASs can be crucial for development and immune cell function (Bennett et al. 2001). APA of different genes has the potential to influence many other cellular functions and is an important aspect to consider in future projects and applications.

References

Ablasser A, Goldeck M, Cavlar T, Deimling T, Witte G, Rohl I, Hopfner KP, Ludwig J & Hornung V (2013), "cGAS produces a 2'-5'-linked cyclic dinucleotide second messenger that activates STING", *Nature,* vol. 498 pp. 380-384, doi:10.1038/nature12306

Agarwal V, Bell GW, Nam JW & Bartel DP (2015), "Predicting effective microRNA target sites in mammalian mRNAs", *Elife,* vol. 4 doi:10.7554/eLife.05005

Agnihotri S, Burrell K, Buczkowicz P, Remke M, Golbourn B, Chornenkyy Y, Gajadhar A, Fernandez NA, Clarke ID, Barszczyk MS, Pajovic S, Ternamian C, Head R, Sabha N, Sobol RW, Taylor MD, Rutka JT, Jones C, Dirks PB, Zadeh G & Hawkins C (2014), "ATM regulates 3-methylpurine-DNA glycosylase and promotes therapeutic resistance to alkylating agents", *Cancer Discov,* vol. 4 pp. 1198-1213, doi:10.1158/2159-8290.CD-14-0157

Ahel J, Lehner A, Vogel A, Schleiffer A, Meinhart A, Haselbach D & Clausen T (2020), "Moyamoya disease factor RNF213 is a giant E3 ligase with a dynein-like core and a distinct ubiquitin-transfer mechanism", *Elife,* vol. 9 doi:10.7554/eLife.56185

Ahmed D, Jaworski A, Roy D, Willmore W, Golshani A & Cassol E (2018), "Transcriptional Profiling Suggests Extensive Metabolic Rewiring of Human and Mouse Macrophages during Early Interferon Alpha Responses", *Mediators Inflamm,* vol. 2018 p. 5906819, doi:10.1155/2018/5906819

Ai D, Jiang H, Westerterp M, Murphy AJ, Wang M, Ganda A, Abramowicz S, Welch C, Almazan F, Zhu Y, Miller YI & Tall AR (2014), "Disruption of mammalian target of rapamycin complex 1 in macrophages decreases chemokine gene expression and atherosclerosis", *Circ Res,* vol. 114 pp. 1576-1584, doi:10.1161/CIRCRESAHA.114.302313

Albina JE, Mills CD, Barbul A, Thirkill CE, Henry WL, Jr., Mastrofrancesco B & Caldwell MD (1988), "Arginine metabolism in wounds", *Am J Physiol,* vol. 254 pp. E459-467, doi:10.1152/ajpendo.1988.254.4.E459

Alonso D & Nungester WJ (1956), "Comparative study of host resistance of guinea pigs and rats. V. The effect of pneumococcal products on glycolysis and oxygen uptake by polymorphonuclear leucocytes", *J Infect Dis,* vol. 99 pp. 174-181, doi:10.1093/infdis/99.2.174

Amarante-Mendes GP, Adjemian S, Branco LM, Zanetti LC, Weinlich R & Bortoluci KR (2018), "Pattern Recognition Receptors and the Host Cell Death Molecular Machinery", *Front Immunol,* vol. 9 p. 2379, doi:10.3389/fimmu.2018.02379

An JJ, Gharami K, Liao GY, Woo NH, Lau AG, Vanevski F, Torre ER, Jones KR, Feng Y, Lu B & Xu B (2008), "Distinct role of long 3' UTR BDNF mRNA in spine morphology and synaptic plasticity in hippocampal neurons", *Cell,* vol. 134 pp. 175-187, doi:10.1016/j.cell.2008.05.045

Anderson CF & Mosser DM (2002), "A novel phenotype for an activated macrophage: the type 2 activated macrophage", *J Leukoc Biol,* vol. 72 pp. 101-106,

Andreou A, Trantza S, Filippou D, Sipsas N & Tsiodras S (2020), "COVID-19: The Potential Role of Copper and N-acetylcysteine (NAC) in a Combination of Candidate Antiviral Treatments Against SARS-CoV-2", *In Vivo,* vol. 34 pp. 1567-1588, doi:10.21873/invivo.11946

Arango Duque G & Descoteaux A (2014), "Macrophage cytokines: involvement in immunity and infectious diseases", *Front Immunol,* vol. 5 p. 491, doi:10.3389/fimmu.2014.00491

Asano K, Nabeyama A, Miyake Y, Qiu CH, Kurita A, Tomura M, Kanagawa O, Fujii S & Tanaka M (2011), "CD169-positive macrophages dominate antitumor immunity by crosspresenting dead cell-associated antigens", *Immunity,* vol. 34 pp. 85-95, doi:10.1016/j.immuni.2010.12.011

Baardman J, Verberk SGS, Prange KHM, van Weeghel M, van der Velden S, Ryan DG, Wust RCI, Neele AE, Speijer D, Denis SW, Witte ME, Houtkooper RH, O'Neill L A, Knatko EV, Dinkova-Kostova AT, Lutgens E, de Winther MPJ & Van den Bossche J (2018), "A Defective Pentose Phosphate Pathway Reduces Inflammatory Macrophage Responses during Hypercholesterolemia", *Cell Rep,* vol. 25 pp. 2044-2052 e2045, doi:10.1016/j.celrep.2018.10.092

Baez MV & Boccaccio GL (2005), "Mammalian Smaug is a translational repressor that forms cytoplasmic foci similar to stress granules", *J Biol Chem,* vol. 280 pp. 43131-43140, doi:10.1074/jbc.M508374200

Bai Y, Auperin TC, Chou CY, Chang GG, Manley JL & Tong L (2007), "Crystal structure of murine CstF-77: dimeric association and implications for polyadenylation of mRNA precursors", *Mol Cell,* vol. 25 pp. 863-875, doi:10.1016/j.molcel.2007.01.034

Bambouskova M, Gorvel L, Lampropoulou V, Sergushichev A, Loginicheva E, Johnson K, Korenfeld D, Mathyer ME, Kim H, Huang LH, Duncan D, Bregman H, Keskin A, Santeford A, Apte RS, Sehgal R, Johnson B, Amarasinghe GK, Soares MP, Satoh T, Akira S, Hai T, de Guzman Strong C, Auclair K, Roddy TP, Biller SA, Jovanovic M, Klechevsky E, Stewart KM, Randolph GJ & Artyomov MN (2018), "Electrophilic properties of itaconate and derivatives regulate the IkappaBzeta-ATF3 inflammatory axis", *Nature,* vol. 556 pp. 501-504, doi:10.1038/s41586-018-0052-z

Banko JL, Poulin F, Hou L, DeMaria CT, Sonenberg N & Klann E (2005), "The translation repressor 4E-BP2 is critical for eIF4F complex formation, synaptic plasticity, and memory in the hippocampus", *J Neurosci,* vol. 25 pp. 9581-9590, doi:10.1523/JNEUROSCI.2423-05.2005

Barr SD, Smiley JR & Bushman FD (2008), "The interferon response inhibits HIV particle production by induction of TRIM22", *PLoS Pathog,* vol. 4 p. e1000007, doi:10.1371/journal.ppat.1000007

Bartel DP (2009), "MicroRNAs: target recognition and regulatory functions", *Cell,* vol. 136 pp. 215-233, doi:10.1016/j.cell.2009.01.002

Barth ML, Fensom A & Harris A (1993), "Prevalence of common mutations in the arylsulphatase A gene in metachromatic leukodystrophy patients diagnosed in Britain", *Hum Genet,* vol. 91 pp. 73-77, doi:10.1007/BF00230227

Basu SK, Malik R, Huggins CJ, Lee S, Sebastian T, Sakchaisri K, Quinones OA, Alvord WG & Johnson PF (2011), "3'UTR elements inhibit Ras-induced C/EBPbeta post-translational activation and senescence in tumour cells", *EMBO J,* vol. 30 pp. 3714-3728, doi:10.1038/emboj.2011.250

Battelli C, Nikopoulos GN, Mitchell JG & Verdi JM (2006), "The RNA-binding protein Musashi-1 regulates neural development through the translational repression of p21WAF-1", *Mol Cell Neurosci,* vol. 31 pp. 85-96, doi:10.1016/j.mcn.2005.09.003

Bauer KE, Segura I, Gaspar I, Scheuss V, Illig C, Ammer G, Hutten S, Basyuk E, Fernandez-Moya SM, Ehses J, Bertrand E & Kiebler MA (2019), "Live cell imaging reveals 3'-UTR dependent mRNA sorting to synapses", *Nat Commun,* vol. 10 p. 3178, doi:10.1038/s41467-019-11123-x

Bava FA, Eliscovich C, Ferreira PG, Minana B, Ben-Dov C, Guigo R, Valcarcel J & Mendez R (2013), "CPEB1 coordinates alternative 3'-UTR formation with translational regulation", *Nature,* vol. 495 pp. 121-125, doi:10.1038/nature11901

Beaudoing E, Freier S, Wyatt JR, Claverie JM & Gautheret D (2000), "Patterns of variant polyadenylation signal usage in human genes", *Genome Res,* vol. 10 pp. 1001-1010, doi:10.1101/gr.10.7.1001

Bekisz J, Baron S, Balinsky C, Morrow A & Zoon KC (2010), "Antiproliferative Properties of Type I and Type II Interferon", *Pharmaceuticals (Basel),* vol. 3 pp. 994-1015, doi:10.3390/ph3040994

Belgnaoui SM, Paz S, Samuel S, Goulet ML, Sun Q, Kikkert M, Iwai K, Dikic I, Hiscott J & Lin R (2012), "Linear ubiquitination of NEMO negatively regulates the interferon antiviral response through disruption of the MAVS-TRAF3 complex", *Cell Host Microbe,* vol. 12 pp. 211-222, doi:10.1016/j.chom.2012.06.009

Bellows CF & Jaffe BM (1999), "Glutamine is essential for nitric oxide synthesis by murine macrophages", *J Surg Res,* vol. 86 pp. 213-219, doi:10.1006/jsre.1999.5713

Ben-Sasson SZ, Hu-Li J, Quiel J, Cauchetaux S, Ratner M, Shapira I, Dinarello CA & Paul WE (2009), "IL-1 acts directly on CD4 T cells to enhance their antigen-driven expansion and differentiation", *Proc Natl Acad Sci U S A,* vol. 106 pp. 7119-7124, doi:10.1073/pnas.0902745106

Bender S, Reuter A, Eberle F, Einhorn E, Binder M & Bartenschlager R (2015), "Activation of Type I and III Interferon Response by Mitochondrial and Peroxisomal MAVS and Inhibition by Hepatitis C Virus", *PLoS Pathog,* vol. 11 p. e1005264, doi:10.1371/journal.ppat.1005264

Bennett CL, Brunkow ME, Ramsdell F, O'Briant KC, Zhu Q, Fuleihan RL, Shigeoka AO, Ochs HD & Chance PF (2001), "A rare polyadenylation signal mutation of the FOXP3 gene (AAUAAA-->AAUGAA) leads to the IPEX syndrome", *Immunogenetics,* vol. 53 pp. 435-439, doi:10.1007/s002510100358

Berg MG, Singh LN, Younis I, Liu Q, Pinto AM, Kaida D, Zhang Z, Cho S, Sherrill-Mix S, Wan L & Dreyfuss G (2012), "U1 snRNP determines mRNA length and regulates isoform expression", *Cell,* vol. 150 pp. 53-64, doi:10.1016/j.cell.2012.05.029

Berkovits BD & Mayr C (2015), "Alternative 3' UTRs act as scaffolds to regulate membrane protein localization", *Nature,* vol. 522 pp. 363-367, doi:10.1038/nature14321

Berod L, Friedrich C, Nandan A, Freitag J, Hagemann S, Harmrolfs K, Sandouk A, Hesse C, Castro CN, Bahre H, Tschirner SK, Gorinski N, Gohmert M, Mayer CT, Huehn J, Ponimaskin E, Abraham WR, Muller R, Lochner M & Sparwasser T (2014), "De novo fatty acid synthesis controls the fate between regulatory T and T helper 17 cells", *Nat Med,* vol. 20 pp. 1327-1333, doi:10.1038/nm.3704

Bienroth S, Keller W & Wahle E (1993), "Assembly of a processive messenger RNA polyadenylation complex", *EMBO J,* vol. 12 pp. 585-594,

Blander JM (2016), "The comings and goings of MHC class I molecules herald a new dawn in cross-presentation", *Immunol Rev,* vol. 272 pp. 65-79, doi:10.1111/imr.12428

Blandino-Rosano M, Scheys JO, Jimenez-Palomares M, Barbaresso R, Bender AS, Yanagiya A, Liu M, Rui L, Sonenberg N & Bernal-Mizrachi E (2016), "4E-BP2/SH2B1/IRS2 Are Part of a Novel Feedback Loop That Controls beta-Cell Mass", *Diabetes,* vol. 65 pp. 2235-2248, doi:10.2337/db15-1443

Bluyssen HA, Vlietstra RJ, van der Made A & Trapman J (1994), "The interferon-stimulated gene 54 K promoter contains two adjacent functional interferon-stimulated response elements of different strength, which act synergistically for maximal interferon-alpha inducibility", *Eur J Biochem,* vol. 220 pp. 395-402, doi:10.1111/j.1432-1033.1994.tb18636.x

Bogunovic D, Byun M, Durfee LA, Abhyankar A, Sanal O, Mansouri D, Salem S, Radovanovic I, Grant AV, Adimi P, Mansouri N, Okada S, Bryant VL, Kong XF, Kreins A, Velez MM, Boisson B, Khalilzadeh S, Ozcelik U, Darazam IA, Schoggins JW, Rice CM, Al-Muhsen S, Behr M, Vogt G, Puel A, Bustamante J, Gros P, Huibregtse JM, Abel L, Boisson-Dupuis S & Casanova JL (2012), "Mycobacterial disease and impaired IFN-gamma immunity in humans with inherited ISG15 deficiency", *Science,* vol. 337 pp. 1684-1688, doi:10.1126/science.1224026

Bohl F, Kruse C, Frank A, Ferring D & Jansen RP (2000), "She2p, a novel RNA-binding protein tethers ASH1 mRNA to the Myo4p myosin motor via She3p", *EMBO J,* vol. 19 pp. 5514-5524, doi:10.1093/emboj/19.20.5514

Boulland ML, Marquet J, Molinier-Frenkel V, Moller P, Guiter C, Lasoudris F, Copie-Bergman C, Baia M, Gaulard P, Leroy K & Castellano F (2007), "Human IL4I1 is a secreted L-phenylalanine oxidase expressed by mature dendritic cells that inhibits T-lymphocyte proliferation", *Blood,* vol. 110 pp. 220-227, doi:10.1182/blood-2006-07-036210

Boutet SC, Cheung TH, Quach NL, Liu L, Prescott SL, Edalati A, Iori K & Rando TA (2012), "Alternative polyadenylation mediates microRNA regulation of muscle stem cell function", *Cell Stem Cell,* vol. 10 pp. 327-336, doi:10.1016/j.stem.2012.01.017

Bozym RA, Delorme-Axford E, Harris K, Morosky S, Ikizler M, Dermody TS, Sarkar SN & Coyne CB (2012), "Focal adhesion kinase is a component of antiviral RIG-I-like receptor signaling", *Cell Host Microbe,* vol. 11 pp. 153-166, doi:10.1016/j.chom.2012.01.008

Brisse M & Ly H (2019), "Comparative Structure and Function Analysis of the RIG-I-Like Receptors: RIG-I and MDA5", *Front Immunol,* vol. 10 p. 1586, doi:10.3389/fimmu.2019.01586

Brumbaugh J, Di Stefano B, Wang X, Borkent M, Forouzmand E, Clowers KJ, Ji F, Schwarz BA, Kalocsay M, Elledge SJ, Chen Y, Sadreyev RI, Gygi SP, Hu G, Shi Y & Hochedlinger K (2018), "Nudt21 Controls Cell Fate by Connecting Alternative Polyadenylation to Chromatin Signaling", *Cell,* vol. 172 pp. 106-120 e121, doi:10.1016/j.cell.2017.11.023

Bruni R, Marcantonio C, Tritarelli E, Tataseo P, Stellacci E, Costantino A, Villano U, Battistini A & Ciccaglione AR (2011), "An integrated approach identifies IFN-

regulated microRNAs and targeted mRNAs modulated by different HCV replicon clones", *BMC Genomics,* vol. 12 p. 485, doi:10.1186/1471-2164-12-485

Brunn GJ, Hudson CC, Sekulic A, Williams JM, Hosoi H, Houghton PJ, Lawrence JC, Jr. & Abraham RT (1997), "Phosphorylation of the translational repressor PHAS-I by the mammalian target of rapamycin", *Science,* vol. 277 pp. 99-101, doi:10.1126/science.277.5322.99

Bruns AM, Leser GP, Lamb RA & Horvath CM (2014), "The innate immune sensor LGP2 activates antiviral signaling by regulating MDA5-RNA interaction and filament assembly", *Mol Cell,* vol. 55 pp. 771-781, doi:10.1016/j.molcel.2014.07.003

Buchmann K (2014), "Evolution of Innate Immunity: Clues from Invertebrates via Fish to Mammals", *Front Immunol,* vol. 5 p. 459, doi:10.3389/fimmu.2014.00459

Buechler MB, Kim KW, Onufer EJ, Williams JW, Little CC, Dominguez CX, Li Q, Sandoval W, Cooper JE, Harris CA, Junttila MR, Randolph GJ & Turley SJ (2019), "A Stromal Niche Defined by Expression of the Transcription Factor WT1 Mediates Programming and Homeostasis of Cavity-Resident Macrophages", *Immunity,* vol. 51 pp. 119-130 e115, doi:10.1016/j.immuni.2019.05.010

Burdette DL, Monroe KM, Sotelo-Troha K, Iwig JS, Eckert B, Hyodo M, Hayakawa Y & Vance RE (2011), "STING is a direct innate immune sensor of cyclic di-GMP", *Nature,* vol. 478 pp. 515-518, doi:10.1038/nature10429

Burnett PE, Barrow RK, Cohen NA, Snyder SH & Sabatini DM (1998), "RAFT1 phosphorylation of the translational regulators p70 S6 kinase and 4E-BP1", *Proc Natl Acad Sci U S A,* vol. 95 pp. 1432-1437, doi:10.1073/pnas.95.4.1432

Canton J, Neculai D & Grinstein S (2013), "Scavenger receptors in homeostasis and immunity", *Nat Rev Immunol,* vol. 13 pp. 621-634, doi:10.1038/nri3515

Cao Z, Henzel WJ & Gao X (1996), "IRAK: a kinase associated with the interleukin-1 receptor", *Science,* vol. 271 pp. 1128-1131, doi:10.1126/science.271.5252.1128

Carmi Y, Voronov E, Dotan S, Lahat N, Rahat MA, Fogel M, Huszar M, White MR, Dinarello CA & Apte RN (2009), "The role of macrophage-derived IL-1 in induction and maintenance of angiogenesis", *J Immunol,* vol. 183 pp. 4705-4714, doi:10.4049/jimmunol.0901511

Caron E, Self AJ & Hall A (2000), "The GTPase Rap1 controls functional activation of macrophage integrin alphaMbeta2 by LPS and other inflammatory mediators", *Curr Biol,* vol. 10 pp. 974-978, doi:10.1016/s0960-9822(00)00641-2

Carpenter KL, van der Veen C, Taylor SE, Hardwick SJ, Clare K, Hegyi L & Mitchinson MJ (1995), "Macrophages, lipid oxidation, ceroid accumulation and

alpha-tocopherol depletion in human atherosclerotic lesions", *Gerontology,* vol. 41 Suppl 2 pp. 53-67, doi:10.1159/000213725

Carswell EA, Old LJ, Kassel RL, Green S, Fiore N & Williamson B (1975), "An endotoxin-induced serum factor that causes necrosis of tumors", *Proc Natl Acad Sci U S A,* vol. 72 pp. 3666-3670, doi:10.1073/pnas.72.9.3666

Casanova JL (2015), "Severe infectious diseases of childhood as monogenic inborn errors of immunity", *Proc Natl Acad Sci U S A,* vol. 112 pp. E7128-7137, doi:10.1073/pnas.1521651112

Castanier C, Zemirli N, Portier A, Garcin D, Bidere N, Vazquez A & Arnoult D (2012), "MAVS ubiquitination by the E3 ligase TRIM25 and degradation by the proteasome is involved in type I interferon production after activation of the antiviral RIG-I-like receptors", *BMC Biol,* vol. 10 p. 44, doi:10.1186/1741-7007-10-44

Cen S, Khorchid A, Javanbakht H, Gabor J, Stello T, Shiba K, Musier-Forsyth K & Kleiman L (2001), "Incorporation of lysyl-tRNA synthetase into human immunodeficiency virus type 1", *J Virol,* vol. 75 pp. 5043-5048, doi:10.1128/JVI.75.11.5043-5048.2001

Chadban SJ, Tesch GH, Foti R, Lan HY, Atkins RC & Nikolic-Paterson DJ (1998), "Interleukin-10 differentially modulates MHC class II expression by mesangial cells and macrophages in vitro and in vivo", *Immunology,* vol. 94 pp. 72-78, doi:10.1046/j.1365-2567.1998.00487.x

Chan S, Choi EA & Shi Y (2011), "Pre-mRNA 3'-end processing complex assembly and function", *Wiley Interdiscip Rev RNA,* vol. 2 pp. 321-335, doi:10.1002/wrna.54

Chan SL, Huppertz I, Yao C, Weng L, Moresco JJ, Yates JR, 3rd, Ule J, Manley JL & Shi Y (2014), "CPSF30 and Wdr33 directly bind to AAUAAA in mammalian mRNA 3' processing", *Genes Dev,* vol. 28 pp. 2370-2380, doi:10.1101/gad.250993.114

Chang JW, Zhang W, Yeh HS, de Jong EP, Jun S, Kim KH, Bae SS, Beckman K, Hwang TH, Kim KS, Kim DH, Griffin TJ, Kuang R & Yong J (2015), "mRNA 3'-UTR shortening is a molecular signature of mTORC1 activation", *Nat Commun,* vol. 6 p. 7218, doi:10.1038/ncomms8218

Chanput W, Mes JJ, Savelkoul HF & Wichers HJ (2013), "Characterization of polarized THP-1 macrophages and polarizing ability of LPS and food compounds", *Food Funct,* vol. 4 pp. 266-276, doi:10.1039/c2fo30156c

Chanput W, Mes JJ & Wichers HJ (2014), "THP-1 cell line: an in vitro cell model for immune modulation approach", *Int Immunopharmacol,* vol. 23 pp. 37-45, doi:10.1016/j.intimp.2014.08.002

Chapman NM, Boothby MR & Chi H (2020), "Metabolic coordination of T cell quiescence and activation", *Nat Rev Immunol,* vol. 20 pp. 55-70, doi:10.1038/s41577-019-0203-y

Chartron JW, Hunt KC & Frydman J (2016), "Cotranslational signal-independent SRP preloading during membrane targeting", *Nature,* vol. 536 pp. 224-228, doi:10.1038/nature19309

Chen CY, Chen ST, Juan HF & Huang HC (2012), "Lengthening of 3'UTR increases with morphological complexity in animal evolution", *Bioinformatics,* vol. 28 pp. 3178-3181, doi:10.1093/bioinformatics/bts623

Chen CY & Shyu AB (1995), "AU-rich elements: characterization and importance in mRNA degradation", *Trends Biochem Sci,* vol. 20 pp. 465-470, doi:10.1016/s0968-0004(00)89102-1

Chen HW, Heiniger HJ & Kandutsch AA (1975), "Relationship between sterol synthesis and DNA synthesis in phytohemagglutinin-stimulated mouse lymphocytes", *Proc Natl Acad Sci U S A,* vol. 72 pp. 1950-1954, doi:10.1073/pnas.72.5.1950

Cheng LC, Zheng D, Baljinnyam E, Sun F, Ogami K, Yeung PL, Hoque M, Lu CW, Manley JL & Tian B (2020), "Widespread transcript shortening through alternative polyadenylation in secretory cell differentiation", *Nat Commun,* vol. 11 p. 3182, doi:10.1038/s41467-020-16959-2

Cheng M, Si Y, Niu Y, Liu X, Li X, Zhao J, Jin Q & Yang W (2013), "High-throughput profiling of alpha interferon- and interleukin-28B-regulated microRNAs and identification of let-7s with anti-hepatitis C virus activity by targeting IGF2BP1", *J Virol,* vol. 87 pp. 9707-9718, doi:10.1128/JVI.00802-13

Cheon H, Holvey-Bates EG, Schoggins JW, Forster S, Hertzog P, Imanaka N, Rice CM, Jackson MW, Junk DJ & Stark GR (2013), "IFNbeta-dependent increases in STAT1, STAT2, and IRF9 mediate resistance to viruses and DNA damage", *EMBO J,* vol. 32 pp. 2751-2763, doi:10.1038/emboj.2013.203

Cheon H & Stark GR (2009), "Unphosphorylated STAT1 prolongs the expression of interferon-induced immune regulatory genes", *Proc Natl Acad Sci U S A,* vol. 106 pp. 9373-9378, doi:10.1073/pnas.0903487106

Chiang HS, Zhao Y, Song JH, Liu S, Wang N, Terhorst C, Sharpe AH, Basavappa M, Jeffrey KL & Reinecker HC (2014), "GEF-H1 controls microtubule-dependent sensing of nucleic acids for antiviral host defenses", *Nat Immunol,* vol. 15 pp. 63-71, doi:10.1038/ni.2766

Christoforidis S, McBride HM, Burgoyne RD & Zerial M (1999), "The Rab5 effector EEA1 is a core component of endosome docking", *Nature,* vol. 397 pp. 621-625, doi:10.1038/17618

Chuvpilo S, Zimmer M, Kerstan A, Glockner J, Avots A, Escher C, Fischer C, Inashkina I, Jankevics E, Berberich-Siebelt F, Schmitt E & Serfling E (1999), "Alternative polyadenylation events contribute to the induction of NF-ATc in effector T cells", *Immunity,* vol. 10 pp. 261-269, doi:10.1016/s1074-7613(00)80026-6

Clayton AL & Mahadevan LC (2003), "MAP kinase-mediated phosphoacetylation of histone H3 and inducible gene regulation", *FEBS Lett,* vol. 546 pp. 51-58, doi:10.1016/s0014-5793(03)00451-4

Clementi E, Brown GC, Feelisch M & Moncada S (1998), "Persistent inhibition of cell respiration by nitric oxide: crucial role of S-nitrosylation of mitochondrial complex I and protective action of glutathione", *Proc Natl Acad Sci U S A,* vol. 95 pp. 7631-7636, doi:10.1073/pnas.95.13.7631

Clerici M, Faini M, Muckenfuss LM, Aebersold R & Jinek M (2018), "Structural basis of AAUAAA polyadenylation signal recognition by the human CPSF complex", *Nat Struct Mol Biol,* vol. 25 pp. 135-138, doi:10.1038/s41594-017-0020-6

Coccia EM, Severa M, Giacomini E, Monneron D, Remoli ME, Julkunen I, Cella M, Lande R & Uze G (2004), "Viral infection and Toll-like receptor agonists induce a differential expression of type I and lambda interferons in human plasmacytoid and monocyte-derived dendritic cells", *Eur J Immunol,* vol. 34 pp. 796-805, doi:10.1002/eji.200324610

Cohen KW, Dugast AS, Alter G, McElrath MJ & Stamatatos L (2015), "HIV-1 single-stranded RNA induces CXCL13 secretion in human monocytes via TLR7 activation and plasmacytoid dendritic cell-derived type I IFN", *J Immunol,* vol. 194 pp. 2769-2775, doi:10.4049/jimmunol.1400952

Colonna M, Krug A & Cella M (2002), "Interferon-producing cells: on the front line in immune responses against pathogens", *Curr Opin Immunol,* vol. 14 pp. 373-379, doi:10.1016/s0952-7915(02)00349-7

Cordes T, Wallace M, Michelucci A, Divakaruni AS, Sapcariu SC, Sousa C, Koseki H, Cabrales P, Murphy AN, Hiller K & Metallo CM (2016), "Immunoresponsive Gene 1 and Itaconate Inhibit Succinate Dehydrogenase to Modulate Intracellular Succinate Levels", *J Biol Chem,* vol. 291 pp. 14274-14284, doi:10.1074/jbc.M115.685792

Cotsapas C, Saarela J, Farmer JR, Scaria V & Abraham RS (2021), "Do monogenic inborn errors of immunity cause susceptibility to severe COVID-19?", *J Clin Invest,* vol. 131 doi:10.1172/JCI149459

Couret J, Tasker C, Kim J, Sihvonen T, Fruitwala S, Quayle AJ, Lespinasse P, Heller DS & Chang TL (2017), "Differential regulation of IFNalpha, IFNbeta and IFNepsilon gene expression in human cervical epithelial cells", *Cell Biosci,* vol. 7 p. 57, doi:10.1186/s13578-017-0185-z

Cox J & Mann M (2008), "MaxQuant enables high peptide identification rates, individualized p.p.b.-range mass accuracies and proteome-wide protein quantification", *Nat Biotechnol,* vol. 26 pp. 1367-1372, doi:10.1038/nbt.1511

Creek DJ, Jankevics A, Burgess KE, Breitling R & Barrett MP (2012), "IDEOM: an Excel interface for analysis of LC-MS-based metabolomics data", *Bioinformatics,* vol. 28 pp. 1048-1049, doi:10.1093/bioinformatics/bts069

Cruz FM, Colbert JD, Merino E, Kriegsman BA & Rock KL (2017), "The Biology and Underlying Mechanisms of Cross-Presentation of Exogenous Antigens on MHC-I Molecules", *Annu Rev Immunol,* vol. 35 pp. 149-176, doi:10.1146/annurev-immunol-041015-055254

Dalpke AH, Opper S, Zimmermann S & Heeg K (2001), "Suppressors of cytokine signaling (SOCS)-1 and SOCS-3 are induced by CpG-DNA and modulate cytokine responses in APCs", *J Immunol,* vol. 166 pp. 7082-7089, doi:10.4049/jimmunol.166.12.7082

Darnell JE, Jr., Kerr IM & Stark GR (1994), "Jak-STAT pathways and transcriptional activation in response to IFNs and other extracellular signaling proteins", *Science,* vol. 264 pp. 1415-1421, doi:10.1126/science.8197455

Darnell RB (2010), "HITS-CLIP: panoramic views of protein-RNA regulation in living cells", *Wiley Interdiscip Rev RNA,* vol. 1 pp. 266-286, doi:10.1002/wrna.31

Dawson JE, Bah A, Zhang Z, Vernon RM, Lin H, Chong PA, Vanama M, Sonenberg N, Gradinaru CC & Forman-Kay JD (2020), "Non-cooperative 4E-BP2 folding with exchange between eIF4E-binding and binding-incompatible states tunes cap-dependent translation inhibition", *Nat Commun,* vol. 11 p. 3146, doi:10.1038/s41467-020-16783-8

de Klerk E, Venema A, Anvar SY, Goeman JJ, Hu O, Trollet C, Dickson G, den Dunnen JT, van der Maarel SM, Raz V & t Hoen PA (2012), "Poly(A) binding protein nuclear 1 levels affect alternative polyadenylation", *Nucleic Acids Res,* vol. 40 pp. 9089-9101, doi:10.1093/nar/gks655

De Souza DP, Achuthan A, Lee MK, Binger KJ, Lee MC, Davidson S, Tull DL, McConville MJ, Cook AD, Murphy AJ, Hamilton JA & Fleetwood AJ (2019), "Autocrine IFN-I inhibits isocitrate dehydrogenase in the TCA cycle of LPS-stimulated macrophages", *J Clin Invest,* vol. 129 pp. 4239-4244, doi:10.1172/JCI127597

de Vries H, Ruegsegger U, Hubner W, Friedlein A, Langen H & Keller W (2000), "Human pre-mRNA cleavage factor II(m) contains homologs of yeast proteins and bridges two other cleavage factors", *EMBO J,* vol. 19 pp. 5895-5904, doi:10.1093/emboj/19.21.5895

de Weerd NA, Samarajiwa SA & Hertzog PJ (2007), "Type I interferon receptors: biochemistry and biological functions", *J Biol Chem,* vol. 282 pp. 20053-20057, doi:10.1074/jbc.R700006200

de Weerd NA, Vivian JP, Nguyen TK, Mangan NE, Gould JA, Braniff SJ, Zaker-Tabrizi L, Fung KY, Forster SC, Beddoe T, Reid HH, Rossjohn J & Hertzog PJ (2013), "Structural basis of a unique interferon-beta signaling axis mediated via the receptor IFNAR1", *Nat Immunol,* vol. 14 pp. 901-907, doi:10.1038/ni.2667

Deak M, Clifton AD, Lucocq LM & Alessi DR (1998), "Mitogen- and stress-activated protein kinase-1 (MSK1) is directly activated by MAPK and SAPK2/p38, and may mediate activation of CREB", *EMBO J,* vol. 17 pp. 4426-4441, doi:10.1093/emboj/17.15.4426

Decker T, Lew DJ, Mirkovitch J & Darnell JE, Jr. (1991), "Cytoplasmic activation of GAF, an IFN-gamma-regulated DNA-binding factor", *EMBO J,* vol. 10 pp. 927-932,

Defrance T, Vanbervliet B, Briere F, Durand I, Rousset F & Banchereau J (1992), "Interleukin 10 and transforming growth factor beta cooperate to induce anti-CD40-activated naive human B cells to secrete immunoglobulin A", *J Exp Med,* vol. 175 pp. 671-682, doi:10.1084/jem.175.3.671

Delgoffe GM & Vignali DA (2013), "STAT heterodimers in immunity: A mixed message or a unique signal?", *JAKSTAT,* vol. 2 p. e23060, doi:10.4161/jkst.23060

Deng Y, Singer RH & Gu W (2008), "Translation of ASH1 mRNA is repressed by Puf6p-Fun12p/eIF5B interaction and released by CK2 phosphorylation", *Genes Dev,* vol. 22 pp. 1037-1050, doi:10.1101/gad.1611308

Derti A, Garrett-Engele P, Macisaac KD, Stevens RC, Sriram S, Chen R, Rohl CA, Johnson JM & Babak T (2012), "A quantitative atlas of polyadenylation in five mammals", *Genome Res,* vol. 22 pp. 1173-1183, doi:10.1101/gr.132563.111

Desjardins M (1995), "Biogenesis of phagolysosomes: the 'kiss and run' hypothesis", *Trends Cell Biol,* vol. 5 pp. 183-186, doi:10.1016/s0962-8924(00)88989-8

Dettwiler S, Aringhieri C, Cardinale S, Keller W & Barabino SM (2004), "Distinct sequence motifs within the 68-kDa subunit of cleavage factor Im mediate RNA binding, protein-protein interactions, and subcellular localization", *J Biol Chem,* vol. 279 pp. 35788-35797, doi:10.1074/jbc.M403927200

Dhillon B, Aleithan F, Abdul-Sater Z & Abdul-Sater AA (2019), "The Evolving Role of TRAFs in Mediating Inflammatory Responses", *Front Immunol,* vol. 10 p. 104, doi:10.3389/fimmu.2019.00104

Di Giammartino DC, Li W, Ogami K, Yashinskie JJ, Hoque M, Tian B & Manley JL (2014), "RBBP6 isoforms regulate the human polyadenylation machinery and modulate expression of mRNAs with AU-rich 3' UTRs", *Genes Dev,* vol. 28 pp. 2248-2260, doi:10.1101/gad.245787.114

Dinarello CA (2007), "Historical insights into cytokines", *Eur J Immunol,* vol. 37 Suppl 1 pp. S34-45, doi:10.1002/eji.200737772

Dixit E, Boulant S, Zhang Y, Lee AS, Odendall C, Shum B, Hacohen N, Chen ZJ, Whelan SP, Fransen M, Nibert ML, Superti-Furga G & Kagan JC (2010), "Peroxisomes are signaling platforms for antiviral innate immunity", *Cell,* vol. 141 pp. 668-681, doi:10.1016/j.cell.2010.04.018

Dominguez-Andres J, Novakovic B, Li Y, Scicluna BP, Gresnigt MS, Arts RJW, Oosting M, Moorlag S, Groh LA, Zwaag J, Koch RM, Ter Horst R, Joosten LAB, Wijmenga C, Michelucci A, van der Poll T, Kox M, Pickkers P, Kumar V, Stunnenberg H & Netea MG (2019), "The Itaconate Pathway Is a Central Regulatory Node Linking Innate Immune Tolerance and Trained Immunity", *Cell Metab,* vol. 29 pp. 211-220 e215, doi:10.1016/j.cmet.2018.09.003

Donnelly RP, Loftus RM, Keating SE, Liou KT, Biron CA, Gardiner CM & Finlay DK (2014), "mTORC1-dependent metabolic reprogramming is a prerequisite for NK cell effector function", *J Immunol,* vol. 193 pp. 4477-4484, doi:10.4049/jimmunol.1401558

Dorman SE & Holland SM (2000), "Interferon-gamma and interleukin-12 pathway defects and human disease", *Cytokine Growth Factor Rev,* vol. 11 pp. 321-333, doi:10.1016/s1359-6101(00)00010-1

Dorrello NV, Peschiaroli A, Guardavaccaro D, Colburn NH, Sherman NE & Pagano M (2006), "S6K1- and betaTRCP-mediated degradation of PDCD4 promotes protein translation and cell growth", *Science,* vol. 314 pp. 467-471, doi:10.1126/science.1130276

Dos Santos PF & Mansur DS (2017), "Beyond ISGlylation: Functions of Free Intracellular and Extracellular ISG15", *J Interferon Cytokine Res,* vol. 37 pp. 246-253, doi:10.1089/jir.2016.0103

Doughty CA, Bleiman BF, Wagner DJ, Dufort FJ, Mataraza JM, Roberts MF & Chiles TC (2006), "Antigen receptor-mediated changes in glucose metabolism in B lymphocytes: role of phosphatidylinositol 3-kinase signaling in the glycolytic control of growth", *Blood,* vol. 107 pp. 4458-4465, doi:10.1182/blood-2005-12-4788

Dowling RJ, Topisirovic I, Alain T, Bidinosti M, Fonseca BD, Petroulakis E, Wang X, Larsson O, Selvaraj A, Liu Y, Kozma SC, Thomas G & Sonenberg N (2010), "mTORC1-mediated cell proliferation, but not cell growth, controlled by the 4E-BPs", *Science,* vol. 328 pp. 1172-1176, doi:10.1126/science.1187532

Doyle SE, O'Connell RM, Miranda GA, Vaidya SA, Chow EK, Liu PT, Suzuki S, Suzuki N, Modlin RL, Yeh WC, Lane TF & Cheng G (2004), "Toll-like receptors induce a phagocytic gene program through p38", *J Exp Med,* vol. 199 pp. 81-90, doi:10.1084/jem.20031237

Du Y, Duan T, Feng Y, Liu Q, Lin M, Cui J & Wang RF (2018), "LRRC25 inhibits type I IFN signaling by targeting ISG15-associated RIG-I for autophagic degradation", *EMBO J,* vol. 37 pp. 351-366, doi:10.15252/embj.201796781

Duchon AA, St Gelais C, Titkemeier N, Hatterschide J, Wu L & Musier-Forsyth K (2017), "HIV-1 Exploits a Dynamic Multi-aminoacyl-tRNA Synthetase Complex To Enhance Viral Replication", *J Virol,* vol. 91 doi:10.1128/JVI.01240-17

Dufort FJ, Gumina MR, Ta NL, Tao Y, Heyse SA, Scott DA, Richardson AD, Seyfried TN & Chiles TC (2014), "Glucose-dependent de novo lipogenesis in B lymphocytes: a requirement for atp-citrate lyase in lipopolysaccharide-induced differentiation", *J Biol Chem,* vol. 289 pp. 7011-7024, doi:10.1074/jbc.M114.551051

Duncan CD & Mata J (2011), "Widespread cotranslational formation of protein complexes", *PLoS Genet,* vol. 7 p. e1002398, doi:10.1371/journal.pgen.1002398

Dustin ML (2016), "Complement Receptors in Myeloid Cell Adhesion and Phagocytosis", *Microbiol Spectr,* vol. 4 doi:10.1128/microbiolspec.MCHD-0034-2016

Dutta O, Espinosa V, Wang K, Avina S & Rivera A (2020), "Dectin-1 Promotes Type I and III Interferon Expression to Support Optimal Antifungal Immunity in the Lung", *Front Cell Infect Microbiol,* vol. 10 p. 321, doi:10.3389/fcimb.2020.00321

Ealick SE, Cook WJ, Vijay-Kumar S, Carson M, Nagabhushan TL, Trotta PP & Bugg CE (1991), "Three-dimensional structure of recombinant human interferon-gamma", *Science,* vol. 252 pp. 698-702, doi:10.1126/science.1902591

Ecker J, Liebisch G, Englmaier M, Grandl M, Robenek H & Schmitz G (2010), "Induction of fatty acid synthesis is a key requirement for phagocytic differentiation of human monocytes", *Proc Natl Acad Sci U S A,* vol. 107 pp. 7817-7822, doi:10.1073/pnas.0912059107

El Chartouni C, Schwarzfischer L & Rehli M (2010), "Interleukin-4 induced interferon regulatory factor (Irf) 4 participates in the regulation of alternative

macrophage priming", *Immunobiology,* vol. 215 pp. 821-825, doi:10.1016/j.imbio.2010.05.031

Elkon R, Drost J, van Haaften G, Jenal M, Schrier M, Oude Vrielink JA & Agami R (2012), "E2F mediates enhanced alternative polyadenylation in proliferation", *Genome Biol,* vol. 13 p. R59, doi:10.1186/gb-2012-13-7-r59

Emamian ES, Leon JM, Lessard CJ, Grandits M, Baechler EC, Gaffney PM, Segal B, Rhodus NL & Moser KL (2009), "Peripheral blood gene expression profiling in Sjogren's syndrome", *Genes Immun,* vol. 10 pp. 285-296, doi:10.1038/gene.2009.20

Enders M, Franken L, Philipp MS, Kessler N, Baumgart AK, Eichler M, Wiertz EJH, Garbi N & Kurts C (2020), "Splenic Red Pulp Macrophages Cross-Prime Early Effector CTL That Provide Rapid Defense against Viral Infections", *J Immunol,* vol. 204 pp. 87-100, doi:10.4049/jimmunol.1900021

Endo TA, Masuhara M, Yokouchi M, Suzuki R, Sakamoto H, Mitsui K, Matsumoto A, Tanimura S, Ohtsubo M, Misawa H, Miyazaki T, Leonor N, Taniguchi T, Fujita T, Kanakura Y, Komiya S & Yoshimura A (1997), "A new protein containing an SH2 domain that inhibits JAK kinases", *Nature,* vol. 387 pp. 921-924, doi:10.1038/43213

Everts B, Amiel E, Huang SC, Smith AM, Chang CH, Lam WY, Redmann V, Freitas TC, Blagih J, van der Windt GJ, Artyomov MN, Jones RG, Pearce EL & Pearce EJ (2014), "TLR-driven early glycolytic reprogramming via the kinases TBK1-IKKvarepsilon supports the anabolic demands of dendritic cell activation", *Nat Immunol,* vol. 15 pp. 323-332, doi:10.1038/ni.2833

Ezekowitz RA, Sastry K, Bailly P & Warner A (1990), "Molecular characterization of the human macrophage mannose receptor: demonstration of multiple carbohydrate recognition-like domains and phagocytosis of yeasts in Cos-1 cells", *J Exp Med,* vol. 172 pp. 1785-1794, doi:10.1084/jem.172.6.1785

Fang R, Jiang Q, Zhou X, Wang C, Guan Y, Tao J, Xi J, Feng JM & Jiang Z (2017), "MAVS activates TBK1 and IKKepsilon through TRAFs in NEMO dependent and independent manner", *PLoS Pathog,* vol. 13 p. e1006720, doi:10.1371/journal.ppat.1006720

Farrar MA & Schreiber RD (1993), "The molecular cell biology of interferon-gamma and its receptor", *Annu Rev Immunol,* vol. 11 pp. 571-611, doi:10.1146/annurev.iy.11.040193.003035

Feingold KR, Shigenaga JK, Kazemi MR, McDonald CM, Patzek SM, Cross AS, Moser A & Grunfeld C (2012), "Mechanisms of triglyceride accumulation in activated macrophages", *J Leukoc Biol,* vol. 92 pp. 829-839, doi:10.1189/jlb.1111537

Fernandes N & Buchan JR (2020), "RPS28B mRNA acts as a scaffold promoting cis-translational interaction of proteins driving P-body assembly", *Nucleic Acids Res,* vol. 48 pp. 6265-6279, doi:10.1093/nar/gkaa352

Ferrao R & Lupardus PJ (2017), "The Janus Kinase (JAK) FERM and SH2 Domains: Bringing Specificity to JAK-Receptor Interactions", *Front Endocrinol (Lausanne),* vol. 8 p. 71, doi:10.3389/fendo.2017.00071

Fiorentino DF, Zlotnik A, Mosmann TR, Howard M & O'Garra A (1991), "IL-10 inhibits cytokine production by activated macrophages", *J Immunol,* vol. 147 pp. 3815-3822,

Fiorucci G, Chiantore MV, Mangino G & Romeo G (2015), "MicroRNAs in virus-induced tumorigenesis and IFN system", *Cytokine Growth Factor Rev,* vol. 26 pp. 183-194, doi:10.1016/j.cytogfr.2014.11.002

Flajnik MF & Kasahara M (2010), "Origin and evolution of the adaptive immune system: genetic events and selective pressures", *Nat Rev Genet,* vol. 11 pp. 47-59, doi:10.1038/nrg2703

Flannagan RS, Jaumouille V & Grinstein S (2012), "The cell biology of phagocytosis", *Annu Rev Pathol,* vol. 7 pp. 61-98, doi:10.1146/annurev-pathol-011811-132445

Flavell SW, Kim TK, Gray JM, Harmin DA, Hemberg M, Hong EJ, Markenscoff-Papadimitriou E, Bear DM & Greenberg ME (2008), "Genome-wide analysis of MEF2 transcriptional program reveals synaptic target genes and neuronal activity-dependent polyadenylation site selection", *Neuron,* vol. 60 pp. 1022-1038, doi:10.1016/j.neuron.2008.11.029

Fletcher CM, McGuire AM, Gingras AC, Li H, Matsuo H, Sonenberg N & Wagner G (1998), "4E binding proteins inhibit the translation factor eIF4E without folded structure", *Biochemistry,* vol. 37 pp. 9-15, doi:10.1021/bi972494r

Fogg DK, Sibon C, Miled C, Jung S, Aucouturier P, Littman DR, Cumano A & Geissmann F (2006), "A clonogenic bone marrow progenitor specific for macrophages and dendritic cells", *Science,* vol. 311 pp. 83-87, doi:10.1126/science.1117729

Forster SC, Tate MD & Hertzog PJ (2015), "MicroRNA as Type I Interferon-Regulated Transcripts and Modulators of the Innate Immune Response", *Front Immunol,* vol. 6 p. 334, doi:10.3389/fimmu.2015.00334

Francois-Newton V, Magno de Freitas Almeida G, Payelle-Brogard B, Monneron D, Pichard-Garcia L, Piehler J, Pellegrini S & Uze G (2011), "USP18-based negative feedback control is induced by type I and type III interferons and specifically inactivates interferon alpha response", *PLoS One,* vol. 6 p. e22200, doi:10.1371/journal.pone.0022200

Freeman SA, Goyette J, Furuya W, Woods EC, Bertozzi CR, Bergmeier W, Hinz B, van der Merwe PA, Das R & Grinstein S (2016), "Integrins Form an Expanding Diffusional Barrier that Coordinates Phagocytosis", *Cell,* vol. 164 pp. 128-140, doi:10.1016/j.cell.2015.11.048

Freeman SA & Grinstein S (2014), "Phagocytosis: receptors, signal integration, and the cytoskeleton", *Immunol Rev,* vol. 262 pp. 193-215, doi:10.1111/imr.12212

Freigang S, Ampenberger F, Weiss A, Kanneganti TD, Iwakura Y, Hersberger M & Kopf M (2013), "Fatty acid-induced mitochondrial uncoupling elicits inflammasome-independent IL-1alpha and sterile vascular inflammation in atherosclerosis", *Nat Immunol,* vol. 14 pp. 1045-1053, doi:10.1038/ni.2704

Fritzen AM, Lundsgaard AM & Kiens B (2020), "Tuning fatty acid oxidation in skeletal muscle with dietary fat and exercise", *Nat Rev Endocrinol,* vol. 16 pp. 683-696, doi:10.1038/s41574-020-0405-1

Frodin M & Gammeltoft S (1999), "Role and regulation of 90 kDa ribosomal S6 kinase (RSK) in signal transduction", *Mol Cell Endocrinol,* vol. 151 pp. 65-77, doi:10.1016/s0303-7207(99)00061-1

Fu Y, Sun Y, Li Y, Li J, Rao X, Chen C & Xu A (2011), "Differential genome-wide profiling of tandem 3' UTRs among human breast cancer and normal cells by high-throughput sequencing", *Genome Res,* vol. 21 pp. 741-747, doi:10.1101/gr.115295.110

Fukuyo A, In Y, Ishida T & Tomoo K (2011), "Structural scaffold for eIF4E binding selectivity of 4E-BP isoforms: crystal structure of eIF4E binding region of 4E-BP2 and its comparison with that of 4E-BP1", *J Pept Sci,* vol. 17 pp. 650-657, doi:10.1002/psc.1384

Fukuzumi M, Shinomiya H, Shimizu Y, Ohishi K & Utsumi S (1996), "Endotoxin-induced enhancement of glucose influx into murine peritoneal macrophages via GLUT1", *Infect Immun,* vol. 64 pp. 108-112, doi:10.1128/iai.64.1.108-112.1996

Fung KY, Mangan NE, Cumming H, Horvat JC, Mayall JR, Stifter SA, De Weerd N, Roisman LC, Rossjohn J, Robertson SA, Schjenken JE, Parker B, Gargett CE, Nguyen HP, Carr DJ, Hansbro PM & Hertzog PJ (2013), "Interferon-epsilon protects the female reproductive tract from viral and bacterial infection", *Science,* vol. 339 pp. 1088-1092, doi:10.1126/science.1233321

Fusco DN, Brisac C, John SP, Huang YW, Chin CR, Xie T, Zhao H, Jilg N, Zhang L, Chevaliez S, Wambua D, Lin W, Peng L, Chung RT & Brass AL (2013), "A genetic screen identifies interferon-alpha effector genes required to suppress hepatitis C virus replication", *Gastroenterology,* vol. 144 pp. 1438-1449, 1449 e1431-1439, doi:10.1053/j.gastro.2013.02.026

Gack MU, Shin YC, Joo CH, Urano T, Liang C, Sun L, Takeuchi O, Akira S, Chen Z, Inoue S & Jung JU (2007), "TRIM25 RING-finger E3 ubiquitin ligase is essential for RIG-I-mediated antiviral activity", *Nature,* vol. 446 pp. 916-920, doi:10.1038/nature05732

Gad HH, Dellgren C, Hamming OJ, Vends S, Paludan SR & Hartmann R (2009), "Interferon-lambda is functionally an interferon but structurally related to the interleukin-10 family", *J Biol Chem,* vol. 284 pp. 20869-20875, doi:10.1074/jbc.M109.002923

Gan X, Wang J, Wang C, Sommer E, Kozasa T, Srinivasula S, Alessi D, Offermanns S, Simon MI & Wu D (2012), "PRR5L degradation promotes mTORC2-mediated PKC-delta phosphorylation and cell migration downstream of Galpha12", *Nat Cell Biol,* vol. 14 pp. 686-696, doi:10.1038/ncb2507

Gao D, Wu J, Wu YT, Du F, Aroh C, Yan N, Sun L & Chen ZJ (2013), "Cyclic GMP-AMP synthase is an innate immune sensor of HIV and other retroviruses", *Science,* vol. 341 pp. 903-906, doi:10.1126/science.1240933

Gao P, Ascano M, Wu Y, Barchet W, Gaffney BL, Zillinger T, Serganov AA, Liu Y, Jones RA, Hartmann G, Tuschl T & Patel DJ (2013), "Cyclic [G(2',5')pA(3',5')p] is the metazoan second messenger produced by DNA-activated cyclic GMP-AMP synthase", *Cell,* vol. 153 pp. 1094-1107, doi:10.1016/j.cell.2013.04.046

Gao Y, Li L, Amos CI & Li W (2021), "Analysis of alternative polyadenylation from single-cell RNA-seq using scDaPars reveals cell subpopulations invisible to gene expression", *Genome Res,* vol. doi:10.1101/gr.271346.120

Garcia-Martinez JM & Alessi DR (2008), "mTOR complex 2 (mTORC2) controls hydrophobic motif phosphorylation and activation of serum- and glucocorticoid-induced protein kinase 1 (SGK1)", *Biochem J,* vol. 416 pp. 375-385, doi:10.1042/BJ20081668

Gautier EL, Shay T, Miller J, Greter M, Jakubzick C, Ivanov S, Helft J, Chow A, Elpek KG, Gordonov S, Mazloom AR, Ma'ayan A, Chua WJ, Hansen TH, Turley SJ, Merad M, Randolph GJ & Immunological Genome C (2012), "Gene-expression profiles and transcriptional regulatory pathways that underlie the identity and diversity of mouse tissue macrophages", *Nat Immunol,* vol. 13 pp. 1118-1128, doi:10.1038/ni.2419

Ghislain JJ, Wong T, Nguyen M & Fish EN (2001), "The interferon-inducible Stat2:Stat1 heterodimer preferentially binds in vitro to a consensus element found in the promoters of a subset of interferon-stimulated genes", *J Interferon Cytokine Res,* vol. 21 pp. 379-388, doi:10.1089/107999001750277853

Gilchrist M, Thorsson V, Li B, Rust AG, Korb M, Roach JC, Kennedy K, Hai T, Bolouri H & Aderem A (2006), "Systems biology approaches identify ATF3 as a

negative regulator of Toll-like receptor 4", *Nature,* vol. 441 pp. 173-178, doi:10.1038/nature04768

Gilmartin GM & Nevins JR (1991), "Molecular analyses of two poly(A) site-processing factors that determine the recognition and efficiency of cleavage of the pre-mRNA", *Mol Cell Biol,* vol. 11 pp. 2432-2438, doi:10.1128/mcb.11.5.2432-2438.1991

Ginhoux F, Schultze JL, Murray PJ, Ochando J & Biswas SK (2016), "New insights into the multidimensional concept of macrophage ontogeny, activation and function", *Nat Immunol,* vol. 17 pp. 34-40, doi:10.1038/ni.3324

Githaka JM, Tripathi N, Kirschenman R, Patel N, Pandya V, Kramer DA, Montpetit R, Zhu LF, Sonenberg N, Fahlman RP, Danial NN, Underhill DA & Goping IS (2021), "BAD regulates mammary gland morphogenesis by 4E-BP1-mediated control of localized translation in mouse and human models", *Nat Commun,* vol. 12 p. 2939, doi:10.1038/s41467-021-23269-8

Gitlin L, Barchet W, Gilfillan S, Cella M, Beutler B, Flavell RA, Diamond MS & Colonna M (2006), "Essential role of mda-5 in type I IFN responses to polyriboinosinic:polyribocytidylic acid and encephalomyocarditis picornavirus", *Proc Natl Acad Sci U S A,* vol. 103 pp. 8459-8464, doi:10.1073/pnas.0603082103

Gordon S (2016), "Elie Metchnikoff, the Man and the Myth", *J Innate Immun,* vol. 8 pp. 223-227, doi:10.1159/000443331

Gordon S & Martinez-Pomares L (2017), "Physiological roles of macrophages", *Pflugers Arch,* vol. 469 pp. 365-374, doi:10.1007/s00424-017-1945-7

Goritzka M, Durant LR, Pereira C, Salek-Ardakani S, Openshaw PJ & Johansson C (2014), "Alpha/beta interferon receptor signaling amplifies early proinflammatory cytokine production in the lung during respiratory syncytial virus infection", *J Virol,* vol. 88 pp. 6128-6136, doi:10.1128/JVI.00333-14

Gosselin D, Link VM, Romanoski CE, Fonseca GJ, Eichenfield DZ, Spann NJ, Stender JD, Chun HB, Garner H, Geissmann F & Glass CK (2014), "Environment drives selection and function of enhancers controlling tissue-specific macrophage identities", *Cell,* vol. 159 pp. 1327-1340, doi:10.1016/j.cell.2014.11.023

Goujon C, Moncorge O, Bauby H, Doyle T, Ward CC, Schaller T, Hue S, Barclay WS, Schulz R & Malim MH (2013), "Human MX2 is an interferon-induced post-entry inhibitor of HIV-1 infection", *Nature,* vol. 502 pp. 559-562, doi:10.1038/nature12542

Griffin GK, Newton G, Tarrio ML, Bu DX, Maganto-Garcia E, Azcutia V, Alcaide P, Grabie N, Luscinskas FW, Croce KJ & Lichtman AH (2012), "IL-17 and TNF-alpha sustain neutrophil recruitment during inflammation through synergistic

effects on endothelial activation", *J Immunol,* vol. 188 pp. 6287-6299, doi:10.4049/jimmunol.1200385

Grimson A, Farh KK, Johnston WK, Garrett-Engele P, Lim LP & Bartel DP (2007), "MicroRNA targeting specificity in mammals: determinants beyond seed pairing", *Mol Cell,* vol. 27 pp. 91-105, doi:10.1016/j.molcel.2007.06.017

Grolleau A, Sonenberg N, Wietzerbin J & Beretta L (1999), "Differential regulation of 4E-BP1 and 4E-BP2, two repressors of translation initiation, during human myeloid cell differentiation", *J Immunol,* vol. 162 pp. 3491-3497,

Gruber AJ, Schmidt R, Gruber AR, Martin G, Ghosh S, Belmadani M, Keller W & Zavolan M (2016), "A comprehensive analysis of 3' end sequencing data sets reveals novel polyadenylation signals and the repressive role of heterogeneous ribonucleoprotein C on cleavage and polyadenylation", *Genome Res,* vol. 26 pp. 1145-1159, doi:10.1101/gr.202432.115

Gruber AR, Martin G, Keller W & Zavolan M (2012), "Cleavage factor Im is a key regulator of 3' UTR length", *RNA Biol,* vol. 9 pp. 1405-1412, doi:10.4161/rna.22570

Gruber AR, Martin G, Muller P, Schmidt A, Gruber AJ, Gumienny R, Mittal N, Jayachandran R, Pieters J, Keller W, van Nimwegen E & Zavolan M (2014), "Global 3' UTR shortening has a limited effect on protein abundance in proliferating T cells", *Nat Commun,* vol. 5 p. 5465, doi:10.1038/ncomms6465

Gu TL, Nardone J, Wang Y, Loriaux M, Villen J, Beausoleil S, Tucker M, Kornhauser J, Ren J, MacNeill J, Gygi SP, Druker BJ, Heinrich MC, Rush J & Polakiewicz RD (2011), "Survey of activated FLT3 signaling in leukemia", *PLoS One,* vol. 6 p. e19169, doi:10.1371/journal.pone.0019169

Guo F, Cen S, Niu M, Javanbakht H & Kleiman L (2003), "Specific inhibition of the synthesis of human lysyl-tRNA synthetase results in decreases in tRNA(Lys) incorporation, tRNA(3)(Lys) annealing to viral RNA, and viral infectivity in human immunodeficiency virus type 1", *J Virol,* vol. 77 pp. 9817-9822, doi:10.1128/jvi.77.18.9817-9822.2003

Gupta I, Clauder-Munster S, Klaus B, Jarvelin AI, Aiyar RS, Benes V, Wilkening S, Huber W, Pelechano V & Steinmetz LM (2014), "Alternative polyadenylation diversifies post-transcriptional regulation by selective RNA-protein interactions", *Mol Syst Biol,* vol. 10 p. 719, doi:10.1002/msb.135068

Ha M & Kim VN (2014), "Regulation of microRNA biogenesis", *Nat Rev Mol Cell Biol,* vol. 15 pp. 509-524, doi:10.1038/nrm3838

Hacker H, Redecke V, Blagoev B, Kratchmarova I, Hsu LC, Wang GG, Kamps MP, Raz E, Wagner H, Hacker G, Mann M & Karin M (2006), "Specificity in Toll-

like receptor signalling through distinct effector functions of TRAF3 and TRAF6", *Nature,* vol. 439 pp. 204-207, doi:10.1038/nature04369

Haldar M, Kohyama M, So AY, Kc W, Wu X, Briseno CG, Satpathy AT, Kretzer NM, Arase H, Rajasekaran NS, Wang L, Egawa T, Igarashi K, Baltimore D, Murphy TL & Murphy KM (2014), "Heme-mediated SPI-C induction promotes monocyte differentiation into iron-recycling macrophages", *Cell,* vol. 156 pp. 1223-1234, doi:10.1016/j.cell.2014.01.069

Hamilton JA, Vairo G & Lingelbach SR (1986), "CSF-1 stimulates glucose uptake in murine bone marrow-derived macrophages", *Biochem Biophys Res Commun,* vol. 138 pp. 445-454, doi:10.1016/0006-291x(86)90301-3

Han TW, Kato M, Xie S, Wu LC, Mirzaei H, Pei J, Chen M, Xie Y, Allen J, Xiao G & McKnight SL (2012), "Cell-free formation of RNA granules: bound RNAs identify features and components of cellular assemblies", *Cell,* vol. 149 pp. 768-779, doi:10.1016/j.cell.2012.04.016

Hans F, Senarisoy M, Bhaskar Naidu C & Timmins J (2020), "Focus on DNA Glycosylases-A Set of Tightly Regulated Enzymes with a High Potential as Anticancer Drug Targets", *Int J Mol Sci,* vol. 21 doi:10.3390/ijms21239226

Hao Y, Liang JF, Chow AW, Cheung WT & Ko WH (2014), "P2Y6 receptor-mediated proinflammatory signaling in human bronchial epithelia", *PLoS One,* vol. 9 p. e106235, doi:10.1371/journal.pone.0106235

Hardbower DM, Asim M, Luis PB, Singh K, Barry DP, Yang C, Steeves MA, Cleveland JL, Schneider C, Piazuelo MB, Gobert AP & Wilson KT (2017), "Ornithine decarboxylase regulates M1 macrophage activation and mucosal inflammation via histone modifications", *Proc Natl Acad Sci U S A,* vol. 114 pp. E751-E760, doi:10.1073/pnas.1614958114

Harris BD, Schreiter J, Chevrier M, Jordan JL & Walter MR (2018), "Human interferon- and interferon-kappa exhibit low potency and low affinity for cell-surface IFNAR and the poxvirus antagonist B18R", *J Biol Chem,* vol. 293 pp. 16057-16068, doi:10.1074/jbc.RA118.003617

Harrison PF, Pattison AD, Powell DR & Beilharz TH (2019), "Topconfects: a package for confident effect sizes in differential expression analysis provides a more biologically useful ranked gene list", *Genome Biol,* vol. 20 p. 67, doi:10.1186/s13059-019-1674-7

Harrison PF, Powell DR, Clancy JL, Preiss T, Boag PR, Traven A, Seemann T & Beilharz TH (2015), "PAT-seq: a method to study the integration of 3'-UTR dynamics with gene expression in the eukaryotic transcriptome", *RNA,* vol. 21 pp. 1502-1510, doi:10.1261/rna.048355.114

Harvey JS, Carey WF & Morris CP (1998), "Importance of the glycosylation and polyadenylation variants in metachromatic leukodystrophy pseudodeficiency phenotype", *Hum Mol Genet,* vol. 7 pp. 1215-1219, doi:10.1093/hmg/7.8.1215

Haschemi A, Kosma P, Gille L, Evans CR, Burant CF, Starkl P, Knapp B, Haas R, Schmid JA, Jandl C, Amir S, Lubec G, Park J, Esterbauer H, Bilban M, Brizuela L, Pospisilik JA, Otterbein LE & Wagner O (2012), "The sedoheptulose kinase CARKL directs macrophage polarization through control of glucose metabolism", *Cell Metab,* vol. 15 pp. 813-826, doi:10.1016/j.cmet.2012.04.023

Hashimoto D, Chow A, Noizat C, Teo P, Beasley MB, Leboeuf M, Becker CD, See P, Price J, Lucas D, Greter M, Mortha A, Boyer SW, Forsberg EC, Tanaka M, van Rooijen N, Garcia-Sastre A, Stanley ER, Ginhoux F, Frenette PS & Merad M (2013), "Tissue-resident macrophages self-maintain locally throughout adult life with minimal contribution from circulating monocytes", *Immunity,* vol. 38 pp. 792-804, doi:10.1016/j.immuni.2013.04.004

Hayes JD & Dinkova-Kostova AT (2014), "The Nrf2 regulatory network provides an interface between redox and intermediary metabolism", *Trends Biochem Sci,* vol. 39 pp. 199-218, doi:10.1016/j.tibs.2014.02.002

He D, Wu H, Xiang J, Ruan X, Peng P, Ruan Y, Chen YG, Wang Y, Yu Q, Zhang H, Habib SL, De Pinho RA, Liu H & Li B (2020), "Gut stem cell aging is driven by mTORC1 via a p38 MAPK-p53 pathway", *Nat Commun,* vol. 11 p. 37, doi:10.1038/s41467-019-13911-x

He J, Ji Y, Li A, Zhang Q, Song W, Li Y, Huang H, Qian J, Zhai A, Yu X, Zhao J, Shang Q, Wei L & Zhang F (2014), "MiR-122 directly inhibits human papillomavirus E6 gene and enhances interferon signaling through blocking suppressor of cytokine signaling 1 in SiHa cells", *PLoS One,* vol. 9 p. e108410, doi:10.1371/journal.pone.0108410

He TS, Chen T, Wang DD & Xu LG (2018), "HAUS8 regulates RLRVISA antiviral signaling positively by targeting VISA", *Mol Med Rep,* vol. 18 pp. 2458-2466, doi:10.3892/mmr.2018.9171

He X, Zhu Y, Zhang Y, Geng Y, Gong J, Geng J, Zhang P, Zhang X, Liu N, Peng Y, Wang C, Wang Y, Liu X, Wan L, Gong F, Wei C & Zhong H (2019), "RNF34 functions in immunity and selective mitophagy by targeting MAVS for autophagic degradation", *EMBO J,* vol. 38 p. e100978, doi:10.15252/embj.2018100978

Heinz S, Benner C, Spann N, Bertolino E, Lin YC, Laslo P, Cheng JX, Murre C, Singh H & Glass CK (2010), "Simple combinations of lineage-determining transcription factors prime cis-regulatory elements required for macrophage and B cell identities", *Mol Cell,* vol. 38 pp. 576-589, doi:10.1016/j.molcel.2010.05.004

Herbst S, Schaible UE & Schneider BE (2011), "Interferon gamma activated macrophages kill mycobacteria by nitric oxide induced apoptosis", *PLoS One,* vol. 6 p. e19105, doi:10.1371/journal.pone.0019105

Herdy B, Jaramillo M, Svitkin YV, Rosenfeld AB, Kobayashi M, Walsh D, Alain T, Sean P, Robichaud N, Topisirovic I, Furic L, Dowling RJO, Sylvestre A, Rong L, Colina R, Costa-Mattioli M, Fritz JH, Olivier M, Brown E, Mohr I & Sonenberg N (2012), "Translational control of the activation of transcription factor NF-kappaB and production of type I interferon by phosphorylation of the translation factor eIF4E", *Nat Immunol,* vol. 13 pp. 543-550, doi:10.1038/ni.2291

Hernandez N, Bucciol G, Moens L, Le Pen J, Shahrooei M, Goudouris E, Shirkani A, Changi-Ashtiani M, Rokni-Zadeh H, Sayar EH, Reisli I, Lefevre-Utile A, Zijlmans D, Jurado A, Pholien R, Drutman S, Belkaya S, Cobat A, Boudewijns R, Jochmans D, Neyts J, Seeleuthner Y, Lorenzo-Diaz L, Enemchukwu C, Tietjen I, Hoffmann HH, Momenilandi M, Poyhonen L, Siqueira MM, de Lima SMB, de Souza Matos DC, Homma A, Maia MLS, da Costa Barros TA, de Oliveira PMN, Mesquita EC, Gijsbers R, Zhang SY, Seligman SJ, Abel L, Hertzog P, Marr N, Martins RM, Meyts I, Zhang Q, MacDonald MR, Rice CM, Casanova JL, Jouanguy E & Bossuyt X (2019), "Inherited IFNAR1 deficiency in otherwise healthy patients with adverse reaction to measles and yellow fever live vaccines", *J Exp Med,* vol. 216 pp. 2057-2070, doi:10.1084/jem.20182295

Herre J, Marshall AS, Caron E, Edwards AD, Williams DL, Schweighoffer E, Tybulewicz V, Reis e Sousa C, Gordon S & Brown GD (2004), "Dectin-1 uses novel mechanisms for yeast phagocytosis in macrophages", *Blood,* vol. 104 pp. 4038-4045, doi:10.1182/blood-2004-03-1140

Hertzog PJ & Williams BR (2013), "Fine tuning type I interferon responses", *Cytokine Growth Factor Rev,* vol. 24 pp. 217-225, doi:10.1016/j.cytogfr.2013.04.002

Higgs DR, Goodbourn SE, Lamb J, Clegg JB, Weatherall DJ & Proudfoot NJ (1983), "Alpha-thalassaemia caused by a polyadenylation signal mutation", *Nature,* vol. 306 pp. 398-400, doi:10.1038/306398a0

Hirokawa N, Noda Y, Tanaka Y & Niwa S (2009), "Kinesin superfamily motor proteins and intracellular transport", *Nat Rev Mol Cell Biol,* vol. 10 pp. 682-696, doi:10.1038/nrm2774

Ho BC, Yu IS, Lu LF, Rudensky A, Chen HY, Tsai CW, Chang YL, Wu CT, Chang LY, Shih SR, Lin SW, Lee CN, Yang PC & Yu SL (2014), "Inhibition of miR-146a prevents enterovirus-induced death by restoring the production of type I interferon", *Nat Commun,* vol. 5 p. 3344, doi:10.1038/ncomms4344

Hoffman RM & Han Q (2020), "Oral Methioninase for Covid-19 Methionine-restriction Therapy", *In Vivo,* vol. 34 pp. 1593-1596, doi:10.21873/invivo.11948

Hoffman Y, Bublik DR, Ugalde AP, Elkon R, Biniashvili T, Agami R, Oren M & Pilpel Y (2016), "3'UTR Shortening Potentiates MicroRNA-Based Repression of Pro-differentiation Genes in Proliferating Human Cells", *PLoS Genet,* vol. 12 p. e1005879, doi:10.1371/journal.pgen.1005879

Holz MK, Ballif BA, Gygi SP & Blenis J (2005), "mTOR and S6K1 mediate assembly of the translation preinitiation complex through dynamic protein interchange and ordered phosphorylation events", *Cell,* vol. 123 pp. 569-580, doi:10.1016/j.cell.2005.10.024

Hooftman A, Angiari S, Hester S, Corcoran SE, Runtsch MC, Ling C, Ruzek MC, Slivka PF, McGettrick AF, Banahan K, Hughes MM, Irvine AD, Fischer R & O'Neill LAJ (2020), "The Immunomodulatory Metabolite Itaconate Modifies NLRP3 and Inhibits Inflammasome Activation", *Cell Metab,* vol. 32 pp. 468-478 e467, doi:10.1016/j.cmet.2020.07.016

Hoque M, Ji Z, Zheng D, Luo W, Li W, You B, Park JY, Yehia G & Tian B (2013), "Analysis of alternative cleavage and polyadenylation by 3' region extraction and deep sequencing", *Nat Methods,* vol. 10 pp. 133-139, doi:10.1038/nmeth.2288

Horhold F, Eisel D, Oswald M, Kolte A, Roll D, Osen W, Eichmuller SB & Konig R (2020), "Reprogramming of macrophages employing gene regulatory and metabolic network models", *PLoS Comput Biol,* vol. 16 p. e1007657, doi:10.1371/journal.pcbi.1007657

Horner SM, Liu HM, Park HS, Briley J & Gale M, Jr. (2011), "Mitochondrial-associated endoplasmic reticulum membranes (MAM) form innate immune synapses and are targeted by hepatitis C virus", *Proc Natl Acad Sci U S A,* vol. 108 pp. 14590-14595, doi:10.1073/pnas.1110133108

Hou E, Sun N, Zhang F, Zhao C, Usa K, Liang M & Tian Z (2017), "Malate and Aspartate Increase L-Arginine and Nitric Oxide and Attenuate Hypertension", *Cell Rep,* vol. 19 pp. 1631-1639, doi:10.1016/j.celrep.2017.04.071

Hou F, Sun L, Zheng H, Skaug B, Jiang QX & Chen ZJ (2011), "MAVS forms functional prion-like aggregates to activate and propagate antiviral innate immune response", *Cell,* vol. 146 pp. 448-461, doi:10.1016/j.cell.2011.06.041

Hrecka K, Hao C, Gierszewska M, Swanson SK, Kesik-Brodacka M, Srivastava S, Florens L, Washburn MP & Skowronski J (2011), "Vpx relieves inhibition of HIV-1 infection of macrophages mediated by the SAMHD1 protein", *Nature,* vol. 474 pp. 658-661, doi:10.1038/nature10195

Hsieh AC, Liu Y, Edlind MP, Ingolia NT, Janes MR, Sher A, Shi EY, Stumpf CR, Christensen C, Bonham MJ, Wang S, Ren P, Martin M, Jessen K, Feldman ME, Weissman JS, Shokat KM, Rommel C & Ruggero D (2012), "The translational landscape of mTOR signalling steers cancer initiation and metastasis", *Nature,* vol. 485 pp. 55-61, doi:10.1038/nature10912

Hu J, Lutz CS, Wilusz J & Tian B (2005), "Bioinformatic identification of candidate cis-regulatory elements involved in human mRNA polyadenylation", *RNA,* vol. 11 pp. 1485-1493, doi:10.1261/rna.2107305

Huang H, Liu H & Sun X (2013), "Nucleosome distribution near the 3' ends of genes in the human genome", *Biosci Biotechnol Biochem,* vol. 77 pp. 2051-2055, doi:10.1271/bbb.130399

Huang J, Dibble CC, Matsuzaki M & Manning BD (2008), "The TSC1-TSC2 complex is required for proper activation of mTOR complex 2", *Mol Cell Biol,* vol. 28 pp. 4104-4115, doi:10.1128/MCB.00289-08

Huang SC, Everts B, Ivanova Y, O'Sullivan D, Nascimento M, Smith AM, Beatty W, Love-Gregory L, Lam WY, O'Neill CM, Yan C, Du H, Abumrad NA, Urban JF, Jr., Artyomov MN, Pearce EL & Pearce EJ (2014), "Cell-intrinsic lysosomal lipolysis is essential for alternative activation of macrophages", *Nat Immunol,* vol. 15 pp. 846-855, doi:10.1038/ni.2956

Hubel P, Urban C, Bergant V, Schneider WM, Knauer B, Stukalov A, Scaturro P, Mann A, Brunotte L, Hoffmann HH, Schoggins JW, Schwemmle M, Mann M, Rice CM & Pichlmair A (2019), "A protein-interaction network of interferon-stimulated genes extends the innate immune system landscape", *Nat Immunol,* vol. 20 pp. 493-502, doi:10.1038/s41590-019-0323-3

Hughes AL (1995), "The evolution of the type I interferon gene family in mammals", *J Mol Evol,* vol. 41 pp. 539-548, doi:10.1007/BF00175811

Hultquist JF, Lengyel JA, Refsland EW, LaRue RS, Lackey L, Brown WL & Harris RS (2011), "Human and rhesus APOBEC3D, APOBEC3F, APOBEC3G, and APOBEC3H demonstrate a conserved capacity to restrict Vif-deficient HIV-1", *J Virol,* vol. 85 pp. 11220-11234, doi:10.1128/JVI.05238-11

Hung V, Udeshi ND, Lam SS, Loh KH, Cox KJ, Pedram K, Carr SA & Ting AY (2016), "Spatially resolved proteomic mapping in living cells with the engineered peroxidase APEX2", *Nat Protoc,* vol. 11 pp. 456-475, doi:10.1038/nprot.2016.018

Hurst SM, Wilkinson TS, McLoughlin RM, Jones S, Horiuchi S, Yamamoto N, Rose-John S, Fuller GM, Topley N & Jones SA (2001), "Il-6 and its soluble receptor orchestrate a temporal switch in the pattern of leukocyte recruitment seen during acute inflammation", *Immunity,* vol. 14 pp. 705-714, doi:10.1016/s1074-7613(01)00151-0

Huttelmaier S, Illenberger S, Grosheva I, Rudiger M, Singer RH & Jockusch BM (2001), "Raver1, a dual compartment protein, is a ligand for PTB/hnRNPI and microfilament attachment proteins", *J Cell Biol,* vol. 155 pp. 775-786, doi:10.1083/jcb.200105044

Huynh A, DuPage M, Priyadharshini B, Sage PT, Quiros J, Borges CM, Townamchai N, Gerriets VA, Rathmell JC, Sharpe AH, Bluestone JA & Turka LA (2015), "Control of PI(3) kinase in Treg cells maintains homeostasis and lineage stability", *Nat Immunol,* vol. 16 pp. 188-196, doi:10.1038/ni.3077

Iacobazzi V, Infantino V, Castegna A, Menga A, Palmieri EM, Convertini P & Palmieri F (2017), "Mitochondrial carriers in inflammation induced by bacterial endotoxin and cytokines", *Biol Chem,* vol. 398 pp. 303-317, doi:10.1515/hsz-2016-0260

Infantino V, Convertini P, Cucci L, Panaro MA, Di Noia MA, Calvello R, Palmieri F & Iacobazzi V (2011), "The mitochondrial citrate carrier: a new player in inflammation", *Biochem J,* vol. 438 pp. 433-436, doi:10.1042/BJ20111275

Infantino V, Iacobazzi V, Menga A, Avantaggiati ML & Palmieri F (2014), "A key role of the mitochondrial citrate carrier (SLC25A1) in TNFalpha- and IFNgamma-triggered inflammation", *Biochim Biophys Acta,* vol. 1839 pp. 1217-1225, doi:10.1016/j.bbagrm.2014.07.013

Inoki K, Li Y, Zhu T, Wu J & Guan KL (2002), "TSC2 is phosphorylated and inhibited by Akt and suppresses mTOR signalling", *Nat Cell Biol,* vol. 4 pp. 648-657, doi:10.1038/ncb839

Isaacs A & Lindenmann J (1957), "Virus interference. I. The interferon", *Proc R Soc Lond B Biol Sci,* vol. 147 pp. 258-267, doi:10.1098/rspb.1957.0048

Ishikawa E, Ishikawa T, Morita YS, Toyonaga K, Yamada H, Takeuchi O, Kinoshita T, Akira S, Yoshikai Y & Yamasaki S (2009), "Direct recognition of the mycobacterial glycolipid, trehalose dimycolate, by C-type lectin Mincle", *J Exp Med,* vol. 206 pp. 2879-2888, doi:10.1084/jem.20091750

Isobe M, Toya H, Mito M, Chiba T, Asahara H, Hirose T & Nakagawa S (2020), "Forced isoform switching of Neat1_1 to Neat1_2 leads to the loss of Neat1_1 and the hyperformation of paraspeckles but does not affect the development and growth of mice", *RNA,* vol. 26 pp. 251-264, doi:10.1261/rna.072587.119

Jacinto E, Loewith R, Schmidt A, Lin S, Ruegg MA, Hall A & Hall MN (2004), "Mammalian TOR complex 2 controls the actin cytoskeleton and is rapamycin insensitive", *Nat Cell Biol,* vol. 6 pp. 1122-1128, doi:10.1038/ncb1183

Jaguin M, Houlbert N, Fardel O & Lecureur V (2013), "Polarization profiles of human M-CSF-generated macrophages and comparison of M1-markers in classically activated macrophages from GM-CSF and M-CSF origin", *Cell Immunol,* vol. 281 pp. 51-61, doi:10.1016/j.cellimm.2013.01.010

Jain M, Nilsson R, Sharma S, Madhusudhan N, Kitami T, Souza AL, Kafri R, Kirschner MW, Clish CB & Mootha VK (2012), "Metabolite profiling identifies a

key role for glycine in rapid cancer cell proliferation", *Science,* vol. 336 pp. 1040-1044, doi:10.1126/science.1218595

Jaks E, Gavutis M, Uze G, Martal J & Piehler J (2007), "Differential receptor subunit affinities of type I interferons govern differential signal activation", *J Mol Biol,* vol. 366 pp. 525-539, doi:10.1016/j.jmb.2006.11.053

Jansen RP (1999), "RNA-cytoskeletal associations", *FASEB J,* vol. 13 pp. 455-466,

Jarret A, McFarland AP, Horner SM, Kell A, Schwerk J, Hong M, Badil S, Joslyn RC, Baker DP, Carrington M, Hagedorn CH, Gale M, Jr. & Savan R (2016), "Hepatitis-C-virus-induced microRNAs dampen interferon-mediated antiviral signaling", *Nat Med,* vol. 22 pp. 1475-1481, doi:10.1038/nm.4211

Javed A & Reder AT (2006), "Therapeutic role of beta-interferons in multiple sclerosis", *Pharmacol Ther,* vol. 110 pp. 35-56, doi:10.1016/j.pharmthera.2005.08.011

Jellusova J (2020), "Metabolic control of B cell immune responses", *Curr Opin Immunol,* vol. 63 pp. 21-28, doi:10.1016/j.coi.2019.11.002

Jenal M, Elkon R, Loayza-Puch F, van Haaften G, Kuhn U, Menzies FM, Oude Vrielink JA, Bos AJ, Drost J, Rooijers K, Rubinsztein DC & Agami R (2012), "The poly(A)-binding protein nuclear 1 suppresses alternative cleavage and polyadenylation sites", *Cell,* vol. 149 pp. 538-553, doi:10.1016/j.cell.2012.03.022

Jha AK, Huang SC, Sergushichev A, Lampropoulou V, Ivanova Y, Loginicheva E, Chmielewski K, Stewart KM, Ashall J, Everts B, Pearce EJ, Driggers EM & Artyomov MN (2015), "Network integration of parallel metabolic and transcriptional data reveals metabolic modules that regulate macrophage polarization", *Immunity,* vol. 42 pp. 419-430, doi:10.1016/j.immuni.2015.02.005

Ji S, Yang Z, Gozali L, Kenney T, Kocabas A, Jinsook Park C & Hynes M (2021), "Distinct expression of select and transcriptome-wide isolated 3'UTRs suggests critical roles in development and transition states", *PLoS One,* vol. 16 p. e0250669, doi:10.1371/journal.pone.0250669

Ji Z, Lee JY, Pan Z, Jiang B & Tian B (2009), "Progressive lengthening of 3' untranslated regions of mRNAs by alternative polyadenylation during mouse embryonic development", *Proc Natl Acad Sci U S A,* vol. 106 pp. 7028-7033, doi:10.1073/pnas.0900028106

Ji Z & Tian B (2009), "Reprogramming of 3' untranslated regions of mRNAs by alternative polyadenylation in generation of pluripotent stem cells from different cell types", *PLoS One,* vol. 4 p. e8419, doi:10.1371/journal.pone.0008419

Jia Q, Nie H, Yu P, Xie B, Wang C, Yang F, Wei G & Ni T (2019), "HNRNPA1-mediated 3' UTR length changes of HN1 contributes to cancer- and senescence-associated phenotypes", *Aging (Albany NY),* vol. 11 pp. 4407-4437, doi:10.18632/aging.102060

Jia X, Yuan S, Wang Y, Fu Y, Ge Y, Ge Y, Lan X, Feng Y, Qiu F, Li P, Chen S & Xu A (2017), "The role of alternative polyadenylation in the antiviral innate immune response", *Nat Commun,* vol. 8 p. 14605, doi:10.1038/ncomms14605

Jiang M, Osterlund P, Fagerlund R, Rios DN, Hoffmann A, Poranen MM, Bamford DH & Julkunen I (2015), "MAP kinase p38alpha regulates type III interferon (IFN-lambda1) gene expression in human monocyte-derived dendritic cells in response to RNA stimulation", *J Leukoc Biol,* vol. 97 pp. 307-320, doi:10.1189/jlb.2A0114-059RR

Jiao X, Chang JH, Kilic T, Tong L & Kiledjian M (2013), "A mammalian pre-mRNA 5' end capping quality control mechanism and an unexpected link of capping to pre-mRNA processing", *Mol Cell,* vol. 50 pp. 104-115, doi:10.1016/j.molcel.2013.02.017

Jin S, Tian S, Luo M, Xie W, Liu T, Duan T, Wu Y & Cui J (2017), "Tetherin Suppresses Type I Interferon Signaling by Targeting MAVS for NDP52-Mediated Selective Autophagic Degradation in Human Cells", *Mol Cell,* vol. 68 pp. 308-322 e304, doi:10.1016/j.molcel.2017.09.005

Jones W & Bianchi K (2015), "Aerobic glycolysis: beyond proliferation", *Front Immunol,* vol. 6 p. 227, doi:10.3389/fimmu.2015.00227

Joshi S, Kaur S, Redig AJ, Goldsborough K, David K, Ueda T, Watanabe-Fukunaga R, Baker DP, Fish EN, Fukunaga R & Platanias LC (2009), "Type I interferon (IFN)-dependent activation of Mnk1 and its role in the generation of growth inhibitory responses", *Proc Natl Acad Sci U S A,* vol. 106 pp. 12097-12102, doi:10.1073/pnas.0900562106

Joshi S & Platanias LC (2014), "Mnk kinase pathway: Cellular functions and biological outcomes", *World J Biol Chem,* vol. 5 pp. 321-333, doi:10.4331/wjbc.v5.i3.321

Kaida D, Berg MG, Younis I, Kasim M, Singh LN, Wan L & Dreyfuss G (2010), "U1 snRNP protects pre-mRNAs from premature cleavage and polyadenylation", *Nature,* vol. 468 pp. 664-668, doi:10.1038/nature09479

Kane M, Yadav SS, Bitzegeio J, Kutluay SB, Zang T, Wilson SJ, Schoggins JW, Rice CM, Yamashita M, Hatziioannou T & Bieniasz PD (2013), "MX2 is an interferon-induced inhibitor of HIV-1 infection", *Nature,* vol. 502 pp. 563-566, doi:10.1038/nature12653

Kaplan DH, Li MO, Jenison MC, Shlomchik WD, Flavell RA & Shlomchik MJ (2007), "Autocrine/paracrine TGFbeta1 is required for the development of epidermal Langerhans cells", *J Exp Med,* vol. 204 pp. 2545-2552, doi:10.1084/jem.20071401

Karpusas M, Nolte M, Benton CB, Meier W, Lipscomb WN & Goelz S (1997), "The crystal structure of human interferon beta at 2.2-A resolution", *Proc Natl Acad Sci U S A,* vol. 94 pp. 11813-11818, doi:10.1073/pnas.94.22.11813

Kato M, Han TW, Xie S, Shi K, Du X, Wu LC, Mirzaei H, Goldsmith EJ, Longgood J, Pei J, Grishin NV, Frantz DE, Schneider JW, Chen S, Li L, Sawaya MR, Eisenberg D, Tycko R & McKnight SL (2012), "Cell-free formation of RNA granules: low complexity sequence domains form dynamic fibers within hydrogels", *Cell,* vol. 149 pp. 753-767, doi:10.1016/j.cell.2012.04.017

Kawai T, Takahashi K, Sato S, Coban C, Kumar H, Kato H, Ishii KJ, Takeuchi O & Akira S (2005), "IPS-1, an adaptor triggering RIG-I- and Mda5-mediated type I interferon induction", *Nat Immunol,* vol. 6 pp. 981-988, doi:10.1038/ni1243

Kawasaki T & Kawai T (2014), "Toll-like receptor signaling pathways", *Front Immunol,* vol. 5 p. 461, doi:10.3389/fimmu.2014.00461

Kerwitz Y, Kuhn U, Lilie H, Knoth A, Scheuermann T, Friedrich H, Schwarz E & Wahle E (2003), "Stimulation of poly(A) polymerase through a direct interaction with the nuclear poly(A) binding protein allosterically regulated by RNA", *EMBO J,* vol. 22 pp. 3705-3714, doi:10.1093/emboj/cdg347

Kim J, Kundu M, Viollet B & Guan KL (2011), "AMPK and mTOR regulate autophagy through direct phosphorylation of Ulk1", *Nat Cell Biol,* vol. 13 pp. 132-141, doi:10.1038/ncb2152

Kinchen JM & Ravichandran KS (2008), "Phagosome maturation: going through the acid test", *Nat Rev Mol Cell Biol,* vol. 9 pp. 781-795, doi:10.1038/nrm2515

Knight E, Jr. & Korant BD (1979), "Fibroblast interferon induces synthesis of four proteins in human fibroblast cells", *Proc Natl Acad Sci U S A,* vol. 76 pp. 1824-1827, doi:10.1073/pnas.76.4.1824

Ko K, Franek BS, Marion M, Kaufman KM, Langefeld CD, Harley JB & Niewold TB (2012), "Genetic ancestry, serum interferon-alpha activity, and autoantibodies in systemic lupus erythematosus", *J Rheumatol,* vol. 39 pp. 1238-1240, doi:10.3899/jrheum.111467

Kobayashi EH, Suzuki T, Funayama R, Nagashima T, Hayashi M, Sekine H, Tanaka N, Moriguchi T, Motohashi H, Nakayama K & Yamamoto M (2016), "Nrf2 suppresses macrophage inflammatory response by blocking proinflammatory cytokine transcription", *Nat Commun,* vol. 7 p. 11624, doi:10.1038/ncomms11624

Kobayashi N, Karisola P, Pena-Cruz V, Dorfman DM, Jinushi M, Umetsu SE, Butte MJ, Nagumo H, Chernova I, Zhu B, Sharpe AH, Ito S, Dranoff G, Kaplan GG, Casasnovas JM, Umetsu DT, Dekruyff RH & Freeman GJ (2007), "TIM-1 and TIM-4 glycoproteins bind phosphatidylserine and mediate uptake of apoptotic cells", *Immunity,* vol. 27 pp. 927-940, doi:10.1016/j.immuni.2007.11.011

Kobayashi T, Walsh MC & Choi Y (2004), "The role of TRAF6 in signal transduction and the immune response", *Microbes Infect,* vol. 6 pp. 1333-1338, doi:10.1016/j.micinf.2004.09.001

Komander D & Rape M (2012), "The ubiquitin code", *Annu Rev Biochem,* vol. 81 pp. 203-229, doi:10.1146/annurev-biochem-060310-170328

Konno H, Yamamoto T, Yamazaki K, Gohda J, Akiyama T, Semba K, Goto H, Kato A, Yujiri T, Imai T, Kawaguchi Y, Su B, Takeuchi O, Akira S, Tsunetsugu-Yokota Y & Inoue J (2009), "TRAF6 establishes innate immune responses by activating NF-kappaB and IRF7 upon sensing cytosolic viral RNA and DNA", *PLoS One,* vol. 4 p. e5674, doi:10.1371/journal.pone.0005674

Kotenko SV, Gallagher G, Baurin VV, Lewis-Antes A, Shen M, Shah NK, Langer JA, Sheikh F, Dickensheets H & Donnelly RP (2003), "IFN-lambdas mediate antiviral protection through a distinct class II cytokine receptor complex", *Nat Immunol,* vol. 4 pp. 69-77, doi:10.1038/ni875

Kotlyarov A & Gaestel M (2002), "Is MK2 (mitogen-activated protein kinase-activated protein kinase 2) the key for understanding post-transcriptional regulation of gene expression?", *Biochem Soc Trans,* vol. 30 pp. 959-963, doi:10.1042/bst0300959

Kouloulia S, Hallin EI, Simbriger K, Amorim IS, Lach G, Amvrosiadis T, Chalkiadaki K, Kampaite A, Truong VT, Hooshmandi M, Jafarnejad SM, Skehel P, Kursula P, Khoutorsky A & Gkogkas CG (2019), "Raptor-Mediated Proteasomal Degradation of Deamidated 4E-BP2 Regulates Postnatal Neuronal Translation and NF-kappaB Activity", *Cell Rep,* vol. 29 pp. 3620-3635 e3627, doi:10.1016/j.celrep.2019.11.023

Kowalinski E, Lunardi T, McCarthy AA, Louber J, Brunel J, Grigorov B, Gerlier D & Cusack S (2011), "Structural basis for the activation of innate immune pattern-recognition receptor RIG-I by viral RNA", *Cell,* vol. 147 pp. 423-435, doi:10.1016/j.cell.2011.09.039

Krapp C, Hotter D, Gawanbacht A, McLaren PJ, Kluge SF, Sturzel CM, Mack K, Reith E, Engelhart S, Ciuffi A, Hornung V, Sauter D, Telenti A & Kirchhoff F (2016), "Guanylate Binding Protein (GBP) 5 Is an Interferon-Inducible Inhibitor of HIV-1 Infectivity", *Cell Host Microbe,* vol. 19 pp. 504-514, doi:10.1016/j.chom.2016.02.019

Krausgruber T, Blazek K, Smallie T, Alzabin S, Lockstone H, Sahgal N, Hussell T, Feldmann M & Udalova IA (2011), "IRF5 promotes inflammatory macrophage polarization and TH1-TH17 responses", *Nat Immunol,* vol. 12 pp. 231-238, doi:10.1038/ni.1990

Krawczyk CM, Holowka T, Sun J, Blagih J, Amiel E, DeBerardinis RJ, Cross JR, Jung E, Thompson CB, Jones RG & Pearce EJ (2010), "Toll-like receptor-induced changes in glycolytic metabolism regulate dendritic cell activation", *Blood,* vol. 115 pp. 4742-4749, doi:10.1182/blood-2009-10-249540

Kristof AS, Marks-Konczalik J, Billings E & Moss J (2003), "Stimulation of signal transducer and activator of transcription-1 (STAT1)-dependent gene transcription by lipopolysaccharide and interferon-gamma is regulated by mammalian target of rapamycin", *J Biol Chem,* vol. 278 pp. 33637-33644, doi:10.1074/jbc.M301053200

Kubo T, Wada T, Yamaguchi Y, Shimizu A & Handa H (2006), "Knock-down of 25 kDa subunit of cleavage factor Im in Hela cells alters alternative polyadenylation within 3'-UTRs", *Nucleic Acids Res,* vol. 34 pp. 6264-6271, doi:10.1093/nar/gkl794

Kumar S & Dikshit M (2019), "Metabolic Insight of Neutrophils in Health and Disease", *Front Immunol,* vol. 10 p. 2099, doi:10.3389/fimmu.2019.02099

Kwon B, Fansler MM, Patel ND, Lee J, Ma W & Mayr C (2021), "Enhancers regulate 3′ end processing activity to control expression of alternative 3′UTR isoforms", *bioRxiv,* vol. p. 2020.2008.2017.254193, doi:10.1101/2020.08.17.254193

Kyriakis JM, App H, Zhang XF, Banerjee P, Brautigan DL, Rapp UR & Avruch J (1992), "Raf-1 activates MAP kinase-kinase", *Nature,* vol. 358 pp. 417-421, doi:10.1038/358417a0

Labzin LI, Schmidt SV, Masters SL, Beyer M, Krebs W, Klee K, Stahl R, Lutjohann D, Schultze JL, Latz E & De Nardo D (2015), "ATF3 Is a Key Regulator of Macrophage IFN Responses", *J Immunol,* vol. 195 pp. 4446-4455, doi:10.4049/jimmunol.1500204

Lackford B, Yao C, Charles GM, Weng L, Zheng X, Choi EA, Xie X, Wan J, Xing Y, Freudenberg JM, Yang P, Jothi R, Hu G & Shi Y (2014), "Fip1 regulates mRNA alternative polyadenylation to promote stem cell self-renewal", *EMBO J,* vol. 33 pp. 878-889, doi:10.1002/embj.201386537

LaFleur DW, Nardelli B, Tsareva T, Mather D, Feng P, Semenuk M, Taylor K, Buergin M, Chinchilla D, Roshke V, Chen G, Ruben SM, Pitha PM, Coleman TA & Moore PA (2001), "Interferon-kappa, a novel type I interferon expressed in human keratinocytes", *J Biol Chem,* vol. 276 pp. 39765-39771, doi:10.1074/jbc.M102502200

Laguette N, Sobhian B, Casartelli N, Ringeard M, Chable-Bessia C, Segeral E, Yatim A, Emiliani S, Schwartz O & Benkirane M (2011), "SAMHD1 is the dendritic- and myeloid-cell-specific HIV-1 restriction factor counteracted by Vpx", *Nature,* vol. 474 pp. 654-657, doi:10.1038/nature10117

Lampropoulou V, Sergushichev A, Bambouskova M, Nair S, Vincent EE, Loginicheva E, Cervantes-Barragan L, Ma X, Huang SC, Griss T, Weinheimer CJ, Khader S, Randolph GJ, Pearce EJ, Jones RG, Diwan A, Diamond MS & Artyomov MN (2016), "Itaconate Links Inhibition of Succinate Dehydrogenase with Macrophage Metabolic Remodeling and Regulation of Inflammation", *Cell Metab,* vol. 24 pp. 158-166, doi:10.1016/j.cmet.2016.06.004

Langmead B & Salzberg SL (2012), "Fast gapped-read alignment with Bowtie 2", *Nat Methods,* vol. 9 pp. 357-359, doi:10.1038/nmeth.1923

Larner AC, Jonak G, Cheng YS, Korant B, Knight E & Darnell JE, Jr. (1984), "Transcriptional induction of two genes in human cells by beta interferon", *Proc Natl Acad Sci U S A,* vol. 81 pp. 6733-6737, doi:10.1073/pnas.81.21.6733

Lau AG, Irier HA, Gu J, Tian D, Ku L, Liu G, Xia M, Fritsch B, Zheng JQ, Dingledine R, Xu B, Lu B & Feng Y (2010), "Distinct 3'UTRs differentially regulate activity-dependent translation of brain-derived neurotrophic factor (BDNF)", *Proc Natl Acad Sci U S A,* vol. 107 pp. 15945-15950, doi:10.1073/pnas.1002929107

Lavoie TB, Kalie E, Crisafulli-Cabatu S, Abramovich R, DiGioia G, Moolchan K, Pestka S & Schreiber G (2011), "Binding and activity of all human alpha interferon subtypes", *Cytokine,* vol. 56 pp. 282-289, doi:10.1016/j.cyto.2011.07.019

Lazear HM, Lancaster A, Wilkins C, Suthar MS, Huang A, Vick SC, Clepper L, Thackray L, Brassil MM, Virgin HW, Nikolich-Zugich J, Moses AV, Gale M, Jr., Fruh K & Diamond MS (2013), "IRF-3, IRF-5, and IRF-7 coordinately regulate the type I IFN response in myeloid dendritic cells downstream of MAVS signaling", *PLoS Pathog,* vol. 9 p. e1003118, doi:10.1371/journal.ppat.1003118

Le Tortorec A & Neil SJ (2009), "Antagonism to and intracellular sequestration of human tetherin by the human immunodeficiency virus type 2 envelope glycoprotein", *J Virol,* vol. 83 pp. 11966-11978, doi:10.1128/JVI.01515-09

Lee EY, Lee HC, Kim HK, Jang SY, Park SJ, Kim YH, Kim JH, Hwang J, Kim JH, Kim TH, Arif A, Kim SY, Choi YK, Lee C, Lee CH, Jung JU, Fox PL, Kim S, Lee JS & Kim MH (2016), "Infection-specific phosphorylation of glutamyl-prolyl tRNA synthetase induces antiviral immunity", *Nat Immunol,* vol. 17 pp. 1252-1262, doi:10.1038/ni.3542

Lee J, Walsh MC, Hoehn KL, James DE, Wherry EJ & Choi Y (2014), "Regulator of fatty acid metabolism, acetyl coenzyme a carboxylase 1, controls T cell immunity", *J Immunol,* vol. 192 pp. 3190-3199, doi:10.4049/jimmunol.1302985

Lee SH & Mayr C (2019), "Gain of Additional BIRC3 Protein Functions through 3'-UTR-Mediated Protein Complex Formation", *Mol Cell,* vol. 74 pp. 701-712 e709, doi:10.1016/j.molcel.2019.03.006

Lekmine F, Uddin S, Sassano A, Parmar S, Brachmann SM, Majchrzak B, Sonenberg N, Hay N, Fish EN & Platanias LC (2003), "Activation of the p70 S6 kinase and phosphorylation of the 4E-BP1 repressor of mRNA translation by type I interferons", *J Biol Chem,* vol. 278 pp. 27772-27780, doi:10.1074/jbc.M301364200

Levin R, Grinstein S & Canton J (2016), "The life cycle of phagosomes: formation, maturation, and resolution", *Immunol Rev,* vol. 273 pp. 156-179, doi:10.1111/imr.12439

Levy DE & Darnell JE, Jr. (2002), "Stats: transcriptional control and biological impact", *Nat Rev Mol Cell Biol,* vol. 3 pp. 651-662, doi:10.1038/nrm909

Levy DE, Kessler DS, Pine R & Darnell JE, Jr. (1989), "Cytoplasmic activation of ISGF3, the positive regulator of interferon-alpha-stimulated transcription, reconstituted in vitro", *Genes Dev,* vol. 3 pp. 1362-1371, doi:10.1101/gad.3.9.1362

Levy ED, De S & Teichmann SA (2012), "Cellular crowding imposes global constraints on the chemistry and evolution of proteomes", *Proc Natl Acad Sci U S A,* vol. 109 pp. 20461-20466, doi:10.1073/pnas.1209312109

Li A, Song W, Qian J, Li Y, He J, Zhang Q, Li W, Zhai A, Kao W, Hu Y, Li H, Wu J, Ling H, Zhong Z & Zhang F (2013), "MiR-122 modulates type I interferon expression through blocking suppressor of cytokine signaling 1", *Int J Biochem Cell Biol,* vol. 45 pp. 858-865, doi:10.1016/j.biocel.2013.01.008

Li G, Xiang Y, Sabapathy K & Silverman RH (2004), "An apoptotic signaling pathway in the interferon antiviral response mediated by RNase L and c-Jun NH2-terminal kinase", *J Biol Chem,* vol. 279 pp. 1123-1131, doi:10.1074/jbc.M305893200

Li K & Underhill DM (2020), "C-Type Lectin Receptors in Phagocytosis", *Curr Top Microbiol Immunol,* vol. 429 pp. 1-18, doi:10.1007/82_2020_198

Li L, Huang KL, Gao Y, Cui Y, Wang G, Elrod ND, Li Y, Chen YE, Ji P, Peng F, Russell WK, Wagner EJ & Li W (2021), "An atlas of alternative polyadenylation quantitative trait loci contributing to complex trait and disease heritability", *Nat Genet,* vol. doi:10.1038/s41588-021-00864-5

Li M, Kao E, Gao X, Sandig H, Limmer K, Pavon-Eternod M, Jones TE, Landry S, Pan T, Weitzman MD & David M (2012), "Codon-usage-based inhibition of HIV

protein synthesis by human schlafen 11", *Nature,* vol. 491 pp. 125-128, doi:10.1038/nature11433

Li S, Strelow A, Fontana EJ & Wesche H (2002), "IRAK-4: a novel member of the IRAK family with the properties of an IRAK-kinase", *Proc Natl Acad Sci U S A,* vol. 99 pp. 5567-5572, doi:10.1073/pnas.082100399

Li S, Zheng H, Mao AP, Zhong B, Li Y, Liu Y, Gao Y, Ran Y, Tien P & Shu HB (2010), "Regulation of virus-triggered signaling by OTUB1- and OTUB2-mediated deubiquitination of TRAF3 and TRAF6", *J Biol Chem,* vol. 285 pp. 4291-4297, doi:10.1074/jbc.M109.074971

Li T, Li X, Attri KS, Liu C, Li L, Herring LE, Asara JM, Lei YL, Singh PK, Gao C & Wen H (2018), "O-GlcNAc Transferase Links Glucose Metabolism to MAVS-Mediated Antiviral Innate Immunity", *Cell Host Microbe,* vol. 24 pp. 791-803 e796, doi:10.1016/j.chom.2018.11.001

Li T, Yang X, Li W, Song J, Li Z, Zhu X, Wu X & Liu Y (2021), "ADAR1 Stimulation by IFN-alpha Downregulates the Expression of MAVS via RNA Editing to Regulate the Anti-HBV Response", *Mol Ther,* vol. 29 pp. 1335-1348, doi:10.1016/j.ymthe.2020.11.031

Li W, Park JY, Zheng D, Hoque M, Yehia G & Tian B (2016), "Alternative cleavage and polyadenylation in spermatogenesis connects chromatin regulation with post-transcriptional control", *BMC Biol,* vol. 14 p. 6, doi:10.1186/s12915-016-0229-6

Li W, You B, Hoque M, Zheng D, Luo W, Ji Z, Park JY, Gunderson SI, Kalsotra A, Manley JL & Tian B (2015), "Systematic profiling of poly(A)+ transcripts modulated by core 3' end processing and splicing factors reveals regulatory rules of alternative cleavage and polyadenylation", *PLoS Genet,* vol. 11 p. e1005166, doi:10.1371/journal.pgen.1005166

Li X & Gao T (2014), "mTORC2 phosphorylates protein kinase Czeta to regulate its stability and activity", *EMBO Rep,* vol. 15 pp. 191-198, doi:10.1002/embr.201338119

Li Y, Batra S, Sassano A, Majchrzak B, Levy DE, Gaestel M, Fish EN, Davis RJ & Platanias LC (2005), "Activation of mitogen-activated protein kinase kinase (MKK) 3 and MKK6 by type I interferons", *J Biol Chem,* vol. 280 pp. 10001-10010, doi:10.1074/jbc.M410972200

Li Y, Sassano A, Majchrzak B, Deb DK, Levy DE, Gaestel M, Nebreda AR, Fish EN & Platanias LC (2004), "Role of p38alpha Map kinase in Type I interferon signaling", *J Biol Chem,* vol. 279 pp. 970-979, doi:10.1074/jbc.M309927200

Li Y, Sun Y, Fu Y, Li M, Huang G, Zhang C, Liang J, Huang S, Shen G, Yuan S, Chen L, Chen S & Xu A (2012), "Dynamic landscape of tandem 3' UTRs during

zebrafish development", *Genome Res,* vol. 22 pp. 1899-1906, doi:10.1101/gr.128488.111

Lianoglou S, Garg V, Yang JL, Leslie CS & Mayr C (2013), "Ubiquitously transcribed genes use alternative polyadenylation to achieve tissue-specific expression", *Genes Dev,* vol. 27 pp. 2380-2396, doi:10.1101/gad.229328.113

Liao B, Hu Y & Brewer G (2007), "Competitive binding of AUF1 and TIAR to MYC mRNA controls its translation", *Nat Struct Mol Biol,* vol. 14 pp. 511-518, doi:10.1038/nsmb1249

Lin Y, Li Z, Ozsolak F, Kim SW, Arango-Argoty G, Liu TT, Tenenbaum SA, Bailey T, Monaghan AP, Milos PM & John B (2012), "An in-depth map of polyadenylation sites in cancer", *Nucleic Acids Res,* vol. 40 pp. 8460-8471, doi:10.1093/nar/gks637

Liu B, Zhang M, Chu H, Zhang H, Wu H, Song G, Wang P, Zhao K, Hou J, Wang X, Zhang L & Gao C (2017), "The ubiquitin E3 ligase TRIM31 promotes aggregation and activation of the signaling adaptor MAVS through Lys63-linked polyubiquitination", *Nat Immunol,* vol. 18 pp. 214-224, doi:10.1038/ni.3641

Liu PS, Wang H, Li X, Chao T, Teav T, Christen S, Di Conza G, Cheng WC, Chou CH, Vavakova M, Muret C, Debackere K, Mazzone M, Huang HD, Fendt SM, Ivanisevic J & Ho PC (2017), "alpha-ketoglutarate orchestrates macrophage activation through metabolic and epigenetic reprogramming", *Nat Immunol,* vol. 18 pp. 985-994, doi:10.1038/ni.3796

Liu S, Cai X, Wu J, Cong Q, Chen X, Li T, Du F, Ren J, Wu YT, Grishin NV & Chen ZJ (2015), "Phosphorylation of innate immune adaptor proteins MAVS, STING, and TRIF induces IRF3 activation", *Science,* vol. 347 p. aaa2630, doi:10.1126/science.aaa2630

Liu S, Chen J, Cai X, Wu J, Chen X, Wu YT, Sun L & Chen ZJ (2013), "MAVS recruits multiple ubiquitin E3 ligases to activate antiviral signaling cascades", *Elife,* vol. 2 p. e00785, doi:10.7554/eLife.00785

Liu XY, Wei B, Shi HX, Shan YF & Wang C (2010), "Tom70 mediates activation of interferon regulatory factor 3 on mitochondria", *Cell Res,* vol. 20 pp. 994-1011, doi:10.1038/cr.2010.103

Liu Y, Beyer A & Aebersold R (2016), "On the Dependency of Cellular Protein Levels on mRNA Abundance", *Cell,* vol. 165 pp. 535-550, doi:10.1016/j.cell.2016.03.014

Livingstone M, Sikstrom K, Robert PA, Uze G, Larsson O & Pellegrini S (2015), "Assessment of mTOR-Dependent Translational Regulation of Interferon Stimulated Genes", *PLoS One,* vol. 10 p. e0133482, doi:10.1371/journal.pone.0133482

Loya A, Pnueli L, Yosefzon Y, Wexler Y, Ziv-Ukelson M & Arava Y (2008), "The 3'-UTR mediates the cellular localization of an mRNA encoding a short plasma membrane protein", *RNA,* vol. 14 pp. 1352-1365, doi:10.1261/rna.867208

Lu J, Pan Q, Rong L, He W, Liu SL & Liang C (2011), "The IFITM proteins inhibit HIV-1 infection", *J Virol,* vol. 85 pp. 2126-2137, doi:10.1128/JVI.01531-10

Luo W, Hu H, Chang R, Zhong J, Knabel M, O'Meally R, Cole RN, Pandey A & Semenza GL (2011), "Pyruvate kinase M2 is a PHD3-stimulated coactivator for hypoxia-inducible factor 1", *Cell,* vol. 145 pp. 732-744, doi:10.1016/j.cell.2011.03.054

Luo W, Ji Z, Pan Z, You B, Hoque M, Li W, Gunderson SI & Tian B (2013), "The conserved intronic cleavage and polyadenylation site of CstF-77 gene imparts control of 3' end processing activity through feedback autoregulation and by U1 snRNP", *PLoS Genet,* vol. 9 p. e1003613, doi:10.1371/journal.pgen.1003613

Ma EH, Bantug G, Griss T, Condotta S, Johnson RM, Samborska B, Mainolfi N, Suri V, Guak H, Balmer ML, Verway MJ, Raissi TC, Tsui H, Boukhaled G, Henriques da Costa S, Frezza C, Krawczyk CM, Friedman A, Manfredi M, Richer MJ, Hess C & Jones RG (2017), "Serine Is an Essential Metabolite for Effector T Cell Expansion", *Cell Metab,* vol. 25 p. 482, doi:10.1016/j.cmet.2017.01.014

Ma W & Mayr C (2018), "A Membraneless Organelle Associated with the Endoplasmic Reticulum Enables 3'UTR-Mediated Protein-Protein Interactions", *Cell,* vol. 175 pp. 1492-1506 e1419, doi:10.1016/j.cell.2018.10.007

Ma W, Zhen G, Xie W & Mayr C (2020), "Unstructured mRNAs form multivalent RNA-RNA interactions to generate TIS granule networks", *bioRxiv,* vol.

MacDonald CC, Wilusz J & Shenk T (1994), "The 64-kilodalton subunit of the CstF polyadenylation factor binds to pre-mRNAs downstream of the cleavage site and influences cleavage site location", *Mol Cell Biol,* vol. 14 pp. 6647-6654, doi:10.1128/mcb.14.10.6647-6654.1994

MacMicking J, Xie QW & Nathan C (1997), "Nitric oxide and macrophage function", *Annu Rev Immunol,* vol. 15 pp. 323-350, doi:10.1146/annurev.immunol.15.1.323

MacMicking JD, Nathan C, Hom G, Chartrain N, Fletcher DS, Trumbauer M, Stevens K, Xie QW, Sokol K, Hutchinson N & et al. (1995), "Altered responses to bacterial infection and endotoxic shock in mice lacking inducible nitric oxide synthase", *Cell,* vol. 81 pp. 641-650, doi:10.1016/0092-8674(95)90085-3

Mak J & Kleiman L (1997), "Primer tRNAs for reverse transcription", *J Virol,* vol. 71 pp. 8087-8095, doi:10.1128/JVI.71.11.8087-8095.1997

Makowska Z, Duong FH, Trincucci G, Tough DF & Heim MH (2011), "Interferon-beta and interferon-lambda signaling is not affected by interferon-induced refractoriness to interferon-alpha in vivo", *Hepatology,* vol. 53 pp. 1154-1163, doi:10.1002/hep.24189

Malakhov MP, Malakhova OA, Kim KI, Ritchie KJ & Zhang DE (2002), "UBP43 (USP18) specifically removes ISG15 from conjugated proteins", *J Biol Chem,* vol. 277 pp. 9976-9981, doi:10.1074/jbc.M109078200

Malakhova OA, Kim KI, Luo JK, Zou W, Kumar KG, Fuchs SY, Shuai K & Zhang DE (2006), "UBP43 is a novel regulator of interferon signaling independent of its ISG15 isopeptidase activity", *EMBO J,* vol. 25 pp. 2358-2367, doi:10.1038/sj.emboj.7601149

Malandrino MI, Fucho R, Weber M, Calderon-Dominguez M, Mir JF, Valcarcel L, Escote X, Gomez-Serrano M, Peral B, Salvado L, Fernandez-Veledo S, Casals N, Vazquez-Carrera M, Villarroya F, Vendrell JJ, Serra D & Herrero L (2015), "Enhanced fatty acid oxidation in adipocytes and macrophages reduces lipid-induced triglyceride accumulation and inflammation", *Am J Physiol Endocrinol Metab,* vol. 308 pp. E756-769, doi:10.1152/ajpendo.00362.2014

Mandel CR, Kaneko S, Zhang H, Gebauer D, Vethantham V, Manley JL & Tong L (2006), "Polyadenylation factor CPSF-73 is the pre-mRNA 3'-end-processing endonuclease", *Nature,* vol. 444 pp. 953-956, doi:10.1038/nature05363

Manning BD, Tee AR, Logsdon MN, Blenis J & Cantley LC (2002), "Identification of the tuberous sclerosis complex-2 tumor suppressor gene product tuberin as a target of the phosphoinositide 3-kinase/akt pathway", *Mol Cell,* vol. 10 pp. 151-162, doi:10.1016/s1097-2765(02)00568-3

Mansfield KD & Keene JD (2012), "Neuron-specific ELAV/Hu proteins suppress HuR mRNA during neuronal differentiation by alternative polyadenylation", *Nucleic Acids Res,* vol. 40 pp. 2734-2746, doi:10.1093/nar/gkr1114

Mao K, Chen S, Chen M, Ma Y, Wang Y, Huang B, He Z, Zeng Y, Hu Y, Sun S, Li J, Wu X, Wang X, Strober W, Chen C, Meng G & Sun B (2013), "Nitric oxide suppresses NLRP3 inflammasome activation and protects against LPS-induced septic shock", *Cell Res,* vol. 23 pp. 201-212, doi:10.1038/cr.2013.6

Marais R & Marshall CJ (1996), "Control of the ERK MAP kinase cascade by Ras and Raf", *Cancer Surv,* vol. 27 pp. 101-125,

Mariella E, Marotta F, Grassi E, Gilotto S & Provero P (2019), "The Length of the Expressed 3' UTR Is an Intermediate Molecular Phenotype Linking Genetic Variants to Complex Diseases", *Front Genet,* vol. 10 p. 714, doi:10.3389/fgene.2019.00714

Marini F, Scherzinger D & Danckwardt S (2021), "TREND-DB-a transcriptome-wide atlas of the dynamic landscape of alternative polyadenylation", *Nucleic Acids Res,* vol. 49 pp. D243-D253, doi:10.1093/nar/gkaa722

Marquez-Jurado S, Nogales A, Zuniga S, Enjuanes L & Almazan F (2015), "Identification of a gamma interferon-activated inhibitor of translation-like RNA motif at the 3' end of the transmissible gastroenteritis coronavirus genome modulating innate immune response", *mBio,* vol. 6 p. e00105, doi:10.1128/mBio.00105-15

Martin G, Gruber AR, Keller W & Zavolan M (2012), "Genome-wide analysis of pre-mRNA 3' end processing reveals a decisive role of human cleavage factor I in the regulation of 3' UTR length", *Cell Rep,* vol. 1 pp. 753-763, doi:10.1016/j.celrep.2012.05.003

Martinez-Reyes I & Chandel NS (2020), "Mitochondrial TCA cycle metabolites control physiology and disease", *Nat Commun,* vol. 11 p. 102, doi:10.1038/s41467-019-13668-3

Marzluff WF (2005), "Metazoan replication-dependent histone mRNAs: a distinct set of RNA polymerase II transcripts", *Curr Opin Cell Biol,* vol. 17 pp. 274-280, doi:10.1016/j.ceb.2005.04.010

Mateu-Regue A, Christiansen J, Bagger FO, Winther O, Hellriegel C & Nielsen FC (2019), "Single mRNP Analysis Reveals that Small Cytoplasmic mRNP Granules Represent mRNA Singletons", *Cell Rep,* vol. 29 pp. 736-748 e734, doi:10.1016/j.celrep.2019.09.018

Mathis D & Shoelson SE (2011), "Immunometabolism: an emerging frontier", *Nat Rev Immunol,* vol. 11 p. 81, doi:10.1038/nri2922

Mayr C & Bartel DP (2009), "Widespread shortening of 3'UTRs by alternative cleavage and polyadenylation activates oncogenes in cancer cells", *Cell,* vol. 138 pp. 673-684, doi:10.1016/j.cell.2009.06.016

Mazan-Mamczarz K, Lal A, Martindale JL, Kawai T & Gorospe M (2006), "Translational repression by RNA-binding protein TIAR", *Mol Cell Biol,* vol. 26 pp. 2716-2727, doi:10.1128/MCB.26.7.2716-2727.2006

McCormick C & Khaperskyy DA (2017), "Translation inhibition and stress granules in the antiviral immune response", *Nat Rev Immunol,* vol. 17 pp. 647-660, doi:10.1038/nri.2017.63

McCracken S, Fong N, Yankulov K, Ballantyne S, Pan G, Greenblatt J, Patterson SD, Wickens M & Bentley DL (1997), "The C-terminal domain of RNA polymerase II couples mRNA processing to transcription", *Nature,* vol. 385 pp. 357-361, doi:10.1038/385357a0

McGuire VA, Rosner D, Ananieva O, Ross EA, Elcombe SE, Naqvi S, van den Bosch MMW, Monk CE, Ruiz-Zorrilla Diez T, Clark AR & Arthur JSC (2017), "Beta Interferon Production Is Regulated by p38 Mitogen-Activated Protein Kinase in Macrophages via both MSK1/2- and Tristetraprolin-Dependent Pathways", *Mol Cell Biol,* vol. 37 doi:10.1128/MCB.00454-16

McNab F, Mayer-Barber K, Sher A, Wack A & O'Garra A (2015), "Type I interferons in infectious disease", *Nat Rev Immunol,* vol. 15 pp. 87-103, doi:10.1038/nri3787

Medzhitov R, Preston-Hurlburt P, Kopp E, Stadlen A, Chen C, Ghosh S & Janeway CA, Jr. (1998), "MyD88 is an adaptor protein in the hToll/IL-1 receptor family signaling pathways", *Mol Cell,* vol. 2 pp. 253-258, doi:10.1016/s1097-2765(00)80136-7

Mendoza JL, Schneider WM, Hoffmann HH, Vercauteren K, Jude KM, Xiong A, Moraga I, Horton TM, Glenn JS, de Jong YP, Rice CM & Garcia KC (2017), "The IFN-lambda-IFN-lambdaR1-IL-10Rbeta Complex Reveals Structural Features Underlying Type III IFN Functional Plasticity", *Immunity,* vol. 46 pp. 379-392, doi:10.1016/j.immuni.2017.02.017

Mertins P, Qiao JW, Patel J, Udeshi ND, Clauser KR, Mani DR, Burgess MW, Gillette MA, Jaffe JD & Carr SA (2013), "Integrated proteomic analysis of post-translational modifications by serial enrichment", *Nat Methods,* vol. 10 pp. 634-637, doi:10.1038/nmeth.2518

Meylan E, Curran J, Hofmann K, Moradpour D, Binder M, Bartenschlager R & Tschopp J (2005), "Cardif is an adaptor protein in the RIG-I antiviral pathway and is targeted by hepatitis C virus", *Nature,* vol. 437 pp. 1167-1172, doi:10.1038/nature04193

Mi H, Muruganujan A, Huang X, Ebert D, Mills C, Guo X & Thomas PD (2019), "Protocol Update for large-scale genome and gene function analysis with the PANTHER classification system (v.14.0)", *Nat Protoc,* vol. 14 pp. 703-721, doi:10.1038/s41596-019-0128-8

Miao F, Bouziane M, Dammann R, Masutani C, Hanaoka F, Pfeifer G & O'Connor TR (2000), "3-Methyladenine-DNA glycosylase (MPG protein) interacts with human RAD23 proteins", *J Biol Chem,* vol. 275 pp. 28433-28438, doi:10.1074/jbc.M001064200

Michalek RD, Gerriets VA, Jacobs SR, Macintyre AN, MacIver NJ, Mason EF, Sullivan SA, Nichols AG & Rathmell JC (2011), "Cutting edge: distinct glycolytic and lipid oxidative metabolic programs are essential for effector and regulatory CD4+ T cell subsets", *J Immunol,* vol. 186 pp. 3299-3303, doi:10.4049/jimmunol.1003613

Michelucci A, Cordes T, Ghelfi J, Pailot A, Reiling N, Goldmann O, Binz T, Wegner A, Tallam A, Rausell A, Buttini M, Linster CL, Medina E, Balling R & Hiller K (2013), "Immune-responsive gene 1 protein links metabolism to immunity by catalyzing itaconic acid production", *Proc Natl Acad Sci U S A,* vol. 110 pp. 7820-7825, doi:10.1073/pnas.1218599110

Michl J, Ohlbaum DJ & Silverstein SC (1976), "2-Deoxyglucose selectively inhibits Fc and complement receptor-mediated phagocytosis in mouse peritoneal macrophages. I. Description of the inhibitory effect", *J Exp Med,* vol. 144 pp. 1465-1483, doi:10.1084/jem.144.6.1465

Mikkelsen SS, Jensen SB, Chiliveru S, Melchjorsen J, Julkunen I, Gaestel M, Arthur JS, Flavell RA, Ghosh S & Paludan SR (2009), "RIG-I-mediated activation of p38 MAPK is essential for viral induction of interferon and activation of dendritic cells: dependence on TRAF2 and TAK1", *J Biol Chem,* vol. 284 pp. 10774-10782, doi:10.1074/jbc.M807272200

Miles WO, Lembo A, Volorio A, Brachtel E, Tian B, Sgroi D, Provero P & Dyson N (2016), "Alternative Polyadenylation in Triple-Negative Breast Tumors Allows NRAS and c-JUN to Bypass PUMILIO Posttranscriptional Regulation", *Cancer Res,* vol. 76 pp. 7231-7241, doi:10.1158/0008-5472.CAN-16-0844

Miller S, Yasuda M, Coats JK, Jones Y, Martone ME & Mayford M (2002), "Disruption of dendritic translation of CaMKIIalpha impairs stabilization of synaptic plasticity and memory consolidation", *Neuron,* vol. 36 pp. 507-519, doi:10.1016/s0896-6273(02)00978-9

Millevoi S, Loulergue C, Dettwiler S, Karaa SZ, Keller W, Antoniou M & Vagner S (2006), "An interaction between U2AF 65 and CF I(m) links the splicing and 3' end processing machineries", *EMBO J,* vol. 25 pp. 4854-4864, doi:10.1038/sj.emboj.7601331

Mills EL, Ryan DG, Prag HA, Dikovskaya D, Menon D, Zaslona Z, Jedrychowski MP, Costa ASH, Higgins M, Hams E, Szpyt J, Runtsch MC, King MS, McGouran JF, Fischer R, Kessler BM, McGettrick AF, Hughes MM, Carroll RG, Booty LM, Knatko EV, Meakin PJ, Ashford MLJ, Modis LK, Brunori G, Sevin DC, Fallon PG, Caldwell ST, Kunji ERS, Chouchani ET, Frezza C, Dinkova-Kostova AT, Hartley RC, Murphy MP & O'Neill LA (2018), "Itaconate is an anti-inflammatory metabolite that activates Nrf2 via alkylation of KEAP1", *Nature,* vol. 556 pp. 113-117, doi:10.1038/nature25986

Minakami R & Sumimotoa H (2006), "Phagocytosis-coupled activation of the superoxide-producing phagocyte oxidase, a member of the NADPH oxidase (nox) family", *Int J Hematol,* vol. 84 pp. 193-198, doi:10.1532/IJH97.06133

Miranda M, Morici JF, Zanoni MB & Bekinschtein P (2019), "Brain-Derived Neurotrophic Factor: A Key Molecule for Memory in the Healthy and the

Pathological Brain", *Front Cell Neurosci,* vol. 13 p. 363, doi:10.3389/fncel.2019.00363

Mishra BB, Rathinam VA, Martens GW, Martinot AJ, Kornfeld H, Fitzgerald KA & Sassetti CM (2013), "Nitric oxide controls the immunopathology of tuberculosis by inhibiting NLRP3 inflammasome-dependent processing of IL-1beta", *Nat Immunol,* vol. 14 pp. 52-60, doi:10.1038/ni.2474

Mittleman BE, Pott S, Warland S, Zeng T, Mu Z, Kaur M, Gilad Y & Li Y (2020), "Alternative polyadenylation mediates genetic regulation of gene expression", *Elife,* vol. 9 doi:10.7554/eLife.57492

Miura P, Shenker S, Andreu-Agullo C, Westholm JO & Lai EC (2013), "Widespread and extensive lengthening of 3' UTRs in the mammalian brain", *Genome Res,* vol. 23 pp. 812-825, doi:10.1101/gr.146886.112

Modic M, Grosch M, Rot G, Schirge S, Lepko T, Yamazaki T, Lee FCY, Rusha E, Shaposhnikov D, Palo M, Merl-Pham J, Cacchiarelli D, Rogelj B, Hauck SM, von Mering C, Meissner A, Lickert H, Hirose T, Ule J & Drukker M (2019), "Cross-Regulation between TDP-43 and Paraspeckles Promotes Pluripotency-Differentiation Transition", *Mol Cell,* vol. 74 pp. 951-965 e913, doi:10.1016/j.molcel.2019.03.041

Moon JS, Hisata S, Park MA, DeNicola GM, Ryter SW, Nakahira K & Choi AMK (2015a), "mTORC1-Induced HK1-Dependent Glycolysis Regulates NLRP3 Inflammasome Activation", *Cell Rep,* vol. 12 pp. 102-115, doi:10.1016/j.celrep.2015.05.046

Moon JS, Lee S, Park MA, Siempos, II, Haslip M, Lee PJ, Yun M, Kim CK, Howrylak J, Ryter SW, Nakahira K & Choi AM (2015b), "UCP2-induced fatty acid synthase promotes NLRP3 inflammasome activation during sepsis", *J Clin Invest,* vol. 125 pp. 665-680, doi:10.1172/JCI78253

Moore CL & Sharp PA (1985), "Accurate cleavage and polyadenylation of exogenous RNA substrate", *Cell,* vol. 41 pp. 845-855, doi:10.1016/s0092-8674(85)80065-9

Mordstein M, Neugebauer E, Ditt V, Jessen B, Rieger T, Falcone V, Sorgeloos F, Ehl S, Mayer D, Kochs G, Schwemmle M, Gunther S, Drosten C, Michiels T & Staeheli P (2010), "Lambda interferon renders epithelial cells of the respiratory and gastrointestinal tracts resistant to viral infections", *J Virol,* vol. 84 pp. 5670-5677, doi:10.1128/JVI.00272-10

Moriguchi T, Kuroyanagi N, Yamaguchi K, Gotoh Y, Irie K, Kano T, Shirakabe K, Muro Y, Shibuya H, Matsumoto K, Nishida E & Hagiwara M (1996), "A novel kinase cascade mediated by mitogen-activated protein kinase kinase 6 and MKK3", *J Biol Chem,* vol. 271 pp. 13675-13679, doi:10.1074/jbc.271.23.13675

Morita M, Gravel SP, Chenard V, Sikstrom K, Zheng L, Alain T, Gandin V, Avizonis D, Arguello M, Zakaria C, McLaughlan S, Nouet Y, Pause A, Pollak M, Gottlieb E, Larsson O, St-Pierre J, Topisirovic I & Sonenberg N (2013), "mTORC1 controls mitochondrial activity and biogenesis through 4E-BP-dependent translational regulation", *Cell Metab,* vol. 18 pp. 698-711, doi:10.1016/j.cmet.2013.10.001

Morita M, Prudent J, Basu K, Goyon V, Katsumura S, Hulea L, Pearl D, Siddiqui N, Strack S, McGuirk S, St-Pierre J, Larsson O, Topisirovic I, Vali H, McBride HM, Bergeron JJ & Sonenberg N (2017), "mTOR Controls Mitochondrial Dynamics and Cell Survival via MTFP1", *Mol Cell,* vol. 67 pp. 922-935 e925, doi:10.1016/j.molcel.2017.08.013

Moritz A, Li Y, Guo A, Villen J, Wang Y, MacNeill J, Kornhauser J, Sprott K, Zhou J, Possemato A, Ren JM, Hornbeck P, Cantley LC, Gygi SP, Rush J & Comb MJ (2010), "Akt-RSK-S6 kinase signaling networks activated by oncogenic receptor tyrosine kinases", *Sci Signal,* vol. 3 p. ra64, doi:10.1126/scisignal.2000998

Morrissey MA, Kern N & Vale RD (2020), "CD47 Ligation Repositions the Inhibitory Receptor SIRPA to Suppress Integrin Activation and Phagocytosis", *Immunity,* vol. 53 pp. 290-302 e296, doi:10.1016/j.immuni.2020.07.008

Muller M, Briscoe J, Laxton C, Guschin D, Ziemiecki A, Silvennoinen O, Harpur AG, Barbieri G, Witthuhn BA, Schindler C & et al. (1993), "The protein tyrosine kinase JAK1 complements defects in interferon-alpha/beta and -gamma signal transduction", *Nature,* vol. 366 pp. 129-135, doi:10.1038/366129a0

Muntjewerff EM, Meesters LD & van den Bogaart G (2020), "Antigen Cross-Presentation by Macrophages", *Front Immunol,* vol. 11 p. 1276, doi:10.3389/fimmu.2020.01276

Murphy C & Newsholme P (1998), "Importance of glutamine metabolism in murine macrophages and human monocytes to L-arginine biosynthesis and rates of nitrite or urea production", *Clin Sci (Lond),* vol. 95 pp. 397-407,

Nagano Y & Kojima Y (1954), "[Immunizing property of vaccinia virus inactivated by ultraviolets rays]", *C R Seances Soc Biol Fil,* vol. 148 pp. 1700-1702,

Nam JW, Rissland OS, Koppstein D, Abreu-Goodger C, Jan CH, Agarwal V, Yildirim MA, Rodriguez A & Bartel DP (2014), "Global analyses of the effect of different cellular contexts on microRNA targeting", *Mol Cell,* vol. 53 pp. 1031-1043, doi:10.1016/j.molcel.2014.02.013

Nasr N, Maddocks S, Turville SG, Harman AN, Woolger N, Helbig KJ, Wilkinson J, Bye CR, Wright TK, Rambukwelle D, Donaghy H, Beard MR & Cunningham AL (2012), "HIV-1 infection of human macrophages directly induces viperin which inhibits viral production", *Blood,* vol. 120 pp. 778-788, doi:10.1182/blood-2012-01-407395

Naujoks J, Tabeling C, Dill BD, Hoffmann C, Brown AS, Kunze M, Kempa S, Peter A, Mollenkopf HJ, Dorhoi A, Kershaw O, Gruber AD, Sander LE, Witzenrath M, Herold S, Nerlich A, Hocke AC, van Driel I, Suttorp N, Bedoui S, Hilbi H, Trost M & Opitz B (2016), "IFNs Modify the Proteome of Legionella-Containing Vacuoles and Restrict Infection Via IRG1-Derived Itaconic Acid", *PLoS Pathog,* vol. 12 p. e1005408, doi:10.1371/journal.ppat.1005408

Nelson VL, Nguyen HCB, Garcia-Canaveras JC, Briggs ER, Ho WY, DiSpirito JR, Marinis JM, Hill DA & Lazar MA (2018), "PPARgamma is a nexus controlling alternative activation of macrophages via glutamine metabolism", *Genes Dev,* vol. 32 pp. 1035-1044, doi:10.1101/gad.312355.118

Newsholme P, Curi R, Gordon S & Newsholme EA (1986), "Metabolism of glucose, glutamine, long-chain fatty acids and ketone bodies by murine macrophages", *Biochem J,* vol. 239 pp. 121-125, doi:10.1042/bj2390121

Nguyen H, Ramana CV, Bayes J & Stark GR (2001), "Roles of phosphatidylinositol 3-kinase in interferon-gamma-dependent phosphorylation of STAT1 on serine 727 and activation of gene expression", *J Biol Chem,* vol. 276 pp. 33361-33368, doi:10.1074/jbc.M105070200

Nguyen KB, Watford WT, Salomon R, Hofmann SR, Pien GC, Morinobu A, Gadina M, O'Shea JJ & Biron CA (2002), "Critical role for STAT4 activation by type 1 interferons in the interferon-gamma response to viral infection", *Science,* vol. 297 pp. 2063-2066, doi:10.1126/science.1074900

Nimmerjahn F & Ravetch JV (2010), "Antibody-mediated modulation of immune responses", *Immunol Rev,* vol. 236 pp. 265-275, doi:10.1111/j.1600-065X.2010.00910.x

Nishimoto N & Kishimoto T (2004), "Inhibition of IL-6 for the treatment of inflammatory diseases", *Curr Opin Pharmacol,* vol. 4 pp. 386-391, doi:10.1016/j.coph.2004.03.005

Norbury CC, Hewlett LJ, Prescott AR, Shastri N & Watts C (1995), "Class I MHC presentation of exogenous soluble antigen via macropinocytosis in bone marrow macrophages", *Immunity,* vol. 3 pp. 783-791, doi:10.1016/1074-7613(95)90067-5

O'Connell RM, Saha SK, Vaidya SA, Bruhn KW, Miranda GA, Zarnegar B, Perry AK, Nguyen BO, Lane TF, Taniguchi T, Miller JF & Cheng G (2004), "Type I interferon production enhances susceptibility to Listeria monocytogenes infection", *J Exp Med,* vol. 200 pp. 437-445, doi:10.1084/jem.20040712

O'Sullivan D, van der Windt GJ, Huang SC, Curtis JD, Chang CH, Buck MD, Qiu J, Smith AM, Lam WY, DiPlato LM, Hsu FF, Birnbaum MJ, Pearce EJ & Pearce EL (2014), "Memory CD8(+) T cells use cell-intrinsic lipolysis to support the

metabolic programming necessary for development", *Immunity,* vol. 41 pp. 75-88, doi:10.1016/j.immuni.2014.06.005

Odendall C, Dixit E, Stavru F, Bierne H, Franz KM, Durbin AF, Boulant S, Gehrke L, Cossart P & Kagan JC (2014), "Diverse intracellular pathogens activate type III interferon expression from peroxisomes", *Nat Immunol,* vol. 15 pp. 717-726, doi:10.1038/ni.2915

Ogorodnikov A, Levin M, Tattikota S, Tokalov S, Hoque M, Scherzinger D, Marini F, Poetsch A, Binder H, Macher-Goppinger S, Probst HC, Tian B, Schaefer M, Lackner KJ, Westermann F & Danckwardt S (2018), "Transcriptome 3'end organization by PCF11 links alternative polyadenylation to formation and neuronal differentiation of neuroblastoma", *Nat Commun,* vol. 9 p. 5331, doi:10.1038/s41467-018-07580-5

OhAinle M, Helms L, Vermeire J, Roesch F, Humes D, Basom R, Delrow JJ, Overbaugh J & Emerman M (2018), "A virus-packageable CRISPR screen identifies host factors mediating interferon inhibition of HIV", *Elife,* vol. 7 doi:10.7554/eLife.39823

Ohno M, Natsume A, Kondo Y, Iwamizu H, Motomura K, Toda H, Ito M, Kato T & Wakabayashi T (2009), "The modulation of microRNAs by type I IFN through the activation of signal transducers and activators of transcription 3 in human glioma", *Mol Cancer Res,* vol. 7 pp. 2022-2030, doi:10.1158/1541-7786.MCR-09-0319

Olagnier D, Brandtoft AM, Gunderstofte C, Villadsen NL, Krapp C, Thielke AL, Laustsen A, Peri S, Hansen AL, Bonefeld L, Thyrsted J, Bruun V, Iversen MB, Lin L, Artegoitia VM, Su C, Yang L, Lin R, Balachandran S, Luo Y, Nyegaard M, Marrero B, Goldbach-Mansky R, Motwani M, Ryan DG, Fitzgerald KA, O'Neill LA, Hollensen AK, Damgaard CK, de Paoli FV, Bertram HC, Jakobsen MR, Poulsen TB & Holm CK (2018), "Nrf2 negatively regulates STING indicating a link between antiviral sensing and metabolic reprogramming", *Nat Commun,* vol. 9 p. 3506, doi:10.1038/s41467-018-05861-7

Oldenborg PA, Zheleznyak A, Fang YF, Lagenaur CF, Gresham HD & Lindberg FP (2000), "Role of CD47 as a marker of self on red blood cells", *Science,* vol. 288 pp. 2051-2054, doi:10.1126/science.288.5473.2051

Orecchioni M, Ghosheh Y, Pramod AB & Ley K (2019), "Macrophage Polarization: Different Gene Signatures in M1(LPS+) vs. Classically and M2(LPS-) vs. Alternatively Activated Macrophages", *Front Immunol,* vol. 10 p. 1084, doi:10.3389/fimmu.2019.01084

Oren R, Farnham AE, Saito K, Milofsky E & Karnovsky ML (1963), "Metabolic patterns in three types of phagocytizing cells", *J Cell Biol,* vol. 17 pp. 487-501, doi:10.1083/jcb.17.3.487

Orkin SH, Cheng TC, Antonarakis SE & Kazazian HH, Jr. (1985), "Thalassemia due to a mutation in the cleavage-polyadenylation signal of the human beta-globin gene", *EMBO J,* vol. 4 pp. 453-456,

Orkin SH & Zon LI (2008), "Hematopoiesis: an evolving paradigm for stem cell biology", *Cell,* vol. 132 pp. 631-644, doi:10.1016/j.cell.2008.01.025

Oshiumi H, Matsumoto M, Funami K, Akazawa T & Seya T (2003a), "TICAM-1, an adaptor molecule that participates in Toll-like receptor 3-mediated interferon-beta induction", *Nat Immunol,* vol. 4 pp. 161-167, doi:10.1038/ni886

Oshiumi H, Sasai M, Shida K, Fujita T, Matsumoto M & Seya T (2003b), "TIR-containing adapter molecule (TICAM)-2, a bridging adapter recruiting to toll-like receptor 4 TICAM-1 that induces interferon-beta", *J Biol Chem,* vol. 278 pp. 49751-49762, doi:10.1074/jbc.M305820200

Palmieri EM, Gonzalez-Cotto M, Baseler WA, Davies LC, Ghesquiere B, Maio N, Rice CM, Rouault TA, Cassel T, Higashi RM, Lane AN, Fan TW, Wink DA & McVicar DW (2020), "Nitric oxide orchestrates metabolic rewiring in M1 macrophages by targeting aconitase 2 and pyruvate dehydrogenase", *Nat Commun,* vol. 11 p. 698, doi:10.1038/s41467-020-14433-7

Palmieri F (2004), "The mitochondrial transporter family (SLC25): physiological and pathological implications", *Pflugers Arch,* vol. 447 pp. 689-709, doi:10.1007/s00424-003-1099-7

Palsson-McDermott EM, Curtis AM, Goel G, Lauterbach MA, Sheedy FJ, Gleeson LE, van den Bosch MW, Quinn SR, Domingo-Fernandez R, Johnston DG, Jiang JK, Israelsen WJ, Keane J, Thomas C, Clish C, Vander Heiden M, Xavier RJ & O'Neill LA (2015), "Pyruvate kinase M2 regulates Hif-1alpha activity and IL-1beta induction and is a critical determinant of the warburg effect in LPS-activated macrophages", *Cell Metab,* vol. 21 pp. 65-80, doi:10.1016/j.cmet.2014.12.005

Papachristou DJ, Batistatou A, Sykiotis GP, Varakis I & Papavassiliou AG (2003), "Activation of the JNK-AP-1 signal transduction pathway is associated with pathogenesis and progression of human osteosarcomas", *Bone,* vol. 32 pp. 364-371, doi:10.1016/s8756-3282(03)00026-7

Papadopoulou AS, Dooley J, Linterman MA, Pierson W, Ucar O, Kyewski B, Zuklys S, Hollander GA, Matthys P, Gray DH, De Strooper B & Liston A (2011), "The thymic epithelial microRNA network elevates the threshold for infection-associated thymic involution via miR-29a mediated suppression of the IFN-alpha receptor", *Nat Immunol,* vol. 13 pp. 181-187, doi:10.1038/ni.2193

Pareek V, Pedley AM & Benkovic SJ (2021), "Human de novo purine biosynthesis", *Crit Rev Biochem Mol Biol,* vol. 56 pp. 1-16, doi:10.1080/10409238.2020.1832438

Patel JR, Jain A, Chou YY, Baum A, Ha T & Garcia-Sastre A (2013), "ATPase-driven oligomerization of RIG-I on RNA allows optimal activation of type-I interferon", *EMBO Rep,* vol. 14 pp. 780-787, doi:10.1038/embor.2013.102

Patsoukis N, Bardhan K, Chatterjee P, Sari D, Liu B, Bell LN, Karoly ED, Freeman GJ, Petkova V, Seth P, Li L & Boussiotis VA (2015), "PD-1 alters T-cell metabolic reprogramming by inhibiting glycolysis and promoting lipolysis and fatty acid oxidation", *Nat Commun,* vol. 6 p. 6692, doi:10.1038/ncomms7692

Pedersen IM, Cheng G, Wieland S, Volinia S, Croce CM, Chisari FV & David M (2007), "Interferon modulation of cellular microRNAs as an antiviral mechanism", *Nature,* vol. 449 pp. 919-922, doi:10.1038/nature06205

Peisley A, Wu B, Yao H, Walz T & Hur S (2013), "RIG-I forms signaling-competent filaments in an ATP-dependent, ubiquitin-independent manner", *Mol Cell,* vol. 51 pp. 573-583, doi:10.1016/j.molcel.2013.07.024

Pelka K, Bertheloot D, Reimer E, Phulphagar K, Schmidt SV, Christ A, Stahl R, Watson N, Miyake K, Hacohen N, Haas A, Brinkmann MM, Marshak-Rothstein A, Meissner F & Latz E (2018), "The Chaperone UNC93B1 Regulates Toll-like Receptor Stability Independently of Endosomal TLR Transport", *Immunity,* vol. 48 pp. 911-922 e917, doi:10.1016/j.immuni.2018.04.011

Perez Canadillas JM & Varani G (2003), "Recognition of GU-rich polyadenylation regulatory elements by human CstF-64 protein", *EMBO J,* vol. 22 pp. 2821-2830, doi:10.1093/emboj/cdg259

Perez-Caballero D, Zang T, Ebrahimi A, McNatt MW, Gregory DA, Johnson MC & Bieniasz PD (2009), "Tetherin inhibits HIV-1 release by directly tethering virions to cells", *Cell,* vol. 139 pp. 499-511, doi:10.1016/j.cell.2009.08.039

Pesce JT, Ramalingam TR, Mentink-Kane MM, Wilson MS, El Kasmi KC, Smith AM, Thompson RW, Cheever AW, Murray PJ & Wynn TA (2009), "Arginase-1-expressing macrophages suppress Th2 cytokine-driven inflammation and fibrosis", *PLoS Pathog,* vol. 5 p. e1000371, doi:10.1371/journal.ppat.1000371

Petroulakis E, Parsyan A, Dowling RJ, LeBacquer O, Martineau Y, Bidinosti M, Larsson O, Alain T, Rong L, Mamane Y, Paquet M, Furic L, Topisirovic I, Shahbazian D, Livingstone M, Costa-Mattioli M, Teodoro JG & Sonenberg N (2009), "p53-dependent translational control of senescence and transformation via 4E-BPs", *Cancer Cell,* vol. 16 pp. 439-446, doi:10.1016/j.ccr.2009.09.025

Pfaller CK, Donohue RC, Nersisyan S, Brodsky L & Cattaneo R (2018), "Extensive editing of cellular and viral double-stranded RNA structures accounts for innate immunity suppression and the proviral activity of ADAR1p150", *PLoS Biol,* vol. 16 p. e2006577, doi:10.1371/journal.pbio.2006577

Phillips C, Pachikara N & Gunderson SI (2004), "U1A inhibits cleavage at the immunoglobulin M heavy-chain secretory poly(A) site by binding between the two downstream GU-rich regions", *Mol Cell Biol,* vol. 24 pp. 6162-6171, doi:10.1128/MCB.24.14.6162-6171.2004

Pidugu VK, Pidugu HB, Wu MM, Liu CJ & Lee TC (2019), "Emerging Functions of Human IFIT Proteins in Cancer", *Front Mol Biosci,* vol. 6 p. 148, doi:10.3389/fmolb.2019.00148

Pijet B, Pijet M, Litwiniuk A, Gajewska M, Pajak B & Orzechowski A (2013), "TNF-alpha and IFN-s-dependent muscle decay is linked to NF-kappaB- and STAT-1alpha-stimulated Atrogin1 and MuRF1 genes in C2C12 myotubes", *Mediators Inflamm,* vol. 2013 p. 171437, doi:10.1155/2013/171437

Platanias LC (2005), "Mechanisms of type-I- and type-II-interferon-mediated signalling", *Nat Rev Immunol,* vol. 5 pp. 375-386, doi:10.1038/nri1604

Platanias LC & Sweet ME (1994), "Interferon alpha induces rapid tyrosine phosphorylation of the vav proto-oncogene product in hematopoietic cells", *J Biol Chem,* vol. 269 pp. 3143-3146,

Platanias LC, Uddin S, Yetter A, Sun XJ & White MF (1996), "The type I interferon receptor mediates tyrosine phosphorylation of insulin receptor substrate 2", *J Biol Chem,* vol. 271 pp. 278-282, doi:10.1074/jbc.271.1.278

Platanitis E & Decker T (2018), "Regulatory Networks Involving STATs, IRFs, and NFkappaB in Inflammation", *Front Immunol,* vol. 9 p. 2542, doi:10.3389/fimmu.2018.02542

Plumlee CR, Lee C, Beg AA, Decker T, Shuman HA & Schindler C (2009), "Interferons direct an effective innate response to Legionella pneumophila infection", *J Biol Chem,* vol. 284 pp. 30058-30066, doi:10.1074/jbc.M109.018283

Poli G, Orenstein JM, Kinter A, Folks TM & Fauci AS (1989), "Interferon-alpha but not AZT suppresses HIV expression in chronically infected cell lines", *Science,* vol. 244 pp. 575-577, doi:10.1126/science.2470148

Porstmann T, Santos CR, Griffiths B, Cully M, Wu M, Leevers S, Griffiths JR, Chung YL & Schulze A (2008), "SREBP activity is regulated by mTORC1 and contributes to Akt-dependent cell growth", *Cell Metab,* vol. 8 pp. 224-236, doi:10.1016/j.cmet.2008.07.007

Posokhova EN, Khoshchenko OM, Chasovskikh MI, Pivovarova EN & Dushkin MI (2008), "Lipid synthesis in macrophages during inflammation in vivo: effect of agonists of peroxisome proliferator activated receptors alpha and gamma and of retinoid X receptors", *Biochemistry (Mosc),* vol. 73 pp. 296-304, doi:10.1134/s0006297908030097

Poulin F, Gingras AC, Olsen H, Chevalier S & Sonenberg N (1998), "4E-BP3, a new member of the eukaryotic initiation factor 4E-binding protein family", *J Biol Chem,* vol. 273 pp. 14002-14007, doi:10.1074/jbc.273.22.14002

Prchal-Murphy M, Semper C, Lassnig C, Wallner B, Gausterer C, Teppner-Klymiuk I, Kobolak J, Muller S, Kolbe T, Karaghiosoff M, Dinnyes A, Rulicke T, Leitner NR, Strobl B & Muller M (2012), "TYK2 kinase activity is required for functional type I interferon responses in vivo", *PLoS One,* vol. 7 p. e39141, doi:10.1371/journal.pone.0039141

Prokunina-Olsson L (2019), "Genetics of the Human Interferon Lambda Region", *J Interferon Cytokine Res,* vol. 39 pp. 599-608, doi:10.1089/jir.2019.0043

Prokunina-Olsson L, Muchmore B, Tang W, Pfeiffer RM, Park H, Dickensheets H, Hergott D, Porter-Gill P, Mumy A, Kohaar I, Chen S, Brand N, Tarway M, Liu L, Sheikh F, Astemborski J, Bonkovsky HL, Edlin BR, Howell CD, Morgan TR, Thomas DL, Rehermann B, Donnelly RP & O'Brien TR (2013), "A variant upstream of IFNL3 (IL28B) creating a new interferon gene IFNL4 is associated with impaired clearance of hepatitis C virus", *Nat Genet,* vol. 45 pp. 164-171, doi:10.1038/ng.2521

Proudfoot NJ, Furger A & Dye MJ (2002), "Integrating mRNA processing with transcription", *Cell,* vol. 108 pp. 501-512, doi:10.1016/s0092-8674(02)00617-7

Raingeaud J, Whitmarsh AJ, Barrett T, Derijard B & Davis RJ (1996), "MKK3- and MKK6-regulated gene expression is mediated by the p38 mitogen-activated protein kinase signal transduction pathway", *Mol Cell Biol,* vol. 16 pp. 1247-1255, doi:10.1128/MCB.16.3.1247

Randal M & Kossiakoff AA (2001), "The structure and activity of a monomeric interferon-gamma:alpha-chain receptor signaling complex", *Structure,* vol. 9 pp. 155-163, doi:10.1016/s0969-2126(01)00567-6

Rani MR, Hibbert L, Sizemore N, Stark GR & Ransohoff RM (2002), "Requirement of phosphoinositide 3-kinase and Akt for interferon-beta-mediated induction of the beta-R1 (SCYB11) gene", *J Biol Chem,* vol. 277 pp. 38456-38461, doi:10.1074/jbc.M203204200

Rappsilber J, Ryder U, Lamond AI & Mann M (2002), "Large-scale proteomic analysis of the human spliceosome", *Genome Res,* vol. 12 pp. 1231-1245, doi:10.1101/gr.473902

Rath M, Muller I, Kropf P, Closs EI & Munder M (2014), "Metabolism via Arginase or Nitric Oxide Synthase: Two Competing Arginine Pathways in Macrophages", *Front Immunol,* vol. 5 p. 532, doi:10.3389/fimmu.2014.00532

Rathinam VA, Jiang Z, Waggoner SN, Sharma S, Cole LE, Waggoner L, Vanaja SK, Monks BG, Ganesan S, Latz E, Hornung V, Vogel SN, Szomolanyi-Tsuda E

& Fitzgerald KA (2010), "The AIM2 inflammasome is essential for host defense against cytosolic bacteria and DNA viruses", *Nat Immunol,* vol. 11 pp. 395-402, doi:10.1038/ni.1864

Ren J, Chen X & Chen ZJ (2014), "IKKbeta is an IRF5 kinase that instigates inflammation", *Proc Natl Acad Sci U S A,* vol. 111 pp. 17438-17443, doi:10.1073/pnas.1418516111

Ren Z, Ding T, Zuo Z, Xu Z, Deng J & Wei Z (2020), "Regulation of MAVS Expression and Signaling Function in the Antiviral Innate Immune Response", *Front Immunol,* vol. 11 p. 1030, doi:10.3389/fimmu.2020.01030

Ribeiro DM, Prod'homme A, Teixeira A, Zanzoni A & Brun C (2020), "The role of 3'UTR-protein complexes in the regulation of protein multifunctionality and subcellular localization", *Nucleic Acids Res,* vol. 48 pp. 6491-6502, doi:10.1093/nar/gkaa462

Richardson RB, Ohlson MB, Eitson JL, Kumar A, McDougal MB, Boys IN, Mar KB, De La Cruz-Rivera PC, Douglas C, Konopka G, Xing C & Schoggins JW (2018), "A CRISPR screen identifies IFI6 as an ER-resident interferon effector that blocks flavivirus replication", *Nat Microbiol,* vol. 3 pp. 1214-1223, doi:10.1038/s41564-018-0244-1

Rink J, Ghigo E, Kalaidzidis Y & Zerial M (2005), "Rab conversion as a mechanism of progression from early to late endosomes", *Cell,* vol. 122 pp. 735-749, doi:10.1016/j.cell.2005.06.043

Robertson AB, Klungland A, Rognes T & Leiros I (2009), "DNA repair in mammalian cells: Base excision repair: the long and short of it", *Cell Mol Life Sci,* vol. 66 pp. 981-993, doi:10.1007/s00018-009-8736-z

Robinson MD & Oshlack A (2010), "A scaling normalization method for differential expression analysis of RNA-seq data", *Genome Biol,* vol. 11 p. R25, doi:10.1186/gb-2010-11-3-r25

Rodriguez-Prados JC, Traves PG, Cuenca J, Rico D, Aragones J, Martin-Sanz P, Cascante M & Bosca L (2010), "Substrate fate in activated macrophages: a comparison between innate, classic, and alternative activation", *J Immunol,* vol. 185 pp. 605-614, doi:10.4049/jimmunol.0901698

Roesch F, OhAinle M & Emerman M (2018), "A CRISPR screen for factors regulating SAMHD1 degradation identifies IFITMs as potent inhibitors of lentiviral particle delivery", *Retrovirology,* vol. 15 p. 26, doi:10.1186/s12977-018-0409-2

Rohrig F & Schulze A (2016), "The multifaceted roles of fatty acid synthesis in cancer", *Nat Rev Cancer,* vol. 16 pp. 732-749, doi:10.1038/nrc.2016.89

Rothenfusser S, Goutagny N, DiPerna G, Gong M, Monks BG, Schoenemeyer A, Yamamoto M, Akira S & Fitzgerald KA (2005), "The RNA helicase Lgp2 inhibits TLR-independent sensing of viral replication by retinoic acid-inducible gene-I", *J Immunol,* vol. 175 pp. 5260-5268, doi:10.4049/jimmunol.175.8.5260

Rubio D, Xu RH, Remakus S, Krouse TE, Truckenmiller ME, Thapa RJ, Balachandran S, Alcami A, Norbury CC & Sigal LJ (2013), "Crosstalk between the type 1 interferon and nuclear factor kappa B pathways confers resistance to a lethal virus infection", *Cell Host Microbe,* vol. 13 pp. 701-710, doi:10.1016/j.chom.2013.04.015

Ruegsegger U, Beyer K & Keller W (1996), "Purification and characterization of human cleavage factor Im involved in the 3' end processing of messenger RNA precursors", *J Biol Chem,* vol. 271 pp. 6107-6113, doi:10.1074/jbc.271.11.6107

Ruepp MD, Schweingruber C, Kleinschmidt N & Schumperli D (2011), "Interactions of CstF-64, CstF-77, and symplekin: implications on localisation and function", *Mol Biol Cell,* vol. 22 pp. 91-104, doi:10.1091/mbc.E10-06-0543

Rusinova I, Forster S, Yu S, Kannan A, Masse M, Cumming H, Chapman R & Hertzog PJ (2013), "Interferome v2.0: an updated database of annotated interferon-regulated genes", *Nucleic Acids Res,* vol. 41 pp. D1040-1046, doi:10.1093/nar/gks1215

Ryan DG & O'Neill LAJ (2020), "Krebs Cycle Reborn in Macrophage Immunometabolism", *Annu Rev Immunol,* vol. 38 pp. 289-313, doi:10.1146/annurev-immunol-081619-104850

Sabbah A, Chang TH, Harnack R, Frohlich V, Tominaga K, Dube PH, Xiang Y & Bose S (2009), "Activation of innate immune antiviral responses by Nod2", *Nat Immunol,* vol. 10 pp. 1073-1080, doi:10.1038/ni.1782

Sachs AB, Sarnow P & Hentze MW (1997), "Starting at the beginning, middle, and end: translation initiation in eukaryotes", *Cell,* vol. 89 pp. 831-838, doi:10.1016/s0092-8674(00)80268-8

Saha SK & Cheng G (2006), "TRAF3: a new regulator of type I interferons", *Cell Cycle,* vol. 5 pp. 804-807, doi:10.4161/cc.5.8.2637

Saha SK, Pietras EM, He JQ, Kang JR, Liu SY, Oganesyan G, Shahangian A, Zarnegar B, Shiba TL, Wang Y & Cheng G (2006), "Regulation of antiviral responses by a direct and specific interaction between TRAF3 and Cardif", *EMBO J,* vol. 25 pp. 3257-3263, doi:10.1038/sj.emboj.7601220

Saleiro D, Mehrotra S, Kroczynska B, Beauchamp EM, Lisowski P, Majchrzak-Kita B, Bhagat TD, Stein BL, McMahon B, Altman JK, Kosciuczuk EM, Baker DP, Jie C, Jafari N, Thompson CB, Levine RL, Fish EN, Verma AK & Platanias LC

(2015), "Central role of ULK1 in type I interferon signaling", *Cell Rep,* vol. 11 pp. 605-617, doi:10.1016/j.celrep.2015.03.056

Samokhvalov IM (2014), "Deconvoluting the ontogeny of hematopoietic stem cells", *Cell Mol Life Sci,* vol. 71 pp. 957-978, doi:10.1007/s00018-013-1364-7

Sandberg R, Neilson JR, Sarma A, Sharp PA & Burge CB (2008), "Proliferating cells express mRNAs with shortened 3' untranslated regions and fewer microRNA target sites", *Science,* vol. 320 pp. 1643-1647, doi:10.1126/science.1155390

Sarbassov DD, Guertin DA, Ali SM & Sabatini DM (2005), "Phosphorylation and regulation of Akt/PKB by the rictor-mTOR complex", *Science,* vol. 307 pp. 1098-1101, doi:10.1126/science.1106148

Sato M, Hata N, Asagiri M, Nakaya T, Taniguchi T & Tanaka N (1998), "Positive feedback regulation of type I IFN genes by the IFN-inducible transcription factor IRF-7", *FEBS Lett,* vol. 441 pp. 106-110, doi:10.1016/s0014-5793(98)01514-2

Satoh T, Takeuchi O, Vandenbon A, Yasuda K, Tanaka Y, Kumagai Y, Miyake T, Matsushita K, Okazaki T, Saitoh T, Honma K, Matsuyama T, Yui K, Tsujimura T, Standley DM, Nakanishi K, Nakai K & Akira S (2010), "The Jmjd3-Irf4 axis regulates M2 macrophage polarization and host responses against helminth infection", *Nat Immunol,* vol. 11 pp. 936-944, doi:10.1038/ni.1920

Schairer DO, Chouake JS, Nosanchuk JD & Friedman AJ (2012), "The potential of nitric oxide releasing therapies as antimicrobial agents", *Virulence,* vol. 3 pp. 271-279, doi:10.4161/viru.20328

Scheltema RA, Jankevics A, Jansen RC, Swertz MA & Breitling R (2011), "PeakML/mzMatch: a file format, Java library, R library, and tool-chain for mass spectrometry data analysis", *Anal Chem,* vol. 83 pp. 2786-2793, doi:10.1021/ac2000994

Schindler C, Fu XY, Improta T, Aebersold R & Darnell JE, Jr. (1992a), "Proteins of transcription factor ISGF-3: one gene encodes the 91-and 84-kDa ISGF-3 proteins that are activated by interferon alpha", *Proc Natl Acad Sci U S A,* vol. 89 pp. 7836-7839, doi:10.1073/pnas.89.16.7836

Schindler C, Shuai K, Prezioso VR & Darnell JE, Jr. (1992b), "Interferon-dependent tyrosine phosphorylation of a latent cytoplasmic transcription factor", *Science,* vol. 257 pp. 809-813, doi:10.1126/science.1496401

Schliehe C, Redaelli C, Engelhardt S, Fehlings M, Mueller M, van Rooijen N, Thiry M, Hildner K, Weller H & Groettrup M (2011), "CD8- dendritic cells and macrophages cross-present poly(D,L-lactate-co-glycolate) acid microsphere-encapsulated antigen in vivo", *J Immunol,* vol. 187 pp. 2112-2121, doi:10.4049/jimmunol.1002084

Schoenemeyer A, Barnes BJ, Mancl ME, Latz E, Goutagny N, Pitha PM, Fitzgerald KA & Golenbock DT (2005), "The interferon regulatory factor, IRF5, is a central mediator of toll-like receptor 7 signaling", *J Biol Chem,* vol. 280 pp. 17005-17012, doi:10.1074/jbc.M412584200

Schoggins JW (2019), "Interferon-Stimulated Genes: What Do They All Do?", *Annu Rev Virol,* vol. 6 pp. 567-584, doi:10.1146/annurev-virology-092818-015756

Schoggins JW, Wilson SJ, Panis M, Murphy MY, Jones CT, Bieniasz P & Rice CM (2011), "A diverse range of gene products are effectors of the type I interferon antiviral response", *Nature,* vol. 472 pp. 481-485, doi:10.1038/nature09907

Schonemann L, Kuhn U, Martin G, Schafer P, Gruber AR, Keller W, Zavolan M & Wahle E (2014), "Reconstitution of CPSF active in polyadenylation: recognition of the polyadenylation signal by WDR33", *Genes Dev,* vol. 28 pp. 2381-2393, doi:10.1101/gad.250985.114

Schulz C, Gomez Perdiguero E, Chorro L, Szabo-Rogers H, Cagnard N, Kierdorf K, Prinz M, Wu B, Jacobsen SE, Pollard JW, Frampton J, Liu KJ & Geissmann F (2012), "A lineage of myeloid cells independent of Myb and hematopoietic stem cells", *Science,* vol. 336 pp. 86-90, doi:10.1126/science.1219179

Schwich OD, Blumel N, Keller M, Wegener M, Setty ST, Brunstein ME, Poser I, Mozos IRL, Suess B, Munch C, McNicoll F, Zarnack K & Muller-McNicoll M (2021), "SRSF3 and SRSF7 modulate 3'UTR length through suppression or activation of proximal polyadenylation sites and regulation of CFIm levels", *Genome Biol,* vol. 22 p. 82, doi:10.1186/s13059-021-02298-y

Scott CC, Dobson W, Botelho RJ, Coady-Osberg N, Chavrier P, Knecht DA, Heath C, Stahl P & Grinstein S (2005), "Phosphatidylinositol-4,5-bisphosphate hydrolysis directs actin remodeling during phagocytosis", *J Cell Biol,* vol. 169 pp. 139-149, doi:10.1083/jcb.200412162

Scott R, Siegrist F, Foser S & Certa U (2011), "Interferon-alpha induces reversible DNA demethylation of the interferon-induced transmembrane protein-3 core promoter in human melanoma cells", *J Interferon Cytokine Res,* vol. 31 pp. 601-608, doi:10.1089/jir.2010.0134

Sedgwick B, Bates PA, Paik J, Jacobs SC & Lindahl T (2007), "Repair of alkylated DNA: recent advances", *DNA Repair (Amst),* vol. 6 pp. 429-442, doi:10.1016/j.dnarep.2006.10.005

Seth RB, Sun L, Ea CK & Chen ZJ (2005), "Identification and characterization of MAVS, a mitochondrial antiviral signaling protein that activates NF-kappaB and IRF 3", *Cell,* vol. 122 pp. 669-682, doi:10.1016/j.cell.2005.08.012

Severt WL, Biber TU, Wu X, Hecht NB, DeLorenzo RJ & Jakoi ER (1999), "The suppression of testis-brain RNA binding protein and kinesin heavy chain disrupts mRNA sorting in dendrites", *J Cell Sci,* vol. 112 (Pt 21) pp. 3691-3702,

Shah AD, Goode RJA, Huang C, Powell DR & Schittenhelm RB (2020), "LFQ-Analyst: An Easy-To-Use Interactive Web Platform To Analyze and Visualize Label-Free Proteomics Data Preprocessed with MaxQuant", *J Proteome Res,* vol. 19 pp. 204-211, doi:10.1021/acs.jproteome.9b00496

Shang G, Zhu D, Li N, Zhang J, Zhu C, Lu D, Liu C, Yu Q, Zhao Y, Xu S & Gu L (2012), "Crystal structures of STING protein reveal basis for recognition of cyclic di-GMP", *Nat Struct Mol Biol,* vol. 19 pp. 725-727, doi:10.1038/nsmb.2332

Shaw AE, Hughes J, Gu Q, Behdenna A, Singer JB, Dennis T, Orton RJ, Varela M, Gifford RJ, Wilson SJ & Palmarini M (2017), "Fundamental properties of the mammalian innate immune system revealed by multispecies comparison of type I interferon responses", *PLoS Biol,* vol. 15 p. e2004086, doi:10.1371/journal.pbio.2004086

Sheehy AM, Gaddis NC, Choi JD & Malim MH (2002), "Isolation of a human gene that inhibits HIV-1 infection and is suppressed by the viral Vif protein", *Nature,* vol. 418 pp. 646-650, doi:10.1038/nature00939

Shell SA, Hesse C, Morris SM, Jr. & Milcarek C (2005), "Elevated levels of the 64-kDa cleavage stimulatory factor (CstF-64) in lipopolysaccharide-stimulated macrophages influence gene expression and induce alternative poly(A) site selection", *J Biol Chem,* vol. 280 pp. 39950-39961, doi:10.1074/jbc.M508848200

Shen Z, Paquin N, Forget A & Chartrand P (2009), "Nuclear shuttling of She2p couples ASH1 mRNA localization to its translational repression by recruiting Loc1p and Puf6p", *Mol Biol Cell,* vol. 20 pp. 2265-2275, doi:10.1091/mbc.E08-11-1151

Shi HX, Yang K, Liu X, Liu XY, Wei B, Shan YF, Zhu LH & Wang C (2010), "Positive regulation of interferon regulatory factor 3 activation by Herc5 via ISG15 modification", *Mol Cell Biol,* vol. 30 pp. 2424-2436, doi:10.1128/MCB.01466-09

Shi JH & Sun SC (2018), "Tumor Necrosis Factor Receptor-Associated Factor Regulation of Nuclear Factor kappaB and Mitogen-Activated Protein Kinase Pathways", *Front Immunol,* vol. 9 p. 1849, doi:10.3389/fimmu.2018.01849

Shi LZ, Wang R, Huang G, Vogel P, Neale G, Green DR & Chi H (2011), "HIF1alpha-dependent glycolytic pathway orchestrates a metabolic checkpoint for the differentiation of TH17 and Treg cells", *J Exp Med,* vol. 208 pp. 1367-1376, doi:10.1084/jem.20110278

Shi Y, Di Giammartino DC, Taylor D, Sarkeshik A, Rice WJ, Yates JR, 3rd, Frank J & Manley JL (2009), "Molecular architecture of the human pre-mRNA 3'

processing complex", *Mol Cell,* vol. 33 pp. 365-376, doi:10.1016/j.molcel.2008.12.028

Shin JH, Yang JY, Jeon BY, Yoon YJ, Cho SN, Kang YH, Ryu DH & Hwang GS (2011), "(1)H NMR-based metabolomic profiling in mice infected with Mycobacterium tuberculosis", *J Proteome Res,* vol. 10 pp. 2238-2247, doi:10.1021/pr101054m

Shulman ED & Elkon R (2020), "Systematic identification of functional SNPs interrupting 3'UTR polyadenylation signals", *PLoS Genet,* vol. 16 p. e1008977, doi:10.1371/journal.pgen.1008977

Signer RA, Qi L, Zhao Z, Thompson D, Sigova AA, Fan ZP, DeMartino GN, Young RA, Sonenberg N & Morrison SJ (2016), "The rate of protein synthesis in hematopoietic stem cells is limited partly by 4E-BPs", *Genes Dev,* vol. 30 pp. 1698-1703, doi:10.1101/gad.282756.116

Smith CA, Want EJ, O'Maille G, Abagyan R & Siuzdak G (2006), "XCMS: processing mass spectrometry data for metabolite profiling using nonlinear peak alignment, matching, and identification", *Anal Chem,* vol. 78 pp. 779-787, doi:10.1021/ac051437y

Smyth GK (2004), "Linear models and empirical bayes methods for assessing differential expression in microarray experiments", *Stat Appl Genet Mol Biol,* vol. 3 p. Article3, doi:10.2202/1544-6115.1027

So L, Lee J, Palafox M, Mallya S, Woxland CG, Arguello M, Truitt ML, Sonenberg N, Ruggero D & Fruman DA (2016), "The 4E-BP-eIF4E axis promotes rapamycin-sensitive growth and proliferation in lymphocytes", *Sci Signal,* vol. 9 p. ra57, doi:10.1126/scisignal.aad8463

Soloaga A, Thomson S, Wiggin GR, Rampersaud N, Dyson MH, Hazzalin CA, Mahadevan LC & Arthur JS (2003), "MSK2 and MSK1 mediate the mitogen- and stress-induced phosphorylation of histone H3 and HMG-14", *EMBO J,* vol. 22 pp. 2788-2797, doi:10.1093/emboj/cdg273

Sommereyns C, Paul S, Staeheli P & Michiels T (2008), "IFN-lambda (IFN-lambda) is expressed in a tissue-dependent fashion and primarily acts on epithelial cells in vivo", *PLoS Pathog,* vol. 4 p. e1000017, doi:10.1371/journal.ppat.1000017

Song F, Yi Y, Li C, Hu Y, Wang J, Smith DE & Jiang H (2018), "Regulation and biological role of the peptide/histidine transporter SLC15A3 in Toll-like receptor-mediated inflammatory responses in macrophage", *Cell Death Dis,* vol. 9 p. 770, doi:10.1038/s41419-018-0809-1

Song JS, Gomez J, Stancato LF & Rivera J (1996), "Association of a p95 Vav-containing signaling complex with the FcepsilonRI gamma chain in the RBL-2H3

mast cell line. Evidence for a constitutive in vivo association of Vav with Grb2, Raf-1, and ERK2 in an active complex", *J Biol Chem,* vol. 271 pp. 26962-26970, doi:10.1074/jbc.271.43.26962

Song N, Qi Q, Cao R, Qin B, Wang B, Wang Y, Zhao L, Li W, Du X, Liu F, Yan Y, Yi W, Jiang H, Li T, Zhou T, Li HY, Xia Q, Zhang XM, Zhong W, Li AL & Duan X (2019), "MAVS O-GlcNAcylation Is Essential for Host Antiviral Immunity against Lethal RNA Viruses", *Cell Rep,* vol. 28 pp. 2386-2396 e2385, doi:10.1016/j.celrep.2019.07.085

Soonthornvacharin S, Rodriguez-Frandsen A, Zhou Y, Galvez F, Huffmaster NJ, Tripathi S, Balasubramaniam VR, Inoue A, de Castro E, Moulton H, Stein DA, Sanchez-Aparicio MT, De Jesus PD, Nguyen Q, Konig R, Krogan NJ, Garcia-Sastre A, Yoh SM & Chanda SK (2017), "Systems-based analysis of RIG-I-dependent signalling identifies KHSRP as an inhibitor of RIG-I receptor activation", *Nat Microbiol,* vol. 2 p. 17022, doi:10.1038/nmicrobiol.2017.22

Soudja SM, Ruiz AL, Marie JC & Lauvau G (2012), "Inflammatory monocytes activate memory CD8(+) T and innate NK lymphocytes independent of cognate antigen during microbial pathogen invasion", *Immunity,* vol. 37 pp. 549-562, doi:10.1016/j.immuni.2012.05.029

Spies N, Burge CB & Bartel DP (2013), "3' UTR-isoform choice has limited influence on the stability and translational efficiency of most mRNAs in mouse fibroblasts", *Genome Res,* vol. 23 pp. 2078-2090, doi:10.1101/gr.156919.113

Stahl PD, Rodman JS, Miller MJ & Schlesinger PH (1978), "Evidence for receptor-mediated binding of glycoproteins, glycoconjugates, and lysosomal glycosidases by alveolar macrophages", *Proc Natl Acad Sci U S A,* vol. 75 pp. 1399-1403, doi:10.1073/pnas.75.3.1399

Stanley SA, Johndrow JE, Manzanillo P & Cox JS (2007), "The Type I IFN response to infection with Mycobacterium tuberculosis requires ESX-1-mediated secretion and contributes to pathogenesis", *J Immunol,* vol. 178 pp. 3143-3152, doi:10.4049/jimmunol.178.5.3143

Stetson DB & Medzhitov R (2006), "Type I interferons in host defense", *Immunity,* vol. 25 pp. 373-381, doi:10.1016/j.immuni.2006.08.007

Stifter SA, Matthews AY, Mangan NE, Fung KY, Drew A, Tate MD, Soares da Costa TP, Hampsey D, Mayall J, Hansbro PM, Garcia Minambres A, Eid SG, Mak J, Scoble J, Lovrecz G, deWeerd NA & Hertzog PJ (2018), "Defining the distinct, intrinsic properties of the novel type I interferon, IFN", *J Biol Chem,* vol. 293 pp. 3168-3179, doi:10.1074/jbc.M117.800755

Stincone A, Prigione A, Cramer T, Wamelink MM, Campbell K, Cheung E, Olin-Sandoval V, Gruning NM, Kruger A, Tauqeer Alam M, Keller MA, Breitenbach M, Brindle KM, Rabinowitz JD & Ralser M (2015), "The return of metabolism:

biochemistry and physiology of the pentose phosphate pathway", *Biol Rev Camb Philos Soc,* vol. 90 pp. 927-963, doi:10.1111/brv.12140

Stopak K, de Noronha C, Yonemoto W & Greene WC (2003), "HIV-1 Vif blocks the antiviral activity of APOBEC3G by impairing both its translation and intracellular stability", *Mol Cell,* vol. 12 pp. 591-601, doi:10.1016/s1097-2765(03)00353-8

Strelko CL, Lu W, Dufort FJ, Seyfried TN, Chiles TC, Rabinowitz JD & Roberts MF (2011), "Itaconic acid is a mammalian metabolite induced during macrophage activation", *J Am Chem Soc,* vol. 133 pp. 16386-16389, doi:10.1021/ja2070889

Stremlau M, Owens CM, Perron MJ, Kiessling M, Autissier P & Sodroski J (2004), "The cytoplasmic body component TRIM5alpha restricts HIV-1 infection in Old World monkeys", *Nature,* vol. 427 pp. 848-853, doi:10.1038/nature02343

Striz I, Brabcova E, Kolesar L & Sekerkova A (2014), "Cytokine networking of innate immunity cells: a potential target of therapy", *Clin Sci (Lond),* vol. 126 pp. 593-612, doi:10.1042/CS20130497

Sullivan KD, Steiniger M & Marzluff WF (2009), "A core complex of CPSF73, CPSF100, and Symplekin may form two different cleavage factors for processing of poly(A) and histone mRNAs", *Mol Cell,* vol. 34 pp. 322-332, doi:10.1016/j.molcel.2009.04.024

Sun L, Wu J, Du F, Chen X & Chen ZJ (2013), "Cyclic GMP-AMP synthase is a cytosolic DNA sensor that activates the type I interferon pathway", *Science,* vol. 339 pp. 786-791, doi:10.1126/science.1232458

Susor A, Jansova D, Cerna R, Danylevska A, Anger M, Toralova T, Malik R, Supolikova J, Cook MS, Oh JS & Kubelka M (2015), "Temporal and spatial regulation of translation in the mammalian oocyte via the mTOR-eIF4F pathway", *Nat Commun,* vol. 6 p. 6078, doi:10.1038/ncomms7078

Swaminathan A, Harrison PF, Preiss T & Beilharz TH (2019), "PAT-Seq: A Method for Simultaneous Quantitation of Gene Expression, Poly(A)-Site Selection and Poly(A)-Length Distribution in Yeast Transcriptomes", *Methods Mol Biol,* vol. 2049 pp. 141-164, doi:10.1007/978-1-4939-9736-7_9

Swiecki M, Omattage NS & Brett TJ (2013), "BST-2/tetherin: structural biology, viral antagonism, and immunobiology of a potent host antiviral factor", *Mol Immunol,* vol. 54 pp. 132-139, doi:10.1016/j.molimm.2012.11.008

Szklarczyk D, Franceschini A, Wyder S, Forslund K, Heller D, Huerta-Cepas J, Simonovic M, Roth A, Santos A, Tsafou KP, Kuhn M, Bork P, Jensen LJ & von Mering C (2015), "STRING v10: protein-protein interaction networks, integrated over the tree of life", *Nucleic Acids Res,* vol. 43 pp. D447-452, doi:10.1093/nar/gku1003

Szklarczyk D, Gable AL, Nastou KC, Lyon D, Kirsch R, Pyysalo S, Doncheva NT, Legeay M, Fang T, Bork P, Jensen LJ & von Mering C (2021), "The STRING database in 2021: customizable protein-protein networks, and functional characterization of user-uploaded gene/measurement sets", *Nucleic Acids Res,* vol. 49 pp. D605-D612, doi:10.1093/nar/gkaa1074

Takagaki Y & Manley JL (1997), "RNA recognition by the human polyadenylation factor CstF", *Mol Cell Biol,* vol. 17 pp. 3907-3914, doi:10.1128/MCB.17.7.3907

—— (2000), "Complex protein interactions within the human polyadenylation machinery identify a novel component", *Mol Cell Biol,* vol. 20 pp. 1515-1525, doi:10.1128/MCB.20.5.1515-1525.2000

Takagaki Y, Manley JL, MacDonald CC, Wilusz J & Shenk T (1990), "A multisubunit factor, CstF, is required for polyadenylation of mammalian pre-mRNAs", *Genes Dev,* vol. 4 pp. 2112-2120, doi:10.1101/gad.4.12a.2112

Takagaki Y, Seipelt RL, Peterson ML & Manley JL (1996), "The polyadenylation factor CstF-64 regulates alternative processing of IgM heavy chain pre-mRNA during B cell differentiation", *Cell,* vol. 87 pp. 941-952, doi:10.1016/s0092-8674(00)82000-0

Takahara T, Amemiya Y, Sugiyama R, Maki M & Shibata H (2020), "Amino acid-dependent control of mTORC1 signaling: a variety of regulatory modes", *J Biomed Sci,* vol. 27 p. 87, doi:10.1186/s12929-020-00679-2

Takayanagi H, Kim S, Koga T, Nishina H, Isshiki M, Yoshida H, Saiura A, Isobe M, Yokochi T, Inoue J, Wagner EF, Mak TW, Kodama T & Taniguchi T (2002), "Induction and activation of the transcription factor NFATc1 (NFAT2) integrate RANKL signaling in terminal differentiation of osteoclasts", *Dev Cell,* vol. 3 pp. 889-901, doi:10.1016/s1534-5807(02)00369-6

Takeda K, Tanaka T, Shi W, Matsumoto M, Minami M, Kashiwamura S, Nakanishi K, Yoshida N, Kishimoto T & Akira S (1996), "Essential role of Stat6 in IL-4 signalling", *Nature,* vol. 380 pp. 627-630, doi:10.1038/380627a0

Takele Y, Abebe T, Weldegebreal T, Hailu A, Hailu W, Hurissa Z, Ali J, Diro E, Sisay Y, Cloke T, Modolell M, Munder M, Tacchini-Cottier F, Muller I & Kropf P (2013), "Arginase activity in the blood of patients with visceral leishmaniasis and HIV infection", *PLoS Negl Trop Dis,* vol. 7 p. e1977, doi:10.1371/journal.pntd.0001977

Takizawa PA & Vale RD (2000), "The myosin motor, Myo4p, binds Ash1 mRNA via the adapter protein, She3p", *Proc Natl Acad Sci U S A,* vol. 97 pp. 5273-5278, doi:10.1073/pnas.080585897

Tang ED & Wang CY (2009), "MAVS self-association mediates antiviral innate immune signaling", *J Virol,* vol. 83 pp. 3420-3428, doi:10.1128/JVI.02623-08

—— (2010), "TRAF5 is a downstream target of MAVS in antiviral innate immune signaling", *PLoS One,* vol. 5 p. e9172, doi:10.1371/journal.pone.0009172

Tang-Huau TL, Gueguen P, Goudot C, Durand M, Bohec M, Baulande S, Pasquier B, Amigorena S & Segura E (2018), "Human in vivo-generated monocyte-derived dendritic cells and macrophages cross-present antigens through a vacuolar pathway", *Nat Commun,* vol. 9 p. 2570, doi:10.1038/s41467-018-04985-0

Tannahill GM, Curtis AM, Adamik J, Palsson-McDermott EM, McGettrick AF, Goel G, Frezza C, Bernard NJ, Kelly B, Foley NH, Zheng L, Gardet A, Tong Z, Jany SS, Corr SC, Haneklaus M, Caffrey BE, Pierce K, Walmsley S, Beasley FC, Cummins E, Nizet V, Whyte M, Taylor CT, Lin H, Masters SL, Gottlieb E, Kelly VP, Clish C, Auron PE, Xavier RJ & O'Neill LA (2013), "Succinate is an inflammatory signal that induces IL-1beta through HIF-1alpha", *Nature,* vol. 496 pp. 238-242, doi:10.1038/nature11986

Taylor PR, Martinez-Pomares L, Stacey M, Lin HH, Brown GD & Gordon S (2005), "Macrophage receptors and immune recognition", *Annu Rev Immunol,* vol. 23 pp. 901-944, doi:10.1146/annurev.immunol.23.021704.115816

ten Klooster JP, Leeuwen I, Scheres N, Anthony EC & Hordijk PL (2007), "Rac1-induced cell migration requires membrane recruitment of the nuclear oncogene SET", *EMBO J,* vol. 26 pp. 336-345, doi:10.1038/sj.emboj.7601518

Thoreen CC, Chantranupong L, Keys HR, Wang T, Gray NS & Sabatini DM (2012), "A unifying model for mTORC1-mediated regulation of mRNA translation", *Nature,* vol. 485 pp. 109-113, doi:10.1038/nature11083

Thornley TB, Fang Z, Balasubramanian S, Larocca RA, Gong W, Gupta S, Csizmadia E, Degauque N, Kim BS, Koulmanda M, Kuchroo VK & Strom TB (2014), "Fragile TIM-4-expressing tissue resident macrophages are migratory and immunoregulatory", *J Clin Invest,* vol. 124 pp. 3443-3454, doi:10.1172/JCI73527

Tian B, Hu J, Zhang H & Lutz CS (2005), "A large-scale analysis of mRNA polyadenylation of human and mouse genes", *Nucleic Acids Res,* vol. 33 pp. 201-212, doi:10.1093/nar/gki158

Tissot C & Mechti N (1995), "Molecular cloning of a new interferon-induced factor that represses human immunodeficiency virus type 1 long terminal repeat expression", *J Biol Chem,* vol. 270 pp. 14891-14898, doi:10.1074/jbc.270.25.14891

Travis MA & Sheppard D (2014), "TGF-beta activation and function in immunity", *Annu Rev Immunol,* vol. 32 pp. 51-82, doi:10.1146/annurev-immunol-032713-120257

Trifilo MJ, Montalto-Morrison C, Stiles LN, Hurst KR, Hardison JL, Manning JE, Masters PS & Lane TE (2004), "CXC chemokine ligand 10 controls viral infection in the central nervous system: evidence for a role in innate immune response through recruitment and activation of natural killer cells", *J Virol,* vol. 78 pp. 585-594, doi:10.1128/jvi.78.2.585-594.2004

Tseng PH, Matsuzawa A, Zhang W, Mino T, Vignali DA & Karin M (2010), "Different modes of ubiquitination of the adaptor TRAF3 selectively activate the expression of type I interferons and proinflammatory cytokines", *Nat Immunol,* vol. 11 pp. 70-75, doi:10.1038/ni.1819

Tsukiyama-Kohara K, Vidal SM, Gingras AC, Glover TW, Hanash SM, Heng H & Sonenberg N (1996), "Tissue distribution, genomic structure, and chromosome mapping of mouse and human eukaryotic initiation factor 4E-binding proteins 1 and 2", *Genomics,* vol. 38 pp. 353-363, doi:10.1006/geno.1996.0638

Tsuno T, Mejido J, Zhao T, Schmeisser H, Morrow A & Zoon KC (2009), "IRF9 is a key factor for eliciting the antiproliferative activity of IFN-alpha", *J Immunother,* vol. 32 pp. 803-816, doi:10.1097/CJI.0b013e3181ad4092

Turner RE, Henneken LM, Liem-Weits M, Harrison PF, Swaminathan A, Vary R, Nikolic I, Simpson KJ, Powell DR, Beilharz TH & Dichtl B (2020), "Requirement for cleavage factor IIm in the control of alternative polyadenylation in breast cancer cells", *RNA,* vol. 26 pp. 969-981, doi:10.1261/rna.075226.120

Uddin S, Lekmine F, Sharma N, Majchrzak B, Mayer I, Young PR, Bokoch GM, Fish EN & Platanias LC (2000), "The Rac1/p38 mitogen-activated protein kinase pathway is required for interferon alpha-dependent transcriptional activation but not serine phosphorylation of Stat proteins", *J Biol Chem,* vol. 275 pp. 27634-27640, doi:10.1074/jbc.M003170200

Uddin S, Majchrzak B, Woodson J, Arunkumar P, Alsayed Y, Pine R, Young PR, Fish EN & Platanias LC (1999), "Activation of the p38 mitogen-activated protein kinase by type I interferons", *J Biol Chem,* vol. 274 pp. 30127-30131, doi:10.1074/jbc.274.42.30127

Uddin S, Sweet M, Colamonici OR, Krolewski JJ & Platanias LC (1997), "The vav proto-oncogene product (p95vav) interacts with the Tyk-2 protein tyrosine kinase", *FEBS Lett,* vol. 403 pp. 31-34, doi:10.1016/s0014-5793(97)00023-9

Uddin S, Yenush L, Sun XJ, Sweet ME, White MF & Platanias LC (1995), "Interferon-alpha engages the insulin receptor substrate-1 to associate with the phosphatidylinositol 3'-kinase", *J Biol Chem,* vol. 270 pp. 15938-15941, doi:10.1074/jbc.270.27.15938

Ulitsky I, Shkumatava A, Jan CH, Subtelny AO, Koppstein D, Bell GW, Sive H & Bartel DP (2012), "Extensive alternative polyadenylation during zebrafish development", *Genome Res,* vol. 22 pp. 2054-2066, doi:10.1101/gr.139733.112

Uribe-Querol E & Rosales C (2020), "Phagocytosis: Our Current Understanding of a Universal Biological Process", *Front Immunol,* vol. 11 p. 1066, doi:10.3389/fimmu.2020.01066

van de Laar L, Saelens W, De Prijck S, Martens L, Scott CL, Van Isterdael G, Hoffmann E, Beyaert R, Saeys Y, Lambrecht BN & Guilliams M (2016), "Yolk Sac Macrophages, Fetal Liver, and Adult Monocytes Can Colonize an Empty Niche and Develop into Functional Tissue-Resident Macrophages", *Immunity,* vol. 44 pp. 755-768, doi:10.1016/j.immuni.2016.02.017

Van den Bossche J, Baardman J, Otto NA, van der Velden S, Neele AE, van den Berg SM, Luque-Martin R, Chen HJ, Boshuizen MC, Ahmed M, Hoeksema MA, de Vos AF & de Winther MP (2016), "Mitochondrial Dysfunction Prevents Repolarization of Inflammatory Macrophages", *Cell Rep,* vol. 17 pp. 684-696, doi:10.1016/j.celrep.2016.09.008

van der Windt GJ, O'Sullivan D, Everts B, Huang SC, Buck MD, Curtis JD, Chang CH, Smith AM, Ai T, Faubert B, Jones RG, Pearce EJ & Pearce EL (2013), "CD8 memory T cells have a bioenergetic advantage that underlies their rapid recall ability", *Proc Natl Acad Sci U S A,* vol. 110 pp. 14336-14341, doi:10.1073/pnas.1221740110

van Liempt E, Bank CM, Mehta P, Garcia-Vallejo JJ, Kawar ZS, Geyer R, Alvarez RA, Cummings RD, Kooyk Y & van Die I (2006), "Specificity of DC-SIGN for mannose- and fucose-containing glycans", *FEBS Lett,* vol. 580 pp. 6123-6131, doi:10.1016/j.febslet.2006.10.009

Vander Heiden MG, Cantley LC & Thompson CB (2009), "Understanding the Warburg effect: the metabolic requirements of cell proliferation", *Science,* vol. 324 pp. 1029-1033, doi:10.1126/science.1160809

Varinou L, Ramsauer K, Karaghiosoff M, Kolbe T, Pfeffer K, Muller M & Decker T (2003), "Phosphorylation of the Stat1 transactivation domain is required for full-fledged IFN-gamma-dependent innate immunity", *Immunity,* vol. 19 pp. 793-802, doi:10.1016/s1074-7613(03)00322-4

Varol C, Mildner A & Jung S (2015), "Macrophages: development and tissue specialization", *Annu Rev Immunol,* vol. 33 pp. 643-675, doi:10.1146/annurev-immunol-032414-112220

Vats D, Mukundan L, Odegaard JI, Zhang L, Smith KL, Morel CR, Wagner RA, Greaves DR, Murray PJ & Chawla A (2006), "Oxidative metabolism and PGC-

1beta attenuate macrophage-mediated inflammation", *Cell Metab,* vol. 4 pp. 13-24, doi:10.1016/j.cmet.2006.05.011

Velazquez L, Fellous M, Stark GR & Pellegrini S (1992), "A protein tyrosine kinase in the interferon alpha/beta signaling pathway", *Cell,* vol. 70 pp. 313-322, doi:10.1016/0092-8674(92)90105-l

Venkataraman K, Brown KM & Gilmartin GM (2005), "Analysis of a noncanonical poly(A) site reveals a tripartite mechanism for vertebrate poly(A) site recognition", *Genes Dev,* vol. 19 pp. 1315-1327, doi:10.1101/gad.1298605

Veraldi KL, Arhin GK, Martincic K, Chung-Ganster LH, Wilusz J & Milcarek C (2001), "hnRNP F influences binding of a 64-kilodalton subunit of cleavage stimulation factor to mRNA precursors in mouse B cells", *Mol Cell Biol,* vol. 21 pp. 1228-1238, doi:10.1128/MCB.21.4.1228-1238.2001

Villarroya-Beltri C, Baixauli F, Mittelbrunn M, Fernandez-Delgado I, Torralba D, Moreno-Gonzalo O, Baldanta S, Enrich C, Guerra S & Sanchez-Madrid F (2016), "ISGylation controls exosome secretion by promoting lysosomal degradation of MVB proteins", *Nat Commun,* vol. 7 p. 13588, doi:10.1038/ncomms13588

Viola A, Munari F, Sanchez-Rodriguez R, Scolaro T & Castegna A (2019), "The Metabolic Signature of Macrophage Responses", *Front Immunol,* vol. 10 p. 1462, doi:10.3389/fimmu.2019.01462

Volkman HE, Cambier S, Gray EE & Stetson DB (2019), "Tight nuclear tethering of cGAS is essential for preventing autoreactivity", *Elife,* vol. 8 doi:10.7554/eLife.47491

Wahle E (1995), "Poly(A) tail length control is caused by termination of processive synthesis", *J Biol Chem,* vol. 270 pp. 2800-2808, doi:10.1074/jbc.270.6.2800

Wahle E & Kuhn U (1997), "The mechanism of 3' cleavage and polyadenylation of eukaryotic pre-mRNA", *Prog Nucleic Acid Res Mol Biol,* vol. 57 pp. 41-71, doi:10.1016/s0079-6603(08)60277-9

Wakefield JK, Wolf AG & Morrow CD (1995), "Human immunodeficiency virus type 1 can use different tRNAs as primers for reverse transcription but selectively maintains a primer binding site complementary to tRNA(3Lys)", *J Virol,* vol. 69 pp. 6021-6029, doi:10.1128/JVI.69.10.6021-6029.1995

Wallace C & Keast D (1992), "Glutamine and macrophage function", *Metabolism,* vol. 41 pp. 1016-1020, doi:10.1016/0026-0495(92)90130-3

Walsh MC, Lee J & Choi Y (2015), "Tumor necrosis factor receptor- associated factor 6 (TRAF6) regulation of development, function, and homeostasis of the immune system", *Immunol Rev,* vol. 266 pp. 72-92, doi:10.1111/imr.12302

Wang BX & Fish EN (2019), "Global virus outbreaks: Interferons as 1st responders", *Semin Immunol,* vol. 43 p. 101300, doi:10.1016/j.smim.2019.101300

Wang C, Deng L, Hong M, Akkaraju GR, Inoue J & Chen ZJ (2001), "TAK1 is a ubiquitin-dependent kinase of MKK and IKK", *Nature,* vol. 412 pp. 346-351, doi:10.1038/35085597

Wang F, Zhang S, Vuckovic I, Jeon R, Lerman A, Folmes CD, Dzeja PP & Herrmann J (2018), "Glycolytic Stimulation Is Not a Requirement for M2 Macrophage Differentiation", *Cell Metab,* vol. 28 pp. 463-475 e464, doi:10.1016/j.cmet.2018.08.012

Wang H, Horbinski C, Wu H, Liu Y, Sheng S, Liu J, Weiss H, Stromberg AJ & Wang C (2016), "NanoStringDiff: a novel statistical method for differential expression analysis based on NanoString nCounter data", *Nucleic Acids Res,* vol. 44 p. e151, doi:10.1093/nar/gkw677

Wang J, Li H, Xue B, Deng R, Huang X, Xu Y, Chen S, Tian R, Wang X, Xun Z, Sang M & Zhu H (2020), "IRF1 Promotes the Innate Immune Response to Viral Infection by Enhancing the Activation of IRF3", *J Virol,* vol. 94 doi:10.1128/JVI.01231-20

Wang P, Hou J, Lin L, Wang C, Liu X, Li D, Ma F, Wang Z & Cao X (2010), "Inducible microRNA-155 feedback promotes type I IFN signaling in antiviral innate immunity by targeting suppressor of cytokine signaling 1", *J Immunol,* vol. 185 pp. 6226-6233, doi:10.4049/jimmunol.1000491

Wang P, Yang L, Cheng G, Yang G, Xu Z, You F, Sun Q, Lin R, Fikrig E & Sutton RE (2013), "UBXN1 interferes with Rig-I-like receptor-mediated antiviral immune response by targeting MAVS", *Cell Rep,* vol. 3 pp. 1057-1070, doi:10.1016/j.celrep.2013.02.027

Wang Q, Zhang X, Han Y, Wang X & Gao G (2016), "M2BP inhibits HIV-1 virion production in a vimentin filaments-dependent manner", *Sci Rep,* vol. 6 p. 32736, doi:10.1038/srep32736

Wang R, Dillon CP, Shi LZ, Milasta S, Carter R, Finkelstein D, McCormick LL, Fitzgerald P, Chi H, Munger J & Green DR (2011), "The transcription factor Myc controls metabolic reprogramming upon T lymphocyte activation", *Immunity,* vol. 35 pp. 871-882, doi:10.1016/j.immuni.2011.09.021

Wang R, Nambiar R, Zheng D & Tian B (2018), "PolyA_DB 3 catalogs cleavage and polyadenylation sites identified by deep sequencing in multiple genomes", *Nucleic Acids Res,* vol. 46 pp. D315-D319, doi:10.1093/nar/gkx1000

Wang R, Zheng D, Wei L, Ding Q & Tian B (2019), "Regulation of Intronic Polyadenylation by PCF11 Impacts mRNA Expression of Long Genes", *Cell Rep,* vol. 26 pp. 2766-2778 e2766, doi:10.1016/j.celrep.2019.02.049

Wang T, Liu H, Lian G, Zhang SY, Wang X & Jiang C (2017), "HIF1alpha-Induced Glycolysis Metabolism Is Essential to the Activation of Inflammatory Macrophages", *Mediators Inflamm,* vol. 2017 p. 9029327, doi:10.1155/2017/9029327

Wang X, Destrument A & Tournier C (2007a), "Physiological roles of MKK4 and MKK7: insights from animal models", *Biochim Biophys Acta,* vol. 1773 pp. 1349-1357, doi:10.1016/j.bbamcr.2006.10.016

Wang X, Hinson ER & Cresswell P (2007b), "The interferon-inducible protein viperin inhibits influenza virus release by perturbing lipid rafts", *Cell Host Microbe,* vol. 2 pp. 96-105, doi:10.1016/j.chom.2007.06.009

Wang X, Yue P, Chan CB, Ye K, Ueda T, Watanabe-Fukunaga R, Fukunaga R, Fu H, Khuri FR & Sun SY (2007c), "Inhibition of mammalian target of rapamycin induces phosphatidylinositol 3-kinase-dependent and Mnk-mediated eukaryotic translation initiation factor 4E phosphorylation", *Mol Cell Biol,* vol. 27 pp. 7405-7413, doi:10.1128/MCB.00760-07

Waskiewicz AJ, Flynn A, Proud CG & Cooper JA (1997), "Mitogen-activated protein kinases activate the serine/threonine kinases Mnk1 and Mnk2", *EMBO J,* vol. 16 pp. 1909-1920, doi:10.1093/emboj/16.8.1909

Watanabe T, Asano N, Fichtner-Feigl S, Gorelick PL, Tsuji Y, Matsumoto Y, Chiba T, Fuss IJ, Kitani A & Strober W (2010), "NOD1 contributes to mouse host defense against Helicobacter pylori via induction of type I IFN and activation of the ISGF3 signaling pathway", *J Clin Invest,* vol. 120 pp. 1645-1662, doi:10.1172/JCI39481

Watanabe Y (2004), "Fifty years of interference", *Nat Immunol,* vol. 5 p. 1193, doi:10.1038/ni1204-1193

Wei J, Long L, Yang K, Guy C, Shrestha S, Chen Z, Wu C, Vogel P, Neale G, Green DR & Chi H (2016), "Autophagy enforces functional integrity of regulatory T cells by coupling environmental cues and metabolic homeostasis", *Nat Immunol,* vol. 17 pp. 277-285, doi:10.1038/ni.3365

Weiss M, Schrimpf S, Hengartner MO, Lercher MJ & von Mering C (2010), "Shotgun proteomics data from multiple organisms reveals remarkable quantitative conservation of the eukaryotic core proteome", *Proteomics,* vol. 10 pp. 1297-1306, doi:10.1002/pmic.200900414

Weng T, Huang J, Wagner EJ, Ko J, Wu M, Wareing NE, Xiang Y, Chen NY, Ji P, Molina JG, Volcik KA, Han L, Mayes MD, Blackburn MR & Assassi S (2020),

"Downregulation of CFIm25 amplifies dermal fibrosis through alternative polyadenylation", *J Exp Med,* vol. 217 doi:10.1084/jem.20181384

West S & Proudfoot NJ (2008), "Human Pcf11 enhances degradation of RNA polymerase II-associated nascent RNA and transcriptional termination", *Nucleic Acids Res,* vol. 36 pp. 905-914, doi:10.1093/nar/gkm1112

Whitmarsh AJ & Davis RJ (1996), "Transcription factor AP-1 regulation by mitogen-activated protein kinase signal transduction pathways", *J Mol Med (Berl),* vol. 74 pp. 589-607, doi:10.1007/s001090050063

Wiegand HL, Doehle BP, Bogerd HP & Cullen BR (2004), "A second human antiretroviral factor, APOBEC3F, is suppressed by the HIV-1 and HIV-2 Vif proteins", *EMBO J,* vol. 23 pp. 2451-2458, doi:10.1038/sj.emboj.7600246

Wilks AF, Harpur AG, Kurban RR, Ralph SJ, Zurcher G & Ziemiecki A (1991), "Two novel protein-tyrosine kinases, each with a second phosphotransferase-related catalytic domain, define a new class of protein kinase", *Mol Cell Biol,* vol. 11 pp. 2057-2065, doi:10.1128/mcb.11.4.2057-2065.1991

Wilusz J, Shenk T, Takagaki Y & Manley JL (1990), "A multicomponent complex is required for the AAUAAA-dependent cross-linking of a 64-kilodalton protein to polyadenylation substrates", *Mol Cell Biol,* vol. 10 pp. 1244-1248, doi:10.1128/mcb.10.3.1244-1248.1990

Wong P, Althammer S, Hildebrand A, Kirschner A, Pagel P, Geissler B, Smialowski P, Blochl F, Oesterheld M, Schmidt T, Strack N, Theis FJ, Ruepp A & Frishman D (2008), "An evolutionary and structural characterization of mammalian protein complex organization", *BMC Genomics,* vol. 9 p. 629, doi:10.1186/1471-2164-9-629

Wood KH, Johnson BS, Welsh SA, Lee JY, Cui Y, Krizman E, Brodkin ES, Blendy JA, Robinson MB, Bartolomei MS & Zhou Z (2016), "Tagging methyl-CpG-binding domain proteins reveals different spatiotemporal expression and supports distinct functions", *Epigenomics,* vol. 8 pp. 455-473, doi:10.2217/epi-2015-0004

Wu B, Peisley A, Richards C, Yao H, Zeng X, Lin C, Chu F, Walz T & Hur S (2013), "Structural basis for dsRNA recognition, filament formation, and antiviral signal activation by MDA5", *Cell,* vol. 152 pp. 276-289, doi:10.1016/j.cell.2012.11.048

Wu D, Sanin DE, Everts B, Chen Q, Qiu J, Buck MD, Patterson A, Smith AM, Chang CH, Liu Z, Artyomov MN, Pearce EL, Cella M & Pearce EJ (2016), "Type 1 Interferons Induce Changes in Core Metabolism that Are Critical for Immune Function", *Immunity,* vol. 44 pp. 1325-1336, doi:10.1016/j.immuni.2016.06.006

Wu H, Zhou J, Zhu T, Cohen I & Dictenberg J (2020), "A kinesin adapter directly mediates dendritic mRNA localization during neural development in mice", *J Biol Chem,* vol. 295 pp. 6605-6628, doi:10.1074/jbc.RA118.005616

Wu Q, Chen X, Li J & Sun S (2020), "Serine and Metabolism Regulation: A Novel Mechanism in Antitumor Immunity and Senescence", *Aging Dis,* vol. 11 pp. 1640-1653, doi:10.14336/AD.2020.0314

Wu X & Bartel DP (2017), "Widespread Influence of 3'-End Structures on Mammalian mRNA Processing and Stability", *Cell,* vol. 169 pp. 905-917 e911, doi:10.1016/j.cell.2017.04.036

Wuest TR & Carr DJ (2008), "Dysregulation of CXCR3 signaling due to CXCL10 deficiency impairs the antiviral response to herpes simplex virus 1 infection", *J Immunol,* vol. 181 pp. 7985-7993, doi:10.4049/jimmunol.181.11.7985

Wyatt MD, Allan JM, Lau AY, Ellenberger TE & Samson LD (1999), "3-methyladenine DNA glycosylases: structure, function, and biological importance", *Bioessays,* vol. 21 pp. 668-676, doi:10.1002/(SICI)1521-1878(199908)21:8<668::AID-BIES6>3.0.CO;2-D

Xiang K, Tong L & Manley JL (2014), "Delineating the structural blueprint of the pre-mRNA 3'-end processing machinery", *Mol Cell Biol,* vol. 34 pp. 1894-1910, doi:10.1128/MCB.00084-14

Xing D, Zhao H & Li QQ (2008), "Arabidopsis CLP1-SIMILAR PROTEIN3, an ortholog of human polyadenylation factor CLP1, functions in gametophyte, embryo, and postembryonic development", *Plant Physiol,* vol. 148 pp. 2059-2069, doi:10.1104/pp.108.129817

Xing J, Zhang A, Minze LJ, Li XC & Zhang Z (2018), "TRIM29 Negatively Regulates the Type I IFN Production in Response to RNA Virus", *J Immunol,* vol. 201 pp. 183-192, doi:10.4049/jimmunol.1701569

Xu C & Zhang J (2018), "Alternative Polyadenylation of Mammalian Transcripts Is Generally Deleterious, Not Adaptive", *Cell Syst,* vol. 6 pp. 734-742 e734, doi:10.1016/j.cels.2018.05.007

Xu D, Han Q, Hou Z, Zhang C & Zhang J (2017), "miR-146a negatively regulates NK cell functions via STAT1 signaling", *Cell Mol Immunol,* vol. 14 pp. 712-720, doi:10.1038/cmi.2015.113

Xu L, Peng L, Gu T, Yu D & Yao YG (2019), "The 3'UTR of human MAVS mRNA contains multiple regulatory elements for the control of protein expression and subcellular localization", *Biochim Biophys Acta Gene Regul Mech,* vol. 1862 pp. 47-57, doi:10.1016/j.bbagrm.2018.10.017

Xu L, Wang W, Li Y, Zhou X, Yin Y, Wang Y, de Man RA, van der Laan LJW, Huang F, Kamar N, Peppelenbosch MP & Pan Q (2017), "RIG-I is a key antiviral interferon-stimulated gene against hepatitis E virus regardless of interferon production", *Hepatology,* vol. 65 pp. 1823-1839, doi:10.1002/hep.29105

Xue B, Li H, Guo M, Wang J, Xu Y, Zou X, Deng R, Li G & Zhu H (2018), "TRIM21 Promotes Innate Immune Response to RNA Viral Infection through Lys27-Linked Polyubiquitination of MAVS", *J Virol,* vol. 92 doi:10.1128/JVI.00321-18

Xue J, Schmidt SV, Sander J, Draffehn A, Krebs W, Quester I, De Nardo D, Gohel TD, Emde M, Schmidleithner L, Ganesan H, Nino-Castro A, Mallmann MR, Labzin L, Theis H, Kraut M, Beyer M, Latz E, Freeman TC, Ulas T & Schultze JL (2014), "Transcriptome-based network analysis reveals a spectrum model of human macrophage activation", *Immunity,* vol. 40 pp. 274-288, doi:10.1016/j.immuni.2014.01.006

Yalcin A, Telang S, Clem B & Chesney J (2009), "Regulation of glucose metabolism by 6-phosphofructo-2-kinase/fructose-2,6-bisphosphatases in cancer", *Exp Mol Pathol,* vol. 86 pp. 174-179, doi:10.1016/j.yexmp.2009.01.003

Yan C, Wei H, Minjuan Z, Yan X, Jingyue Y, Wenchao L & Sheng H (2014), "The mTOR inhibitor rapamycin synergizes with a fatty acid synthase inhibitor to induce cytotoxicity in ER/HER2-positive breast cancer cells", *PLoS One,* vol. 9 p. e97697, doi:10.1371/journal.pone.0097697

Yan W, Guo H, Suo F, Han C, Zheng H & Chen T (2017), "The effect of miR-146a on STAT1 expression and apoptosis in acute lymphoblastic leukemia Jurkat cells", *Oncol Lett,* vol. 13 pp. 151-154, doi:10.3892/ol.2016.5395

Yang Q, Coseno M, Gilmartin GM & Doublie S (2011), "Crystal structure of a human cleavage factor CFI(m)25/CFI(m)68/RNA complex provides an insight into poly(A) site recognition and RNA looping", *Structure,* vol. 19 pp. 368-377, doi:10.1016/j.str.2010.12.021

Yang Q, Gilmartin GM & Doublie S (2010), "Structural basis of UGUA recognition by the Nudix protein CFI(m)25 and implications for a regulatory role in mRNA 3' processing", *Proc Natl Acad Sci U S A,* vol. 107 pp. 10062-10067, doi:10.1073/pnas.1000848107

Yang S, Deng P, Zhu Z, Zhu J, Wang G, Zhang L, Chen AF, Wang T, Sarkar SN, Billiar TR & Wang Q (2014), "Adenosine deaminase acting on RNA 1 limits RIG-I RNA detection and suppresses IFN production responding to viral and endogenous RNAs", *J Immunol,* vol. 193 pp. 3436-3445, doi:10.4049/jimmunol.1401136

Yao C, Biesinger J, Wan J, Weng L, Xing Y, Xie X & Shi Y (2012), "Transcriptome-wide analyses of CstF64-RNA interactions in global regulation of

mRNA alternative polyadenylation", *Proc Natl Acad Sci U S A,* vol. 109 pp. 18773-18778, doi:10.1073/pnas.1211101109

Yao C, Choi EA, Weng L, Xie X, Wan J, Xing Y, Moresco JJ, Tu PG, Yates JR, 3rd & Shi Y (2013), "Overlapping and distinct functions of CstF64 and CstF64tau in mammalian mRNA 3' processing", *RNA,* vol. 19 pp. 1781-1790, doi:10.1261/rna.042317.113

Yao R, Ma YL, Liang W, Li HH, Ma ZJ, Yu X & Liao YH (2012), "MicroRNA-155 modulates Treg and Th17 cells differentiation and Th17 cell function by targeting SOCS1", *PLoS One,* vol. 7 p. e46082, doi:10.1371/journal.pone.0046082

Yona S, Kim KW, Wolf Y, Mildner A, Varol D, Breker M, Strauss-Ayali D, Viukov S, Guilliams M, Misharin A, Hume DA, Perlman H, Malissen B, Zelzer E & Jung S (2013), "Fate mapping reveals origins and dynamics of monocytes and tissue macrophages under homeostasis", *Immunity,* vol. 38 pp. 79-91, doi:10.1016/j.immuni.2012.12.001

Yoneyama M, Kikuchi M, Natsukawa T, Shinobu N, Imaizumi T, Miyagishi M, Taira K, Akira S & Fujita T (2004), "The RNA helicase RIG-I has an essential function in double-stranded RNA-induced innate antiviral responses", *Nat Immunol,* vol. 5 pp. 730-737, doi:10.1038/ni1087

Yoo YS, Park YY, Kim JH, Cho H, Kim SH, Lee HS, Kim TH, Sun Kim Y, Lee Y, Kim CJ, Jung JU, Lee JS & Cho H (2015), "The mitochondrial ubiquitin ligase MARCH5 resolves MAVS aggregates during antiviral signalling", *Nat Commun,* vol. 6 p. 7910, doi:10.1038/ncomms8910

Yoshida R, Takaesu G, Yoshida H, Okamoto F, Yoshioka T, Choi Y, Akira S, Kawai T, Yoshimura A & Kobayashi T (2008), "TRAF6 and MEKK1 play a pivotal role in the RIG-I-like helicase antiviral pathway", *J Biol Chem,* vol. 283 pp. 36211-36220, doi:10.1074/jbc.M806576200

You F, Sun H, Zhou X, Sun W, Liang S, Zhai Z & Jiang Z (2009), "PCBP2 mediates degradation of the adaptor MAVS via the HECT ubiquitin ligase AIP4", *Nat Immunol,* vol. 10 pp. 1300-1308, doi:10.1038/ni.1815

Yu W, Wang Z, Zhang K, Chi Z, Xu T, Jiang D, Chen S, Li W, Yang X, Zhang X, Wu Y & Wang D (2019), "One-Carbon Metabolism Supports S-Adenosylmethionine and Histone Methylation to Drive Inflammatory Macrophages", *Mol Cell,* vol. 75 pp. 1147-1160 e1145, doi:10.1016/j.molcel.2019.06.039

Zaessinger S, Busseau I & Simonelig M (2006), "Oskar allows nanos mRNA translation in Drosophila embryos by preventing its deadenylation by Smaug/CCR4", *Development,* vol. 133 pp. 4573-4583, doi:10.1242/dev.02649

Zhang C, Shang G, Gui X, Zhang X, Bai XC & Chen ZJ (2019), "Structural basis of STING binding with and phosphorylation by TBK1", *Nature,* vol. 567 pp. 394-398, doi:10.1038/s41586-019-1000-2

Zhang P & Samuel CE (2008), "Induction of protein kinase PKR-dependent activation of interferon regulatory factor 3 by vaccinia virus occurs through adapter IPS-1 signaling", *J Biol Chem,* vol. 283 pp. 34580-34587, doi:10.1074/jbc.M807029200

Zhang Q, Bastard P, Liu Z, Le Pen J, Moncada-Velez M, Chen J, Ogishi M, Sabli IKD, Hodeib S, Korol C, Rosain J, Bilguvar K, Ye J, Bolze A, Bigio B, Yang R, Arias AA, Zhou Q, Zhang Y, Onodi F, Korniotis S, Karpf L, Philippot Q, Chbihi M, Bonnet-Madin L, Dorgham K, Smith N, Schneider WM, Razooky BS, Hoffmann HH, Michailidis E, Moens L, Han JE, Lorenzo L, Bizien L, Meade P, Neehus AL, Ugurbil AC, Corneau A, Kerner G, Zhang P, Rapaport F, Seeleuthner Y, Manry J, Masson C, Schmitt Y, Schluter A, Le Voyer T, Khan T, Li J, Fellay J, Roussel L, Shahrooei M, Alosaimi MF, Mansouri D, Al-Saud H, Al-Mulla F, Almourfi F, Al-Muhsen SZ, Alsohime F, Al Turki S, Hasanato R, van de Beek D, Biondi A, Bettini LR, D'Angio M, Bonfanti P, Imberti L, Sottini A, Paghera S, Quiros-Roldan E, Rossi C, Oler AJ, Tompkins MF, Alba C, Vandernoot I, Goffard JC, Smits G, Migeotte I, Haerynck F, Soler-Palacin P, Martin-Nalda A, Colobran R, Morange PE, Keles S, Colkesen F, Ozcelik T, Yasar KK, Senoglu S, Karabela SN, Rodriguez-Gallego C, Novelli G, Hraiech S, Tandjaoui-Lambiotte Y, Duval X, Laouenan C, Clinicians C-S, Clinicians C, Imagine CG, French CCSG, Co VCC, Amsterdam UMCC-B, Effort CHG, Group N-UTCI, Snow AL, Dalgard CL, Milner JD, Vinh DC, Mogensen TH, Marr N, Spaan AN, Boisson B, Boisson-Dupuis S, Bustamante J, Puel A, Ciancanelli MJ, Meyts I, Maniatis T, Soumelis V, Amara A, Nussenzweig M, Garcia-Sastre A, Krammer F, Pujol A, Duffy D, Lifton RP, Zhang SY, Gorochov G, Beziat V, Jouanguy E, Sancho-Shimizu V, Rice CM, Abel L, Notarangelo LD, Cobat A, Su HC & Casanova JL (2020), "Inborn errors of type I IFN immunity in patients with life-threatening COVID-19", *Science,* vol. 370 doi:10.1126/science.abd4570

Zhang S, Zhang X, Lei W, Liang J, Xu Y, Liu H & Ma S (2019), "Genome-wide profiling reveals alternative polyadenylation of mRNA in human non-small cell lung cancer", *J Transl Med,* vol. 17 p. 257, doi:10.1186/s12967-019-1986-0

Zhao H, Lin W, Kumthip K, Cheng D, Fusco DN, Hofmann O, Jilg N, Tai AW, Goto K, Zhang L, Hide W, Jang JY, Peng LF & Chung RT (2012), "A functional genomic screen reveals novel host genes that mediate interferon-alpha's effects against hepatitis C virus", *J Hepatol,* vol. 56 pp. 326-333, doi:10.1016/j.jhep.2011.07.026

Zhao J, Hyman L & Moore C (1999), "Formation of mRNA 3' ends in eukaryotes: mechanism, regulation, and interrelationships with other steps in mRNA synthesis", *Microbiol Mol Biol Rev,* vol. 63 pp. 405-445, doi:10.1128/MMBR.63.2.405-445.1999

Zhao Y, Sun X, Nie X, Sun L, Tang TS, Chen D & Sun Q (2012), "COX5B regulates MAVS-mediated antiviral signaling through interaction with ATG5 and repressing ROS production", *PLoS Pathog,* vol. 8 p. e1003086, doi:10.1371/journal.ppat.1003086

Zheng YH, Irwin D, Kurosu T, Tokunaga K, Sata T & Peterlin BM (2004), "Human APOBEC3F is another host factor that blocks human immunodeficiency virus type 1 replication", *J Virol,* vol. 78 pp. 6073-6076, doi:10.1128/JVI.78.11.6073-6076.2004

Zhong B, Zhang Y, Tan B, Liu TT, Wang YY & Shu HB (2010), "The E3 ubiquitin ligase RNF5 targets virus-induced signaling adaptor for ubiquitination and degradation", *J Immunol,* vol. 184 pp. 6249-6255, doi:10.4049/jimmunol.0903748

Zhou Z, Hamming OJ, Ank N, Paludan SR, Nielsen AL & Hartmann R (2007), "Type III interferon (IFN) induces a type I IFN-like response in a restricted subset of cells through signaling pathways involving both the Jak-STAT pathway and the mitogen-activated protein kinases", *J Virol,* vol. 81 pp. 7749-7758, doi:10.1128/JVI.02438-06

Zhu Y, Wang X, Forouzmand E, Jeong J, Qiao F, Sowd GA, Engelman AN, Xie X, Hertel KJ & Shi Y (2018), "Molecular Mechanisms for CFIm-Mediated Regulation of mRNA Alternative Polyadenylation", *Mol Cell,* vol. 69 pp. 62-74 e64, doi:10.1016/j.molcel.2017.11.031

Zmuda EJ, Viapiano M, Grey ST, Hadley G, Garcia-Ocana A & Hai T (2010), "Deficiency of Atf3, an adaptive-response gene, protects islets and ameliorates inflammation in a syngeneic mouse transplantation model", *Diabetologia,* vol. 53 pp. 1438-1450, doi:10.1007/s00125-010-1696-x

Curriculum Vitae

Appendix

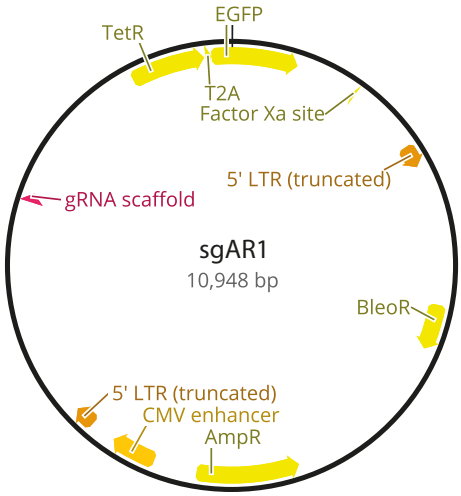

Appendix Figure 1: sgAR1 plasmid map. Plasmid used to knockout IFNAR1.

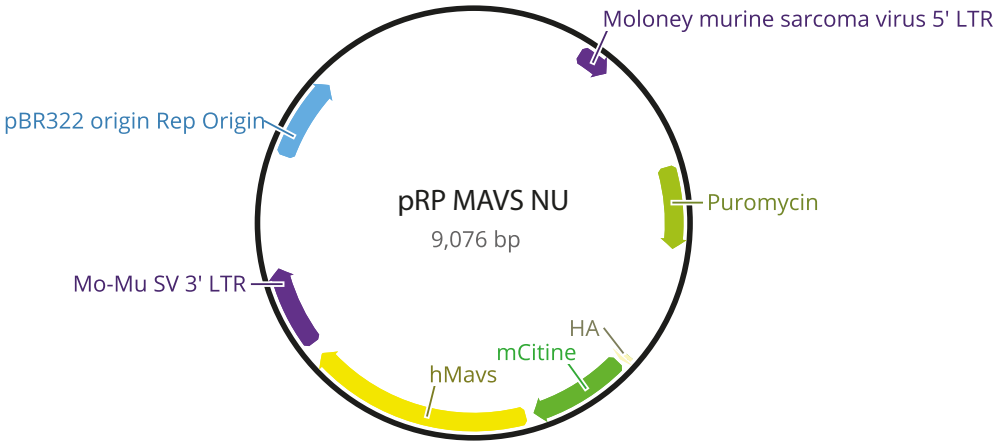

Appendix Figure 2: pRP MAVS NU plasmid map. Plasmid used for MAVS expression from a transcript without a 3'-UTR.

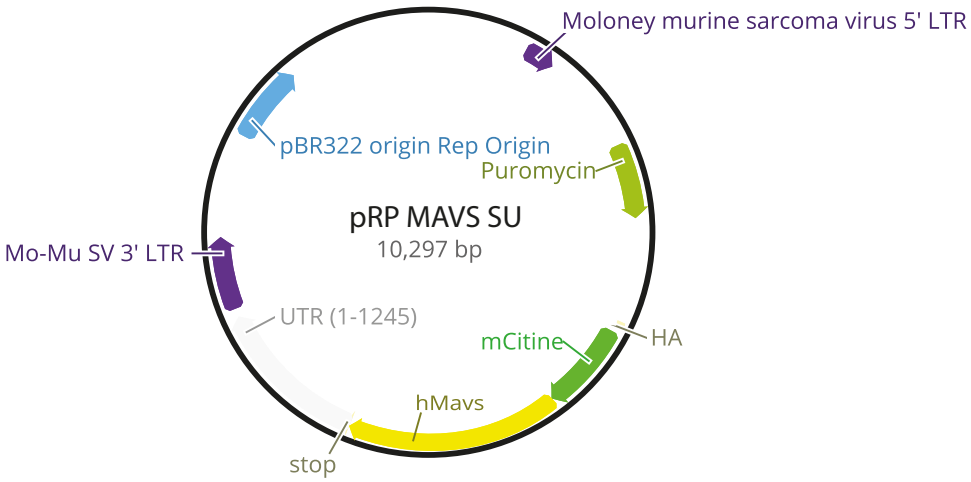

Appendix Figure 3: pRP MAVS SU plasmid map. Plasmid used for MAVS expression from SU transcript.

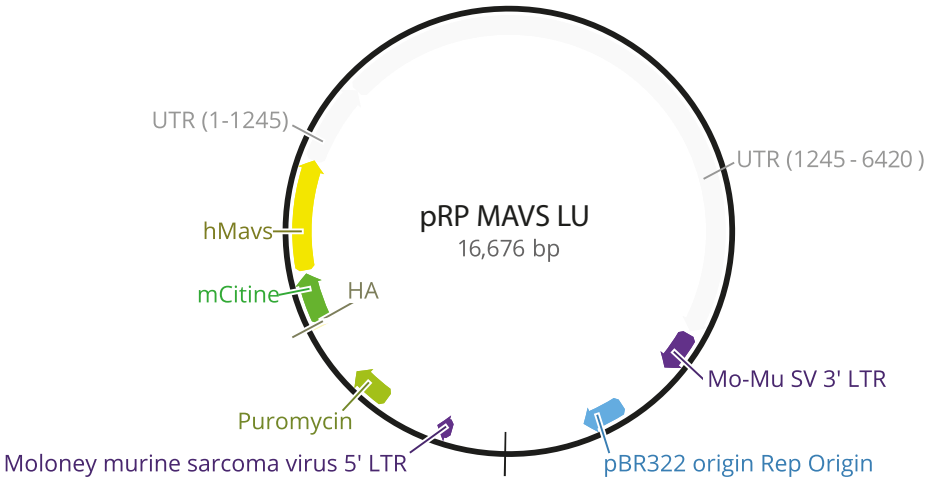

Appendix Figure 4: pRP MAVS LU plasmid map. Plasmid used for MAVS expression from LU transcript.

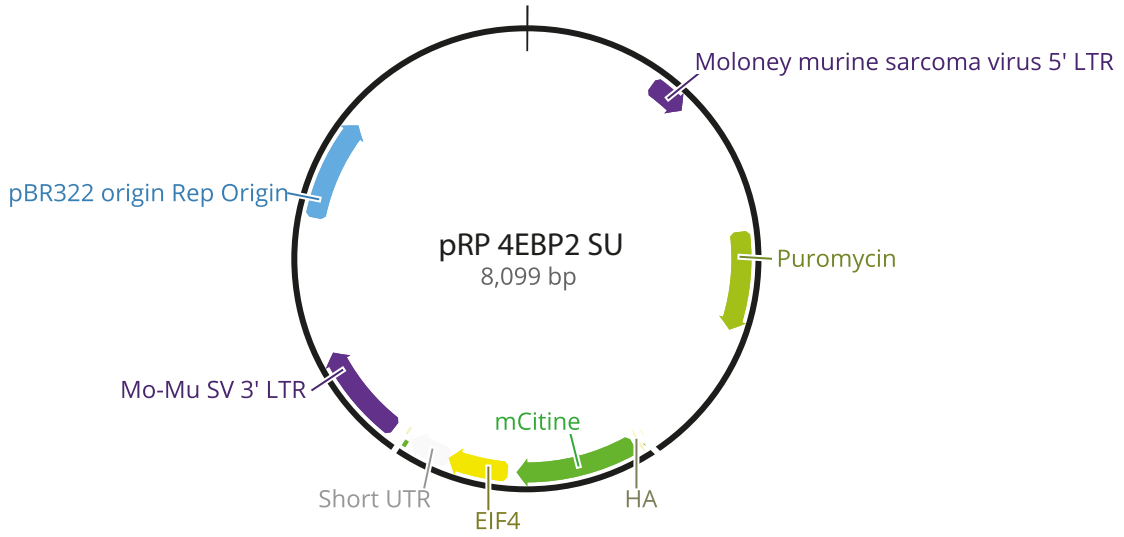

Appendix Figure 5: pRP 4EBP2 SU plasmid map. Plasmid used for 4EBP2 expression from SU transcript.

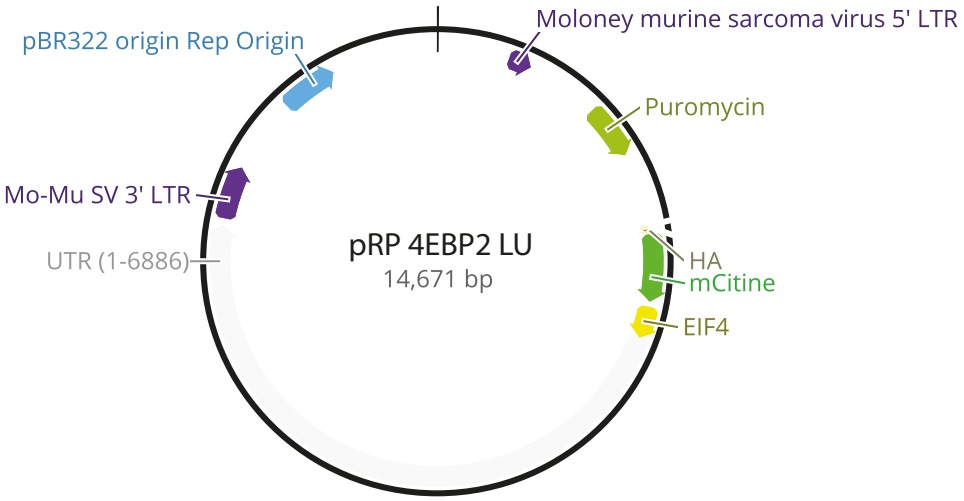

Appendix Figure 6: pRP 4EBP2 LU plasmid map. Plasmid used for 4EBP2 expression from LU transcript.

Appendix Table 1: Top 50 downregulated genes in BMDMs after 3 h of IFNβ treatment

Gene	Log_2 Fold Change	Confect	Average Expression	Ensembl ID
9930012k11Rik	-4.849	-1.026	-1.696	ENSMUSG00000044551
Fam222a	-4.730	-0.918	-2.308	ENSMUSG00000041930
Gm24620	-4.468	-0.704	-2.446	ENSMUSG00000064558
Ddit4	-4.392	-0.672	-1.926	ENSMUSG00000020108
Myl2	-3.969	-1.139	0.074	ENSMUSG00000013936
Gm37198	-3.868	-0.304	-2.756	ENSMUSG00000104069
Gm3604	-3.740	-0.387	-1.934	ENSMUSG00000094942
Zfyve28	-3.651	-0.444	-1.023	ENSMUSG00000037224
4833411c07Rik	-3.615	-0.153	-2.868	ENSMUSG00000109089
Snhg7	-3.519	-0.019	-2.937	ENSMUSG00000064858
Gm9889	-3.386	-0.277	-2.181	ENSMUSG00000052769
Sema6d	-3.350	-0.414	-0.723	ENSMUSG00000027200
Plekhg5	-3.338	-0.328	-1.640	ENSMUSG00000039713
Gm45050	-3.266	-0.372	-2.232	ENSMUSG00000108371
Lipt2	-3.262	-0.303	-1.270	ENSMUSG00000030725
F830115b05Rik	-3.110	-0.251	-1.561	ENSMUSG00000104576
Gm15503	-3.095	-0.585	-0.349	ENSMUSG00000084964
Ac159810.1	-3.070	-0.451	-0.952	ENSMUSG00000111844
Il16	-3.055	-1.171	1.866	ENSMUSG00000001741
Gm28557	-2.985	-0.469	-1.008	ENSMUSG00000100235
Per2	-2.973	-0.369	-1.441	ENSMUSG00000055866
Gm37276	-2.828	-0.133	-1.427	ENSMUSG00000103283
Fgd3	-2.759	-1.327	3.610	ENSMUSG00000037946
Gm29291	-2.749	-0.513	-0.310	ENSMUSG00000101903
Gm10369	-2.711	-0.09	-2.041	ENSMUSG00000072573
Cd300lb	-2.688	-1.625	5.805	ENSMUSG00000063193
Plat	-2.670	-0.065	-1.341	ENSMUSG00000031538
Plk3	-2.663	-0.687	-0.197	ENSMUSG00000028680
Adrb2	-2.647	-1.273	2.306	ENSMUSG00000045730
Plekhh3	-2.628	-1.269	1.633	ENSMUSG00000035172
Fut7	-2.624	-0.542	-0.338	ENSMUSG00000036587
Irs2	-2.583	-1.63	3.110	ENSMUSG00000038894
Sesn1	-2.553	-1.234	4.434	ENSMUSG00000038332
Nol4l	-2.545	-0.86	0.955	ENSMUSG00000061411
S1pr1	-2.541	-1.425	4.956	ENSMUSG00000045092
Znrf3	-2.504	-0.04	-0.440	ENSMUSG00000041961

N4bp3	-2.501	-0.685	1.141	ENSMUSG00000001053
Sox4	-2.487	-0.56	0.560	ENSMUSG00000076431
Gpr183	-2.471	-1.247	2.841	ENSMUSG00000051212
Mnt	-2.458	-1.377	4.646	ENSMUSG00000000282
Slc10a6	-2.455	-0.105	-1.634	ENSMUSG00000029321
Tfap4	-2.398	-0.966	1.384	ENSMUSG00000005718
Tfeb	-2.393	-1.5	3.579	ENSMUSG00000023990
Bhlhe41	-2.379	-1.414	5.582	ENSMUSG00000030256
Nhlrc1	-2.349	-0.148	-0.594	ENSMUSG00000044231
Mir6403	-2.332	-0.37	-0.144	ENSMUSG00000099289
Gm15513	-2.331	-0.318	-1.292	ENSMUSG00000086291
Hyls1	-2.296	-0.327	-0.022	ENSMUSG00000050555
Frat2	-2.290	-1.246	2.345	ENSMUSG00000047604
Lpin1	-2.245	-0.916	2.334	ENSMUSG00000020593

Appendix Table 2: Top 50 upregulated genes in BMDMs after 3 h of IFNβ treatment

Gene	**Log_2 Fold Change**	**Confect**	**Average Expression**	**Ensembl ID**
Serpina3f	8.511	4.511	1.501	ENSMUSG00000066363
Cd69	7.857	3.974	1.811	ENSMUSG00000030156
Misp	7.506	2.864	-1.032	ENSMUSG00000035852
Cxcl10	7.395	6.341	9.179	ENSMUSG00000034855
Serpina3g	7.358	3.938	1.970	ENSMUSG00000041481
Iigp1	7.154	5.647	6.128	ENSMUSG00000054072
Amotl2	7.133	3.928	1.431	ENSMUSG00000032531
Lhx2	7.081	3.947	1.533	ENSMUSG00000000247
Arsi	6.984	2.506	-1.293	ENSMUSG00000036412
Gbp5	6.979	4.586	3.068	ENSMUSG00000105504
Cish	6.918	2.474	-1.326	ENSMUSG00000032578
Cxcl9	6.917	2.699	0.663	ENSMUSG00000029417
Klrk1	6.914	2.458	-1.328	ENSMUSG00000030149
Rsad2	6.870	5.966	8.078	ENSMUSG00000020641
Socs1	6.688	5.697	6.087	ENSMUSG00000038037
Ifi206	6.687	2.32	-1.442	ENSMUSG00000037849
Ccl12	6.647	4.841	3.987	ENSMUSG00000035352
Gbp11	6.626	2.338	-0.917	ENSMUSG00000092021
Ifit1	6.618	5.748	8.062	ENSMUSG00000034459
Gm12250	6.583	5.111	5.306	ENSMUSG00000082292

Ch25h	6.548	5.014	4.359	ENSMUSG00000050370
Trim30c	6.547	2.894	0.512	ENSMUSG00000078616
Acod1	6.484	4.968	4.312	ENSMUSG00000022126
F830016b08Rik	6.400	2.108	-1.588	ENSMUSG00000090942
Cmpk2	6.388	5.803	9.380	ENSMUSG00000020638
Ifit1bl1	6.379	5.014	5.906	ENSMUSG00000079339
Tgtp1	6.339	4.191	2.795	ENSMUSG00000078922
Msh4	6.282	2.86	0.658	ENSMUSG00000005493
Clcn1	6.267	2.014	-1.652	ENSMUSG00000029862
Tnfsf10	6.261	4.191	2.771	ENSMUSG00000039304
Tgtp2	6.220	5.004	5.179	ENSMUSG00000078921
Gbp4	6.183	2.757	1.239	ENSMUSG00000079363
Batf2	6.168	5.014	5.509	ENSMUSG00000039699
Pou3f1	6.165	4.457	3.997	ENSMUSG00000090125
Gm4841	6.165	2.274	-0.310	ENSMUSG00000068606
Gm4951	6.035	4.738	4.697	ENSMUSG00000073555
Trim30d	6.034	3.485	1.797	ENSMUSG00000057596
Sectm1a	6.012	3.439	1.774	ENSMUSG00000025165
Mx1	5.977	4.968	5.361	ENSMUSG00000000386
Il10	5.965	3.576	1.937	ENSMUSG00000016529
Ifi209	5.939	4.076	3.017	ENSMUSG00000043263
Ccl8	5.900	4.047	3.139	ENSMUSG00000009185
A530040e14Rik	5.786	2.67	0.682	ENSMUSG00000072109
Ifi214	5.784	2.34	-0.052	ENSMUSG00000070501
Cxcl11	5.768	2.22	-0.049	ENSMUSG00000060183
Trim30b	5.767	1.661	-1.348	ENSMUSG00000052749
Akap12	5.753	2.321	-0.067	ENSMUSG00000038587
Gipc3	5.752	1.615	-1.913	ENSMUSG00000034872
Ifit2	5.732	4.813	6.382	ENSMUSG00000045932
Socs2	5.722	1.631	-0.821	ENSMUSG00000020027

Appendix Table 3: Top 50 downregulated genes in BMDMs after 12 h of IFNβ treatment

Gene	Log_2 Fold Change	Confect	Average Expression	Ensembl ID
Clmp	-5.327	-2.048	-0.272	ENSMUSG00000032024
Sema6d	-5.292	-1.847	-1.140	ENSMUSG00000027200
Rnf125	-5.063	-1.675	-1.255	ENSMUSG00000033107
Cyp39a1	-4.473	-1.256	-1.550	ENSMUSG00000023963

Pald1	-4.419	-1.907	0.553	ENSMUSG00000020092
Myh6	-4.295	-0.784	-2.244	ENSMUSG00000040752
Gm29291	-4.244	-1.207	-0.807	ENSMUSG00000101903
Fn3k	-4.217	-1.064	-1.677	ENSMUSG00000025175
Lrfn4	-4.214	-1.921	1.014	ENSMUSG00000045045
Gm17233	-4.184	-1.027	-1.697	ENSMUSG00000090706
Cx3cr1	-4.137	-2.952	3.698	ENSMUSG00000052336
Prokr1	-4.122	-1.004	-1.735	ENSMUSG00000049409
B3gnt7	-4.081	-0.98	-1.745	ENSMUSG00000079445
Ptpn4	-4.033	-1.079	-0.400	ENSMUSG00000026384
Rfx2	-4.023	-1.079	-1.239	ENSMUSG00000024206
Tle2	-4.002	-0.931	-1.787	ENSMUSG00000034771
Gja1	-3.972	-1.158	-0.739	ENSMUSG00000050953
Stk26	-3.940	-1.279	-0.265	ENSMUSG00000031112
Pacsin3	-3.933	-0.934	-0.949	ENSMUSG00000027257
Grk4	-3.818	-0.788	-1.878	ENSMUSG00000052783
F830115b05Rik	-3.793	-0.748	-1.895	ENSMUSG00000104576
Smim10l2a	-3.775	-0.777	-1.899	ENSMUSG00000054850
Mki67	-3.729	-2.765	4.614	ENSMUSG00000031004
Osbpl10	-3.695	-0.733	-1.941	ENSMUSG00000040875
C5ar2	-3.658	-0.626	-2.000	ENSMUSG00000074361
Mfap3l	-3.658	-1.368	0.666	ENSMUSG00000031647
Satb1	-3.650	-0.695	-1.960	ENSMUSG00000023927
Wtip	-3.650	-0.667	-1.970	ENSMUSG00000036459
Btbd17	-3.646	-0.774	-1.411	ENSMUSG00000000202
Myl2	-3.621	-0.461	-0.754	ENSMUSG00000013936
Gfod1	-3.595	-0.641	-1.150	ENSMUSG00000051335
Gm43313	-3.588	-0.949	-1.267	ENSMUSG00000107083
Chml	-3.584	-1.006	0.328	ENSMUSG00000078185
Kif21a	-3.581	-0.967	-0.654	ENSMUSG00000022629
Zfp827	-3.516	-0.842	-1.216	ENSMUSG00000071064
2510046g10Rik	-3.471	-0.59	-2.051	ENSMUSG00000066175
Zfp651	-3.455	-0.578	-2.068	ENSMUSG00000013419
Mb	-3.447	-0.178	-2.482	ENSMUSG00000018893
Lama3	-3.426	-0.633	-0.965	ENSMUSG00000024421
Alox5	-3.393	-2.028	2.692	ENSMUSG00000025701
Acot1	-3.391	-1.311	0.736	ENSMUSG00000072949
Sacs	-3.380	-1.051	-0.330	ENSMUSG00000048279
Mafa	-3.363	-0.632	-1.228	ENSMUSG00000047591
Kcnn1	-3.358	-0.477	-1.565	ENSMUSG00000002908

Mt2	-3.350	-2.42	3.892	ENSMUSG00000031762
Gm5141	-3.341	-0.451	-1.631	ENSMUSG00000091183
Fam46b	-3.319	-0.494	-2.126	ENSMUSG00000046694
Asb10	-3.313	-1.247	0.588	ENSMUSG00000038204
Pccb	-3.297	-1.907	2.554	ENSMUSG00000032527
Uck2	-3.292	-1.68	1.869	ENSMUSG00000026558

Appendix Table 4: Top 50 upregulated genes in BMDMs after 12 h of IFNβ treatment

Gene	Log_2 Fold Change	Confect	Average Expression	Ensembl ID
Ddx4	8.050	4.023	0.242	ENSMUSG00000021758
Misp	7.981	3.821	-0.886	ENSMUSG00000035852
Apol9b	7.889	5.292	3.301	ENSMUSG00000068246
Ifi214	7.656	4.28	0.786	ENSMUSG00000070501
Klrk1	7.519	3.471	-1.116	ENSMUSG00000030149
Gm2619	7.454	3.705	-0.063	ENSMUSG00000091199
Slfn1	7.385	5.689	4.344	ENSMUSG00000078763
Cxcl9	7.323	3.954	1.377	ENSMUSG00000029417
Slfn4	7.222	3.453	0.165	ENSMUSG00000000204
Prm1	7.113	3.259	-0.765	ENSMUSG00000022501
Piwil4	7.088	3.145	-1.333	ENSMUSG00000036912
Apol9a	7.083	4.047	2.504	ENSMUSG00000057346
Gbp10	7.024	3.56	0.222	ENSMUSG00000105096
Ifit1bl1	6.990	5.596	6.180	ENSMUSG00000079339
Sectm1a	6.966	4.537	2.149	ENSMUSG00000025165
Ccl8	6.928	5.185	3.560	ENSMUSG00000009185
Clcn1	6.809	2.932	-1.473	ENSMUSG00000029862
F8	6.796	3.08	-0.373	ENSMUSG00000031196
Ifi208	6.791	3.605	0.552	ENSMUSG00000066677
Hap1	6.714	3.76	1.201	ENSMUSG00000006930
Isg15	6.710	5.94	9.629	ENSMUSG00000035692
Trim30d	6.709	4.49	2.348	ENSMUSG00000057596
Cxcl11	6.694	3.373	0.320	ENSMUSG00000060183
Isg20	6.687	5.803	6.469	ENSMUSG00000039236
Hdc	6.679	3.886	1.110	ENSMUSG00000027360
Phf11a	6.656	4.902	3.689	ENSMUSG00000044703
Treml2	6.653	4.82	3.163	ENSMUSG00000071068
Ms4a4c	6.588	5.775	6.698	ENSMUSG00000024675

Gbp4	6.557	3.45	1.199	ENSMUSG00000079363
Lipg	6.552	3.615	0.807	ENSMUSG00000053846
Csprs	6.541	2.983	-0.339	ENSMUSG00000062783
Gm7582	6.532	2.857	-0.334	ENSMUSG00000061852
A530040e14Rik	6.508	3.57	0.783	ENSMUSG00000072109
Cfb	6.420	5.125	4.670	ENSMUSG00000090231
Sell	6.288	2.517	-1.733	ENSMUSG00000026581
Hsh2d	6.242	2.388	-1.230	ENSMUSG00000062007
Ly6a	6.237	5.259	5.139	ENSMUSG00000075602
Ifi206	6.227	2.388	-1.787	ENSMUSG00000037849
Aw112010	6.222	4.538	3.842	ENSMUSG00000075010
Mx1	6.216	5.259	5.409	ENSMUSG00000000386
Ifit2	6.192	5.315	6.543	ENSMUSG00000045932
Dnase1l3	6.169	2.756	-0.397	ENSMUSG00000025279
Ifit3b	6.165	5.259	5.461	ENSMUSG00000062488
Apod	6.153	2.83	-0.200	ENSMUSG00000022548
Gbp2b	6.138	4.901	4.752	ENSMUSG00000040264
Tgtp1	6.118	4.412	2.889	ENSMUSG00000078922
Gm13822	6.073	3.306	1.400	ENSMUSG00000087477
Ifi209	6.064	4.392	3.036	ENSMUSG00000043263
Socs2	6.035	2.423	-0.992	ENSMUSG00000020027
Gbp6	6.022	3.596	1.336	ENSMUSG00000104713

Appendix Table 5: Top 50 shortened genes in BMDMs after 3 h of IFNβ treatment

Gene	3'-UTR Log_2 Fold Change	Confect	Average Expression	Ensembl ID
Trim56	-0.499	-0.281	4.287	ENSMUSG00000043279
Nat8l	-0.442	-0.131	1.802	ENSMUSG00000048142
Rasa2	-0.371	-0.01	1.816	ENSMUSG00000032413
Chchd5	-0.302	-0.117	5.021	ENSMUSG00000037938
Btbd9	-0.292	-0.118	5.448	ENSMUSG00000062202
March1	-0.288	-0.087	4.793	ENSMUSG00000036469
Etv1	-0.268	-0.015	2.937	ENSMUSG00000004151
Creb1	-0.268	-0.038	3.971	ENSMUSG00000025958
Nupl2	-0.267	-0.018	3.161	ENSMUSG00000048439
Pgm2l1	-0.262	-0.027	3.693	ENSMUSG00000030729
Ifi203	-0.254	-0.079	6.384	ENSMUSG00000039997
Brd3	-0.250	-0.062	4.878	ENSMUSG00000026918
Mllt3	-0.250	-0.018	3.615	ENSMUSG00000028496
Cdc73	-0.249	-0.04	4.227	ENSMUSG00000026361
Naa25	-0.247	-0.051	5.145	ENSMUSG00000042719
Asxl2	-0.245	-0.006	3.268	ENSMUSG00000037486
Tmem106b	-0.242	-0.036	4.501	ENSMUSG00000029571
Fam219b	-0.241	-0.019	3.604	ENSMUSG00000032305
Twistnb	-0.236	-0.058	4.516	ENSMUSG00000020561
Ube3a	-0.235	-0.063	5.026	ENSMUSG00000025326
Thg1l	-0.230	-0.023	3.840	ENSMUSG00000011254
Herc6	-0.229	-0.037	5.188	ENSMUSG00000029798
Sec14l1	-0.219	-0.09	6.674	ENSMUSG00000020823
Pdlim5	-0.215	-0.063	5.593	ENSMUSG00000028273
Ssh1	-0.215	-0.029	4.391	ENSMUSG00000042121
Slc35a3	-0.213	-0.029	4.462	ENSMUSG00000027957
Ythdf1	-0.212	-0.114	7.438	ENSMUSG00000038848
Nrp1	-0.210	-0.009	3.728	ENSMUSG00000025810
Tsc22d2	-0.209	-0.017	4.098	ENSMUSG00000027806
Synrg	-0.208	-0.029	4.377	ENSMUSG00000034940
Ascc2	-0.205	-0.024	4.371	ENSMUSG00000020412
Dock8	-0.200	-0.071	5.772	ENSMUSG00000052085
Cd2bp2	-0.199	-0.069	6.017	ENSMUSG00000042502
Spred1	-0.199	-0.099	7.679	ENSMUSG00000027351

Zc3hav1	-0.199	-0.079	6.922	ENSMUSG00000029826
Fmn1	-0.194	-0.028	4.896	ENSMUSG00000044042
Arhgef10l	-0.193	-0.037	5.243	ENSMUSG00000040964
Uqcc1	-0.192	-0.011	4.342	ENSMUSG00000005882
Ubr2	-0.191	-0.041	5.372	ENSMUSG00000023977
Prkaa1	-0.190	-0.025	4.913	ENSMUSG00000050697
Pias1	-0.190	-0.056	5.819	ENSMUSG00000032405
Rps6ka3	-0.190	-0.034	5.277	ENSMUSG00000031309
Tgs1	-0.189	-0.025	3.644	ENSMUSG00000028233
Pten	-0.188	-0.024	5.015	ENSMUSG00000013663
Ccdc93	-0.188	-0.069	6.392	ENSMUSG00000026339
Napg	-0.188	-0.014	4.212	ENSMUSG00000024581
Snx20	-0.185	-0.094	7.324	ENSMUSG00000031662
Kras	-0.184	-0.016	4.262	ENSMUSG00000030265
Srsf10	-0.183	-0.016	4.980	ENSMUSG00000028676
Brcc3	-0.182	-0.01	4.472	ENSMUSG00000031201

Appendix Table 6: All lengthened genes in BMDMs after 3 h of IFNβ treatment

Gene	**3'-UTR Log_2 Fold Change**	**Confect**	**Average Expression**	**Ensembl ID**
Zbp1	0.348	0.215	5.786	ENSMUSG00000027514
Wdr20	0.286	0.063	4.011	ENSMUSG00000037957
Sik3	0.235	0.059	5.424	ENSMUSG00000034135
Vmp1	0.143	0.058	7.000	ENSMUSG00000018171
Wtap	0.179	0.04	5.137	ENSMUSG00000060475
Fcgr1	0.088	0.033	8.447	ENSMUSG00000015947
Prune1	0.215	0.029	3.850	ENSMUSG00000015711
Oas1a	0.087	0.022	5.911	ENSMUSG00000052776
Fxr1	0.140	0.022	5.864	ENSMUSG00000027680
Specc1	0.160	0.018	5.838	ENSMUSG00000042331
Il10ra	0.056	0.018	7.084	ENSMUSG00000032089
Cflar	0.100	0.016	6.630	ENSMUSG00000026031
Dbp	0.172	0.015	5.608	ENSMUSG00000059824
Dnaja2	0.090	0.014	6.916	ENSMUSG00000031701
Gla	0.094	0.013	7.854	ENSMUSG00000031266
Nlrc5	0.182	0.011	4.757	ENSMUSG00000074151
Crem	0.207	0.011	4.431	ENSMUSG00000063889

Il4ra	0.073	0.011	7.201	ENSMUSG00000030748
Nampt	0.083	0.011	7.897	ENSMUSG00000020572
Kxd1	0.025	0.01	11.010	ENSMUSG00000055553
Ahnak	0.063	0.009	8.585	ENSMUSG00000069833
Plekhn1	0.195	0.008	4.161	ENSMUSG00000078485
Nisch	0.048	0.007	6.991	ENSMUSG00000021910
Zyx	0.030	0.007	9.208	ENSMUSG00000029860
Fcgr4	0.100	0.006	6.792	ENSMUSG00000059089
Zfp710	0.042	0.006	6.960	ENSMUSG00000048897
Mbp	0.080	0.002	5.588	ENSMUSG00000041607

Appendix Table 7: Top 50 shortened genes in BMDMs after 12 h of IFNβ treatment

Gene	3'-UTR Log_2 Fold Change	Confect	Average Expression	Ensembl ID
Trim56	-0.674	-0.447	3.636	ENSMUSG00000043279
Ccdc50	-0.495	-0.292	5.144	ENSMUSG00000038127
Utp14b	-0.494	-0.159	3.029	ENSMUSG00000079470
Bcl2	-0.468	-0.101	1.477	ENSMUSG00000057329
Pgap1	-0.457	-0.17	3.585	ENSMUSG00000073678
Creb1	-0.456	-0.148	3.561	ENSMUSG00000025958
Osbpl3	-0.449	-0.12	2.670	ENSMUSG00000029822
Tmem106b	-0.443	-0.173	3.863	ENSMUSG00000029571
Phactr2	-0.407	-0.076	2.844	ENSMUSG00000062866
Katnal1	-0.398	-0.023	1.190	ENSMUSG00000041298
Akap1	-0.391	-0.1	2.338	ENSMUSG00000018428
Zfp462	-0.383	-0.09	2.391	ENSMUSG00000060206
Zfp704	-0.379	-0.076	2.359	ENSMUSG00000040209
Gnb4	-0.376	-0.154	4.269	ENSMUSG00000027669
Pgm2l1	-0.372	-0.049	2.609	ENSMUSG00000030729
Fmn1	-0.368	-0.155	4.313	ENSMUSG00000044042
Dpy19l4	-0.363	0	2.649	ENSMUSG00000045205
Sh3rf1	-0.362	-0.037	2.339	ENSMUSG00000031642
Nktr	-0.362	-0.148	3.908	ENSMUSG00000032525
Slc7a2	-0.357	-0.096	3.326	ENSMUSG00000031596
Klhl2	-0.355	-0.057	2.782	ENSMUSG00000031605
Zdhhc21	-0.355	-0.045	1.611	ENSMUSG00000028403
Impad1	-0.351	-0.15	4.900	ENSMUSG00000066324

Zfp106	-0.351	-0.175	5.326	ENSMUSG00000027288
Gls	-0.346	-0.094	4.481	ENSMUSG00000026103
Rc3h1	-0.346	-0.077	3.115	ENSMUSG00000040423
Zmat3	-0.344	-0.103	3.530	ENSMUSG00000027663
Rbbp8	-0.343	0	1.991	ENSMUSG00000041238
Poc5	-0.343	-0.077	3.234	ENSMUSG00000021671
Nras	-0.343	-0.185	5.867	ENSMUSG00000027852
March1	-0.340	-0.153	4.507	ENSMUSG00000036469
Hook3	-0.334	-0.01	3.195	ENSMUSG00000037234
Pten	-0.332	-0.134	4.738	ENSMUSG00000013663
Reep3	-0.332	-0.193	6.344	ENSMUSG00000019873
Zkscan1	-0.331	-0.086	3.403	ENSMUSG00000029729
Rps6ka3	-0.323	-0.136	4.995	ENSMUSG00000031309
Ubxn7	-0.321	-0.028	2.910	ENSMUSG00000053774
Cuedc1	-0.321	-0.013	2.057	ENSMUSG00000018378
Tfdp2	-0.320	-0.042	3.077	ENSMUSG00000032411
Etv1	-0.317	-0.072	2.828	ENSMUSG00000004151
Rab10	-0.317	-0.185	6.350	ENSMUSG00000020671
Dnmt3a	-0.317	-0.213	7.119	ENSMUSG00000020661
Ccnt2	-0.316	-0.056	2.881	ENSMUSG00000026349
Slain2	-0.314	-0.159	5.710	ENSMUSG00000036087
Sft2d2	-0.312	-0.15	5.646	ENSMUSG00000040848
Xpr1	-0.308	-0.155	5.615	ENSMUSG00000026469
Sepsecs	-0.306	-0.013	2.279	ENSMUSG00000029173
Spag9	-0.302	-0.154	5.433	ENSMUSG00000020859
Cast	-0.299	-0.159	6.048	ENSMUSG00000021585
Mecp2	-0.298	-0.143	5.042	ENSMUSG00000031393

Appendix Table 8: All lengthened genes in BMDMs after 12 h of IFNβ treatment

Gene	**3'-UTR Log_2 Fold Change**	**Confect**	**Average Expression**	**Ensembl ID**
Plekhn1	0.405	0.188	4.418	ENSMUSG00000078485
Hnrnpa2b1	0.256	0.178	9.044	ENSMUSG00000004980
15011B03Rik	0.356	0.14	4.335	ENSMUSG00000072694
Zbp1	0.207	0.114	6.659	ENSMUSG00000027514
Fcgr2b	0.232	0.111	6.208	ENSMUSG00000026656
Itpr1	0.336	0.108	3.814	ENSMUSG00000030102

Qk	0.184	0.081	6.803	ENSMUSG00000062078
Ms4a4b	0.158	0.063	3.777	ENSMUSG00000056290
Tctn1	0.304	0.063	2.825	ENSMUSG00000038593
Gla	0.127	0.061	8.363	ENSMUSG00000031266
Vmp1	0.128	0.06	6.997	ENSMUSG00000018171
Ankrd11	0.206	0.049	3.896	ENSMUSG00000035569
C1326l21Rik	0.196	0.049	5.226	ENSMUSG00000052477
Susd3	0.157	0.049	6.303	ENSMUSG00000021384
Ppt1	0.133	0.049	6.379	ENSMUSG00000028657
Plbd2	0.140	0.047	6.704	ENSMUSG00000029598
Ighm	0.118	0.045	7.829	ENSMUSG00000076617
Hnrnpa1	0.173	0.044	5.560	ENSMUSG00000046434
Ahnak	0.100	0.043	8.365	ENSMUSG00000069833
Zrsr2	0.156	0.04	4.537	ENSMUSG00000031370
Mospd3	0.074	0.035	7.124	ENSMUSG00000037221
Coa5	0.108	0.035	6.678	ENSMUSG00000026112
Sp100	0.102	0.033	7.629	ENSMUSG00000026222
Ubap2l	0.116	0.033	7.049	ENSMUSG00000042520
Eif1	0.075	0.032	8.103	ENSMUSG00000035530
Ctsc	0.063	0.031	7.882	ENSMUSG00000030560
Tmem59	0.064	0.03	8.498	ENSMUSG00000028618
Zwint	0.067	0.026	6.955	ENSMUSG00000019923
Csk	0.051	0.026	8.495	ENSMUSG00000032312
Col18a1	0.099	0.019	5.853	ENSMUSG00000001435
Nop56	0.053	0.018	6.444	ENSMUSG00000027405
Arsb	0.033	0.015	8.613	ENSMUSG00000042082
Ddost	0.064	0.014	7.566	ENSMUSG00000028757
Ncstn	0.103	0.013	5.685	ENSMUSG00000003458
Vps53	0.067	0.012	5.645	ENSMUSG00000017288
Timm13	0.043	0.011	7.831	ENSMUSG00000020219
Pde12	0.182	0.01	3.647	ENSMUSG00000043702
Ak6	0.069	0.01	5.557	ENSMUSG00000052293
Fuca1	0.039	0.01	9.166	ENSMUSG00000028673
Dtx3l	0.047	0.008	6.729	ENSMUSG00000049502
Tmem106a	0.049	0.008	9.478	ENSMUSG00000034947
Snx12	0.079	0.008	5.640	ENSMUSG00000046032
Cd72	0.022	0.007	8.591	ENSMUSG00000028459
Itsn2	0.157	0.006	5.111	ENSMUSG00000020640
Gsto1	0.052	0.006	7.252	ENSMUSG00000025068
Ptpn18	0.033	0.006	8.332	ENSMUSG00000026126

Ctsl	0.014	0.005	11.524	ENSMUSG00000021477
Rasa4	0.026	0.002	7.082	ENSMUSG00000004952
Fes	0.021	0.001	7.489	ENSMUSG00000053158
Pltp	0.009	0.001	10.442	ENSMUSG00000017754
Rps24	0.005	0.001	10.587	ENSMUSG00000025290

Appendix Table 9: Top 50 shortened genes in HMDMs after 12 h of IFNβ treatment

Gene	3'-UTR Log_2 Fold Change	Confect	Average Expression	Ensembl ID
ZC3HAV1	-0.735	-0.494	4.206	ENSG00000105939
SH3PXD2A	-0.539	-0.261	4.455	ENSG00000107957
GPATCH2L	-0.510	-0.161	2.944	ENSG00000089916
RNF217	-0.506	-0.163	2.940	ENSG00000146373
PHC3	-0.501	-0.241	3.726	ENSG00000173889
ATXN1	-0.487	-0.211	3.822	ENSG00000124788
COG8	-0.487	-0.136	2.201	ENSG00000213380
MAP2K4	-0.483	-0.261	4.817	ENSG00000065559
AKT3	-0.479	-0.042	1.270	ENSG00000117020
PSD3	-0.479	-0.193	3.907	ENSG00000156011
CAPN5	-0.475	-0.023	0.899	ENSG00000149260
CLN8	-0.459	-0.263	5.145	ENSG00000182372
ZNF791	-0.441	-0.051	1.222	ENSG00000173875
MDM4	-0.432	-0.023	1.268	ENSG00000198625
MAVS	-0.429	-0.22	5.180	ENSG00000088888
DCANP1	-0.429	-0.121	2.872	ENSG00000251380
MTURN	-0.424	-0.09	2.441	ENSG00000180354
VPS37A	-0.409	-0.193	5.115	ENSG00000155975
SYNJ2BP	-0.409	-0.163	4.220	ENSG00000213463
ACVR2A	-0.403	-0.047	2.011	ENSG00000121989
PTGFRN	-0.403	-0.075	2.796	ENSG00000134247
TMEM170B	-0.403	-0.053	2.113	ENSG00000205269
FAM168B	-0.401	-0.088	3.620	ENSG00000152102
C12orf76	-0.400	-0.047	2.464	ENSG00000174456
ELMOD2	-0.394	-0.056	3.319	ENSG00000179387
ZHX3	-0.387	-0.108	2.081	ENSG00000174306
PPM1F	-0.375	-0.151	4.440	ENSG00000100034
CYP20A1	-0.373	-0.101	3.258	ENSG00000119004

DCAF17	-0.371	-0.035	1.907	ENSG00000115827
UBXN2A	-0.371	-0.066	2.605	ENSG00000173960
RAPGEF3	-0.369	-0.057	3.081	ENSG00000079337
SNX16	-0.366	-0.036	2.310	ENSG00000104497
LPP	-0.361	-0.112	4.184	ENSG00000145012
FAM199X	-0.358	-0.136	4.509	ENSG00000123575
TRPS1	-0.357	-0.058	2.979	ENSG00000104447
RABGAP1L	-0.351	-0.142	5.798	ENSG00000152061
ING5	-0.347	-0.039	2.139	ENSG00000168395
PNPT1	-0.346	-0.161	5.716	ENSG00000138035
CBX5	-0.344	-0.099	4.232	ENSG00000094916
FP565260.3	-0.341	-0.053	3.360	ENSG00000277117
TRIM44	-0.340	-0.135	4.856	ENSG00000166326
FGD4	-0.338	-0.086	4.106	ENSG00000139132
SLC23A2	-0.335	-0.127	5.109	ENSG00000089057
WIPF3	-0.334	-0.023	2.767	ENSG00000122574
NACC2	-0.332	-0.118	4.846	ENSG00000148411
C12orf49	-0.330	-0.1	5.342	ENSG00000111412
TNRC6B	-0.328	-0.075	4.098	ENSG00000100354
REPS2	-0.325	-0.009	2.107	ENSG00000169891
EIF4EBP2	-0.324	-0.135	5.628	ENSG00000148730
ZNF562	-0.322	-0.026	3.169	ENSG00000171466

Appendix Table 10: All lengthened genes in HMDMs after 12 h of IFNβ treatment.

Gene	**3'-UTR Log_2 Fold Change**	**Confect**	**Average Expression**	**Ensembl ID**
CUX1	0.261	0.069	4.815	ENSG00000257923
SNX6	0.152	0.061	8.999	ENSG00000129515
APOBEC3F	0.303	0.053	4.152	ENSG00000128394
ELF2	0.293	0.043	3.471	ENSG00000109381
ADCY7	0.117	0.041	7.283	ENSG00000121281
ASPH	0.152	0.032	6.992	ENSG00000198363
ATRIP	0.102	0.031	6.077	ENSG00000164053
C9orf40	0.490	0.03	0.299	ENSG00000135045
IL12RB1	0.317	0.028	2.523	ENSG00000096996
FGL2	0.227	0.025	5.359	ENSG00000127951
MTRNR2L1	0.055	0.006	7.933	ENSG00000256618

Appendix Table 11: Top 20 downregulated metabolites in BMDMs after 1 h of IFNβ treatment

Sum Formula	Putative Metabolite	FC 1h	FC 3h	FC 16h	FC 24h	t-test 1h	t-test 3h	t-test 16h	t-test 24h
C6H7N5O	3-Methylguanine	74.709	13.424	241.575	464.396	0.005	-	0.001	0.001
C22H47N	di-n-Undecylamine	11.391	0.846	0.952	1.699	0.233	0.576	0.866	0.306
C23H38	3Z,6Z,9Z,12Z,15Z-Tricosapentaene	8.928	0.768	0.887	1.367	0.154	0.402	0.705	0.349
C10H13N4O8P	IMP	6.696	0.779	1.066	1.232	0.038	0.379	0.824	0.407
C5H4N4O	Hypoxanthine	5.560	0.357	1.195	1.170	0.084	0.149	0.784	0.775
CH4O4S	Monomethyl sulfate	4.898	0.912	0.897	0.936	0.164	0.492	0.532	0.675
C10H13N5O4	Adenosine	3.323	2.186	1.939	1.414	0.069	0.015	0.049	0.325
C10H12N4O5	Inosine	2.909	0.231	1.903	2.640	0.014	0.083	0.171	0.095
C4H9NO5S	L-Homocysteic acid	2.493	1.406	2.067	1.049	0.030	0.187	0.110	0.842
C16H31NO	Palmitoleamide	1.899	1.184	2.149	1.057	0.031	0.285	0.166	0.815
C10H17N3O6S	Glutathione	1.898	0.917	1.248	2.724	0.091	0.829	0.500	0.009
C3H7NO2	L-Alanine	1.889	0.991	1.321	1.950	0.029	0.931	0.258	0.000
C5H5N5	Adenine	1.873	1.304	1.217	1.079	0.057	0.260	0.188	0.491
C3H9O6P	sn-Glycerol 3-phosphate	1.728	1.284	1.236	1.706	0.005	0.086	0.283	0.000
C23H45NO4	O-Palmitoyl-R-carnitine	1.690	0.819	1.427	1.294	0.082	0.140	0.009	0.045
C13H27NO2	2S-Amino-tridecanoic acid	1.676	0.677	1.892	0.896	0.439	0.035	0.188	0.482
C9H14N3O7P	dCMP	1.666	0.954	3.289	6.319	0.097	0.931	0.042	0.000
C3H6O3	(S)-Lactate	1.663	1.119	0.865	1.085	0.013	0.379	0.264	0.196
C3H10NO4P	N-Methylethanolamine phosphate	1.601	1.245	2.100	3.504	0.106	0.205	0.080	0.001
C6H6N4O	1-Methylhypoxanthine	1.591	1.431	1.655	1.314	0.059	0.104	0.019	0.157

Appendix Table 12: Top 20 upregulated metabolites in BMDMs after 1 h of IFNβ treatment

Sum Formula	Putative Metabolite	FC 1h	FC 3h	FC 16h	FC 24h	t-test 1h	t-test 3h	t-test 16h	t-test 24h
C44H84NO8P	PE(39:2)	0.256	0.250	0.332	1.262	0.013	0.014	0.017	0.380
C10H14O3	5-Oxo-1,2-campholide	0.293	0.278	0.270	0.277	0.181	0.174	0.170	0.174
C25H50	Pentacosene	0.419	0.594	0.865	0.608	0.099	0.222	0.773	0.224
C6H6N2O2	Urocanate	0.442	0.408	0.823	0.712	0.084	0.077	0.587	0.349
C15H28O2	[FA dimethyl(13:0)]2,5-dimethyl-2E-tridecenoic acid	0.477	0.454	1.050	0.404	0.286	0.268	0.936	0.233
C18H32O2	FA (18:2)	0.501	0.904	0.572	0.564	0.159	0.799	0.252	0.210
C50H75O10P	PG(44:12)	0.511	0.878	0.773	0.463	0.014	0.502	0.253	0.009
C40H80NO8P	PC(32:0)	0.512	1.134	1.660	1.178	0.010	0.319	0.020	0.191
C25H38O3	Testosterone isocaproate	0.531	0.999	0.798	0.717	0.050	0.996	0.379	0.250
C48H79O10P	PG(42:8)	0.532	0.977	1.034	0.553	0.025	0.924	0.922	0.061
C7H14O6	1-O-Methyl-myo-inositol	0.534	0.883	0.547	1.066	0.020	0.684	0.028	0.831
C18H32O3	FA hydroxy (18:2)	0.554	0.940	0.747	0.667	0.112	0.844	0.403	0.212
C16H30O2	FA(16:1)	0.569	0.522	0.886	0.488	0.360	0.316	0.839	0.286
C48H80NO10P	PS(42:7)	0.577	1.157	0.860	0.612	0.145	0.667	0.632	0.206
C18H30O2	FA (18:3)	0.578	1.064	0.578	0.622	0.175	0.863	0.204	0.220
C17H32O2	FA methyl(16:1)	0.583	0.562	0.965	0.507	0.345	0.324	0.953	0.274
C47H81O13P	PI(38:5)	0.589	0.979	0.872	0.852	0.041	0.909	0.469	0.444
C48H82NO10P	PS(42:6)	0.595	1.034	0.880	0.776	0.075	0.889	0.578	0.317
C23H36O3	17beta-Hydroxy-6beta-methyl-5alpha-androstan-3-one propionate	0.597	1.047	0.766	0.626	0.216	0.901	0.481	0.256
C14H26O2	FA (14:1) tetradecenoic acid	0.610	0.538	1.023	0.505	0.333	0.261	0.965	0.233

Appendix Table 13: Top 20 downregulated metabolites in BMDMs after 3 h of IFNβ treatment

Sum Formula	Putative Metabolite	FC 1h	FC 3h	FC 16h	FC 24h	t-test 1h	t-test 3h	t-test 16h	t-test 24h
C10H12N4O5	Inosine	74.709	13.424	241.575	464.396	0.005	NA	0.001	0.001
C44H84NO8P	PE(39:2)	11.391	0.846	0.952	1.699	0.233	0.576	0.866	0.306
C10H14O3	5-Oxo-1,2-campholide	8.928	0.768	0.887	1.367	0.154	0.402	0.705	0.349
C18H30O5	[FA trihydroxy(2:0)] 9S,11R,15S-trihydroxy-2,3-dinor-5Z,13E-prostadienoic acid-cyclo[8S,12R]	6.696	0.779	1.066	1.232	0.038	0.379	0.824	0.407
C5H4N4O	Hypoxanthine	5.560	0.357	1.195	1.170	0.084	0.149	0.784	0.775
C17H33NO4	O-decanoyl-R-carnitine	4.898	0.912	0.897	0.936	0.164	0.492	0.532	0.675
C6H6N2O2	Urocanate	3.323	2.186	1.939	1.414	0.069	0.015	0.049	0.325
C6H5N3O	3-N4-ethenocytosine	2.909	0.231	1.903	2.640	0.014	0.083	0.171	0.095
C15H28O2	[FA dimethyl(13:0)] 2,5-dimethyl-2E-tridecenoic acid	2.493	1.406	2.067	1.049	0.030	0.187	0.110	0.842
C16H30O2	FA(16:1)	1.899	1.184	2.149	1.057	0.031	0.285	0.166	0.815
C14H26O2	FA (14:1) tetradecenoic acid	1.898	0.917	1.248	2.724	0.091	0.829	0.500	0.009
C17H32O2	FA methyl(16:1)	1.889	0.991	1.321	1.950	0.029	0.931	0.258	0.000
C20H36O2	FA (20:2)	1.873	1.304	1.217	1.079	0.057	0.260	0.188	0.491
C25H50	Pentacosene	1.728	1.284	1.236	1.706	0.005	0.086	0.283	0.000

C5H11N3O2	4-Guanidinobutanoate	1.690	0.819	1.427	1.294	0.082	0.140	0.009	0.045
C24H48O2	Tetracosanoic acid	1.676	0.677	1.892	0.896	0.439	0.035	0.188	0.482
C13H27NO2	2S-Amino-tridecanoic acid	1.666	0.954	3.289	6.319	0.097	0.931	0.042	0.000
C25H47NO4	Oleoylcarnitine	1.663	1.119	0.865	1.085	0.013	0.379	0.264	0.196
C15H30O2	FA methyl(14:0)	1.601	1.245	2.100	3.504	0.106	0.205	0.080	0.001
C15H22N2O18P2	UDP-glucuronate	1.591	1.431	1.655	1.314	0.059	0.104	0.019	0.157

Appendix Table 14: Top 20 upregulated metabolites in BMDMs after 3 h of IFNβ treatment

Sum Formula	Putative Metabolite	FC 1h	FC 3h	FC 16h	FC 24h	t-test 1h	t-test 3h	t-test 16h	t-test 24h
C6H7N5O	3-Methylguanine	74.709	13.424	241.575	464.396	0.005	NA	0.001	0.001
C12H23NO4	2-Methylbutyroylcarnitine	0.909	2.709	1.891	2.159	0.789	0.072	0.202	0.223
C10H13N5O4	Adenosine	3.323	2.186	1.939	1.414	0.069	0.015	0.049	0.325
C10H19NO4	O-Propanoylcarnitine	0.703	1.995	2.003	3.650	0.291	0.162	0.085	0.053
C18H35NO3	(+)-Prosopinine	0.983	1.961	1.837	2.360	0.971	0.250	0.380	0.337
C6H10O3	4-Methyl-2-oxopentanoate	0.828	1.855	0.631	0.839	0.205	0.245	0.025	0.265
C19H41N	CTAB	1.425	1.739	1.300	2.163	0.264	0.400	0.483	0.324
C4H10N2O	N-Nitrosodiethylamine	1.337	1.657	0.954	2.416	0.548	0.383	0.899	0.117
C5H10O3	5-Hydroxypentanoate	0.926	1.609	0.806	0.843	0.551	0.155	0.026	0.051
C6H7NO3S	3-Aminobenzenesulfonate	0.954	1.574	0.721	0.848	0.905	0.191	0.293	0.642
C6H9NO4S	a Cysteine adduct	1.369	1.562	1.072	1.322	0.252	0.221	0.697	0.191
C11H19NO9	O-Acetylneuraminic acid	1.270	1.500	1.186	2.578	0.173	0.052	0.518	0.309

C14H26N4O10P2	CMP-N-trimethyl-2-aminoethylphosphonate	1.163	1.499	1.724	3.291	0.434	0.058	0.027	0.012
C6H6N4O	1-Methylhypoxanthine	1.591	1.431	1.655	1.314	0.059	0.104	0.019	0.157
C6H6N2O	Picolinamide	1.210	1.415	1.182	1.109	0.436	0.130	0.389	0.476
C4H9NO5S	L-Homocysteic acid	2.493	1.406	2.067	1.049	0.030	0.187	0.110	0.842
C18H33NO	Linoleamide	1.423	1.406	1.423	0.960	0.027	0.274	0.040	0.779
C5H11NO2	L-Valine	1.373	1.403	1.148	1.234	0.011	0.014	0.197	0.023
C5H9NO3	5-Aminolevulinate	1.243	1.389	1.156	1.460	0.090	0.051	0.179	0.005
C5H6O4	Itaconate	1.435	1.388	2.675	9.471	0.152	0.296	0.084	0.004

Appendix Table 15: Top 20 downregulated metabolites in BMDMs after 16 h of IFNβ treatment

Sum Formula	Putative Metabolite	FC 1h	FC 3h	FC 16h	FC 24h	t-test 1h	t-test 3h	t-test 16h	t-test 24h
C10H14O3	5-Oxo-1,2-campholide	0.293	0.278	0.270	0.277	0.181	0.174	0.170	0.174
C17H33NO4	O-decanoyl-R-carnitine	0.945	0.396	0.277	0.268	0.919	0.033	0.017	0.016
C18H30O5	[FA trihydroxy(2:0)] 9S,11R,15S-trihydroxy-2,3-dinor-5Z,13E-prostadienoic acid-cyclo[8S,12R]	0.807	0.322	0.310	0.074	0.720	0.074	0.073	NA
C44H84NO8P	PE(39:2)	0.256	0.250	0.332	1.262	0.013	0.014	0.017	0.380
C7H14O6	1-O-Methyl-myo-inositol	0.534	0.883	0.547	1.066	0.020	0.684	0.028	0.831
C14H26N4O11P2	CDP-choline	0.944	1.148	0.549	1.114	0.821	0.499	0.067	0.636
C7H12O2	FA methyl(6:1)	0.633	0.782	0.556	1.098	0.018	0.199	0.011	0.592
C18H32O2	FA (18:2)	0.501	0.904	0.572	0.564	0.159	0.799	0.252	0.210
C18H30O2	FA (18:3)	0.578	1.064	0.578	0.622	0.175	0.863	0.204	0.220

C32H58N2O7S	CHAPS	0.739	0.885	0.594	0.950	0.052	0.311	0.006	0.620
C12H24O2	Dodecanoic acid	0.651	1.014	0.610	0.739	0.141	0.962	0.116	0.256
C6H10O3	4-Methyl-2-oxopentanoate	0.828	1.855	0.631	0.839	0.205	0.245	0.025	0.265
C6H10O3	3-Oxo-4-methylpentanoic acid	1.067	1.220	0.646	0.750	0.856	0.450	0.041	0.150
C15H22N2O18P2	UDP-glucuronate	0.896	0.694	0.654	0.829	0.476	0.048	0.099	0.387
C9H19NO2	butyrylcholine	1.551	1.057	0.686	2.157	0.468	0.931	0.557	0.092
C6H7NO3S	3-Aminobenzenesulfonate	0.954	1.574	0.721	0.848	0.905	0.191	0.293	0.642
C18H32O3	FA hydroxy (18:2)	0.554	0.940	0.747	0.667	0.112	0.844	0.403	0.212
C23H36O3	17beta-Hydroxy-6beta-methyl-5alpha-androstan-3-one propionate	0.597	1.047	0.766	0.626	0.216	0.901	0.481	0.256
C50H75O10P	PG(44:12)	0.511	0.878	0.773	0.463	0.014	0.502	0.253	0.009
C6H13N3O3	L-Citrulline	0.762	0.820	0.784	0.958	0.117	0.222	0.235	0.709

Appendix Table 16: Top 20 upregulated metabolites in BMDMs after 16 h of IFNβ treatment

Sum Formula	Putative Metabolite	FC 1h	FC 3h	FC 16h	FC 24h	t-test 1h	t-test 3h	t-test 16h	t-test 24h
C6H7N5O	3-Methylguanine	74.709	13.424	241.575	464.396	0.005	NA	0.001	0.001
C9H14N3O7P	dCMP	1.666	0.954	3.289	6.319	0.097	0.931	0.042	0.000
C5H6O4	Itaconate	1.435	1.388	2.675	9.471	0.152	0.296	0.084	0.004
C11H20N4O10P2	dCDP-ethanolamine	1.357	0.974	2.627	5.158	0.133	0.920	0.019	0.002

C90H160N4O39	Galbeta1-3GalNAcbeta1-4(NeuAcalpha2-8NeuAcalpha2-3)Galbeta1-4Glcbeta-Cer(d18:1/24:0)	1.325	1.253	2.334	2.001	0.484	0.317	0.013	**0.020**
C45H91N2O6P	SM(d18:1/22:0)	1.116	0.987	2.258	1.241	0.717	0.950	0.038	0.278
C71H127N3O31	Ganglioside GM1 (18:1/16:0)	1.249	0.917	2.250	1.894	0.478	0.682	0.045	0.062
C16H31NO	Palmitoleamide	1.899	1.184	2.149	1.057	0.031	0.285	0.166	0.815
C3H10NO4P	N-Methylethanolamine phosphate	1.601	1.245	2.100	3.504	0.106	0.205	0.080	0.001
C4H9NO5S	L-Homocysteic acid	2.493	1.406	2.067	1.049	0.030	0.187	0.110	0.842
C10H19NO4	O-Propanoylcarnitine	0.703	1.995	2.003	3.650	0.291	0.162	0.085	0.053
C10H13N5O4	Adenosine	3.323	2.186	1.939	1.414	0.069	0.015	0.049	0.325
C10H12N4O5	Inosine	2.909	0.231	1.903	2.640	0.014	0.083	0.171	0.095
C13H27NO2	2S-Amino-tridecanoic acid	1.676	0.677	1.892	0.896	0.439	0.035	0.188	0.482
C12H23NO4	2-Methylbutyroylcarnitine	0.909	2.709	1.891	2.159	0.789	0.072	0.202	0.223
C13H23NO4	2-Hexenoylcarnitine	1.423	0.951	1.877	1.431	0.203	0.835	0.074	0.161
C18H35NO3	(+)-Prosopinine	0.983	1.961	1.837	2.360	0.971	0.250	0.380	0.337
C6H6N2O	Isonicotineamide	1.219	1.295	1.832	1.017	0.219	0.225	0.019	0.894
C81H146O17P2	CL(18:2(9Z,12Z)	0.876	0.889	1.824	0.999	0.624	0.377	0.018	0.994
C4H6O2	2-Butenoate	1.174	1.174	1.777	6.164	0.413	0.219	0.104	0.005

Appendix Table 17: Top 20 downregulated metabolites in BMDMs after 24 h of IFNβ treatment

Sum Formula	Putative Metabolite	FC 1h	FC 3h	FC 16h	FC 24h	t-test 1h	t-test 3h	t-test 16h	t-test 24h
C18H30O5	[FA trihydroxy(2:0)] 9S,11R,15S-trihydroxy-2,3-dinor-5Z,13E-prostadienoic acid-cyclo[8S,12R]	74.709	13.424	241.575	464.396	0.005	NA	0.001	0.001
C17H33NO4	O-decanoyl-R-carnitine	11.391	0.846	0.952	1.699	0.233	0.576	0.866	0.306
C10H14O3	5-Oxo-1,2-campholide	8.928	0.768	0.887	1.367	0.154	0.402	0.705	0.349
C44H83NO9	N-(2-hydroxy-15Z-tetracosenoyl)-1-beta-glucosyl-tetradecasphing-4-enine	6.696	0.779	1.066	1.232	0.038	0.379	0.824	0.407
C5H11NO4	N,N-dihydroxyvaline	5.560	0.357	1.195	1.170	0.084	0.149	0.784	0.775
C15H28O2	[FA dimethyl(13:0)] 2,5-dimethyl-2E-tridecenoic acid	4.898	0.912	0.897	0.936	0.164	0.492	0.532	0.675
C49H74O4	[PR] Coenzyme Q8	3.323	2.186	1.939	1.414	0.069	0.015	0.049	0.325
C50H75O10P	PG(44:12)	2.909	0.231	1.903	2.640	0.014	0.083	0.171	0.095
C16H30O2	FA(16:1)	2.493	1.406	2.067	1.049	0.030	0.187	0.110	0.842
C6H6N4	Dihydropteridine	1.899	1.184	2.149	1.057	0.031	0.285	0.166	0.815
C14H26O2	FA (14:1) tetradecenoic acid	1.898	0.917	1.248	2.724	0.091	0.829	0.500	0.009
C17H32O2	FA methyl(16:1)	1.889	0.991	1.321	1.950	0.029	0.931	0.258	0.000
C48H79O10P	PG(42:8)	1.873	1.304	1.217	1.079	0.057	0.260	0.188	0.491

C18H32O2	FA (18:2)	1.728	1.284	1.236	1.706	0.005	0.086	0.283	0.000
C23H34O3	Pregnenolone acetate	1.690	0.819	1.427	1.294	0.082	0.140	0.009	0.045
C25H50	Pentacosene	1.676	0.677	1.892	0.896	0.439	0.035	0.188	0.482
C48H80NO10P	PS(42:7)	1.666	0.954	3.289	6.319	0.097	0.931	0.042	0.000
C18H30O2	FA (18:3)	1.663	1.119	0.865	1.085	0.013	0.379	0.264	0.196
C23H36O3	17beta-Hydroxy-6beta-methyl-5alpha-androstan-3-one propionate	1.601	1.245	2.100	3.504	0.106	0.205	0.080	0.001
C13H22N4O8S2	Asp-Cys-Cys-Ser	1.591	1.431	1.655	1.314	0.059	0.104	0.019	0.157

Appendix Table 18: Top 20 downregulated metabolites in BMDMs after 24 h of IFNβ treatment

Sum Formula	Putative Metabolite	FC 1h	FC 3h	FC 16h	FC 24h	t-test 1h	t-test 3h	t-test 16h	t-test 24h
C6H7N5O	3-Methylguanine	74.709	13.424	241.575	464.396	0.005	NA	0.001	0.001
C5H6O4	Itaconate	1.435	1.388	2.675	9.471	0.152	0.296	0.084	0.004
C9H14N3O7P	dCMP	1.666	0.954	3.289	6.319	0.097	0.931	0.042	0.000
C4H6O2	2-Butenoate	1.174	1.174	1.777	6.164	0.413	0.219	0.104	0.005
C11H20N4O10P2	dCDP-ethanolamine	1.357	0.974	2.627	5.158	0.133	0.920	0.019	0.002
C10H10O4	6-Hydroxymellein	0.784	1.185	0.801	5.019	0.446	0.625	0.497	0.387
C13H15NO6	4-Hydroxyphenyl-acetylglutamic acid	1.323	1.366	1.402	4.779	0.205	0.247	0.284	0.261
C3H8NO6P	O-Phospho-L-serine	1.351	0.789	1.559	4.544	0.406	0.600	0.349	0.070
C9H17NO8	Neuraminic acid	0.946	1.213	1.230	4.192	0.675	0.107	0.233	0.319
C10H19NO4	O-Propanoylcarnitine	0.703	1.995	2.003	3.650	0.291	0.162	0.085	0.053

C3H10NO4P	N-Methylethanolamine phosphate	1.601	1.245	2.100	3.504	0.106	0.205	0.080	0.001
C14H26N4O10P2	CMP-N-trimethyl-2-aminoethylphosphonate	1.163	1.499	1.724	3.291	0.434	0.058	0.027	0.012
C12H23NO10	Lactosamine	1.270	1.328	1.248	3.279	0.278	0.115	0.190	0.312
C10H17N3O6S	Glutathione	1.898	0.917	1.248	2.724	0.091	0.829	0.500	0.009
C3H7N3O2	Guanidinoacetate	1.144	0.980	1.446	2.664	0.607	0.932	0.200	0.001
C10H12N4O5	Inosine	2.909	0.231	1.903	2.640	0.014	0.083	0.171	0.095
C11H19NO9	O-Acetylneuraminic acid	1.270	1.500	1.186	2.578	0.173	0.052	0.518	0.309
C6H12O7	D-Gluconic acid	1.526	1.076	1.551	2.567	0.315	0.828	0.356	0.120
C7H15NO3	L-Carnitine	0.969	1.131	1.564	2.518	0.837	0.475	0.012	0.003
C10H16N5O13P3	ATP	1.163	1.125	1.185	2.453	0.293	0.382	0.523	0.002

Appendix Table 19: NanoString log_2 fold changes of LU vs. total transcript ratio

Gene	HMDM Log_2 FC	HMDM Adj. p-value	THP-1 Log_2 FC	THP-1 Adj. p-value	THP-1 CHX Log_2 FC	THP-1 CHX Adj. p-value	THP-1 mapK Log_2 FC	THP-1 mapK Adj. p-value	THP-1 mTOR Log_2 FC	THP-1 mTOR Adj. p-value	THP-1 JAK Log_2 FC	THP-1 JAK Adj. p-value
ACOX1	-0.800	0.005	-0.886	0.001	-0.247	0.949	-0.386	0.477	-0.517	0.513	-0.110	0.984
AKAP13	-0.110	0.779	-0.349	0.378	-0.115	0.960	-0.219	0.855	0.033	0.958	-0.127	0.984
ARL8B	-0.075	0.779	-0.155	0.554	-0.072	0.960	0.154	0.733	-0.165	0.715	-0.051	0.984
ATP6V1C1	-0.753	0.088	-1.190	0.003	-0.145	0.960	-0.604	0.477	-0.754	0.342	0.161	0.984
ATXN1	-1.079	0.000	-0.351	0.362	-0.376	0.949	0.416	0.733	0.314	0.823	0.613	0.984
C12orf49	-0.271	0.530	-0.803	0.022	-0.027	0.960	-0.519	0.733	-0.113	0.908	0.006	0.984
CD84	-0.396	0.701	-0.017	0.983	-0.190	0.960	0.062	0.979	1.507	0.715	0.955	0.984
CLN8	-1.265	0.000	-1.698	0.000	-0.607	0.822	-1.003	0.477	-1.101	0.342	-0.057	0.984
CYLD	-0.857	0.093	-1.236	0.028	-0.427	0.949	-0.727	0.733	-1.358	0.446	-0.231	0.984
EIF4EBP2	-0.986	0.008	-1.772	0.000	-0.439	0.949	-0.946	0.347	-1.474	0.115	0.034	0.984
FAM168B	-0.437	0.206	-1.124	0.000	-0.032	0.960	-0.325	0.733	-0.755	0.452	0.008	0.984
G3BP1	-1.250	0.000	-1.726	0.000	-0.312	0.949	-1.599	0.001	-1.222	0.115	0.162	0.984
GLG1	-1.029	0.005	-1.663	0.000	-0.398	0.949	-1.295	0.347	-1.447	0.149	0.074	0.984
GNB4	-0.136	0.779	-0.551	0.332	-0.058	0.960	-0.140	0.865	-0.176	0.829	0.097	0.984
MLLT6	-0.213	0.731	-1.057	0.022	-0.230	0.960	-0.439	0.739	-0.602	0.562	-0.152	0.984
NLN	-0.243	0.530	-0.543	0.086	-0.202	0.960	-0.426	0.477	-0.372	0.562	-0.079	0.984
OGFRL1	-0.359	0.351	-0.717	0.028	-0.057	0.960	-0.423	0.477	-0.377	0.529	-0.031	0.984
PAK1	-0.107	0.731	-0.534	0.022	-0.133	0.960	-0.153	0.733	-0.165	0.829	-0.121	0.984
PANK3	-0.515	0.107	-0.701	0.014	-0.153	0.960	-0.216	0.733	-0.341	0.641	0.153	0.984
PARP14	-0.245	0.779	-0.160	0.818	-0.051	0.960	-0.379	0.733	-0.212	0.829	0.017	0.984
PHC3	-0.800	0.031	-1.127	0.001	-0.172	0.960	-0.943	0.410	-1.296	0.149	0.045	0.984

PHC3	-0.800	0.031	-1.127	0.001	-0.172	0.960	-0.943	0.410	-1.296	0.149	0.045	0.984
PSD3	-0.809	0.341	-1.663	0.002	-0.087	0.960	-0.559	0.733	-1.367	0.395	-0.103	0.984
PTGFRN	-0.201	0.779	-0.668	0.554	-0.115	0.960	0.280	0.904	1.259	0.641	-1.025	0.984
RNF217	-0.690	0.298	-1.183	0.075	-0.062	0.960	-1.048	0.731	-1.752	0.395	-0.201	0.984
SPTLC2	-0.698	0.179	-1.757	0.000	-0.375	0.960	-0.881	0.477	-0.866	0.562	0.012	0.984
SRF	-0.327	0.298	-1.073	0.000	-0.222	0.960	-0.387	0.477	-0.427	0.519	-0.078	0.984
TNS1	-0.012	0.979	-0.869	0.170	-0.010	0.989	-0.197	0.917	-1.064	0.672	0.148	0.984
TRIM44	-0.296	0.351	-0.656	0.015	-0.155	0.960	-0.446	0.477	-0.178	0.829	-0.380	0.984
ZC3HAV1	-0.815	0.088	-1.137	0.004	-0.702	0.822	-0.585	0.477	-0.955	0.149	0.090	0.984
ZNF24	-0.460	0.206	-1.116	0.000	-0.120	0.960	-0.459	0.477	-1.028	0.149	-0.075	0.984

Appendix Table 20: Top 20 protein interactors enriched in 4EBP2 SU compared to LU samples

Gene	Uniprot ID	Log_2 FC 4EBP2 SU vs. LU	Log_2 FC EV vs. 4EBP2 LU	Log_2 FC EV vs. 4EBP2 SU	Adj. p-value 4EBP2 SU vs. LU	Adj. p-value EV vs. 4EBP2 LU	Adj. p-value EV vs. 4EBP2 SU
MIB1	Q86YT6	5.570	2.620	-2.950	0.363	0.709	0.552
DCTN1	Q14203	5.260	-2.440	-7.700	0.015	0.313	0.000
EIF4EBP2	Q13542	5.070	-11.000	-16.100	0.096	0.000	0.000
PPP2R2A	P63151	3.570	2.040	-1.540	0.020	0.267	0.318
PFN2	P35080	3.450	0.976	-2.480	0.114	0.760	0.211
SNRPA1	P09661	3.410	1.430	-1.980	0.548	0.821	0.651
RNH1	P13489	3.400	0.383	-3.010	0.352	0.938	0.268
TTLL12	Q14166	3.280	1.660	-1.620	0.246	0.581	0.500
ATP6V1G1	O75348	3.100	0.924	-2.170	0.005	0.527	0.056
TOMM70A	O94826	2.790	0.755	-2.040	0.128	0.784	0.211
TSFM	P43897	2.690	0.787	-1.910	0.075	0.734	0.177
SORD	Q00796	2.690	-1.180	-3.870	0.173	0.621	0.030
MYEOV2	Q8WXC6	2.570	0.584	-1.990	0.365	0.890	0.371
TALDO1	P37837	2.500	1.610	-0.883	0.412	0.587	0.736
HPRT1	P00492	2.350	0.201	-2.140	0.463	0.969	0.343
GMPS	P49915	2.350	-0.151	-2.500	0.315	0.969	0.168
FTO	Q9C0B1	2.330	0.616	-1.720	0.396	0.866	0.427
HSPA8	P11142	2.300	0.839	-1.470	0.082	0.634	0.241
COPS5	Q92905	2.250	0.286	-1.970	0.058	0.895	0.087
CPNE3	O75131	2.240	1.000	-1.240	0.366	0.748	0.552

Appendix Table 21: Top 20 protein interactors enriched in 4EBP2 LU compared to SU samples

Gene	Uniprot ID	Log_2 FC 4EBP2 SU vs. LU	Log_2 FC EV vs. 4EBP2 LU	Log_2 FC EV vs. 4EBP2 SU	Adj. p-value 4EBP2 SU vs. LU	Adj. p-value EV vs. 4EBP2 LU	Adj. p-value EV vs. 4EBP2 SU
MAVS	Q7Z434	-7.170	-6.590	0.582	0.000	0.000	0.704
ALPP	P05187	-5.640	-5.260	0.375	0.000	0.000	0.766
BAG4	O95429	-4.340	-1.870	2.470	0.005	0.298	0.101
TTN	Q8WZ42	-3.850	-3.000	0.852	0.117	0.267	0.755
MFAP1	P55081	-3.290	-0.667	2.630	0.036	0.799	0.087
PLCG1	P19174	-3.220	-3.090	0.128	0.352	0.304	0.977
NENF	Q9UMX5	-3.170	-1.640	1.520	0.158	0.525	0.473
PPP5C	P53041	-3.120	-1.840	1.280	0.058	0.308	0.445
PPP1R14B	Q96C90	-3.110	-2.590	0.526	0.352	0.371	0.874
GOT2	P00505	-2.850	-1.850	1.000	0.363	0.535	0.726
RAD23B	P54727	-2.820	-0.569	2.250	0.315	0.884	0.275
NUMA1	Q14980	-2.800	-0.998	1.800	0.204	0.734	0.330
BANF1	O75531	-2.750	-1.130	1.610	0.472	0.802	0.587
MAPK3	P27361	-2.570	-2.320	0.253	0.475	0.475	0.943
ACTA1	P68133	-2.550	-0.172	2.380	0.729	0.978	0.552
PSIP1	O75475	-2.530	-0.493	2.040	0.363	0.898	0.343
AIFM1	O95831	-2.520	-0.697	1.820	0.336	0.825	0.357
PRCC	Q92733	-2.420	-1.440	0.988	0.075	0.337	0.476
BTF3	P20290	-2.380	-1.820	0.556	0.383	0.489	0.819
MSH6	P52701	-2.340	-2.630	-0.291	0.440	0.299	0.921

Appendix Table 22: Top 20 protein interactors enriched in MAVS SU compared to LU samples

Gene	Uniprot ID	Log_2 FC MAVS SU vs. LU	Log_2 FC EV vs. MAVS NU	Log_2 FC EV vs. MAVS SU	Log_2 FC EV vs. MAVS LU	Log_2 FC MAVS NU vs. SU	Log_2 FC MAVS NU vs. LU	Adj. p-value MAVS SU vs. LU	Adj. p-value EV vs. MAVS NU	Adj. p-value EV vs. MAVS SU	Adj. p-value EV vs. MAVS LU	Adj. p-value MAVS NU vs. SU	Adj. p-value MAVS NU vs. LU
NUDT4	Q9NZJ9	4.960	-4.300	-6.910	-1.950	-2.610	2.340	0.151	0.181	0.025	0.629	0.812	0.600
COA7	Q96BR5	4.040	-1.610	-1.830	2.210	-0.219	3.820	0.022	0.229	0.127	0.135	0.981	0.031
ACTA1	P68133	4.000	0.023	-1.560	2.440	-1.580	2.420	0.163	0.993	0.519	0.425	0.867	0.511
CDK4	P11802	3.980	-4.550	-6.020	-2.040	-1.480	2.500	0.036	0.007	0.001	0.203	0.752	0.213
GRB2	P62993	3.910	-5.100	-4.880	-0.972	0.222	4.130	0.022	0.002	0.001	0.547	0.981	0.022
DUSP3	P51452	3.810	-5.830	-5.430	-1.620	0.404	4.210	0.002	0.000	0.000	0.094	0.898	0.001
FTO	Q9C0B1	3.690	-4.420	-3.740	-0.045	0.679	4.370	0.042	0.008	0.013	0.986	0.905	0.031
ARFGAP1	Q8N6T3	3.680	-4.010	-4.480	-0.807	-0.476	3.200	0.037	0.008	0.003	0.640	0.933	0.091
TRIP6	Q15654	3.640	-5.200	-6.120	-2.470	-0.922	2.720	0.023	0.001	0.000	0.081	0.818	0.116
TTC4	O95801	3.620	-2.500	-3.930	-0.304	-1.430	2.200	0.003	0.014	0.000	0.835	0.596	0.082
MRPS34	P82930	3.570	-3.330	-3.680	-0.109	-0.357	3.220	0.046	0.037	0.014	0.969	0.974	0.121
CPOX	P36551	3.570	-2.730	-4.110	-0.540	-1.380	2.190	0.039	0.053	0.006	0.792	0.752	0.243
mCitrine		3.560	1.890	2.210	5.770	0.314	3.870	0.000	0.009	0.002	0.000	0.896	0.000
LIMD1	Q9UGP4	3.550	-2.800	-4.470	-0.922	-1.670	1.880	0.039	0.045	0.003	0.576	0.751	0.328
AASDHPPT	Q9NRN7	3.540	-2.790	-3.770	-0.228	-0.982	2.560	0.017	0.018	0.002	0.900	0.778	0.093
TPP1	Q5IS74	3.460	-2.090	-3.270	0.190	-1.170	2.280	0.037	0.110	0.012	0.928	0.769	0.190
ARL3	P36405	3.440	-4.280	-4.210	-0.772	0.068	3.500	0.003	0.000	0.000	0.413	0.988	0.002
TYMS	P04818	3.410	-0.892	-1.980	1.420	-1.090	2.310	0.050	0.600	0.139	0.402	0.818	0.258
TCEB1	Q15369	3.270	-2.300	-2.970	0.306	-0.665	2.610	0.046	0.102	0.025	0.892	0.897	0.173
MPDZ	O75970	3.240	0.449	-2.670	0.568	-3.120	0.119	0.004	0.659	0.005	0.603	0.047	0.954

Appendix Table 23: Top 20 protein interactors enriched in MAVS LU compared to SU samples

Gene	Uniprot ID	Log_2 FC MAVS SU vs. LU	Log_2 FC EV vs. MAVS NU	Log_2 FC EV vs. MAVS SU	Log_2 FC EV vs. MAVS LU	Log_2 FC MAVS NU vs. SU	Log_2 FC MAVS NU vs. LU	Adj. p-value MAVS SU vs. LU	Adj. p-value EV vs. MAVS NU	Adj. p-value EV vs. MAVS SU	Adj. p-value EV vs. MAVS LU	Adj. p-value MAVS NU vs. SU	Adj. p-value MAVS NU vs. LU
MYDGF	Q969H8	-5.340	0.560	1.780	-3.560	1.220	-4.120	0.004	0.753	0.165	0.038	0.799	0.031
SNRPA1	P09661	-4.120	0.627	-0.248	-4.370	-0.876	-5.000	0.164	0.862	0.937	0.153	0.946	0.190
PNN	Q9H307	-3.470	1.620	1.610	-1.860	-0.011	-3.480	0.022	0.162	0.123	0.146	1.000	0.025
EDF1	O60869	-3.240	-0.649	0.842	-2.400	1.490	-1.750	0.075	0.746	0.567	0.175	0.763	0.425
COA4	Q9NYJ1	-3.230	1.140	1.940	-1.290	0.800	-2.430	0.113	0.587	0.235	0.566	0.911	0.349
BTF3	P20290	-3.220	-1.490	1.500	-1.720	2.990	-0.230	0.058	0.331	0.255	0.304	0.481	0.944
HMGA1	P17096	-3.070	1.490	1.640	-1.420	0.158	-2.910	0.062	0.316	0.201	0.384	0.983	0.162
CALU	O43852	-3.050	0.470	2.670	-0.378	2.200	-0.848	0.141	0.844	0.121	0.901	0.751	0.762
CALR	P27797	-3.010	0.529	2.660	-0.358	2.130	-0.886	0.139	0.822	0.117	0.904	0.751	0.748
NMT1	P30419	-2.940	-0.515	0.307	-2.640	0.822	-2.120	0.123	0.818	0.861	0.174	0.897	0.383
Q5U7I5	Q5U7I5	-2.920	-1.740	0.507	-2.410	2.250	-0.667	0.364	0.624	0.871	0.526	0.820	0.913
HK1	P19367	-2.860	2.260	2.860	-0.004	0.599	-2.260	0.340	0.469	0.266	1.000	0.979	0.580
ATP5EP2	Q5VTU8	-2.820	0.110	-0.094	-2.910	-0.204	-3.020	0.171	0.971	0.965	0.174	0.983	0.251
TIMM9	Q9Y5J7	-2.790	0.294	1.170	-1.620	0.876	-1.910	0.045	0.835	0.251	0.203	0.813	0.229
NENF	Q9UMX5	-2.670	-0.120	1.090	-1.580	1.210	-1.460	0.096	0.953	0.394	0.328	0.799	0.457
SART3	Q15020	-2.630	0.134	-0.015	-2.640	-0.149	-2.780	0.057	0.938	0.989	0.056	0.983	0.093
HMGN5	P82970	-2.600	1.010	1.280	-1.320	0.267	-2.340	0.067	0.445	0.250	0.348	0.979	0.176
PRCC	Q92733	-2.480	-0.975	1.170	-1.310	2.140	-0.338	0.039	0.312	0.166	0.204	0.481	0.831
RPL35A	P18077	-2.450	0.451	0.761	-1.690	0.311	-2.140	0.039	0.689	0.367	0.105	0.946	0.103
UBA52	P62987	-2.400	0.516	-0.411	-2.810	-0.927	-3.330	0.120	0.766	0.760	0.078	0.834	0.091